Golder Associates
CONSULTING GEOTECHNICAL AND MINING ENGINEERS

REPORT TO

CANMET
ON

IN SITU STRESS DETERMINATIONS
PRINCE AND LINGAN MINES
CAPE BRETON NOVA SCOTIA

CONTRACT SERIAL NUMBER: OSQ85-00063
CONTRACTOR: GOLDER ASSOCIATES (EASTERN CAN.)
DSS REQUISITION NUMBER 23440-5-9004

210 pp + figure pages

Distribution:

15 copies - CANMET
Cape Breton, Nova Scotia

3 copies - Golder Associates
Mississauga, Ontario

MICROMEDIA

851-6025

September 1986

ABSTRACT

An in situ stress measurement program was undertaken at the Prince and Lingan Mines of the Sydney Coalfied, Cape Breton, Nova Scotia. The stresses were determined in 100 mm diameter boreholes using the method of overcoring (with the USBM gauge) and hydrofracture techniques.

Seven successful USBM overcoring tests were completed in each mine in boreholes drilled at different orientations. Complete stress tensors were evaluated from the overcoring test results for each mine. The in situ stresses measured at 222 m below sea level at Prince Mine are slightly anisotropic ($\sigma 1/\sigma 3 = 2$) the major principal stress ($\sigma 1$) is near horizontal and oriented approximately in the E-W direction. The minimum principal stress ($\sigma 3$) is close to vertical and agrees well with the overburden stress.

The in situ stresses at 592 m below sea level at Lingan Mine exhibit relatively higher anisotrophy ($\sigma 1/\sigma 3 = 2.8$). The major principal stress ($\sigma 1$) is near horizontal and oriented approximately in the E-W direction. The minimum principal ($\sigma 3$) stress is off vertical, dipping at 55° to south. The intermediate principal stress is oriented N-S and dips 35° towards the north. This stress system appears to have been influenced by a E-W striking monocline on which the test site was located.

Hydrofracture tests were carried out at the Prince and Lingan Mines in vertical and horizontal boreholes. At Prince Mine distinct vertical fractures were developed in some test zones in the vertical boreholes. The horizontal in situ stresses were interpreted from the breakdown and shut in pressures, the assumed rock tensile strength and pore pressures. The minimum horizontal stress agrees reasonably well with the overcoring test results. The vertical stresses were evaluated in tests where horizontal fractures were induced. They agree reasonably with the overburden stress.

At Lingan Mine, only horizontal fractures were induced in the vertical and horizontal boreholes. In several cases breakdown did not occur in the siltstone strata at pressure levels varying from 20 to 30 MPa. Where horizontal fractures occurred, the vertical stresses were evaluated. The average vertical stress is lower than the overburden stress.

The stress data from different Mines of the Sydney Coalfied were summarized. The results indicated that the in situ stresses increased with depth. The major principal stress is generally horizontal and oriented E-W. The horizontal stress system is fairly isotropic at No. 26 Colliery, Prince and Donkin Mines. The vertical stresses at all the mines agree reasonably well with the overburden stress.

RESUME

Un programme de mesure des contraintes in-situ fut entrepris aux mines Prince et Lingan, près de Sydney, Nouvelle- Ecosse. La détermination des contraintes, par les techniques d'hydrofracture et de surforage (utilisant les cellules du USBM), s'effectua au moyen de trous de sonde de 100 mm de diamètre.

Un total de sept essais de surforage, par la methode du USBM, furent couronnés de succès à chacune des mines. Pour ces essais, les trous de sonde étaient forés selon des orientations différentes, permettant ainsi d'établir la direction et la grandeur de chacune des contraintes. Les contraintes in-situ mesurées 222 m sous le niveau de la mer, à la mine Prince, sont légèrement anisotropiques ($\sigma_1/\sigma_3 \cong 2.0$). La contrainte principale majeure (σ_1) est presqu'horizontale et est orientée approximativement dans l'axe Est-Ouest. La contrainte principale minimum (σ_3) est presque verticale et en accord avec l'épaisseur de la couverture rocheuse.

Les contraintes in-situ mesurées 593 m sous le niveau de la mer, à la mine Lingan, sont relativement plus anisotropiques ($\sigma_1/\sigma_3 \cong 2.8$). La contrainte principal majeure (σ_1) est presqu'horizontal et est orientée approximativement dans l'axe Est-Ouest. La contrainte principale minimum (σ_3) est inclinée, possédant un pendage de 55° vers le Sud. La contrainte principale intermédiaire (σ_2) est orientée Nord-Sud et possède un pendage de 35° vers le Nord.

Ce système de contraintes semble avoir été influencé par une structure monoclinale de direction Est-Ouest dans laquelle les essais furent effectués.

Les essais par la méthode d'hydrofracture furent réalisés à chacune des mines dans des trous de sonde horizontaux et verticaux. A la mine Prince, des fractures verticales distinctes furent developpées dans certaines zones d'essais. Les contraintes in-situ horizontales furent interprétées au moyen des pressions de rupture et résiduelle, de la resistance assumée en tension de la roche et des pressions interstitielles. La contrainte horizontale minimum est raisonnablement en accord avec les résultats des essais par surforage. Les contraintes in-situ verticales furent évaluées au moyen d'essais où des fractures horizontales furent induites. Elles sont en accord avec les contraintes dérivées de l'épaisseur de la couverture rocheuse.

A la mine Lingan, seulement des fractures horizontales furent induites dans les trous de sonde verticaux et horizontaux. Dans plusieurs cas, la rupture n'a pas eu lieu dans le massif de siltstone à des niveaux de pression variants entre 20 et 30 MPa. Là où les fractures horizontales furent induites, les contraintes verticales ont été déterminées. La contrainte verticale moyenne est inférieure à la contrainte dérivée de l'épaisseur de la couverture rocheuse.

Les données relatives aux mesures de contraintes in-situ dans les différentes mines du bassin de Sydney sont résumées. Les résultats indiquent que les contraintes in-situ augmentent avec la profondeur. La contrainte principale majeure est générallement horizontale et orientée dans l'axe Est-Ouest. Le système de contraintes horizontales est modérément isotropique à la houillère No. 26 et aux mines Princes et Donkin Morien. Les contraintes verticales, à toutes les mines, correspondent bien à la contrainte causée par la couverture rocheuse.

TABLE OF CONTENTS

Page No.

ABSTRACT i

1.0 INTRODUCTION 1

2.0 DESCRIPTION OF TEST SITES 2

- 2.1 Prince Mine 2
  - 2.1.1 Location of Test Site 2
  - 2.1.2 Geology 2
- 2.2 Lingan Mine 3
  - 2.2.1 Location of Test Site 3
  - 2.2.2 Geology 4

3.0 INSITU STRESS MEASUREMENT PROGRAMS 5

- 3.1 Test Program for Prince Mine 5
  - 3.1.1 Overcoring Tests 5
  - 3.1.2 Hydrofracture Tests 6
  - 3.1.3 Laboratory Testing 6
- 3.2 Test Program for Lingan Mine 6
  - 3.2.1 Overcoring Tests 7
  - 3.2.2 Hydrofracture Tests 7
  - 3.2.3 Laboratory Testing 8

4.0 OVERCORING TECHNIQUE FOR STRESS MEASUREMENT 9

- 4.1 General Testing Procedure 9
- 4.2 USBM Deformation 9
- 4.3 Biaxial Testing Equipment 10
- 4.4 Drilling Equipment 10
- 4.5 Certification of Testing Equipment 11
- 4.6 Method of Analysis 11

5.0 HYDROFRACTURE TECHNIQUE FOR STRESS MEASUREMENT 13

- 5.1 Hydrofracture Theory 13
  - 5.1.1 Fracture Initiation 13
  - 5.1.2 Fracture Propagation 17
- 5.2 Application of the Hydrofracture Theory to In Situ Stress Determination 18
  - 5.2.1 Initial Fracture 18
  - 5.2.2 Shut-In 19
  - 5.2.3 Refracture 20

TABLE OF CONTENTS (Cont.)

Page No.

- 5.3 Hydrofracture Equipment 22
  - 5.3.1 Straddle Packer 22
  - 5.3.2 Pumping Equipment and Accessories 22
  - 5.3.3 Data Logging 22
  - 5.3.4 Impression Packer 23
- 5.4 Hydrofracture Test Procedures 23
  - 5.4.1 Method of Testing 23
    - 5.4.1.1 Selection of Test Zones 23
    - 5.4.1.2 Installation and Testing of Straddle Packer 24
    - 5.4.1.3 Hydrofracture Test Procedure 26
  - 5.4.2 Data Acquisition 27
  - 5.4.3 Data Analysis 28
    - 5.4.3.1 Test Zone Pressure 28
    - 5.4.3.2 Analysis of Shut-In 28
    - 5.4.3.3 Pressure/Flow Rate Relation 28
    - 5.4.3.4 Determination of the Minimum Horizontal Principal Stress 29
    - 5.4.3.5 Tensile Strength 29
    - 5.4.3.6 Groundwater Pressure 30
  - 5.4.4 Impression Packer 31

6.0 TEST RESULTS FROM PRINCE MINE 32

- 6.1 Overcoring Test Results 32
  - 6.1.1 Overcoring Tests 32
  - 6.1.2 Biaxial Tests 33
  - 6.1.3 Laboratory Tests 34
  - 6.1.4 Evaluation of In Situ Stresses 35
- 6.2 Hydrofracture Test Results 36
  - 6.2.1 Test Data 36
  - 6.2.2 Interpretation of In Situ Stresses from Hydrofracture Test Data 44
    - 6.2.2.1 Classic Hydrofracture Response 45
    - 6.2.2.2 Multiple Hydrofracture Responses 46
    - 6.2.2.3 Fracture of Incipient Weaknesses 47

TABLE OF CONTENTS (Cont.)

Page No.

6.2.2.4 Re-opening of Existing Fractures 48
6.2.3 Summary 48
6.3 Comparison of Stresses Measured by Overcoring and Hydrofracture Tests 49

7.0 TEST RESULTS FROM LINGAN MINE 52

7.1 Overcoring Test Results 52
7.1.1 Overcoring Tests 52
7.1.2 Biaxial Tests 53
7.1.3 Laboratory Tests 54
7.1.4 Evaluation of In Situ Stresses 54
7.2 Hydrofracture Test Results 56
7.2.1 Test Data 56
7.2.2 Interpretation of In Situ Stresses from Hydrofracture Test Data 67
7.2.2.1 Tests in which No Breakdown Occurred 68
7.2.2.2 Tests in which Breakdown Occurred 68
7.2.3 Summary 69

7.3 Comparison of Stresses Measured by Overcoring and Hydrofracture Tests 69

8.0 REGIONAL STRESS DISTRIBUTION IN THE SYDNEY COALFIELD 71

9.0 CONCLUSIONS 73

10.0 ACKNOWLEDGEMENTS 77

LIST OF TABLES

1. Summary of Positions of USBM Overcoring Tests - Prince Mine

2. Summary of Positions of USBM Overcoring Tests - Lingan Mine

3. Magnitudes and Directions of Secondary Principal Stresses Measured from Overcoring Tests - Prince Mine

4. Summary of Biaxial Test Results - Prince Mine

5. Stress Tensor Calculated by Least Squares Solution - Prince Mine

6. Results of Hydrofracture Tests - Prince Mine

7. Magnitudes and Directions of Secondary Principal Stresses Measured from Overcoring Tests - Lingan Mine

8. Summary of Biaxial Test Results - Lingan Mine

9. Stress Tensor Calculated by Least Squares Solution - Lingan Mine

10. Results of Hydrofracture Tests - Lingan Mine

11. Stresses Measured at Different Mines in the Sydney Coalfield

APPENDIX E

E1-1 Uniaxial Compressive Strength Tests - Prince Mine
E1-2 Multistage Triaxial Test Results - Prince Mine
E1-3 Laboratory Tensile Strength Tests - Prince Mine
E2-1 Uniaxial Compressive Strength Tests - Lingan Mine
E2-2 Multistage Triaxial Test Results - Lingan Mine
E2-3 Laboratory Tensile Strength Tests - Lingan Mine

LIST OF FIGURES

1. Site Location Map

2. Site for In Situ Stress Measurement - Prince Mine

3. Site for In Situ Stress Measurement - Lingan Mine

4. Plan Showing Locations of Boreholes for In Situ Stress Measurements - Prince Mine

5. Plan Showing Locations of Boreholes for In Situ Stress Measurements - Lingan Mine

6. Stress Measurement by Overcoring Method

7. Pressure vs. Time - Record of an Idealized Hydrofracture Test

8. Schematic Layout of Hydrofracture Test Equipment

9. Straddle Packer Assembly for Hydrofracture Tests

10. Principal Stress Directions Measured in Sydney Coalfield

11. Stress Components Measured in Different Mines in the Sydney Coalfield

APPENDIX B

B1-1 In Situ Stress Measurement - Prince Mine - USBM Test No. P101

B1-2 In Situ Stress Measurement - Prince Mine - USBM Test No. P104

B1-3 In Situ Stress Measurement - Prince Mine - USBM Test No. P201

B1-4 In Situ Stress Measurement - Prince Mine - USBM Test No. P202

B1-5 In Situ Stress Measurement - Prince Mine - USBM Test No. P301

B1-6 In Situ Stress Measurement - Prince Mine - USBM Test No. P302

LIST OF FIGURES (Cont.)

APPENDIX B (Cont.)

B1-7 In Situ Stress Measurement - Prince Mine - USBM Test No. P401

B1-8 In Situ Stress Measurement - Prince Mine - Biaxial Test No. P103B1

B2-1 In Situ Stress Measurement - Lingan Mine - USBM Test No. L102

B2-2 In Situ Stress Measurement - Lingan Mine - USBM Test No. L103

B2-3 In Situ Stress Measurement - Lingan Mine - USBM Test No. L203

B2-4 In Situ Stress Measurement - Lingan Mine - USBM Test No. L204

B2-5 In Situ Stress Measurement - Lingan Mine - USBM Test No. L301

B2-6 In Situ Stress Measurement - Lingan Mine - USBM Test No. L303

B2-7 In Situ Stress Measurement - Lingan Mine - USBM Test No. L501

B2-8 In Situ Stress Measurement - Lingan Mine - Biaxial Test No. L102B1

APPENDIX C

C1-1 Hydrofracture Test Results - Prince Mine - BH P-3 Test 1, P-5 Test 1

C1-2 Hydrofracture Test Results - Prince Mine - BH P-4 Tests 1 to 6

C1-3 Hydrofracture Pressure/Flow Test - Prince Mine - BH P-4 Test No. 1

C1-4 Hydrofracture Pressure/Flow Test - Prince Mine - BH P-4 Test No. 3

C1-5 Hydrofracture Pressure/Flow Test - Prince Mine - BH P-4 Test No. 4

LIST OF FIGURES (Cont.)

APPENDIX C (Cont.)

C1-6 Hydrofracture Pressure/Flow Test - Prince Mine - BH P-4 Test No. 6

C1-7 Hydrofracture Pressure/Flow Test - Prince Mine - BH P-3 Test No. 1

C1-8 Hydrofracture Pressure/Flow Test - Prince Mine - BH P-5 Test No. 1

C2-1 Hydrofracture Test Results - Lingan Mine - BH L-3 Tests 1 and 2

C2-2 Hydrofracture Test Results - Lingan Mine - BH L-4 Tests 1 and 2

C2-3 Hydrofracture Test Results - Lingan Mine - BH L-4 Tests 3 to 9

C2-4 Hydrofracture Test Results - Lingan Mine - BH L-5 Tests 1 and 2

C2-5 Hydrofracture Pressure/Flow Test - Lingan Mine - BH L-3 Test No. 1

C2-6 Hydrofracture Pressure/Flow Test - Lingan Mine - BH L-3 Test No. 2

C2-7 Hydrofracture Pressure/Flow Test - Lingan Mine - BH L-4 Test No. 1

C2-8 Hydrofracture Pressure/Flow Test - Lingan Mine - BH L-4 Test No. 2

C2-9 Hydrofracture Pressure/Flow Test - Lingan Mine - BH L-4 Test No. 3

C2-10 Hydrofracture Pressure/Flow Test - Lingan Mine - BH L-4 Test No. 4

C2-11 Hydrofracture Pressure/Flow Test - Lingan Mine - BH L-4 Test No. 5

C2-12 Hydrofracture Pressure/Flow Test - Lingan Mine - BH L-4 Test No. 6

C2-13 Hydrofracture Pressure/Flow Test - Lingan Mine - BH L-4 Test No. 7

LIST OF FIGURES (Cont.)

APPENDIX C (Cont.)

C2-14 Hydrofracture Pressure/Flow Test - Lingan Mine - BH L-4 Test No. 8

C2-15 Hydrofracture Pressure/Flow Test - Lingan Mine - BH L-4 Test No. 9

C2-16 Hydrofracture Pressure/Flow Test - Lingan Mine - BH L-5 Test No. 1

C2-17 Hydrofracture Pressure/Flow Test - Lingan Mine - BH L-5 Test No. 2

APPENDIX D

D-1 Co-ordinate Systems for Evaluation of In Situ Stresses

LIST OF PLATES

1. (a) USBM Deformation Gauge
(b) Set-Up for Biaxial Test

2. (a) General Arrangement of Drill Rig at Prince Mine
(b) General Arrangement of Drill Rig at Lingan Mine Showing Hydrofracture Equipment

3. (a) Hydrofracture Straddle Packer Assembly
(b) Hydrofracture Perforated Mandrel

4. (a) Hydrofracture Test Zone and Packer Inflation Pumps
(b) Hydrofracture Chart Recorder and Pressure Transducer

5. Hydrofracture Impression Packer with Typical Fracture Trace Shown

LIST OF APPENDICES

A. Borehole Records

B. Overcoring Test Results

C. Hydrofracture Results

D. Procedure for Evaluation of In Situ Stresses from Overcoring Test Data

E. Laboratory Test Results

F. Specialized Drilling Equipment for Overcoring

G. Nomenclature

1.0 INTRODUCTION

Prince and Lingan Mines are two coal mines currently in production in the Sydney coalfield. They are owned and operated by the Cape Breton Development Corporation (CBDC) in Sydney, Nova Scotia.

Golder Associates was awarded a contract under the auspices of CANMET through Supply and Services Canada (DSS Contract No. 06SQ.23440-5-9004) to undertake a program of in situ stress determinations at Prince and Lingan Mines using the method of overcoring (with the USBM deformation gauge) and hydraulic fracturing (hydrofracture) techniques. The Cape Breton Development Corporation contributed geological and mine services as well as a driller's helper.

Previous in situ stress measurements at the No. 26 Colliery and Donkin Morien Mines also in the Sydney coalfield, have been carried out by Golder Associates on behalf of the Cape Breton Coal Research Laboratory (CBCRL) of CANMET. This report presents the results of the testing programs at Prince and Lingan Mines and discusses the regional in situ stresses encountered in the Sydney coalfield.

2.0 DESCRIPTION OF TEST SITES

The test sites for the in situ stress measurement program were selected jointly with CANMET and CBDC. They are located at sufficient distances from the active mining areas, so that the measured stresses were not influenced by other current or historical mining activity. Geological data available for each of the test sites was provided by the Cape Breton Development Corporation prior to testing.

2.1 Prince Mine

2.1.1 Location of Test Site

Prince Mine is a sub-sea coal mine located at Point Aconi, near North Sydney, Nova Scotia (see Figure 1). The mining development area extends approximately 3 km offshore in a northerly direction.

The test site was located approximately 30 m from the end of the No. 4 deep development (September 1985) at a depth of about 222 m below sea level (Figure 2). The floor of the deep coincides with the base of the workable coal seam (Hub Seam) which is approximately 2.2 m thick and dips gently to the north at 3 to 5 degrees.

2.1.2 Geology

The coal measures sequence immediately overlying and underlying the workable coal seam comprises a series of mudstones, siltstones and sandstones interbedded with subsidiary coal seams. Based on geological data provided by CBDC, a major fault trending in a northeast orientation and located about 3.4 km northwest of the test site was reported to be present. This fault is considered to be an extension of the onshore "Mountain" fault.

The dominant structure/fabric evident from the boreholes is the bedding although a few bedding plane fractures were observed. The majority of the breaks in the core were drilling induced.

The mudstone is thinly bedded, occasionally laminated, and silty. The more silty beds tend to be stronger and the less silty horizons, weaker and laminated.

The siltstone or fine grained sandstone locally has thin carbonaceous bands parallel to the bedding.

The coarse to medium grained sandstone has a few carbonaceous bands.

The coal has frequent joints and cleats.

The geological borehole logs of the test holes, as compiled by CBDC are given in Appendix A.

2.2 Lingan Mine

2.2.1 Location of Test Site

Lingan Mine is a sub-sea coal mine located near New Waterford, Nova Scotia (see Figure 1). The mining development area extends approximately 3.5 km offshore in a near northerly direction.

The test site is located on the top level of the 7 west panel (Figure 3). The level was developed 62.5 m to the west from the centreline of the No. 1 slope for the purposes of this program. The test site is located at a depth of 590 m below sea level. The material level is a 5.2 m (17 ft.) wide arched roadway approximately 3.7 m high and excavated with the floor of the roadway coinciding with the base of the coal seam. The workable coal seam (Harbour seam) is approximately 1.8 m thick and dips at about 13 per cent to the north.

2.2.2 Geology

The coal measures sequence immediately overlying and underlying the workable coal seam comprises a series of mudstones, siltstones and sandstones interbedded with subsidiary coal seams. Based on the geological data provided by CBDC, the test site is located on the up-dip limb of a regional monocline which strikes approximately east-west. Approximately 1500 m down-dip from the test site, the strata are projected to be at the steepest dip about 38 percent. At 2400 m up-dip from the test site, the dip of the strata is 20 percent. Hence there is a slight roll in the strata and it is apparent that the dip is gradually increasing towards the north.

The dominant structure/fabric evident from the boreholes is the bedding, although a few bedding plane fractures were observed, as were intraformational shears in the more muddy horizons. The shear planes were particularly evident in the 0.3 m thick band of muddy siltstone immediately overlying the coal seam. Two main sets of shear planes were observed at 38°/274° (dip/dip direction) and 50°/102°.

The mudstone is thinly bedded, occasionally laminated.

The siltstone or fine grained sandstone locally has thin carbonaceous bands parallel to the bedding. Some core discing was noted over a 0.15 m section in the siltstone between 4.3 and 11 m depth in Borehole L3.

The coarse to medium grained sandstone has a few carbonaceous bands.

The coal has frequent joints and cleats.

The geological borehole logs of the test holes, as compiled by CBDC are given in Appendix A.

3.0 IN SITU STRESS MEASUREMENT PROGRAMS

3.1 Test Program for Prince Mine

The field testing program at Prince Mine commenced on September 24, 1985 and was completed on November 6, 1985. Five test boreholes were drilled for in situ stress determinations. Overcoring tests using the USBM deformation gauge were carried out in four of the holes; P1, P2, P3 and P4. Hydrofracture stress measurements were carried out in three holes, P3, P4 and P5. The locations of the boreholes are shown in Figure 4. Details of the orientations and depths of the boreholes are given in Table 1. The boreholes were logged by CBDC geologists and the records are presented in Appendix A.

3.1.1 Overcoring Tests

Overcoring tests using the USBM deformation gauge were carried out first in Boreholes P1 to P4 starting from a location about 10 m from the collar of each hole. For each hole a minimum of two successful USBM tests were carried out to determine the secondary principal stresses P and Q. These tests were conducted in the siltstone unit immediately overlying the coal seam. Table 1 summarizes the overcoring test positions. To allow a statistical evaluation of the complete stress tensor, the holes were drilled in different orientations as shown in Figure 4.

After completion of the USBM tests in Borehole P1 the hole was extended to a depth of 24.08 m (79 ft) in an attempt to intersect a different strata suitable for USBM tests. The hole intersected a mudstone layer at a depth of 22 m which was too broken to attempt any USBM tests.

After the USBM testing in the vertical downhole P4, this borehole was extended to 30 m for hydrofracture testing.

3.1.2 Hydrofracture Tests

Hydrofracture tests were carried out in Boreholes P3, P4 and P5. Borehole P4, being in the vertical direction intersected different rock units and was used for a major part of the hydrofracture tests. Six tests were carried out in P4 with one test each in the near horizontal holes P3 and P5. Table 6 summarizes the test locations.

3.1.3 Laboratory Testing

Biaxial tests were carried out at the CANMET laboratory on overcore samples recovered from each of the USBM tests, to determine the modulus of the rock. It was noted that the rock exhibited anisotropic deformation behaviour and further testing was carried out on the overcore specimens in Golder Associates laboratory, in Mississauga.

A number of HQ core samples from each of the rock types encountered were sent to the CANMET Mining Research Laboratory in Ottawa, for testing. These tests included Uniaxial compression, Triaxial and Brazilian (Tensile) Tests. A summary of these tests is shown in Appendix E.

3.2 Test Program for Lingan Mine

The start-up of the field testing program for Lingan Mine was delayed due to problems associated with the drill motor. The program commenced on January 16, 1986 and was completed on February 21, 1986. Five test boreholes were drilled for in situ stress determinations. Overcoring tests using the USBM deformation gauge were carried out in four of the holes, L1, L2, L3 and L5. Hydrofracture stress measurements were carried out in three holes, L3, L4 and L5. The location of the boreholes is shown in Figure 5. Details of the orientation and depth of the boreholes are given in Table 2. The boreholes were logged by CBDC geologists and the records are presented in Appendix A.

3.2.1. Overcoring Tests

Overcoring tests using the USBM deformation gauge were carried out first in Boreholes L1 to L3 from a location about 10 m from the collar of each hole. For each hole, except L4, a minimum of two successful USBM tests were carried out to determine the secondary principal stresses P and Q. Table 2 summarizes the overcoring test positions. To allow a statistical evaluation of the complete stress tensor, the holes were drilled in different orientations as shown on Figure 5.

After completion of the USBM tests in Borehole L1, the hole was extended to a depth of 30.4 m (100 ft) in an attempt to intersect a different strata that could be tested. No suitable locations for USBM tests were intersected.

The vertical downholes L4 and L5 were drilled to 31.29 and 25.3 m respectively. USBM tests were carried out only in Borehole L5.

3.2.2 Hydrofracture Tests

Hydrofracture tests were carried out in the two vertical Boreholes, L4 and L5, and the near horizontal hole L3. A total of 15 tests were attempted, two in L3, nine in L4 and four in L5. Table 10 summarizes the test locations.

3.2.3 Laboratory Testing

Biaxial tests were carried out on overcore samples recovered from each of the USBM tests to determine the modulus of the rock. Further testing was also carried out on the overcore samples in Golder Associates laboratory, Mississauga to investigate the anisotropic deformation behaviour of the rock.

A number of HQ core samples from each of the rock types encountered were also sent to the CANMET Mining Research Laboratory in Ottawa, for further laboratory testing. These tests included Uniaxial compression, Triaxial and Brazilian (Tensile) Tests. A summary of these tests are shown in Appendix E.

4.0 OVERCORING TECHNIQUE FOR STRESS MEASUREMENT

4.1 General Testing Procedure

The method of overcoring used for in situ stress determination was developed by the United States Bureau of Mines (USBM) (Hooker and Bickel 1974). The field techniques have been modified to suit the present program.

The general procedure of the overcoring method is illustrated on Figure 6. A 100 mm diameter (H size) hole was drilled to about 250 mm short of the required location for the stress measurement test. A 38 mm diameter (EX size) pilot hole (approximately 600 mm in length) concentric with the 100 mm diameter hole was drilled through the test position. The USBM deformation gauge was then installed in the pilot hole in an area free of joints or fractures, normally at 200-300 mm from the end of the 100 mm diameter hole. The pilot hole was then overcored using a 100 mm diameter thin-walled coring bit to relieve the stresses around the pilot hole. The corresponding changes in the diametral deformations in the pilot hole were monitored during overcoring using the USBM deformation gauge connected to a digital strain indicator, and a switch and balance unit. The stresses were evaluated from the measured changes in the deformation, and the deformation modulus determined by testing the overcored rock specimen. Details of the procedures for the evaluation of the principal stresses are presented in Appendix D.

4.2 USBM Deformation Gauge

The USBM deformation gauge is designed to measure the changes in the deformation of the pilot hole across three diameters (spaced 120° apart). The gauge has three pairs of buttons which provide contact between the surface of the pilot hole and the sensing element of the gauge. Continuous observation of the borehole deformation changes can be made during overcoring. This instrument enables the measurement of the two-dimensional stress field on a plane normal to the axis of the drillhole. Details of this instrument and the operational procedure have been described by Hooker and Bickel (1974).

4.3 Biaxial Testing Equipment

The deformation modulus of the rock at the test position was determined using a "biaxial test cell", the set up of which is shown on Plate 1. The cell essentially consists of a cylindrical steel jacket and seals. The overcored rock specimen recovered from the test position is tested in the cell with the USBM gauge inside the specimen. Hydraulic oil is pumped into the space between the steel jacket and the sealed membrane which is in contact with the overcore. The outer surface of the overcore is therefore subjected to a uniformly distributed radial (biaxial) pressure. During modulus testing, the deformations of the inner hole of the overcore are monitored at various pressure increments and decrements.

4.4. Drilling Equipment

The stress measurement boreholes were drilled using a Longyear 38 underground drill supplied to the project by the Cape Breton Development Corporation. The general arrangements of the drill rig at the Prince and Lingan Mine sites are shown on Plate 2.

Standard HQ wireline equipment was used for drilling the H size borehole with specialized ancillary drilling equipment to facilitate the drilling of the pilot hole and the overcoring operation. A list of the specialized drilling equipment and an outline of the procedure in using this equipment is given in Appendix F.

4.5 Certification of Testing Equipment

In compliance with the statutory requirements of the Coal Mines (CBDC) Safety Regulations, all electrical equipment (including their circuitries) and installation tools used for overcoring stress measurements have been certified by the Mining Research Laboratories of CANMET. This set of equipment was also approved by Labour Canada (Sydney).

4.6 Method of Analysis

The interpretation of the overcoring test data is based on the assumption that the rock is homogeneous and linearly elastic. Two interpretation procedures are considered in this report:

a) Evaluation of the secondary principal stresses on a plane perpendicular to the axis of the borehole using isotropic theory and assuming that the stress changes during overcoring occur under plane strain conditions.

b) Evaluation of the complete three-dimensional stress system by pooling all the data and using the least squares solution for the complete stress tensor. The orientations of the boreholes, diametral deformations and the effects of anisotropic deformation modulus are all taken into account in this interpretation.

Details of the evaluation of the principal stresses by both methods are given in Appendix D. In both cases, the diametral deformation, rock deformation modulus (calculated from Biaxial Tests) and Poisson's Ratios are used for the analysis.

The results include:

- The six independent stress components σx, σy, σz, τxy, τyz and τzx with respect to magnetic north (x, y and z correspond to EW, NS and vertical directions respectively).
- The standard deviations of the stress components and the correlation coefficient of the multilinear regression analysis in the least squares solution.
- The magnitudes and directions of the three principal stresses based on the average values of the six stress components.

5.0 HYDROFRACTURE TECHNIQUE FOR STRESS MEASUREMENT

5.1 Hydrofracture Theory

5.1.1 Fracture Initiation

General concepts for determining the triaxial state of in situ stress by the hydrofracture method have been outlined by Hubbert and Willis (1957), Haimson and Fairhurst (1967) and many subsequent authors.

In essence, the method assumes that the borehole is parallel to one of the principal stresses. It is generally accepted that, except in areas of extreme relief, the vertical stress is a principal stress, so that in the case of a vertical borehole, this assumption is valid. The other two principal stresses are therefore horizontal and may be termed $_H$ and $_h$. Plane strain conditions are applicable and the analysis may be considered in two dimensions.

The principal field stresses are modified by the presence of the borehole according to elastic theory (e.g. Savin, 1961). The modified principal stresses on the borehole wall may be termed σ_θ and σ_r where:

$$\sigma_r = 0$$

$$\sigma_\theta = (\sigma_h + \sigma_H) - 2(\sigma_h - \sigma_H) \cos 2\theta \qquad (5\text{-}1)$$

so that the minimum tangential stress is

$$\sigma_{\theta\ (min)} = 3\ \sigma_h - \sigma_H \qquad (5\text{-}2)$$

at $\theta = 90$, i.e. at the same azimuth as the maximum horizontal principal field stress.

where σr is the radial stress
σ_θ is the tangential stress
σh is the minimum horizontal principal stress
σH is the maximum horizontal principal stress

If the sealed off interval of the borehole is pressurized with fluid, then, assuming no fluid penetration in a non-porous rock material, the stress changes induced on the borehole wall by the fluid pressure (P) are:

$$\Delta \sigma_\theta = -P$$
$$\Delta \sigma_r = P \qquad (5\text{-}3)$$

The vertical stress on the borehole wall is equivalent to the vertical field stress modified by small Poisson's ratio effects due to the horizontal stress changes caused by the presence of the borehole. The vertical stress is not modified by the fluid pressure except near the ends of the interval through deformation of the packers.

Summing the stresses on the borehole wall (Equations 5-2 and 5-3) gives:

$$\sigma_r = P$$

$$\sigma_\theta \text{ (min)} = 3\,\sigma h - \sigma H - P \qquad (5\text{-}4)$$

If the stress on the borehole wall at any point is less (with compression + ve sign convention) than the tensile strength of the rock applicable under these conditions at that point, a rupture will occur or an existing fracture will be opened.

The vertical stresses induced through deformation of the soft rubber packers on the borehole wall rarely result in fracture (Haimson, 1978).

Thus when $\sigma_\theta \leqq - T$ (5-5)

where T is the hydrofracturing tensile strength of the rock (expressed as a positive number) at which rupture occurs through the intact rock or an existing fracture is opened.

Assuming the rock is homogeneous and isotropic with respect to the tensile strength, rupture occurs when

$$\sigma_\theta \text{ (min)} \leqq - T \tag{5-6}$$

Combining equation (5-4) and (5-6) results in the formula

$$P \geqq 3\sigma h - \sigma H + T \tag{5-7}$$

for the rupture

or $$P_c = 3\sigma h - \sigma H + T \tag{5-8}$$

where P_c is the critical fluid pressure for rupture.

The rupture will result in a fracture initiating as a vertical plane parallel to the maximum horizontal principal stress.

If the rock material is now considered to be porous, but not permeable, and contains a fluid under pressure, effective stresses must be used. Thus equation (5-8) becomes:

$$(P_c - P_p) = 3(\sigma_h - P_p) - (\sigma_H - P_p) + T \tag{5-9}$$

where P_p is the pore water pressure

which reduces to:

$$P_c = 3\sigma h - \sigma H - P_p + T \tag{5-10}$$

However, this simple equation for effective stress is valid only if the compressibility of the bulk material is much greater than the matrix compressibility (Bishop, 1953). In rocks, this is not likely to be the case and the more correct form of the equation is given by:

$$(P_c - \alpha P_p) = 3(\sigma_h - \alpha P_p) - (\sigma_H - \alpha P_p) + T \qquad (5\text{-}11)$$

$$\text{where } \alpha = 1 - \frac{C_v}{C_b}$$

where C_v = coefficient of rock matrix compressibility
C_b = coefficient of rock bulk compressibility.

Haimson and Fairhurst (1967) further extended the analysis to account for fluid penetration of a permeable material when the borehole is pressurised and proposed the formula:

$$P_c - P_p = \frac{3\sigma h - \sigma H + T - 2P_p}{K} \qquad (5\text{-}12)$$

$$\text{where } K = 2 - \alpha \frac{(1 - 2\ )}{1 -\ }$$

and therefore $1 \leqq K \leqq 2$

where ν is Poisson's ratio.

However, when the rock material is not porous or permeable $\alpha \rightarrow 0$, $K \rightarrow 2$ and $P_p \rightarrow 0$, so that Equation (5-12) is difficult to reconcile with Equation (5-8). However, K values are reported to be close to 1 in field tests (Haimson, 1978).

A formula may be derived in terms of fracture mechanics criteria (Abou-Sayed and Brechtel, 1978), but provided the tensile strength is determined under the same conditions of hydraulic fracture, the calculations will reduce to the above formulae.

5.1.2 Fracture Propagation

As the fracture propagates away from the borehole, the influence of the borehole on the stress field rapidly diminishes. Fracture mechanics considerations indicate that the stress concentration at the fracture tip will allow the fracture to continue to propagate provided that the fluid pressure within the fracture remains sufficiently in excess of the field stress normal to the fracture to keep the fracture open; and that the plane of propagation is the one which minimises the potential energy involved in keeping the fracture open (e.g. Abou-Sayed and Brechtel, 1978).

In a homogeneous, isotropic rock mass the fracture will therefore propagate in the plane perpendicular to the minimum principal stress provided that the pressure in the fracture is in excess of that minimum principal stress.

It is possible that the initial fracture will propagate along the borehole, eventually bridging the seals to the test section. It is not clear to what extent the stress concentration at the ends of the test section will affect the propagation of the fracture along the borehole wall and influence the shape of the fracture.

When the minimum principal field stress is vertical instead of horizontal, it is considered that where the fracture is initiated in the vertical plane it will tend to rollover so that it eventually propagates perpendicular to the minimum (vertical) principal stress (Zoback and Pollard, 1978).

5.2 Application of the Hydrofracture Theory to In Situ Stress Determination

Application of the above theory to determine the stresses in an isotropic rock is described by Haimson (1973). The sealed off section of the borehole is pressurized by pumping fluid into it to determine the value of P_c, the critical fluid pressure for rupture and hence, development of the initial fracture. Pumping then ceases and the fluid is shut-in. The fracture continues to propogate until the fluid pressure falls below the normal stress across the fracture; the shut-in pressure in the borehole is then constant or falls more slowly due to leakage. Refracture tests may be made to confirm the value of the shut-in pressure. A pressure time record of an idealised test is shown in Figure 7.

The shut-in pressure is assumed to represent the minimum principal stress and the maximum principal stress may then be calculated by application of equations (5-8), (5-10) or (5-12) as appropriate.

These stages in the test are now discussed critically in the light of later published work.

5.2.1 Initial Fracture

The equipment used in the field does not constitute a stiff testing system and energy is stored due to volumetric compression of the hydrofracture fluid and volume changes of the equipment. This results in the fracture being propagated uncontrollably some distance from the borehole immediately after initial breakdown. Assuming a fracture width of 1 mm and typical loss of water of 1 litre at 100 m test depth indicates that for the proposed testing system the fracture typically would propagate for an area of one square metre around the initiation point due to this stored energy.

The rate of pumping before initiation of the fracture also may have some influence on the pressure recorded at breakdown depending on crack propagation velocity, fluid pressure wave velocity and location of the transducer.

As pumping continues, the fluid pressure in the borehole falls to a value dependant upon the rate of pumping. Crack propagation continues as long as this pressure is slightly in excess of the field stress normal to the fracture at its extremity, (Hickman and Zoback, 1982) allowing for small viscous flow losses and the small amount of energy required to propagate the fracture.

5.2.2 Shut-In

If pumping is stopped and the fluid in the system is now shut-in, the pressure will decay rapidly as the fracture propagates until this pressure equals the field stress normal to the fracture. At this point, the pressure in a closed system should remain constant, but under field conditions generally continues to decay at a reduced rate towards the hydrostatic pressure. This is due to leakage past the packers; flow to the natural fracture system of the rock mass; and in some cases through the natural permeability of the rock (McLennan and Roegiers, 1982). Thus, it is frequently difficult to determine the shut-in pressure with confidence and several methods of analysis, such as the semi-log plot of pressure against time (Doe, 1982), the Muskat method (Aamodt and Kuriyagawa, 1982), and the tangent divergence method (Enever and Wooltorton, 1982) have been proposed. It has also been noted that, in some circumstances, the shut-in pressure decays over several cycles of reopening the fracture. In order to determine the field stress normal to the fracture, several authors advocate different approaches to evaluating the shut-in pressure Zoback & Pollard, (1978) suggest that the initial shut-in pressure gives the field stress normal to the fracture; subsequent shut-ins asymptotically approach the minimum in situ stress. Barton (1982) suggests taking the average of first shut-in and minimum shut-in, and Gronseth and Kry (1982) suggest taking cycle 4 shut-in.

It is thus apparent that the shut-in is not an entirely definitive method of determining the minimum in situ stress. In particular, it is difficult to understand the mechanism whereby the shut-in pressure decays noticeably over several cycles of reopening the fracture since it is considered that the normal stress across the fracture near the borehole should dominate the shut-in response especially if this is greater than the stress across the fracture further away. A possible explanation of this phenomenon could be self propping or initial shear failure giving access to a correctly aligned fracture further into the rock mass.

5.2.3 Refracture

If the fluid pressure is released, the fracture should close and a refracture test may be made. Several authors following Bredehoeft et al (1976) consider the difference in peak pressure between the initial fracture and the refracture to be equal to the tensile strength of the rock. However Doe (1982) notes that, if the ratio of horizontal stresses ($\sigma h/\sigma H$) is greater than 2, the stress concentration at the borehole wall by the fracture is less than the minimum principal stress,

i.e.: $3\sigma h - \sigma H < \sigma h$

which implies $\sigma H/\sigma h > 2$

and the fracture will not completely reopen until the pressure exceeds the minimum horizontal principal stress. Zoback and Pollard, (1978) however, report that the opening pressure may be noted if sufficiently low flow rates are used.

Where the principal stress ratio is less than 2, a slightly propped fracture will still have a finite conductivity and, if the pumping rate is slow enough, may still open at a pressure equivalent to or greater than the minimum principal stress, but less than the stress concentration on the borehole wall.

It is, therefore, considered that the refracture does not provide a reliable value of the tensile strength, which must be determined by laboratory hydrofracture tests on hole sizes of a comparable magnitude (Rummel and Winter, 1981) or by fracture mechanics analysis (Ratigan, 1982; Doe, 1982). Where the ratio of horizontal principal stresses perpendicular to the borehole wall exceeds 2, the refracture pressure should provide a clearly defined value of the minimum principal stress.

Step-wise refracture has been used (Rummel, et al 1982; Pine et al, 1983b) which when plotted as a graph of flow rate against pressure indicates a clearly defined breakpoint at fracture reopening. It is suggested that even for horizontal stress ratios of less than 2, the step-wise refracture tests may provide a better determination of the principal stress than the shut-in. Even when the hydraulic fracture breaks into the natural fracture system or changes orientation away from the borehole it is considered that the conductivity of the system will be dominated by the behaviour of the fracture adjacent to the borehole. Stepwise pressure/flow tests should therefore still show a breakpoint as the fracture in the region of the borehole opens against the minimum in situ stress. This procedure was used in examining the hydrofracture data in the present program.

5.3 Hydrofracture Equipment

A schematic layout of the hydrofracture equipment used for the hydrofracture tests in the 100 mm diameter holes is shown in Figure 8. This set of equipment was designed and assembled for this project on behalf of the Coal Research Laboratory of CANMET.

5.3.1 Straddle Packer

The double straddle packer was made up from 89 mm (3.5 in) elements supplied by Baker Production Technology (Lynes Petrotech Ltd.) mounted on a specially designed mandrel built by Rock Mechanics Ltd. (Figure 9). Plate 3 shows the straddle packer assembly. The straddle packer was lowered down the hole on a string of BQ rods. Pressure was transmitted to the test zone by pumping water through the rods. A separate high pressure hose (6 mm i.d.) was used for packer inflation.

5.3.2 Pumping Equipment and Accessories

The pumping equipment comprised two air-driven pumps (Plate 4) supplying manifolds connected to the packer and test zone. The two separate manifolds were each fitted with a bypass valve and pressure gauge. A 4.5 kW pump, rated to 69 MPa, fed the manifold connected to the test section and a 0.25 kW pump, also rated to 69 MPa, fed the manifold connected to the packer inflation line. A single crossover connection could be fitted to allow either pump to feed both manifolds. This equipment was housed in two separate units which were designed and constructed by Haskel Energy Systems Ltd.

5.3.3 Data Logging

A strain gauged diaphragm type pressure transducer rated to 69 MPa, and manufactured by Shape Instruments Ltd. was used to measure the pressure in the test zone.

A hard copy graphical output of the test pressure was recorded on a single channel chart recorder (Model MRD 77110) manufactured by Rapco Electronics Ltd. Plate 5 shows the transducer and chart recorder used for this program. Both of these items have been certified by the Mining Research Laboratory of CANMET.

5.3.4 Impression Packer

For this series of tests the impression packer comprised a 72 mm inflatable element and mandrel supplied by Petrometalic Ltd. A separate high pressure hose was used for packer inflation. An impression wrap supplied by Baker Production Technology (Lynes Petrotech Ltd) was fitted to the packer element to record the fracture details in the borehole wall. Plate 6 shows typical traces of the fractures on the impression wrap.

The impression packer was oriented by the USBM installation rods with which it was lowered into the borehole. This gave an estimated orientation accuracy of ± 5°.

5.4 Hydrofracture Test Procedures

5.4.1 Method of Testing

5.4.1.1 Selection of Test Zones

Each of the test boreholes were cored and the core inspected. Test zones were selected by identifying fracture free zones with minimal inherent fabric. The strata encountered comprised a typical coal measures sequence of sandstones, siltstones, mudstones and coal. The arenaceous lithologies frequently had thin carbonaceous bands present. Sections of the borehole with these present or zones with other inherent fabric were avoided where possible. These zones are potential planes of weakness and as such may open preferentially during pressurization because of the possibly lower tensile strength of these planes compared with massive rock. In situ stress determination of fractures along these places of weakness would be limited and is likely to result in confirmation of the overburden stress only.

Sections with minimum length of 1.0 m were selected for testing. Details of the tests carried out at the two mines are given in Sections 6 and 7.

5.4.1.2 Installation and test of Straddle Packer

Each packer element was fitted to the mandrel on surface prior to being taken underground. It was not possible to check the seals in the mandrel, and the seal between the mandrel and the packer element until the equipment was taken underground.

The straddle packer assembly was tested for leaks after it had been lowered into position in the first borehole (Borehole P4) tested at Prince Mine. Leakage into the test zone occurred during the initial inflation of the packers and it was judged that this was occurring where the mandrel screwed into the fixed end of the packer. This allowed water to pass from the annulus between the mandrel and the packer through to the bore of the mandrel and into the test zone. The packer assembly was recovered from the borehole and the leaking joints tightened and sealed with a thread sealant. The packer assembly was checked for leaks at low pressure in the underground roadway and when a satisfactory seal had been achieved, lowered once more to the first test section. The subsequent performance of the straddle packer assembly indicated that an adequate seal had been achieved.

In general, the deepest location in the borehole to be tested was selected first and subsequent tests were carried out by lifting the complete assembly and removing the BQ placement rods where necessary.

The straddle packer was assembled over the hole and the interval between the top connection and the top and bottom of the test zone was recorded. The straddle packer was placed into the hole on uncentralized BQ rods of standard 1.5 m (5 ft.) length or BQ rods 0.61 m (2 ft.) in length were used to facilitate fixing of the wellhead assembly through the chuck of the drilling rig. Rod joints were greased and wrenched tight. The packer inflation line was fixed to each rod with a cable strap. A careful record of the number of rods in the hole was maintained. When the packer assembly reached the test zone depth, the rods were clamped at the borehole collar. To improve safety during testing, the rods were clamped firmly in the chuck of the drilling rig.

To test the straddle packers, the packers were inflated to 8 MPa and this pressure was shut in for a short period. During this time the test zone was pressurized to approximately 3 MPa and a check made to determine the rate of leakage from the test zone. This procedure was generally carried out at the start of each test.

Leakage out of the test zone occurs in two major areas. Firstly, through the rock because of the permeability of the rock or rock mass and secondly, leakage when the water in the test zone by-passes the packers as a result of ineffective 'seating' of the packers.

During testing, the packer pressure was kept 4 to 6 MPa above the test zone pressure by manually operating the regulator on the pump connected to the packers.

For subsequent tests, the packers were deflated and the straddle packer assembly was raised to the next test location and reset. A careful record was kept of the number of placement rods (BQ rods) removed.

5.4.1.3 Hydrofracture Test Procedure

The test procedure was designed to obtain sufficient data to permit interpretation of the test results by different methods of analysis. The key parameters to be measured were:

- initial fracture breakdown pressure;
- first shut-in pressure;
- subsequent refracture breakdown and shut-in pressures;
- pressures at varying flow rates (stepwise refracture test - Pressure flow rate tests)

The tests were therefore conducted in the following general sequence:

First cycle:
  Quick breakdown, new fracture
  Shut-in

Second Cycle:
  Quick breakdown, refracture
  Shut-in

Third Cycle:
  Quick breakdown, refracture
  Shut-in

Step-wise Refracture:
  Constant pressure/flow rate tests

Last Cycle:
  Quick breakdown, refracture
  Shut-in

Further cycles of quick breakdown and shut-in were made if there had been a substantial drop in breakdown pressure between the third and last cycles. The test procedure for the critical stages is outlined as follows:

Quick Breakdown

The pressure in the test section was increased until there was a sudden drop in pressure and increase in flow rate (this behaviour is termed as the breakdown) or until a maximum pressure was reached. To avoid penetration of the fluid into the rock mass and the fracture, the breakdown (if breakdown occurred) was achieved in less than 120 seconds from start of pumping.

Shut-In

Immediately after breakdown and the establishment of a constant pressure, the pump was turned off to shut in the pressure in the test zone. The pressure decay was monitored and recorded. This part of the test was extended for a sufficient period of time to allow some dissipation of pore water pressures.

Constant Pressure/Flow Rate Test

The injection flow rate was maintained at a constant value so that a stable pressure was obtained. Several such pressure/flow rate relations were observed in step-wise fashion at pressures throughout the range where stable flow rates could be achieved. The flow from these tests was measured by counting the number of pump strokes over a given period of time on the positive displacement pump. Each pump stroke on the GSF 100 pump delivered 0.038 litres.

5.4.2 Data Acquisition

A pressure transducer located at the wellhead measured the test zone pressure which was automatically displayed on the chart recorder. A visual display of the test zone and packer pressures was obtained from the gauges on each pump. These gauges were generally used during the test to control the test.

5.4.3 Data Analysis

5.4.3.1 Test Zone Pressure

Pressure in the test zone was read off the chart record of each test. The chart record pressures could be read to an accuracy of better than ±0.2 MPa. The critical fluid pressure at breakdown was read directly from the chart recorder.

The maximum horizontal stress was determined by rearranging the equation (5-10) for breakdown pressure. In the present case, the sediments were assumed to be porous but relatively impermeable. Equation (5-10) is therefore rearranged in the following form for analysis.

$$\sigma_H = 3\sigma_h - P_c - P_p + T$$

It may be noted that the required input parameters include the critical rupture pressure, minimum horizontal stress (from the shut-in pressure) pore pressure and the tensile strength.

5.4.3.2 Analysis of Shut-In

Analysis of the shut-in was taken from the chart record of the pressure decay generally in the first pressure cycle following the breakdown. The shut-in was interpreted as the change in gradient in the decay curve only when this could be identified. It was supplemented by an analysis of the pressure/flow rate relation described below.

5.4.3.3 Pressure/Flow Rate Relation

The pressure/flow relation was determined by pumping at a constant rate and observing the equilibrium pressure. The pressure in the hole was measured on the chart recorder, and the total flow down the hole over a measured period was recorded from the number of pump strokes. This was repeated for a range of pressures and flows.

Graphical plots of the flow rate against pressure generally showed a linear relation with a sharp change in slope. The fracture reopening pressure was assumed to be at the pressure where the change in slope occurred.

5.4.3.4 Determination of the Minimum Horizontal Principal Stress

When a vertical fracture was identified in a vertical borehole, the minimum horizontal principal stress was determined from the shut-in pressure or fracture reopening pressure at the change in slope of the two linear segments of the graph. Where there was a clear trend of decreasing shut-in pressure over a number of refracture cycles, the shut-in value following fracture initiation was interpreted as the stress perpendicular to the initial fracture. The lowest value of shut-in or reopening pressure was interpreted as being not less than the minimum principal stress.

5.4.3.5 Tensile Strength

The average tensile strength for all rock types apart from the coal was based on the results of the Brazilian (Tensile) tests. The tensile strength of the coal and that for the bedding of the siltstone and sandstone were not determined. For those tests in which the tensile strength of the bedding was required, it was assumed that this was approximately 2 MPa. This was based on data from bedded arenaceous sediments in which the strength along the bedding is typically 40 percent to 60 percent of that for the intact rock.

5.4.3.6 Groundwater Pressure

The groundwater pressure is not known for the areas where the hydrofracture testing was carried out. The sections of the mines where testing was undertaken lie under the Atlantic Ocean and it is not unreasonable to assume that the groundwater pressure head prior to mining development was equivalent to depth below sea level.

During testing, the standing water level in Borehole P4 at Prince Mine was approximately 0.8 m below the invert level of the drift. At Lingan Mine, there was a steady flow of water from each of the vertical boreholes (L4 and L5) which appeared once the boreholes penetrated the sandstone band at a depth of approximately 10 m. The standing water levels at Borehole L4 and L5 were at the invert level of the drift.

Other boreholes used for hydrofracture testing were upward inclined and had been open for several days prior to hydrofracture testing. It is considered that the rock around the immediate vicinity of these boreholes had partially drained and the groundwater pressure was reduced correspondingly. For the purpose of result interpretations, the groundwater pressures during testing were assumed as follows:

Borehole	Assumed Groundwater Pressure
Prince Mine (222m* below sea level)	
P3 (horizontal hole)	1.0 MPa
P4 (vertical hole)	2.5 MPa
Lingan Mine (592m* below seal level)	
L3 (horizontal hole)	2.0 MPa
L4 (vertical hole)	5.4 MPa
L5 (vertical hole)	5.4 MPa

* Depth at test site

5.4.4 Impression Packer

The impression packer was installed at the test zone and inflated to 5 MPa, a pressure considered sufficient to cause the trace of the fractures to be marked on the wrap. The pressure was left for a minimum of 30 minutes.

On removal from the borehole, the impressions on the wrap were sketched and the orientations of any fractures were recorded (Plate 6). If the impression material was found to be in good condition, the impressions were painted over to avoid confusion with subsequent impressions and the impression packer re-run with the same impression rubber. After a maximum of three runs the impression material was stripped from the packer and a new wrap applied.

6.0 TEST RESULTS FROM PRINCE MINE

6.1 Overcoring Test Results

A total of nine overcoring tests was attempted at Prince Mine; four in Borehole P1, two in P2, two in P3 and one in P4. Of these tests, seven were successful, the other two were not successful due to premature breakage of the core at or near the location of the USBM gauge buttons. Where the tests were unsuccessful, the cores tended to break along bedding planes during the overcoring process. The test positions and relevant comments about the tests are given in Table 1. Results of the successful tests are discussed in the following sections.

6.1.1 Overcoring Tests

During the overcoring tests, the diametral deformation of the E-sized pilot hole was monitored. The measured diametral deformations, as calculated from the recorded strain readings, for the three button positions (designated as U1, U2 and U3, respectively) were plotted against the depth of overcoring measured from the collar of the pilot hole. The results of all tests carried out are presented in Figures B1-1 to B1-7 in Appendix B.

Tests that were completely successful included P101, P104, P201, P202, P301, P302 and P401. The results of these tests (Figures B1-1 to B1-7) displayed the classic response curves expected of good overcoring tests. Typically, the readings were stable during the initial stages of overcoring. As the thin walled overcoring bit approached the position of the buttons, a small increase in stress was noted, followed by stress relief at the point where the overcoring bit reached the instrumentation button locations. Once the overcoring bit had past the location of the buttons, a gradual stabilization was noted. The net changes in the diametral deformation used for stress calculations are summarized in Table 3.

6.1.2 Biaxial Tests

Biaxial tests were carried out on the overcore specimens soon after completion of the overcoring tests to determine the rock modulus. Due to the laminated nature of the rock, some samples spilt during their recovery from the hole. Hence it was not always possible to undertake biaxial testing on the recovered overcore.

In addition to the biaxial tests carried out immediately after recovery, further tests were carried out at a later date on the overcore with the USBM gauge at different orientations to assess the anisotropic deformation properties of the rock.

Figure B1-8 shows the results of a typical biaxial test in which the diametral deformation of the pilot hole at the three buttom positions are plotted with respect to the applied radial (biaxial) pressure on the overcore. In general, the curves of deformation vs pressure are fairly linear showing little hysteresis upon unloading. Some anisotropy was noted.

Tables 3 and 5 summarize the average and individual modulus values calculated from the biaxial tests undertaken soon after completion of the overcoring tests (within 2 days generally). Results of more extensive biaxial testing carried out at a later date are presented in Table 4 in which the deformation modulus at different orientations are tabulated. The formula given in Appendix D was used for the calculation of the individual modulus values.

Several points may be noted from the modulus values shown in Tables 3, 4 and 5.

a. Based on the results obtained from the same overcore at different dates, there is a noticeable increase in modulus values with time (over a period of about 150 days). The increase in average modulus ranges from 20 to 50% for the sandstone tested.

b. Results of more detailed biaxial tests on samples from Boreholes P2 and P3 (subhorizontal holes) indicated that the sandstone exhibited modest anisotropic deformation behaviour. The modulus along the direction of the bedding plane (U3 direction in the C series tests in Boreholes P2 and P3 shown in Table 4) is higher than that perpendicular to the bedding (U1 direction in the A series tests in Boreholes P2 and P3). The ratio of maximum to minimum modulus ranges from 1.4 to 1.6.

The implications of these results on the evaluation of the in situ stresses are discussed in Section 6.1.4.

6.1.3. Laboratory Tests

To supplement the data obtained from biaxial tests undertaken for the in situ measurement program, uniaxial and triaxial compression tests as well as Brazilian tensile tests were carried out by the CANMET Mining Research Laboratories on selected core samples. The results of this supplementary laboratory testing are summarized in Tables E1-1 to E1-3 in Appendix E. Details of the laboratory testing programs and results obtained are contained in a separate report prepared by CANMET (Gorski, 1986).

6.1.4 Evaluation of In Situ Stresses

The in situ stresses were evaluated from the measured deformations in the pilot hole during overcoring and the deformation moduli determined from the biaxial tests.

Becker and Hooker (1967) and Tullis (1981) have considered the effects of anisotropic rock on the biaxial stresses interpreted from the USBM tests using isotropic theory. It was noted that for an anisotropic rock having a ratio of maximum to minimum modulus of 1.6, the error in the calculation of the secondary principal stresses, using isotropic theory for the P/Q ratio of 1 to 2 (as in the case of Prince Mine) is less than 10%. Hence for the evaluation of the secondary principal stresses the isotropic theory was used.

For the evaluation of the complete stress tensor the deformation moduli measured in the direction of the USBM gauge button positions were used (Table 5). This procedure allows the effect of anisotropy to be taken into account in calculating the six stress components and the three principal stresses.

As there is an apparent increase in deformation modulus with time, it is considered appropriate to use the modulus values obtained at the time when the overcore samples were still relatively fresh. The modulus values used for each button positions in the stress calculations are presented in Table 5.

The secondary principal stresses calculated at each test position and the stress tensor evaluated by the method of least squares are presented in Table 3 and 5 respectively. It may be noted that the minimum principal stress is near vertical while the maximum and intermediate principal stresses are approximately horizontal. The ratio of the maximum to minimum principal stress is about 2.

The depth of the test site at Prince Mine is about 222 m (730 ft) below sea level. The depth of water above the site is estimated to be about 20 m (60 ft). Hence the overburden pressure at the project location based on a bulk rock density of 2.6 Mg/m^3 and a water density of 1.03 Mg/m^3, is about 5.5 MPa. This compares very well with the magnitude of the average vertical stress component (σz), of 6 MPa calculated from the least squares method (Table 5).

6.2 Hydrofracture Test Results

6.2.1 Test Data

Hydrofracture tests were carried out in Boreholes P3, P4 and P5. Table 6 shows a summary of the test locations in each borehole, the break-down, first fracture shut-in and fracture reopening pressures observed and the fracture orientations obtained from the impression packers for each test. The pressure response curves recorded during the tests are shown in Figures C1-1 and C1-2 in Appendix C, and the pressure flow rate test results are presented in Figures C1-3 to C1-8. Detailed discussions of the data obtained from each test are presented in the following sections.

Borehole P4 Test 1: (26.92 m to 27.43 m) Siltstone

The 1st pressure cycle (Figure C1-2) showed a steady rise in pressure after a brief leakage test at 2.8 MPa and a break in the pump delivery at approximately 7.0 MPa. A peak of 20.6 MPa was ultimately reached followed by a rapid fall to a constant level at 7.5 MPa. A slight break in the decay curve at a pressure of 10.5 MPa was evident. The 2nd, 3rd and 4th pressure cycles all showed rapid rises in pressure to a constant level between 10.5 and 11.2 MPa. The slightly uneven rise in pressure to the maximum pressure on these cycles was the result of uneven control on the test zone pump delivery.

The pressure/flow tests (Figure C1-3) showed a generally increasing relation between pressure and flow.

The 5th and 6th pressure cycles (4th and 5th refractures) showed similar responses to the earlier refracture pressure cycles with a rapid rise to approximately 10.5 MPa.

The pressure following shutting-off the pump in all pressure cycles showed a fall to between 7.0 and 6.3 MPa. It was necessary to vent between all tests as the pressure decay from the test core was relatively slow indicating a well sealed test zone. The fracture reopening pressure and the shut-in pressure identified from the decay of the 1st pressure cycle were consistent. The stress perpendicular to the fracture was interpreted as 10.3 MPa.

An axial fracture dipping vertically and trending 265° was recorded by the impression packer at a depth of 26.5 m (87 ft) to 27.4 m (90 ft). This fracture is within the test zone although the fracture extended beyond the nominal test zone and into the area of the upper packer.

Borehole P4 Test 2: (23.37 m to 23.98 m) Mudstone

The 1st pressure cycle (Figure C1-2) showed a rapid rise in pressure to 20.4 MPa at which pressure the BQ rods started to vibrate. A decision was taken to vent at this pressure in order that the rods could be more securely clamped through the chuck of the drilling rig. After the 1st pressure cycle and when the rods had been secured, the 2nd pressure cycle was started and showed a rapid rise to 28.4 MPa followed by a slow and irregular rise in pressure to 32.3 MPa. This pressure was held for approximtely 6 minutes with no obvious breakdown. It was decided not to increase the test zone pressure above this level because this pressure is close to the maximum design working pressure of the mandrel. The pump was shut-off and the pressure in the test zone decayed rapidly to 1.4 MPa after venting. As it was considered that no fracture had occurred during the 2nd pressure cycle, no pressure flow tests were carried out.

No fractures were evident from the impression wrap after testing of this zone.

Borehole P4 Test 3: (17.98 m to 18.59 m) Siltstone

After a leakage test to a pressure of 4.9 MPa, the 1st pressure cycle (Figure C1-2) showed a rapid rise in pressure to an indistinct peak of 17.9 MPa followed by a gradual fall to 3.2 MPa. The 2nd pressure cycle showed a similar rapid rise in pressure to an equally indistinct peak at a slightly lower pressure of 16.8 MPa followed by a more gradual fall to 4.2 MPa at which pressure the system was vented. It is possible that during the 1st and 2nd pressure cycles, water from the test zone was leaking past the packer.

The 3rd pressure cycle showed a rapid rise in pressure to 18.8 MPa followed by a rapid decay to a constant pressure at 5.6 MPa. This last pressure cycle is believed to be the fracture cycle. The 4th and 5th pressure cycles (1st and 2nd refractures) showed rapid rises in pressure to a constant level of 6.0 MPa in the 4th cycle and 5.3 MPa in the 5th cycle.

The pressure after shutting the pump off in the 3rd, 4th and 5th cycles was constant at approximately 5.3 MPa.

The pressure/flow tests (Figure C1-4) showed a generally increasing relation between pressure and flow.

The 6th pressure cycle (3rd refracture) showed a rapid rise to a peak at 5.3 MPa followed by a constant level of 5.0 MPa.

The fracture reopening pressure and the shut-in pressure identified from the 3rd pressure cycle were consistent. The stress perpendicular to the fracture was interpreted as 5.4 MPa. The shut-in pressure and the fracture reopening pressure are consistent with stress levels (determined by overcoring tests) perpendicular to a horizontal fracture (as observed).

A zone of low angle fractures was recorded at around 18.59 m, at the bottom of the test zone. The dip of these fractures was approximately 5° along the axis of the tunnel and are interpreted as being bedding plane fractures.

Borehole P4 Test 4: (13.61 m to 14.22 m) Siltstone

After a leakage test to a pressure of 4.9 MPa, the 1st pressure cycle (Figure C1-2) showed a rapid but distinctly uneven rise in pressure to a peak of 23.9 MPa followed by a very rapid decay to a constant level of 6.3 MPa. The 2nd pressure cycle (1st refracture) showed a rapid rise to an indistinct peak of 15.4 MPa followed by a gradual decay. The 3rd and 4th pressure cycles were similar in nature to the 1st pressure cycle although the peaks were lower at 18.2 MPa and 13.7 MPa, respectively. The decays in both cycles were very rapid, falling to a constant level of 5.6 MPa.

The pressure/flow tests (Figure C1-5) showed a generally increasing relation between pressure and flow.

The 5th and 6th pressure cycles showed a similar response with relatively low peaks at 5.5 MPa.

The fracture reopening pressure of 5.4 MPa was reasonably consistent with the shut-in pressures identified from the 1st, 3rd and 4th pressure cycles of approximately 6.3 MPa. However, three obvious breakdown peaks were evident in these pressure cycles although the maximum pressure showed a steady fall from 23.9 MPa to 13.7 MPa. This behaviour is believed to be indicative of either temporary leakage passed the packers or fracture on several planes, the lower threshold planes not being fractured during the first and subsequent cycles. The steady fluctuation of the test zone pressure particularly in the 1st pressure cycle also reflected this behaviour. Incipient fractures are considered to be present which are on the point of opening but no fracture is developed into the rock. The pressure rises to a level where a fracture develops at a different orientation.

A zone of low angle fractures was recorded at around 13.51 m which is slightly above the nominal test zone, probably within the 'hold-down' grit zone. (This section of the packer lies close to the metal shoulder of the packer element and is approximately 200 mm in length. It is intended to provide improved grip to the element when pressurized particularly when used within casing) of the upper packer. One of the fractures is near horizontal, one dips around 25° to the north and a short vertical fracture (azimuth 090°/270° with respect to the drift centreline) connects these two low angle fractures. The fractures identified at different orientations on the impression wrap are in agreement with the behaviour of the pressure cycles. The 1st breakdown may have developed on the short axial fracture and the 2nd and 3rd fractures breakdowns, on the 25° and near horizontal fractures respectively.

Borehole P4 Test 5: (11.94 m to 12.55 m) Mudstone

After a leakage test to a pressure of 5.3 MPa the 1st pressure cycle (Figure C1-2) showed an initially irregular rise in pressure with several pressure plateaus until a peak of 30.9 MPa was reached. This was followed by a rapid decay which was masked by a pump cycle although a shut-in could be identified at 12.3 MPa which in turn was followed by a gradual decay to a constant pressure around 4.2 MPa.

The 2nd pressure cycle showed a similar response to the 1st cycle with an irregular rise in pressure with a distinct pressure plateau at around 10.5 MPa, 15.4 MPa and 21.0 MPa, followed by a peak at 30.1 MPa. The pressure fell rapidly but no shut-in comparable to the 1st pressure cycle was observed on the decay curve.

The 3rd pressure cycle was irregular but increased rapidly to a peak at 10.2 MPa following a pressure plateau at 5.3 MPa. This peak could not be maintained by the pump and it is considered that air had entered the test zone system via the inlet supply. After a gradual decay the pressure became constant at 6.3 MPa.

The 4th and 5th pressure cycles showed lower maximum attainable pressures at 3.5 MPa and 2.5 MPa, respectively. On venting after the 3rd, 4th and 5th cycles, the vented water spurted out and was consistent with air passing out of the system. This problem was not fully appreciated until the assembly had been moved to the next test location. No pressure/flow stepwise reopening tests were conducted.

One near vertical fracture and two near horizontal fractures were recorded on the impression wrap. The dip and dip direction of the steep fracture was 80°/91° at a depth of around 12.32 m. The fractures at different orientations were consistent with the behaviour of 1st and 2nd pressure cycles which showed pressure plateau during the steady rise to the breakdown. The peak of the 3rd cycle was indicative of a breakdown on a horizontal fracture.

Borehole P4 Test 6: (7.98 m to 8.59 m) Sandstone

The 1st pressure cycle (Figure C1-6) showed a rapid rise in pressure to a peak of 16.9 MPa followed by a gradual decay and a shut-in identified from the chart at 11.9 MPa. A brief leakage test was conducted at a pressure of 10.2 MPa during the rise in pressure in the 1st pressure cycle.

The 2nd, 3rd and 4th pressure cycles (1st, 2nd and 3rd refractures) all showed a rapid rise to a consistent peak of 11.6 MPa followed by a gradual decay.

The pressure flow tests showed a generally increasing relation between pressure and flow with an interpreted reopening pressure of 11.6 MPa.

The 5th and 6th pressure cycles (4th and 5th refractures) showed similar responses to the 2nd, 3rd and 4th cycles.

The fracture reopening pressure and the shut-in pressures were consistent. The stress perpendicular to the initial fracture orientation was interpreted as 11.6 MPa.

An axial fracture dipping vertically and trending 266° was recorded by the impression wrap at a depth of 8.74 m to 8.94 m. The more dominant trace occurred below the nominal test zone and continued beyond the 'hold-down' grit section of the lower packer.

Borehole P3 Test: 1 (7.26 m to 7.87 m) Sandstone

After a leakage test to a pressure of 4.6 MPa the 1st pressure cycle (Figure C1-1) showed a gradual rise in pressure to a distinct peak at 9.1 MPa followed by a gradual decay to an interpreted shut-in at 6.5 MPa and subsequently a gradual decay.

The 2nd, 3rd and 4th pressure cycles (1st, 2nd and 3rd refractures) were similar in response with a consistent peak at 7.0 MPa.

The pressure flow tests (Figure C1-7) showed a generally increasing relation between pressure and flow and an interpreted reopening pressure at 5.9 MPa.

The 5th and 6th pressure cycles (4th and 5th refractures) were similar to the 2nd, 3rd and 4th pressure cycles (1st, 2nd and 3rd refractures) except that the peaks were slightly lower at 6.3 MPa to 6.7 MPa.

The fracture reopening pressure and the shut-in pressure from the 1st pressure cycle were reasonably consistent. The stress perpendicular to the fracture was interpreted as 5.9 MPa.

A zone of axial (near horizontal) fractures were recorded by the impression packer at a depth of 7.72 m to 8.31 m (Borehole P3 was drilled in a subhorizontal orientation). The majority of the fracture traces were below the nominal test zone and beyond the 'hold-down' grit opposite the lower packer.

Borehole P5 Test 1: (7.47 m to 8.08 m): Coal

After a leakage test to a pressure of 2.5 MPa the 1st pressure cycle (Figure C1-1) showed a gradual rise to a low peak of 3.5 MPa followed by a gradual decay. The 2nd pressure cycle was similar in response to the 1st pressure cycle.

The pressure flow tests (Figure C1-8) showed a generally increasing relation between pressure and flow.

The 3rd and 4th pressure cycles were similar in response to the earlier cycles although the peak pressure attained was slightly higher at 4.2 MPa.

The fracture reopening pressure was interpreted as 3.0 MPa. No shut-in interpretation was possible.

Two main series of fractures or traces were evident from the impression packer record. The first was along bedding and the second approximately 30° to 40° to horizontal. Since the test section was located within the coal seam and had a number of strongly developed incipient or existing weaknesses it was not possible to identify which of these was opened during the pressure cycles.

6.2.2 Interpretation of In Situ Stresses from Hydrofracture Test Data

The discussion of the results can be separated into those tests conducted in the vertical borehole and those in the near horizontal borehole. No in situ stress interpretation is given for tests in the coal. In all cases, it is convenient to divide the tests into the four following categories for discussion:

a. Tests showing a well defined peak pressure response to the first pressure cycle and evidence of an axial or steeply dipping fracture (Borehole P4, Tests 1 and 6).

b. Tests showing well defined peak pressure responses to several cycles with evidence of axial and near horizontal fractures (Borehole P4, Tests 4 and 5).

c. Tests showing peak pressures with evidence of near horizontal fractures (Borehole P4, Test 3 and Borehole P3 Test 1).

d. Tests with evidence of reopening of existing fractures (Borehole P5 Test 1).

6.2.2.1 Classic Hydrofracture Response

Two of the hydrofracture tests (Test 1 and 6 in Borehole P4) produced the classic pressure response to hydrofracturing. A breakdown consisting of a sharp peak followed by a rapid decay to a constant pressure which was repeatable over several pressure cycles. This peak pressure was read directly from the chart record of the first pressure cycle (see Figure C1-2). In these two tests, the interpretation of the minimum horizontal principal stress was made from the pressure/flow tests. In both tests, the shut-in pressure identified from the chart record after the breakdown is similar to the fracture reopening pressure.

It is considered that the hydraulic pressure induced the axial or steeply dipping fracture and orientations of the principal stresses have been determined from these fracture orientations.

Using a tensile strength of 5 MPa (from laboratory Brazilian tensile test) and a pore pressure of 2.5 MPa, the magnitudes and orientations of the horizontal principal stresses determined (in total stresses) from these tests are, based on equation 5-10,

	Test	Borehole Depth (m)	σH (MPa)	σh (MPa)	σH Azimuth
Borehole P4	1	27.13	12.8	10.8	265°
	6	8.23	20.4	11.6	256°

6.2.2.2 Multiple Hydrofracture Response

A multiple hydrofracture response was recorded in two tests (Tests 4 and 5 in Borehole P4). In Test 4, the 1st pressure cycle had an uneven rise to the peak and subsequent pressure cycles had distinct peaks and breakdowns which were lower than the first breakdown. The reopening pressure was interpreted as the minimum pressure across a horizontal fracture. A short axial fracture was recorded which connected one horizontal fracture and one dipping at approximately 25°.

In Test 5, the first and more clearly, the second pressure cycles had distinct plateau before reaching the peak at breakdown. The reason why two almost identical breakdowns occurred is not clear. The 3rd pressure cycle reached a peak equivalent to the lowest plateau in the first two cycles. A short fracture with a dip of 80° was recorded in addition to the near horizontal fractures.

Using a tensile strength of 9 MPa (from laboratory test) and a pore pressure of 2.5 MPa the magnitude and orientation of the principal stresses (in total stresses) determined from these tests are,

	Test	Borehole Depth (m)	σH (MPa)	σh (MPa)	σH Azimuth
Borehole P4	4	13.72	?	?	261°
	5	12.19	12.8*	12.4	261°

The breakdown test pressure in this rock type was significantly higher than those in the siltstone or sandstone. This may be due to the effects of creep in the more muddy sediments compared with the stiffer arenaceous rocks. Similar behaviour to that in Test 5 in Borehole P4 was experienced in Test 2 in Borehole P4 where breakdown was not achieved at a test zone pressure of 32.3 MPa.

6.2.2.3 Fracture of Incipient Weaknesses

Fracture along incipient weaknesses were recorded in two tests (Test 3 - Borehole P4 and Test 1 - Borehole P3). In Test 3 in Borehole P4, the first two pressure cycles did not show distinct breakdowns but the 3rd cycle gave a classic response with a distinct peak followed by a rapid decay. The following cycle gave a maximum close to the overburden stress as did the fracture reopening pressure. A horizontal fracture was recorded.

In Test 1 in Borehole P3, the first pressure cycle gave a distinct peak followed by a rapid decay. Subsequent pressure cycles gave peaks equivalent to the overburden stress as did the fracture reopening pressure. A horizontal fracture was recorded.

The orientation of the minimum horizontal principal stress determined in Tests 1 and 6 in Borehole P4 is approximately parallel to the axis of Borehole P3. The axial fracture in Borehole P3 represents therefore a classic breakdown, the fracture developing on the plane of the maximum principal stress in the vertical plane, i.e. normal to the axis of the borehole. The maximum principal stress interpreted from the breakdown data is therefore the minimum horizontal principal stress.

The magnitude and orientation of the principal stresses determined from this test are,

σ_h* (MPa)	σ_v (MPa)	σ_h Azimuth
9.6	5.9	assumed parallel to borehole axis

*Tensile strength assumed to be 2.0 MPa and groundwater pressure to be 1.0 MPa.

6.2.2.4 Re-Opening of Existing Fractures

No fracture free zone existed in Borehole P5, a borehole which was drilled through the coal. As a result, the test conducted in the coal re-opened existing fractures. The peak was very indistinct and low at 3.5 MPa which is lower than the overburden stress. It is considered that the pressure cycle characteristics of this test reflect the permeability of the coal mass rather than representing the stress levels in the rock.

6.2.3 Summary

The in situ stress at Prince Mine was determined from Tests 1 and 6 in Borehole P4. Additional stress data may be available from Test 5 in Borehole P4 (even though no re-opening pressure information is available) and Test 1 in Borehole P3. The magnitudes of the minimum horizontal stress determined from each of the above four tests is similar although there is apparently a wide range for the maximum horizontal principal stress. This may be due to the different moduli for the various rock types encompassed by these tests. The capacity of individual beds or rock to carry load and the ratio of the principal stresses within each bed may vary depending on the modulus and creep although there is apparently a wide range for the maximum horizontal principal stress. This may be due to the different moduli for the various rock types encompassed by these tests. The capacity of individual beds of rock to carry load and the ratio of the principal stresses within each bed may vary depending on the modulus and creep characteristics of the various rock types. A stiffer, higher modulus rock will tend to carry more load than, say, a less stiff rock such as a mudstone. Stiffer rocks are capable of sustaining a high stress ratios whereas a rock which is susceptible to creep may not. This is particularly the case in a cyclic sequence of horizontally bedded strata such as that in Prince Mine. The sandstone unit will be capable of carrying greater load and will also be capable of sustaining a high horizontal stress ratio compared to the more muddy units. Results of Test Nos. 5 and 6 in Borehole P4 appears to indicate this "decoupling" effect of stresses.

The trend of the maximum horizontal principal stress is relatively consistent, ranging from 256° to 265°.

6.3 Comparison of Stresses Measured by Overcoring and Hydrofracture Tests

The stress components and principal stresses calculated from all the overcoring tests carried out in Borehole P1 to P4 represent statistical averages of the in situ stresses. The average principal stresses and their orientations and the six stress components are as follows:

Overcoring Tests

Principal Stress	Orientation Azimuth/Dip
σ_1 = 11.08 MPa	263.5°/14.2°
σ_2 = 9.54 MPa	352.2°/ 5°
σ_3 = 5.63 MPa	64°/-75°

Stress Components

σ_x ($\sigma_{E - W}$) = 10.76 MPa τ_{xy} = 0.06 MPa
σ_y ($\sigma_{N - S}$) = 9.51 MPa τ_{yz} = 0.48 MPa
σ_z (σ_v) = 6.00 MPa τ_{zx} = 1.25 MPa

vertical stress calculated from overburden weight = 5.5 MPa.

The secondary principal stresses determined from the hydrofracturing tests are summarized below:

Hydrofracture Tests

	Secondary Horizontal Principal Stress	Orientation of σ_H Azimuth/Dip
Borehole P4:	σ_H = 10.3 to 11.6 MPa	
	σ_h = 12.8 to 20.4 MPa	274 to 265/0°

Vertical Stress

Borehole P4	5.4 MPa
Borehole P3	5.9 MPa

The in situ stress system determined from the overcoring tests indicated that the average major and intermediate principal stresses are near horizontal. The orientation of σ_1, agrees with the range of orientation of the maximum horizontal stress 'σ_H', determined from the hydrofracture tests.

The magnitudes of horizontal stresses, $_h$ and $_H$, obtained by the hydrofracturing tests are slightly higher than those determined from the overcoring tests. The maximum horizontal stresses (H) calculated from the hydrofracturing test results however varied considerably from the overcoring test results.

This may be due to the following factors:

- The tensile strength of the rock used for the calculated σH is based on laboratory Brazilian (tensile) test results and may not be representative of the rock fractured as tensile strength can vary considerably in a rock over a short distance.

- The pore water pressure conditions in the immediate vicinity of the test section are complicated by the introduction of a fluid at high pressure. The actual pore pressure may be different from the assumed values.

- The different moduli of the various rock types tested and the consequential effects of this on the load carrying capability of each unit may also introduce factors which would result in differences in the horizontal principal stress levels determined.

The vertical stress from the hydrofracture test in Boreholes P3 and P5, agree reasonably well with the the vertical stress component (σ_z) from the overcoring test, and the vertical stress calculated from the overburden weight.

7.0 TEST RESULTS FROM LINGAN MINE

7.1 Overcoring Test Results

A total of eleven overcoring tests were attempted at Lingan Mine; three in Borehole L1, four in L2, three in L3 and one in L5. Of these tests, seven were successful, the other four were not successful due to premature breakage of the core at or near the location of the USBM gauge buttons or the gauge was loose in the hole. The test positions and relevant comments about the tests are given in Table 2. The results of the successful tests are discussed in the following sections.

7.1.1 Overcoring Tests

During the overcoring tests, the diametral deformation of the EX-sized pilot hole was monitored. The measured diametral deformations, as calculated from the recorded strain readings, for the three button positions (designated as U1, U2 and U3, respectively) are plotted against the depth of overcoring measured from the collar of the pilot hole. The results of all the tests carried out are presented in Figures B2-1 to B2-7 in Appendix B.

Tests that were completely successful included L102 L103, L203, L204, L301, L302 and L501. The results of these tests (Figures B2-1 to B2-7) displayed the classic response curves of good overcoring tests. Typically, the readings were stable during the initial stages of overcoring. As the thin wall bit approached the position of the buttons, a small increase in stress was noted, followed by stress relief at the point where the overcoring bit reached the instrumentation button locations. Once the overcoring bit had past the location of the buttons, a gradual stabilization was noted.

The net changes in the diametral deformation used for stress calculations are summarized in Table 7.

7.1.2 Biaxial Tests

Biaxial tests were carried out on the overcore specimens soon after completion of the overcoring tests for the determination of the rock modulus. Due to the laminated nature of the rock, some samples spilt during recovery from the hole. Hence it was not always possible to test the recovered overcore.

In addition to the biaxial tests carried out immediately after recovery, further tests were carried out at a later date on the overcore with the USBM gauge at different orientations to assess anisotropic deformation properties of the rock.

Figure B2-8 shows the results of a typical biaxial test in which the diametral deformation of the pilot hole at the three buttom positions are plotted with respect to the applied radial (biaxial) pressure on the overcore. In general, the curves of deformation vs pressure are fairly linear showing little hysteresis upon unloading. Some anisotropy was noted.

Tables 7 and 9 summarize the average and individual modulus values calculated from the biaxial tests undertaken soon after completion of the overcoring tests (within 2 days generally). Results of more extensive biaxial testing carried out at a later date are presented in Table 8 in which the deformation modulus at different orientations are tabulated. The formula given in Appendix D was used for the calculation of the individual modulus values.

Several points may be noted from the results shown in Tables 7, 8 and 9.

a. Based on the results obtained from the same overcore at different dates, there is a modest increase in modulus values with time (over a period of about 40 days). The increase in average modulus ranges from 10 to 18% for the siltstone tested. This phenomenon is similar to that observed from the biaxial tests for Prince Mine.

b. Results of more detailed biaxial tests on samples from Boreholes L2 and L3 (sub-horizontal holes) indicated that the siltstone exhibited modest anisotropic deformation behaviour. The modulus along the direction of the bedding plane (U3 direction in the C series tests in Boreholes L2 and L3 shown in Table 8) is higher than that perpendicular to the bedding (U1 direction in the A series tests in Boreholes L2 and L3). The ratio of maximum to minimum modulus ranges from 1.7 to 1.8.

The implications of these results on the evaluation of the in situ stresses are discussed in Section 7.1.4.

7.1.3. Laboratory Tests

To supplement the data obtained from biaxial tests undertaken for the in situ measurement program, uniaxial and triaxial compression tests as well as Brazilian tensile tests were carried out by the CANMET Mining Research Laboratories on selected core samples. The results of these is supplementary laboratory tests selected are summarized in Tables E2-1 to E2-3 in Appendix E. Details of the laboratory testing programs and the results obtained are contained in a separate report prepared by CANMET (Gorski, 1986a).

7.1.4 Evaluation of In Situ Stresses

The in situ stresses were evaluated from the measured deformations in the pilot hole during overcoring and the deformation modulus determined from the biaxial tests.

The ratio of maximum to minimum modulus for the rock tested at Lingan Mine is about 1.8. For this anisotropy ratio, the error involved in the calculation of in situ stresses using the isotropic theory, is less than 10% (Becker and Hooker, 1967 and Tullis 1981). Hence for the evaluation of the secondary principal stresses, the isotorpic theory was used.

For the evaluation of the complete stress tensor, the deformation moduli measured in the direction of the USBM gauge button positions were used (Table 9). This procedure allows the effect of anisotropy to be taken into account in calculating the six stress components and the three principal stresses.

As there is an apparent increase in deformation modulus with time, it is considered appropriate to use the modulus values obtained at the time when the cores were still relatively fresh. The modulus values used for each button position in the stress calculations are presented in Table 9.

The secondary principal stresses calculated at each test position and the stress tensor evaluated by the method of least squares are presented in Tables 7 and 9 respectively. It may be noted that the maximum principal stress is near horizontal and is trending in the E-W orientation. The average minimum principal stress ($\sigma 3$) is off vertical and correspondingly the average intermediate principal stress ($\sigma 2$) is dipping towards to the north at about 34°. The orientations of the major principal stresses appear to be consistent with the E-W trend of the monocline which is known to exist at the test site. The gradual steepening of the limb of the monocline and roll of the strata appears to have caused a minor rotation of the minor and intermediate principal stresses. The ratio of the maximum to minimum principal stresses is 2.8 which is higher than that at Prince Mine.

The depth of the test site is about 593 m (1947 ft) below sea level. The depth of water above the site is estimated to be about 70 m (230 ft). Hence the overburden pressure at the project location based on a bulk rock density of 2.6 Mg/m^3 and a water density of 1.03 Mg/m^3, is about 14.3 MPa. This is consistent with the magnitude of the average vertical stress component (σ_z) of 13 MPa calculated from the least squares method (Table 9).

7.2 Hydrofracture Test Results

7.2.1 Test Data

Hydrofracture tests were carried out in Boreholes L3, L4 and L5. Table 10 shows a summary of the test locations in each borehole, the break-down, first fracture, shut-in and fracture reopening pressures observed and the fracture orientations obtained from the impression packers for each test. The pressure response curves recorded during the tests are shown in Figures C2-1 to C2-4 in Appendix C, and results of the pressure/flow tests are presented in Figures C2-5 to C2-17. Detailed discussions of the data obtained from each test are presented in the following sections.

Borehole L3 Test 1: (7.80 m to 8.41 m) Siltstone

The first pressure cycle (Figure C2-1) showed a steady rise in pressure until a peak of 11.6 MPa was reached followed by a gradual decay after the pump was cut-off at 10.5 MPa. The second pressure cycle showed a steady rise in pressure to a peak of 21.1 MPa followed by a shut-in at 19.3 MPa and then a rapid decay. The 3rd, 4th and 5th pressure cycles all showed a rapid rise in pressure to slightly lower peaks of 19.3 MPa, 18.9 MPa and 18.2 MPa, respectively.

The pressure/flow tests showed a generally increasing relation between pressure and flow (Figure C2-1). During the pressure/flow tests the packer pressure decayed rapidly and the test was abandoned in order to check the packer inflation line. The packer assembly was withdrawn from the borehole but on investigation, no damage was evident in the inflation line.

The pressure plateau following the pump shut off in all pressure cycles showed a fall from 19.3 to 18.2 MPa. It was necessary to vent between all tests. The fracture reopening pressure data may not be reliable as the plateau pressures attained in earlier pressure cycles was not reached because of loss of pressure in the packers. The effect was particulary noticeable during the pressure/flow tests and was probably the result of air entering the hydraulic system of the pump. The stress perpendicular to the fracture was interpreted as 18.2 MPa, the plateau pressure on the last pressure cycle before the packers were deflated.

A fracture along the bedding was identified from the impression at a depth of 8.59 m in the borehole. This fracture is slightly beyond the nominal test zone and into the area of the lower packer.

Borehole L3 Test 2: (6.20 m to 6.81 m) Siltstone

The leakage test (Figure C2-1) indicated a rapid pressure drop from 5.8 MPa to approximately 1.8 MPa after which the pressure decayed very slowly. The 1st pressure cycle showed a rapid rise to 20.3 MPa followed by a very rapid decay to around 1.5 MPa with a shut-in at 18.6 MPa. The 2nd, 3rd and 4th pressure cycles all showed a similar rapid rise in pressure to slightly decaying peaks of 17.5 MPa, 17.5 MPa and 16.8 MPa, respectively. These peaks were followed by very rapid pressure decays after the pump was shut off. The stable pressure attained after shutting the pump off in these cycles was approximately 1.5 MPa.

The pressure/flow tests showed a generally increasing relation between pressure and flow with a reopening pressure of 15.4 MPa identified from the test data (Figure C2-6).

The 5th and 6th pressure cycles showed rapid rises to a consistent peak of 16.5 MPa followed by a very rapid decay in pressure to 1.5 MPa after the pump was shut cff.

The fracture reopening pressure and the shut-in pressure identified from the 1st pressure cycle was not consistent, a difference of 3.2 MPa, although the plateau pressure attainable from succeeding pressure cycles decayed to a final level of 16.5 MPa compared with a fracture reopening pressure of 15.4 MPa.

Two fracture traces were identified from the impression testing, one a bedding plane trace and the other, a near axial trace which has an orientation at an angle of 35° to the bedding direction. Both fracture traces occurred in the section of the borehole 5.64 m to 6.20 m which was just outside the nominal test zone area.

Borehole L4 Test 1: (28.88 m to 29.50 m) Siltstone

The leakage test (Figure C2-2) indicated a rapid pressure decay from 5.2 MPa to zero, indicating significant leakage from the system.

An attempt to prevent or minimize the leakage which may have been due, partially at least, to leakage passed the packers was introduced into the test procedure by increasing the pressure differential between the test zone and packers. This had a minimal effect on the performance of the test and it is likely that most of the leakage was via primary permeability i.e. through the rock pores. To minimize this effect it would have been necessary to introduce a very viscous bentonite mud into the borehole to 'cake' onto the wall of the borehole and so inhibit fluid invasion of the rock during testing. Such a mud was not available on site.

The 1st pressure cycle showed a rapid rise in pressure to a plateau of 26.9 MPa which was sustained for several seconds after which the pump was shut off. The pressure decayed rapidly to approximately 4.9 MPa and then increased to 6.3 MPa after which the system was vented. Back pressure in the rock mass probably caused the pressure in the test zone to increase after the rapid decay.

The 2nd, 3rd and 4th pressure cycles all showed a rapid rise in pressure to plateau of 26.9 MPa, 28.0 MPa and 26.6 MPa, respectively. After the pump was shut off the pressure decayed rapidly followed in each case by a slow decay below 2.3 MPa. No increase in pressure similar to that experienced in the 1st pressure cycle was evident.

The pressure/flow tests showed a generally increasing relation between pressure and flow and plotting of the data confirmed that no breakdown had been achieved in the pressure cycles (Figure C2-7).

The 5th and 6th pressure cycles showed rapid rises in pressure to plateau of 23.4 MPa and 22.4 MPa, respectively. No evidence of breakdown was apparent.

Lower pressures were attainable in these cycles compared with those prior to the pressure/flow tests. This was probably due to a fall in the pressure of the mine compressed air supply during the test.

No evidence of any fractures was found from the impression testing confirming that breakdown had not been achieved.

Borehole L4 Test 2: (27.48 m to 28.09 m) Siltstone

The leakage test (Figure C2-2) showed a rapid decay from a pressure of 4.9 MPa to zero indicating significant flow out of the system.

The 1st pressure cycle showed an unsteady rise in pressure to 24.8 MPa after which the pump was shut off. This was followed by a rapid decay in pressure to zero. This cycle indicated significant leakage from the system and a further leakage test was carried out after tightening of the well head adaptors.

The 2nd, 3rd and 4th pressure cycles all showed a rapid rise in pressure to pressure levels of 24.1 MPa, 24.6 MPa and 22.7 MPa, respectively. In each cycle, higher pressures were not attainable because of leakage from the system probably through the permeability of the rock pores.

The pressure/flow tests showed a generally increasing relation between pressure and flow and a plot of the data confirmed that no breakdown had been achieved during the previous pressure cycles (Figure C2-8).

The 5th and 6th pressure cycles showed a rapid rise to plateau of 21.7 MPa and 20.3 MPa, respectively.

No evidence of any fractures was found from the impression testing, confirming that breakdown had not been achieved.

Borehole L4 Test 3: (24.36 m to 24.97 m) Siltstone

The leakage test indicated a rapid fall in pressure from 4.3 MPa to 0.7 MPa indicating significant leakage from the system.

The 1st pressure cycle showed a rapid rise in pressure to a plateau of 24.8 MPa followed by a rapid decay after the pump was shut off.

The 2nd, 3rd and 4th pressure cycles all showed similar behaviour with a rapid rise in pressure to a plateau decaying from 24.1 MPa in the 2nd cycle to 23.4 MPa in the 3rd cycle and 19.9 MPa in the 4th pressure cycle. The decay after the pump was shut off was rapid.

The pressure/flow tests showed a generally increasing relation between pressure and flow and confirmed that no breakdown had been achieved during the previous pressure cycles (Figure C2-9).

The 5th and 6th pressure cycles were similar, reaching plateau of 22.0 MPa and 20.6 MPa, respectively, after a rapid build up in pressure. In each case, the pressure decay was rapid after the pump was shut off.

No evidence of any fractures was found from the impression testing, confirming that breakdown had not been achieved.

Borehole L4 Test 4: (9.14 m to 9.75 m) Sandstone

The 1st pressure cycle (Figure C2-3) showed a rapid rise in pressure to a peak of 20.4 MPa, followed by a possible shut-in at 11.7 MPa. The 2nd, 3rd and 4th pressure cycles showed a similar response with peaks of 9.9 MPa, 9.2 MPa and 8.9 MPa, respectively. The pressure immediately after the pump was shut off in the 2nd and 3rd cycle was approximately 2.6 MPa. After the rapid decay the pressure increased slowly, probably because of back pressure. This behaviour was not apparent, however, in the 4th pressure cycle.

The pressure/flow tests (Figure C2-10) showed a generally increasing relation between pressure and flow with a reopening pressure of approximately 7.8 MPa.

The 5th and 6th pressure cycles showed a rapid rise to peaks of 8.5 MPa and 7.8 MPa, respectively, followed by an observed shut-in of 7.1 MPa in both cycles.

The fracture reopening pressure at 7.8 MPa and the shut-in pressure from the 5th and 6th cycles were reasonably consistent. The stress perpendicular to the fracture was interpreted as 7.8 MPa.

A near horizontal fracture was recorded at approximately 11.89 m which is slightly above the nominal test zone and probably within the hold down grit zone of the upper packer.

Borehole L4 Test 5: (10.36 m to 10.97 m) Siltstone

The 1st pressure cycle showed a rapid rise to a peak of 20.1 MPa followed by a rapid fall in pressure to zero with no obvious shut-in. The 2nd pressure cycle showed a similar rapid rise in pressure but to a much higher peak of 29.2 MPa followed by a very rapid fall in pressure with a possible shut-in identified at 6.8 MPa. The 3rd pressure cycle was similar to the second, although a higher peak pressure was attained at 30.6 MPa. No shut-in point was identified from the 3rd pressure decay trace.

The 4th and 5th pressure cycles showed a rapid rise in pressure to a plateau of 13.1 MPa which was followed by a rapid decay after the pump had been shut off.

The pressure/flow tests showed a generally increasing relation between pressure and flow with an interpreted reopening pressure of 10.7 MPa (Figure C2-11).

The 6th and 7th pressure cycles were similar to the 4th and 5th cycles although the peak pressures attainable were lower at 12.4 MPa and 11.7 MPa, respectively.

The stress perpendicular to the fracture was interpreted as 10.6 MPa.

A near horizontal fracture was recorded by the impression wrap at a depth of 10.41 m.

Borehole L4 Test 6: (13.09 m to 13.70 m) Siltstone

The 1st pressure cycle (Figure C2-3) showed a rapid rise in pressure to a peak of 33.8 MPa followed by a rapid decay to approximately 2.2 MPa with a possible shut-in at 21.6 MPa.

The 2nd, 3rd and 4th pressure cycles showed a rapid rise in pressure to plateau of 20.5 MPa, 18.8 MPa and 16.0 MPa respectively. After the pump was shut off the pressure decayed rapidly to 4.2 MPa in the case of cycles 2 and 3 and to 2.2 MPa in the 4th cycle. After the rapid decay the pressure decayed gradually until the system was vented.

The pressure/flow tests showed a generally increasing relation between pressure and flow with an interpreted reopening pressure of 12.7 MPa.

The 5th and 6th pressure cycles were similar but the plateau pressure (14.6 MPa) was lower than the pressure cycles prior to the pressure/flow tests (Figure C2-12).

The fracture reopening pressure was considered to be indicative of the stress perpendicular to the fracture and was taken as 12.7 MPa.

A near horizontal fracture was recorded in the impression wrap and was interpreted as a fracture along the bedding.

Borehole L4 Test 7: (16.12 m to 16.73 m) Muddy Siltstone

The 1st pressure cycle (Figure C2-3) showed a rapid rise in pressure to a peak of 27.2 MPa followed by a rapid decay to a plateau at approximately 4.2 MPa. The 2nd and 3rd pressure cycles showed a rapid rise in pressure to plateau of 17.0 MPa and 15.3 MPa, respectively, followed by a gradual and sometimes irregular decay to 5.5 MPa in the case of cycle 2 and 2.4 MPa for cycle 3. An increase in pressure was evident after the decay on the 3rd cycle which is attributed to back pressure developing in the test zone.

The pressure/flow tests showed a generally increasing relation between pressure and flow with an interpreted reopening pressure of 13.6 MPa (Figure C2-13).

The 4th and 5th pressure cycles showed a rapid rise in pressure to plateau at 14.9 MPa and 14.2 MPa, respectively. Following the pump shut off, the pressure decayed rapidly to plateau of 5.8 MPa and 5.1 MPa, respectively.

The reopening pressure was considered to be the pressure perpendicular to the fracture and was taken at 13.6 MPa.

A near horizontal fracture was recorded on the impression wrap at a depth of approximately 16.76 m. This trace was interpreted as being a fracture along the bedding.

Borehole L4 Test 8: (25.60 m to 26.21 m) Siltstone

The first pressure cycle (Figure C2-3) showed a rapid rise to a plateau at 30.1 MPa followed by a rapid decay to zero pressure once the pump was shut off. The 2nd and 3rd pressure cycles had similar characteristics to the 1st cycle apart from the plateau pressures which were attainable and these were lower at 24.1 MPa and 22.7 MPa, respectively. In each case, the pressure decayed to zero after the pump was shut off.

The pressure/flow tests showed a generally increasing relation between pressure and flow. The plot of this data confirmed that no breakdown had occurred (Figure C2-14).

The 4th and 5th pressure cycles were similar to the 2nd and 3rd pressure cycles except that the plateau pressure were lower at 21.0 MPa and 19.9 MPa, respectively.

No evidence of any fractures were found from the impression testing, confirming that breakdown had not been achieved.

Borehole L4 Test 9: (28.22 m to 28.83 m) Siltstone

The 1st pressure cycle (Figure C2-3) showed a rapid rise to an irregular plateau at 20.3 MPa followed by a rapid decay after the pump was shut off. A break in the decay curve was noted at a pressure of 7.3 MPa after which the pressure decayed slowly.

The 2nd and 3rd pressure cycles were similar in response, showing a rapid rise in pressure to plateau of 22.7 MPa and 22.1 MPa, respectively, followed by a rapid decay to zero pressure once the pump had been shut off.

The pressure/flow tests showed a generally increasing relation between pressure and flow and the data confirm that no breakdown had occurred (Figure C2-15).

The 4th and 5th pressure cycles were similar in response to the 2nd and 3rd cycles, although the plateau pressures were lower at 19.9 MPa and 19.2 MPa, respectively.

No evidence of any fractures was found from the impression testing confirming that breakdown had not been achieved.

Borehole L5 Test 1: (11.46 m to 12.07 m) Siltstone

After a leakage test to a pressure of 4.2 MPa the 1st pressure cycle (Figure C2-4) showed a rapid rise to a peak of 21.1 MPa at which breakdown occurred followed by an observed shut-in at approximately 9.9 MPa. The pressure then decayed rapidly to zero.

The 2nd, 3rd and 4th pressure cycles were similar with a rapid rise in pressure to plateau of 8.9 MPa, 8.5 MPa and

8.5 MPa, respectively. The pressure decay after the pump had been shut off was relatively slow.

The pressure/flow tests had a generally increasing relation between pressure and flow with a re-opening pressure of 8.8 MPa determined from the data (Figure C2-16).

The 5th and 6th pressure cycles were similar to the 3rd and 4th pressure cycles with the same plateau pressure of 8.5 MPa.

The re-opening pressure was considered to be the stress normal to the fracture and taken as 8.8 MPa.

A near horizontal fracture was recorded on the impression wrap.

Borehole L5 Test 2: (13.84 m to 14.45 m) Muddy Siltstone

After a leakage test to a pressure of 5.6 MPa the 1st pressure cycle (Figure C2-4) showed a rapid rise to a plateau of 29.5 MPa. After the pump was shut-off the pressure decayed very rapidly to zero. The 2nd and 3rd pressure cycles were similar to the 1st cycle although the plateau pressures were lower at 25.3 MPa and 23.9 MPa, respectively. In both cases, the pressure decayed very rapidly to zero after the pump was shut off.

The pressure/flow tests showed a generally increasing relation between pressure and flow and the data confirm that no breakdown had been achieved (Figure C2-17).

The impression record showed a wide horizontal feature which cannot be reconciled with the performance of the test.

Borehole L5 Test 3: (16.31 m to 16.92 m) Muddy Siltstone

No pressure could be developed in the test section for this test. The reason for this is unclear. It was considered that the packers should be deflated and moved to a nearby zone for a repeat test (Test 4 in Borehole L5).

Borehole L5 Test 4: (15.14 m to 15.75 m) Muddy Siltstone

After the failure to pressurize the test section in Test 3 in this borehole, the packer assembly was moved to position approximately 1.22 m above. Once again the test section was not able to be pressurized and this test was also abandoned.

7.2.2 Interpretation of In Situ Stresses from Hydrofracture Test Data

For analysis purposes equation 5-10 is applicable. The results can be separated into those tests conducted in the vertical boreholes and those in the near horizontal borehole. As none of the tests produced fractures which were other than near horizontal, i.e. along the bedding plane the data cannot be used to determine the magnitudes and directions of the horizontal principal stresses. The data can therefore only be used as an indicator overburden stress. The tests can be divided into two main categories for the purposes of discussions:

a. Tests in which no breakdown occurred (Tests 1, 2, 3, 8 and 9 in Borehole L4 and Tests 2, 3 and 4 in Borehole L5).

b. Tests in which breakdown occurred (Tests 1 and 2 in Borehole L3, Tests 4, 5, 6 and 7 in Borehole L4 and Test 1 in Borehole L5).

7.2.2.1 Tests in Which No Breakdown Occurred

Breakdown was not achieved at eight of the fifteen hydrofracture test positions. Two positions, Tests 3 and 4 in Borehole L5 were not able to be pressurized and these are not included in the following discussion.

The pressures achieved in those boreholes in which breakdown did not occur ranged from 20.3 MPa in Test 9, Borehole L4 to 30.1 MPa in Test 8 Borehole L4. The range in the pressure levels achieved is probably the result of a number of factors including leakage out of the test zone through primary permeability, (i.e. permeability associated with permeability of the rock pores), leakage from the rods and the available mine compressed air supply pressure. In all of these tests, the choke valve which controls the input air pressure was screwed in fully so that the pump was working at the full mine air supply pressure, available from the mine compressed air supply.

At high outlet pump pressures to the test zone, the flow rate from the pump is low and was obviously incapable of increasing the pressure in the test zone above a certain level mainly due to leakage from the test zone system into the surrounding rock because of its permeability.

7.2.2.2 Tests in Which Breakdown Occurred

Breakdown was achieved in seven of the fifteen tests and all fracture traces were near horizontal, i.e. essentially along the bedding plane.

The reopening pressures across the fracture planes varied from 7.8 MPa in Test 4, Borehole L4 to 15.4 MPa in Test 1, Borehole L3. The overburden stress calculated for the depth below ground is estimated to be approximately 14.3 MPa The difference in stress as measured by the reopening pressure to the overburden load is probably the result of pore pressure effects although it is noticeable that pore pressure appears to be completely controlling the pressure level in some tests (Borehole L4 - Test 4, Borehole L5 - Test 1) and only partially in others (Borehole L4, Tests 5 and 6). This may be the result of varying permeability and porosity characteristics of the rock types tested. The reopening pressure for L4 -Test 4 and L5-Test 1 were approximately 7.5 MPa 8.0 MPa respectively whereas for L4 - Test 5 and Test 6 the reopening pressures were approximately 11.0 MPa and 12.5 MPa respectively. All the fractures were horizontal and it is likely that the overburden pressure for all tests is similar. The reason for these large differences could likely be associated with pore pressure effects or possible rotation of the fracture from the horizontal.

7.2.3 Summary

None of the tests in the vertical boreholes produced an axial fracture. The fractures in the near horizontal borehole (L3) produced essentially axial fractures but these were also along bedding planes. All of the tests in which breakdown occurred produced horizontal fractures along bedding. The data produced cannot therefore be used to determine the magnitude and direction of the major principal stress in this area.

To date, all that can be stated is that the minimum principal stress is likely to be the vertical stress. The results of the test programs are summarized in Table 10.

7.3 Comparison of Stresses Measured by Overcoring and Hydrofracturing Tests

The stress components and principal stresses calculated from all the overcoring tests carried out in Borehole P1 to P4 and L5, represent statistical averages of the in situ stresses. The average principal stresses and their orientations, and the six stress components are as follows:

Overcoring Tests

Principal Stress	Orientation Azimuth/Dip
σ_1 = 33.84 MPa	88.3°/ 4.0
σ_2 = 14.49 MPa	355.0/ 34.7
σ_3 = 12.21 MPa	4.0/-55.0

Six Stress Components

σ_x (σ_{E-W}) = 33.72 MPa

σ_y (σ_{N-S}) = 13.76 MPa

σ_z (σ_v) = 13.05 MPa

τ_{xy} = 0.54 MPa

τ_y = 1.11 MPa

τ_{zx} = 1.43 MPa

vertical stress calculated from overburden weight = 14.3 MPa

The vertical stress determined from the hydrofracture tests is as follows:

Range: 7.8 MPa to 15.4 MPa (gauge pressure)
Average: 11.5 MPa

As discussed in Section 7.2.2 the in situ horizontal stresses cannot be evaluated from the hydrofracture test results because vertical fractures were not induced in any of the tests where break down occurred. The vertical stress measured by hydrofracturing varies over a substantial range probably due to pore pressure effects. The average value is slightly lower than that determined by the overcoring tests.

8.0 REGIONAL STRESS DISTRIBUTION IN THE SYDNEY COALFIELD

Stress measurements have been carried out at four sites in the Sydney Coalfield. These sites include the Donkin Mine, No. 26 Colliery, and the Prince and Lingan Mines (present program). The scope of the stress measurement program at each site differed because of different project requirements Results of the stress determinations at Donkin Mine and No. 26 Colliery have been published in Golder Associates reports No. 831-6014 and 821-1296 respectively.

In each test program, the stresses measured have been resolved into components in the N-S, E-W and vertical directions and the stress tensors were evaluated for No. 26 Colliery, the Prince and Lingan Mines by the method of least squares.

As the in situ stress data is an important parameter for the study of the rock/gas outburst problems, it would be of interest to summarize the available data from these four sites.

Table 11 presents a summary of the stresses measured at the four mines in the Sydney Coalfield. Figure 10 shows the directions of the principal stresses measured at the No. 26 Colliery, Prince and Lingan Mines. In general, the major principal stress ($\sigma 1$) is trending E-W and the intermediate principal stress ($\sigma 2$) is oriented N-S. These two principal stresses are close to or slightly off horizontal. The minor principal stress ($\sigma 3$) is close to or slightly off vertical. In No. 26 Colliery, the stress regime is fairly isotropic, and the principal stress directions vary from the general trend.

A plot of the stress components in the E-W, N-S and vertical directions is presented in Figure 11. The general trend is a gradual increase in stress with depth. The vertical stress components measured at the four sites are generally consistent with the overburden stress. The horizontal stress components σ_{E-W} and σ_{N-S} only differ slightly at Donkin Mine, Prince Mine and No. 26 Colliery resulting in a fairly isotropic horizontal stress system at these sites. At Lingan Mine however, σ_{E-W} is significantly higher than σ_{N-S}. This may arise from the influence of the monocline which could cause a slight reduction in the intermediate and minor principal stresses.

The stresses determined from the hydrofracture tests are also plotted on Figure 11. The measured vertical stresses are generally consistent with the overburden stresses. The minimum horizontal stress measured from hydrofracture tests at Prince Mine is slightly higher than those obtained from overcoring tests but the corresponding maximum horizontal stress is however considerably higher.

9.0 CONCLUSIONS

The in situ stress measurement programs for the Prince and Lingan Mines of the Sydney Coalfield, Cape Breton were completed in February 1986. The stresses were determined using the method of overcoring (with the USBM gauge) and hydrofracturing techniques. Five 100 mm diameter boreholes were drilled in each mine at different directions. Hydrofracture tests were carried out in the vertical and selected horizontal boreholes. The conclusions derived from these test programs are summarized below.

a) the hydrofracture testing equipment was designed for this project which was undertaken on behalf of the CANMET Cape Breton Coal Research Laboratory. The equipment performed satisfactorily throughout the test program.

b) Overcoring tests were carried out in the sandstone and siltstone units in Prince and Lingan Mines respectively. Seven successful USBM tests were completed in each mine. The unsuccessful attempts were primarily the result of premature rock breakage along bedding planes or planes of weakness during overcoring. All the successful USBM tests displayed the classic stress relief response.

c) Results from the biaxial tests on the overcore samples indicate that there is an increase in the rock deformation modulus with time. For the sandstone from Prince Mine, the modulus increased by 20 to 50% in about 150 days. Similarly, the siltstone from Lingan Mine increased in modulus by 10 to 18% in about 40 days. For the evaluation of in situ stresses, it was considered appropriate to use the biaxial test data obtained soon after the overcoring test, while the samples were still relatively fresh.

d) Anisotropic deformation behaviour of the rock was noted from the biaxial tests carried out with the USBM gauge positioned at different orientations. The deformation modulus along the bedding is generally higher than that perpendicular to the bedding for both the sandstone and siltstone samples recovered from the Prince and Lingan Mines respectively. The ratio of maximum to minimum modulus for the sandstone from Prince Mine is 1.4 to 1.6, and for the siltstone from Lingan Mine 1.7 to 1.8. Individual modulus values measured at the USBM gauge button positions were used for the evaluation of the complete stress tensor. For the evaluation of secondary principal stresses at individual test positions, the average modulus values were used.

e) The in situ stresses measured at 222 m below sea level at Prince Mine are slightly anisotropic. The results are summarized in Table 5. The major principal stress is near horizontal and oriented approximately in the E-W direction. The minimum principal stress is close to vertical. The ratio of the major and minor principal stress is about 2. The average vertical stress component agrees well with the overburden stress. The "Mountain" fault locted at 3.4 km northwest of the test site does not appear to have influenced the in situ stresses measured.

f) The in situ stresses measured at 593 m below sea level at Lingan Mine exhibit relatively higher anisotropy. The results are summarized in Table 9. The ratio of the major and minor principal stress is about 2.8. The major principal stress is near horizontal and oriented approximately in the E-W direction. The minimum principal stress is off vertical, dipping at 55°. The intermediate principal stress is oriented N-S and dips 35° towards the north. This stress system appears to have been influenced by the monocline as the test site was located on the up-dip limb of this regional structure which strikes approximately E-W.

The ratio of the major and minor principal stress is about 2.8. The average vertical stress component is slightly lower than the overburden pressure.

g) Hydrofracture tests were carried out at the Prince and Lingan Mines in vertical and horizontal boreholes. Pressure flow tests were carried out during the pressure cycles to augment the interpretation of the in situ stresses from the test data. At Prince Mine, distinct vertical fractures were developed in some test zones in the vertical boreholes. However, breakdown did not occur in the mudstone layers. In other test positions in the vertical borehole, either near horizonal fractures or a combination of horizontal and vertical fractures were induced. In the horizontal holes, the induced fractures were invariably horizontal. A very low and indistinct pressure peak was obtained when hydrofracturing the coal because of the presence of existing factures.

At Lingan Mine, only horizontal fractures were induced in both the vertical and horizontal boreholes. In several cases, breakdown did not occur in the siltstone strata at pressure levels varying from 20 to 30 MPa. This could possibly result from a number of factors, including leakage out of the test zone through primary permeability, leakage from the rods and available the mine compressed air supply pressure. These factors could limit the maximum test zone pressure that could be applied. Apparently the pressures required to cause breakdown of the strata is higher than the maximum attainable pressures.

h) The presence of vertical fractures at Prince Mine enabled the determination of the maximum and minimum horizontal stresses from the hydrofracture data based on the shut-in pressures identified from the pressure records or the pressure/flow tests. The minimum horizontal stress ranges from 10.3 to 11.6 MPa which is slightly higher than the results from overcoring tests. The corresponding maximum horizontal stress is estimated to range from 12.8 to 20.4 MPa and are higher than the overcoring test results. The discrepancy may be attributed to the tensile strength and pore pressures assumed for the evaluation of the maximum horizontal stresses. The direction of the maximum horizontal stress was consistently found to be in the E-W orientation and it agrees with that determined from overcoring tests.

Tests which resulted in horizontal fractures provided an indication of the vertical stress component. The vertical stresses evaluated from the hydrofracture data at Prince Mine range from 5.4 to 5.9 MPa and this agrees reasonably well with the overburden stress.

i) At Lingan Mine, only vertical stresses were evaluated from the hydrofracture test data. There is a wider scatter in the results. The measured vertical stresses range from 7.8 to 15.4 MPa. The average value is lower than the overburden stress.

j) Stress measurements have previously been carried out at Donkin Mine and the No. 26 Colliery. A summary of all the stress data available for the Sydney coalfield is presented in Table 11. The following points are noted from the data:

  o the major and intermediate principal stresses are generally oriented in the E-W and N-S directions respectively.

  o the major principal stresses are near horizontal except in No. 26 Colliery where the in situ stress system is approximately isotropic.

  o the minimum principal stresses are close to or slightly off vertical.

- the vertical stress components measured at each mine site generally agree reasonably well with the overburden stress.

- the magnitudes of stresses increase with depth. The horizontal stress system is approximately isotropic at No. 26 Colliery and the Prince and Donkin Mines. At Lingan, the stress system is relatively more anisotropic due probably to the influence a regional monoclinal structure.

10. ACKNOWLEDGEMENTS

Golder Associates would like to thank the Cape Breton Development Corporation for their contributions and assistance during the testing programs at the Prince and Lingan Mines. Personnel at the CANMET Cape Breton Coal Research Laboratory Sydney and in particular Dr. T.R.C. Aston and Mr. W. Gallant, have provided invaluable assistance in organization of the field activities associated with this program. Their contribution is also gratefully acknowledged.

GOLDER ASSOCIATES

C.M.-k. Yuen

C.M.K. Yuen, P. Eng.

J.L. Gilby

CMKY/JLG/pds

REFERENCES

1. Abou-Sayed, A.S. and Brechtel, C.E. "In Situ Stress Determination by Hydrofracturing: A Fracture Mechanics Approach". J. Geophy. Res., 83, B6, 2851-2862, 1978.

2. Aamodt, L. and Kuriyagawa, M. "Measurement of Instantaneous Shut-in Pressure in Crystalline Rock". Proceedings of the Workshop on Hydraulic Fracturing Stress Measurements, U.S. Nat. Comm. on Rock Mech., Washington, D.C., 394-402, 1982.

3. Barton, N. "Hydraulic Fracturing to Estimate Minimum Stress and Rockmass Stability at a Pumped Hydro Project". Proceedings of the Workshop on Hydraulic Fracturing Stress Measurements, U.S. Nat. Comm. on Rock Mech., Washington, D.C., 167-180, 1982.

4. Becker, R.M., and Hooker V.E., 1976. Some Anisotropic Considerations in Rock Stress Determination. U.S. Burea Of Mines Report 6965.

5. Bishop 1953, Personal Communication reported in "Effective Stress in Soils, Concrete and Rocks" in Pore Pressure and Suction in Soils, Butterworths, London, 1961 by Skempton, A.W.

6. Bredehoeft, J.D., Wolff, R.G., Keys, W.S. and Shuter, E. "Hydraulic Fracturing to Determine the Regional In Situ Stress Field, Piceance Basin, Colorado". Geol. Soc. Am. Bull., 87, 250-258, 1976.

7. Doe, T.W. "Determination of the State of Stress at the Stripa Mine, Sweden". Proceedings of the Workshop on Hydraulic Fracturing Stress Measurements, U.S. Nat. Comm. on Rock Mech., Washington, D.C., 305-331, 1982.

8. Enever, J.R. and Woolterton, B.A. "Experience With Hydraulic Fracturing as a Means of Estimating In Situ Stress in Australian Coal Basin sediments". Proceedings of the Workshop on Hydraulic Fracturing Stress Measurements, U.S. Nat. Comm. on Rock Mech., Washington, D.C., 62-102, 1982.

9. Gorski, B., 1986. Strength Determinations of Prince Mine Rocks. CANMET MRL Report. MRL 85-33.

10. Gorski, B., 1986a. Strength Determinations of Lingan Mine Rocks. CANMET MRL Report. MRL 86-45.

REFERENCES (continued)

11. Gronseth, J.M. and Kry, P.R. "Instantaneous Shut-in Pressure and its Relationship to the Minimum In Situ Stress". Proceedings of the Workshop on Hydraulic Fracturing Stress Measurements, U.S. Nat. Comm. on Rock Mech., Washington, D.C., 147-166, 1982.

12. Haimson, B.C. "Earthquake Related Stresses at Rangely, Colorado". In New Horizons in Rock Mechanics, Ed. Hardy, H and Stefanko, R., American Society for Civil Engineers, New York, 689-708, 1973.

13. Haimson, B.C. "The Hydrofracturing Stress Measuring Method and Recent Field Results". Int. J. Rock Mech. Min. Sci. & Geomech. Abstr., 15, 167-168, 1978.

14. Haimson, B.C. and Fairhurst, C. "Initiation and Extension of Hydraulic Fractures in Rock". Soc. Petrol. Engrs. J., 7, 310-318, 1967.

15. Hickman, S.H. and Zoback, M.D. "The Interpretation of Hydraulic Fracturing Pressure Time Data for In Situ Stress Determination". Proceedings of the Workshop on Hydraulic Fracturing Stress Measurements, U.S. Nat. Comm. on Rock Mech., Washington, D.C., 103-146, 1982.

16. Hooker, V.E., and Bickel, D.L. 1974, Overcoring Equipment and Techniques Used in Rock Stress Determinations. U.S. Bureau of Mines Information Circular 8618.

17. Hubbert, M.K. and Willis, D.G. "Mechanics of Hydraulic Fracturing". Trans. Am. Inst. Min. Engrs., 210, 153-163, 1957.

18. McLennan, J.D. and Roegiers, J.C. "Do Instantaneous Shut-in Pressures Accurately Represent the Minimum Principal Stress". Proceedings of the Workshop on Hydraulic Fracturing Stress Measurements, U.S. Nat. Comm. on Rock Mech., Washington, D.C., 181-207, 1982.

19. Obert, L. and Durall, W.I., 1967. Rock Mechanics and the Design of Structures in Rock. John Wiley & Sons, Inc. (Publisher).

20. Panek, L.A., 1966. Calculation of the Average Ground Stress Components from Measurements of the Diametral Deformation of a Drillhole; U.S. Bureau of Mines Report 6732.

REFERENCES (continued)

21. Pine, R.J., Ledingham, P. and Merrifield, C.M. "In Situ Stress Measurement in the Carnmenellis Granite - II. Hydrofracture Tests at Rosemanowas Quarry to Depths of 2000 m". Int. J. Rock Mech. Min. Sci. & Geomech. Abstr., 20, 63-72, 1983.

22. Ratigan, J.L. "A Statistical Fracture Mechanics Determination of the Apparent Tensile Strength in Hydraulic Fracture". Proceedings of the Workshop on Hydraulic Fracturing Stress Measurements, U.S. Nat. Comm. On Rock Mech., Washington, D.C., 444-462, 1982.

23. Rummel, F., Baumgartner, J., and Alheid, H.J. "Hydraulic Fracturing Stress Measurements along the Eastern Boundary of The SW-German Block". Proceedings of the Workshop on Hydraulic Fracturing Stress Measurements, U.S. Nat. Comm. on Rock Mech., Washington, D.C., 1-35, 1982.

24. Rummel, F. and Winter, R.B. "Fracture Mechanics as Applied to Hydraulic Fracturing". Proc. Int. Symp. Physical and Geodynamical Processes in Earthquake Focal Regions, Potsdam, 1981.

25. Savin, G.N. "Stress Concentrations Around Holes". Oxford, 1961.

26. Tullis, T.E., 1981. Stress Measurements Via Shallow Overcoring Near the San Andreas Fault, Geophysical Monograph 24. The Handin Volume.

27. Zoback, M.D. and Pollard, D.D. "Hydraulic Fracture Propagation and Interpretation of Pressure-Time Records for In Situ Stress Determinations". 19th U.S. Symposium on Rock Mechanics, Stateline, Nevada, 1978.

TABLE 1 SUMMARY OF POSITIONS OF USBM OVERCORING TESTS
PRINCE MINE

BOREHOLE NO.	BOREHOLE ORIENTATION				TEST NO.	ROCK TYPE	DEPTH OF TEST FROM COLLAR (m)	COMMENTS ON TEST
	AZIMUTH	DIP	COLLAR ELEVATION (m)	TOTAL DEPTH (m)				
P1	318°	30°	-223.73	24.1	P101	Sandstone	12.34	a, e
					P102	Sandstone	12.95	b, d
					P103	Sandstone	13.50	c, d
					P104	Sandstone	14.63	a, e
P2	320°	4.5°	-224.10	13.3	P201	Sandstone	12.04	a, e
					P202	Sandstone	12.92	a, d
P3	260°	9°	-223.97	9.9	P301	Sandstone	8.81	a, d
					P302	Sandstone	9.51	a, e
P4	-	-90°	-226.09	29.9	P401	Sandstone	8.08	a, d
P5	261°	-1.5°	-224.71	10.3	--	Coal	--	No USBM Tests

1. COMMENTS ON TESTS

   a. Test successful.
   b. Test aborted as USBM gauge was loose in pilot hole.
   c. Rock broke close to USBM gauge buttons during test.
   d. Intact overcore sample recovered from test suitable for Biaxial Testing.
   e. Overcore sample broke during recovery.

2. NOTES:

   Azimuth is referenced to north.

TABLE 2 SUMMARY OF POSITIONS OF USBM OVERCORING TESTS
LINGAN MINE

BOREHOLE NO.	BOREHOLE ORIENTATION				TEST NO.	ROCK TYPE	DEPTH OF TEST FROM COLLAR (m)	COMMENT ON TEST
	AZIMUTH	DIP	COLLAR ELEVATION (m)	TOTAL DEPTH (m)				
L1	330°	27°	-591.36	30.4	L101	Siltstone	8.81	c
					L102	Siltstone	9.51	a, d
					L103	Siltstone	10.19	a, d
L2	330°	6°	-592.00	13.6	L201	Siltstone	10.36	b
					L202	Siltstone	11.96	b
					L203	Siltstone	12.50	a, e
					L204	Siltstone	13.26	a, d
L3	272°	12°	-591.72	11.7	L301	Siltstone	9.65	a, d
					L302	Siltstone	10.21	c
					L303	Siltstone	11.20	a, d
L4	--	-90°	-593.72	31.6	--		--	No USBM Tests
L5	--	-90°	-593.47	25.3	L501	Siltstone	12.80	a, e

1. COMMENTS ON TESTS

   a. Test successful.
   b. Test aborted as USBM gauge was loose in pilot hole.
   c. Rock broke close to USBM gauge buttons during test.
   d. Intact overcore sample recovered from test suitable for Biaxial Testing.
   e. Overcore sample broke during recovery.

2. NOTES:
   Azimuth is referenced to north.

TABLE 3 MAGNITUDES AND DIRECTIONS OF SECONDARY PRINCIPAL STRESSES MEASURED FROM OVERCORING TESTS

PRINCE MINE

DRILL HOLE	ROCK TYPE	TEST NO.	DEPTH OF TEST FROM HOLE COLLAR	DIAMETRAL DISPLACEMENT OF PILOT HOLE (MICROINCH)			SECONDARY PRINCIPAL STRESSES		ORIENTATION OF P FROM DIRECTION OF U1	AVERAGE ELASTIC CONSTANTS USED FOR EVALUATION OF P & Q	
				U1	U2	U3	MAX STRESS P (MPa)	MIN STRESS Q (MPa)		E (GPa)	ν
P1	Sandstone	P101	12.34m	2146	4790	2942	14.06	8.66	68.53	9.91	0.2
	Sandstone	P104	14.63m	1350	2672	3046	9.90	6.35	96.04	9.91*	0.2
P2	Sandstone	P201	12.04m	712	1957	3772	10.78	4.47	108.07	10.20	0.2
	Sandstone	P202	12.92m	1143	1750	3055	9.04	5.04	110.95	10.20*	0.2
P3	Sandstone	P301	8.81m	1968	1901	1971	5.72	5.58	148.86	8.34	0.2
	Sandstone	P302	9.51m	1878	1882	1924	5.54	5.45	115.79	8.34*	0.2
P4	Sandstone	P401	8.08m	2773	4893	2103	16.08	9.48	53.35	11.27	0.2

NOTES:

1. Diametral displacements are presented in microinches using the following calibration factors:
   Button No. 1 = 0.937 (microinch for unit microstrain)
   Button No. 2 = 0.941
   Button No. 3 - 0.943

2. For each test, button set No. 1 was oriented in the vertical plane through the axis of the drill hole. For vertical tests button set No. 1 was oriented along the axis of the tunnel.

3. Only data from successful overcoring tests are used for the calculation of in situ stresses.

4. P and Q are respectively the maximum and minimum stresses (secondary principal stresses) measured on the plane perpendicular to the axis of the drill hole.

5. Orientation of P is measured counterclockwise from the U1 direction.

6. E values are determined from Biaxial Tests undertaken soon after completion of overcoring test. The average values are used to determine P and Q.

7. Orientation of the drill holes are given in Table 1. Test No. P101 indicates test No. 1 in Borehole P1.

8. * No biaxial tests were carried out, E values were assumed.

TABLE 4

SUMMARY OF BIAXIAL TEST RESULTS

PRINCE MINE

Drill Hole	Rock Type	Biaxial Test No.	Depth of Sample from Hole Collar (m)	Modulus of Deformation (GPa)		
				Individual Diameters		Average
P1	Sandstone	P102-A	12.95	U1	15.07	14.92
				U2	14.57	
				U3	15.13	
P1	Sandstone	P103B-A	13.50	U1	46.55	45.00
				U2	36.01	
				U3	52.44	
P2	Sandstone	P202B-A	12.92	U1	10.51	13.84
				U2	11.13	
				U3	19.89	
		P202B-C	12.92	U1	12.78	13.48
				U2	11.32	
				U3	16.35	
P3	Sandstone	P301B-A	8.81	U1	11.21	12.67
				U2	12.57	
				U3	14.22	
		P301B-C	8.81	U1	13.70	13.67
				U2	11.75	
				U3	15.42	
P4	Sandstone	P401B-A	8.08	U1	14.16	13.47
				U2	12.76	
				U3	13.48	
		P401B-C	8.08	U1	15.90	14.71
				U2	13.93	
				U3	14.29	

Notes: 1. Biaxial tests were carried out   days after overcoring tests.

2. Biaxial tests were carried out with the buttons oriented in various positions to check the effect of anisotropy of the modulus. The sketch shows the location of the U1 button oriented for test:

-A vertical
-B 15°
-C 30°
-D 45°
-E 60° (a check for Test A)

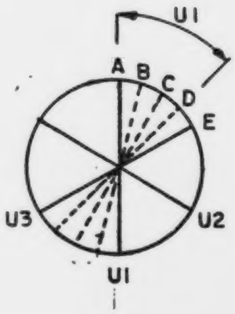

TABLE 5

STRESS TENSOR CALCULATED BY LEAST SQUARES SOLUTION PRINCE MINE

Page 1 of 2

a. INPUT PARAMETERS

DRILL HOLE	DRILL HOLE ORIENTATION (degrees)		TEST NO.	DIAMETRAL DEFORMATION (microinch) U1 (θ = 90°) U2 (θ = 150°) U3 (θ = 30°)	ELASTIC CONSTANTS	
	AZIMUTH α	DIP Ψ			E (GPa)	υ
P1	318	30	P101	U1 = 2146	10.04	0.2
				U2 = 4790	9.67	0.2
				U3 = 2942	10.02	0.2
P1	318	30	P104	U1 = 1350	10.04*	0.2
				U2 = 2672	9.67*	0.2
				U3 = 3046	10.02*	0.2
P2	320	4.5	P201	U1 = 712	7.77	0.2
				U2 = 1957	8.20	0.2
				U3 = 3772	14.62	0.2
P2	320	4.5	P202	U1 = 1143	7.77*	0.2
				U2 = 1750	8.20*	0.2
				U3 = 3055	14.62*	0.2
P3	260	9	P301	U1 = 1968	7.41	0.2
				U2 = 1901	8.27	0.2
				U3 = 1971	9.34	0.2
P3	260	9	P302	U1 = 1878	7.41*	0.2
				U2 = 1882	8.27*	0.2
				U3 = 1924	9.34*	0.2
P4	90	-90	P401	U1 = 2773	11.89	0.2
				U2 = 4893	10.67	0.2
				U3 = 2103	11.25	0.2

NOTE:

1. θ is the angle between the h_1 axis of the drill hole and the diameter across which the deformation was measured (see Figure D.1 in Appendix D for notation of co-ordinate system for drillhole).
2. Only data from successful overcoring tests are used in the least squares solution.
3. E values are determined from biaxial tests undertaken soon after overcoring tests; υ is assumed. Average values are shown in Table 3.
4. * No biaxial tests were carried out. E values were assumed.

TABLE 5 (cont'd)
PRINCE MINE

b. RESULTS OF LEAST SQUARES SOLUTION

(i) AVERAGE STRESS TENSOR

$\sigma_x (\sigma_{E-W}) = 10.76$ MPa

$\tau_{xy} = 0.06$ MPa

$\sigma_y (\sigma_{N-S}) = 9.51$ MPa

$\tau_{yz} = 0.48$ MPa

$\sigma_z = 6.00$ MPa

$\tau_{zx} = 1.25$ MPa

(ii) STATISTICAL INTERPRETATION

° Coefficient of Correlation	$R^2 = 0.85$
° Standard Deviation of Regression Line	$S = 30.46$ µm
° Standard Deviations of the Stress Components	$s(\sigma_x) = 2.45$ MPa $s(\sigma_y) = 1.45$ MPa $s(\sigma_z) = 1.18$ MPa $s(\tau_{xy}) = 1.33$ MPa $s(\tau_{yz}) = 0.92$ MPa $s(\tau_{zx}) = 1.41$ MPa

c. MAGNITUDES AND DIRECTIONS OF PRINCIPAL STRESSES

PRINCIPAL STRESSES	AZIMUTH	DIP
$\sigma_1 = 11.08$ MPa	83.5°	14.3°
$\sigma_2 = 9.54$ MPa	352.2°	5.0°
$\sigma_3 = 5.64$ MPa	63.4°	-74.9°

NOTES: - Azimuth is referenced to north
- Positive dip is upward

TABLE 6

RESULTS OF HYDROFRACTURE TESTS

PRINCE MINE

Borehole (Azimuth/ Dip)	Test No.	Depth of Test Zone (m)	Rock Type	Effective Breakdown Test Pressure (P_c) (MPa)	First Fracture Shut-in Pressure (MPa)	Fracture Reopening Pressure (MPa)	Ground Water Pressure P_p (MPa)	Tensile Strength (MPa)	σ_H Total Stress (MPa)	σ_h Total Stress (MPa)	σ_v* Total Stress (MPa)	Fracture Orientation** Dip	Azimuth	Comments
P4	1	26.92 to 27.53	Siltstone	20.6	10.5	10.3	2.5	5	12.8	10.3	6.2	90°	265°	Axial Fracture
	2	23.37 to 23.98	Mudstone	-	-	-	2.5	5	-	-	6.1	No trace		No breakdown at 32.2 MPa
(-/-90)	3	17.98 to 18.59	Siltstone	18.8	6.2	5.4	2.5	5	?	?	6.0	0 to 5°		Near horizontal fracture
	4	13.61 to 14.26	Siltstone	23.9	6.4	5.4	2.5	5	?	?	5.9	Horizontal 90°	261°	Several fractures
	5	11.94 to 12.55	Mudstone	30.9	12.4	-	2.5	9	12.8	12.4	5.8	Horizontal 84°	261°	Several fractures
	6	7.98 to 8.58	Sandstone	16.9	12.0	11.6	2.5	5	20.4	11.6	5.7	90°	256°	Axial fracture
									σ_h	σ_v	σ_v*			
P3 (260/9)	1	7.26 to 7.87	Sandstone	9.1	6.5	5.9	1.0	-	11.6	6.9	5.7	Horizontal		Opening along bedding
P5 (265/-1.5)	1	7.47 to 8.08	Coal	3.5	?	3.0	0.0	-	?	?	5.7	Not Determined		Several en echelon fractures

* Determined from overburden load

** Determined from impression packer tests

TABLE 7 MAGNITUDES AND DIRECTIONS OF SECONDARY PRINCIPAL STRESSES MEASURED FROM OVERCORING TESTS

LINGAN MINE

DRILL HOLE	ROCK TYPE	TEST NO.	DEPTH OF TEST FROM HOLE COLLAR	DIAMETRAL DISPLACEMENT OF PILOT HOLE (MICROINCH)			SECONDARY PRINCIPAL STRESSES		ORIENTATION OF P FROM DIRECTION OF U1	AVERAGE ELASTIC CONSTANTS USED FOR EVALUATION OF P & Q	
				U1	U2	U3	MAX STRESS P (MPa)	MIN STRESS Q (MPa)		E (GPa)	υ
L1	Siltstone	L102	9.51	843	659	2546	36.59	14.05	122.55	53.90	0.2
	Siltstone	L103	10.19	328	1600	2641	26.25	10.23	103.35	34.41	0.2
L2	Siltstone	L203	12.50	937	1938	2414	29.61	17.88	99.19	38.69	0.2
	Siltstone	L204	13.26	890	1496	1735	22.27	15.38	97.96	39.35	0.2
L3	Siltstone	L301	9.65	1199	753	1094	10.87	8.32	156.53	27.16	0.2
	Siltstone	L303	11.20	896	651	1182	13.73	9.77	133.69	37.10	0.2
L5	Siltstone	L501	12.80	4078	1165	1460	33.00	13.67	177.36	30.00	0.2

NOTES:

1. Diametral displacements are presented in microinches using the following calibration factors:
   Button No. 1 = 0.937 (microinch for unit microstrain)
   Button No. 2 = 0.941
   Button No. 3 = 0.943

2. For each test, button set No. 1 was oriented in the vertical place through the axis of the drill hole. For vertical tests button set No. 1 was oriented along the axis of the tunnel.

3. Only data from successful overcoring tests are used for the calculation of insitu stresses.

4. P and Q are respectively the maximum and minimum stresses (secondary principal stresses) measured on the plane perpendicular to the axis of the drill hole.

5. Orientation of P is measured counterclockwise from the U1 direction.

6. E values are determined from Biaxial Tests. The average values are used to determine P and Q.

7. Orientation of the drill holes are given in Table 2.

TABLE 8

SUMMARY OF BIAXIAL TEST RESULTS

LINGAN MINE

Drill Hole	Rock Type	Biaxial Test No.	Depth of Sample from Hole Collar (m)	Modulus of Deformation (GPa)		
				Individual Diameters		Average
P1	Siltstone	L102B-A	9.51	U1	39.46	47.40
				U2	45.27	
				U3	57.46	
		L102B-B	9.51	U1	42.20	64.23
				U2	43.53	
				U3	106.97	
		L102B-C	9.51	U1	43.76	72.52
				U2	41.28	
				U3	132.53	
		L102B-D	9.51	U1	46.85	68.42
				U2	39.74	
				U3	118.66	
		L102B-E	9.51	U1	52.06	71.78
				U2	39.74	
				U3	123.54	
L1	Siltstone	L103B-A	10.19	U1	30.59	40.65
				U2	42.17	
				U3	49.20	
		L103B-B	10.19	U1	33.41	40.95
				U2	33.86	
				U3	55.58	
		L103B-C	10.19	U1	37.05	40.19
				U2	31.89	
				U3	51.64	
		L103B-D	10.19	U1	44.84	40.91
				U2	31.17	
				U3	46.72	
		L103B-E	10.19	U1	51.28	41.98
				U2	30.89	
				U3	43.76	
L2	Siltstone	L203B-A	12.50	U1	35.46	42.71
				U2	43.24	
				U3	49.44	
L2	Siltstone	L204B-A	13.26	U1	34.73	46.43
				U2	51.85	
				U3	52.71	
		L204B-B	13.26	U1	37.46	46.63
				U2	37.54	
				U3	64.91	
		L204B-C	13.26	U1	39.01	44.81
				U2	34.76	
				U3	60.67	

TABLE 8 (Cont'd)

Drill Hole	Rock Type	Biaxial Test No.	Depth of Sample from Hole Collar (m)	Modulus of Deformation (GPa)		
				Individual Diameters		Average
		L204B-D	13.26	U 1	42.27	41.93
				U 2	32.50	
				U 3	51.02	
		L204B-E	13.26	U.1	46.47	40.89
				U 2	31.05	
				U 3	45.15	
L3	Siltstone	L303B-A	11.20	U 1	31.44	41.98
				U 2	43.17	
				U 3	51.33	
		L303B-B	11.20	U 1	34.38	49.42
				U 2	37.74	
				U 3	76.15	
		L303B-C	11.20	U 1	35.46	43.93
				U 2	34.55	
				U 3	61.77	
		L303B-D	11.20	U 1	38.74	42.54
				U 2	33.30	
				U 3	55.58	
		L303B-E	11.20	U 1	40.59	45.93
				U 2	32.05	
				U 3	65.16	

Note: Biaxial tests were carried out with the buttons oriented in various positions to check the effect of anisotrophy of the modulus. The sketch shows the location of the ul button oriented for test:

-A vertical

-B 15°

-C 30°

-D 45°

-E 60° (a check for Test A)

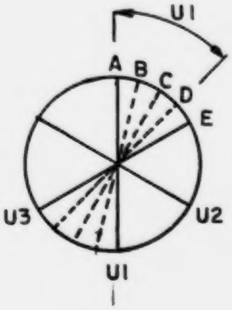

TABLE 9

STRESS TENSOR CALCULATED BY LEAST SQUARES SOLUTION LINGAN MINE

Page 1 of 2

a. INPUT PARAMETERS

DRILL HOLE	DRILL HOLE ORIENTATION		TEST NO.	DIAMETRAL DEFORMATION (microinch) U1 (θ = 90°) U2 (θ = 150°) U3 (θ = 30°)	ELASTIC CONSTANTS	
	AZIMUTH α	DIP Ψ			E (GPa)	ν
L1	330	27	L102	U1 = 843 U2 = 659 U3 = 2546	45.05 51.47 65.18	0.2 0.2 0.2
L1	330	27	L103	U1 = 328 U2 = 1600 U3 = 2641	26.00 35.68 41.55	0.2 0.2 0.2
L2	330	6	L203	U1 = 937 U2 = 1938 U3 = 2414	32.24 39.15 44.67	0.2 0.2 0.2
L2	330	6	L204	U1 = 890 U2 = 1496 U3 = 1735	29.55 43.93 44.57	0.2 0.2 0.2
L3	272	12	L301	U1 = 1199 U2 = 753 U3 = 1094	20.42 27.92 33.13	0.2 0.2 0.2
L3	272	12	L303	U1 = 896 U2 = 651 U3 = 1182	27.90 38.14 45.26	0.2 0.2 0.2
L5	90	-90	L501	U1 = 4078 U2 = 1165 U3 = 1460	30.00 30.00 30.00	0.2 0.2 0.2

NOTE:

1. θ is the angle between the h1 axix of the drill hole and the diameter across which the deformation was measured (see Figure D.1 in Appendix D for notation of co-ordinate system for drillhole).
2. Only data from successful overcoring tests are used in the least squares solution.
3. E values are determined from biaxial tests (see table 2); is assumed.
4. E values for test L501 are assumed.

TABLE 9 (cont'd)
LINGAN MINE

b. RESULTS OF LEAST SQUARES

Page 2 of 2

(i) AVERAGE STRESS TENSOR

$\sigma_x (\sigma_{E-W})$ = 33.73 MPa

$\sigma_y (\sigma N\text{-}S)$ = 13.76 MPa

$\sigma_z (\sigma_v)$ = 13.05 MPa

τ_{xy} = 0.54 MPa

τ_{yz} = 1.11 MPa

τ_{zx} = 1.43 MPa

(ii) STATISTICAL INTERPRETATION

° Coefficient of Correlation	R^2 = 0.95
° Standard Deviation of Regression Line	S = 10.98 µm
° Standard Deviations of the Stress Components	$s(\sigma_x)$ = 2.39 MPa $s(\sigma_y)$ = 1.91 MPa $s(\sigma_z)$ = 1.60 MPa $s(\tau_{xy})$ = 1.60 MPa $s(\tau_{yz})$ = 1.45 MPa $s(\tau_{zx})$ = 1.91 MPa

c. MAGNITUDES AND DIRECTIONS OF PRINCIPAL STRESSES

PRINCIPAL STRESSES	AZIMUTH	DIP
σ_1 = 33.84 MPa	88.3°	4.0°
σ_2 = 14.49 MPa	355.5°	34.7°
σ_3 = 12.21 MPa	4.0°	-55.0°

NOTES: - Azimuth is referenced to north
- Positive dip is upward.

TABLE 10

RESULTS OF HYDROFRACTURE TESTS

LINGAN MINE

Borehole (Azimuth/ Dip)	Test No.	Depth of Test Zone (m)	Rock Type	Effective Breakdown Test Pressure (P_c) (MPa)	First Fracture Shut-in Pressure (MPa)	Fracture Reopening Pressure (MPa)	Ground Water Pressure P_p (MPa)	Tensile Strength (MPa)	σ_H Total Stress (MPa)	σ_n Total Stress (MPa)	σ_{v*} Total Stress (MPa)	Fracture Orientation Dip Azimuth	Comments
L3 (272°/12°)	1	7.8 to 8.41	Siltstone	21.6	19.3	-	2.0	-	-	-	14.2	Near horizontal	Along bedding
	2	6.2 to 6.81	Siltstone	20.3	18.6	15.4	2.0	-	-	-	14.2	Near horizontal	Along bedding
L4 (-/-90°)	1	28.8 to 29.50	Siltstone	-	-	-	5.4	-	-	-	15.1	No trace	No breakdown at 28.0 MPa
	2	27.48 to 28.09	Siltstone	-	-	-	5.4	-	-	-	15.0	No trace	No breakdown at 24.8 MPa
	3	24.36 to 24.97	Siltstone	-	-	-	5.4	-	-	-	15.0	No trace	No breakdown at 24.8 MPa
	4	9.14 to 9.75	Sandstone	20.4	11.7	7.8	5.4	-	-	-	14.5	Near horizontal	Along bedding
	5	10.36 to 10.97	Siltstone	30.6	-	10.7	5.4	-	-	-	14.6	Near horizontal	Along bedding
	6	13.9 to 13.70	Siltstone	33.8	-	12.7	5.4	-	-	-	14.7	Near horizontal	Along bedding
	7	16.12 to 16.73	Siltstone	27.2	-	13.6	5.4	-	-	-	14.7	Near horizontal	Along bedding
	8	25.60 to 26.21	Siltstone	-	-	-	5.4	-	-	-	15.0	No trace	No breakdown at 30.1 MPa
	9	28.22 to 28.83	Siltstone	-	-	-	5.4	-	-	-	15.0	No trace	No breakdown at 20.3 MPa
L5 (-/-90°)	1	11.46 to 12.07	Siltstone	21.1	-	8.8	5.4	-	-	-	14.6	Near horizontal	Along bedding
	2	13.84 to 14.45	Muddy Siltstone	-	-	-	5.4	-	-	-	14.7	No trace	No breakdown at 29.5 MPa
	3	16.31 to 16.92	Muddy Siltstone	-	-	-	5.4	-	-	-	14.7	Not determined	
	4	15.14 to 15.75	Muddy Siltstone	-	-	-	5.4	-	-	-	14.7	Not determined	

* Determined from overburden load

TABLE 11

STRESSES MEASURED AT DIFFERENT MINES IN THE SYDNEY COALFIELD

Mine Site	Depth of (1) Test Site (m)	Method of Stress Measurement	Principal Stresses(2) (MPa) (Azimuth/Dip) (Degrees)			Stress Components$^{(3)}$ (MPa)			Overburden Stress (MPa)
			σ_1	σ_2	σ_3	σ_{E-W}	σ_{N-S}	σ_v	
Donkin Mine	165 (12)	overcoring	-	-	-	9.04	7.93	4.90	4.2
No. 26 Colliery	762 (90)	overcoring	26.3 (278/64)	24.05 (9/-13)	23.2 (270/- 25)	23.31	24.98	25.27	21.7
Prince Mine	222 (20)	overcoring	11.8 (263/14)	9.54 (-7.8/5)	5.1 (64/-75)	10.76	9.51	6.00	5.5
		hydrofracturing	12.8-20.4 (261/0)	10.3-11.6 (351/0)	5.4-5.9 (-)	-	-	-	-
Lingan Mine	593 (70)	overcoring	33.84 (88 /4.0)	14.49 (355/35)	12.21 (4 /-55)	33.73	13.76	13.05	14.3
		hydrofracturing	-	-	7.8-15.4 (-)	-	-	-	

Notes:

(1) Depth below sea level, Figure in ( ) indicates depth of water

(2) σ_1, σ_2, σ_3 : Major, intermediate and minor principal stresses.

(3) σ_{E-W}, σ_{N-S}, σ_v : Stress components in E-W, N-S and vertical directions

SITE LOCATION MAP

FIGURE 1

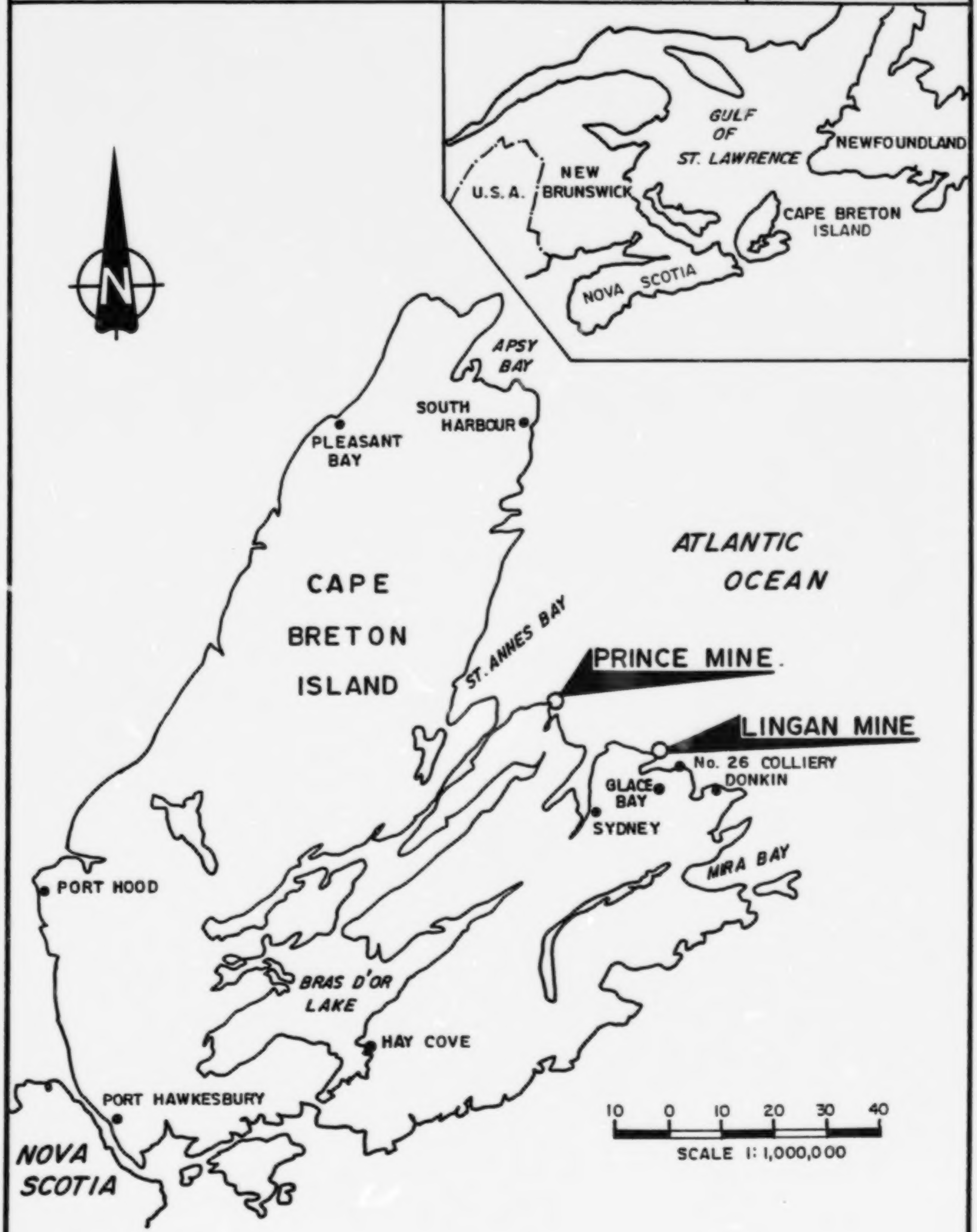
GULF OF ST. LAWRENCE
NEWFOUNDLAND
NEW BRUNSWICK
U.S.A.
CAPE BRETON ISLAND
NOVA SCOTIA
N
APSY BAY
SOUTH HARBOUR
PLEASANT BAY
ATLANTIC OCEAN
CAPE BRETON ISLAND
ST. ANNES BAY
PRINCE MINE
LINGAN MINE
No. 26 COLLIERY
DONKIN
GLACE BAY
SYDNEY
MIRA BAY
PORT HOOD
BRAS D'OR LAKE
HAY COVE
PORT HAWKESBURY
NOVA SCOTIA
10 0 10 20 30 40
SCALE 1: 1,000,000

Date MAY 15, 1986
Project 851-6025

Golder Associates

Drawn D.M.
Chkd. JG

SITE FOR IN SITU STRESS MEASUREMENTS PRINCE MINE

FIGURE 2

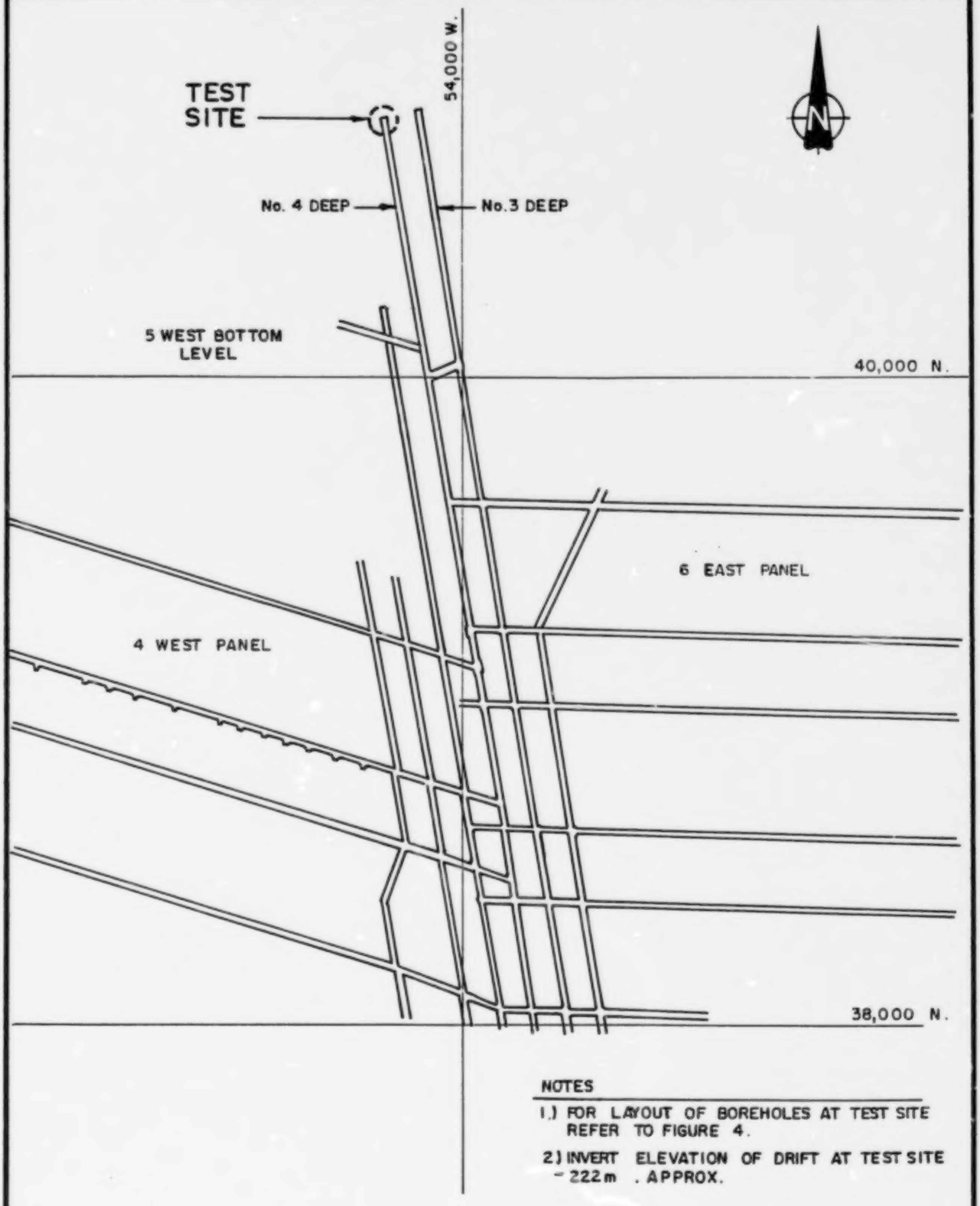
TEST SITE
54,000 W.
No. 4 DEEP
No. 3 DEEP
N
5 WEST BOTTOM LEVEL
40,000 N.
6 EAST PANEL
4 WEST PANEL
38,000 N.

NOTES

1.) FOR LAYOUT OF BOREHOLES AT TEST SITE REFER TO FIGURE 4.

2) INVERT ELEVATION OF DRIFT AT TEST SITE ~222m . APPROX.

SCALE : 1 :4800

Date MAY 16, 1986

Project 851-6025

Golder Associates

Drawn D. M.

Chkd. JLG

SITE FOR IN SITU STRESS MEASUREMENT
LINGAN MINE

FIGURE 3

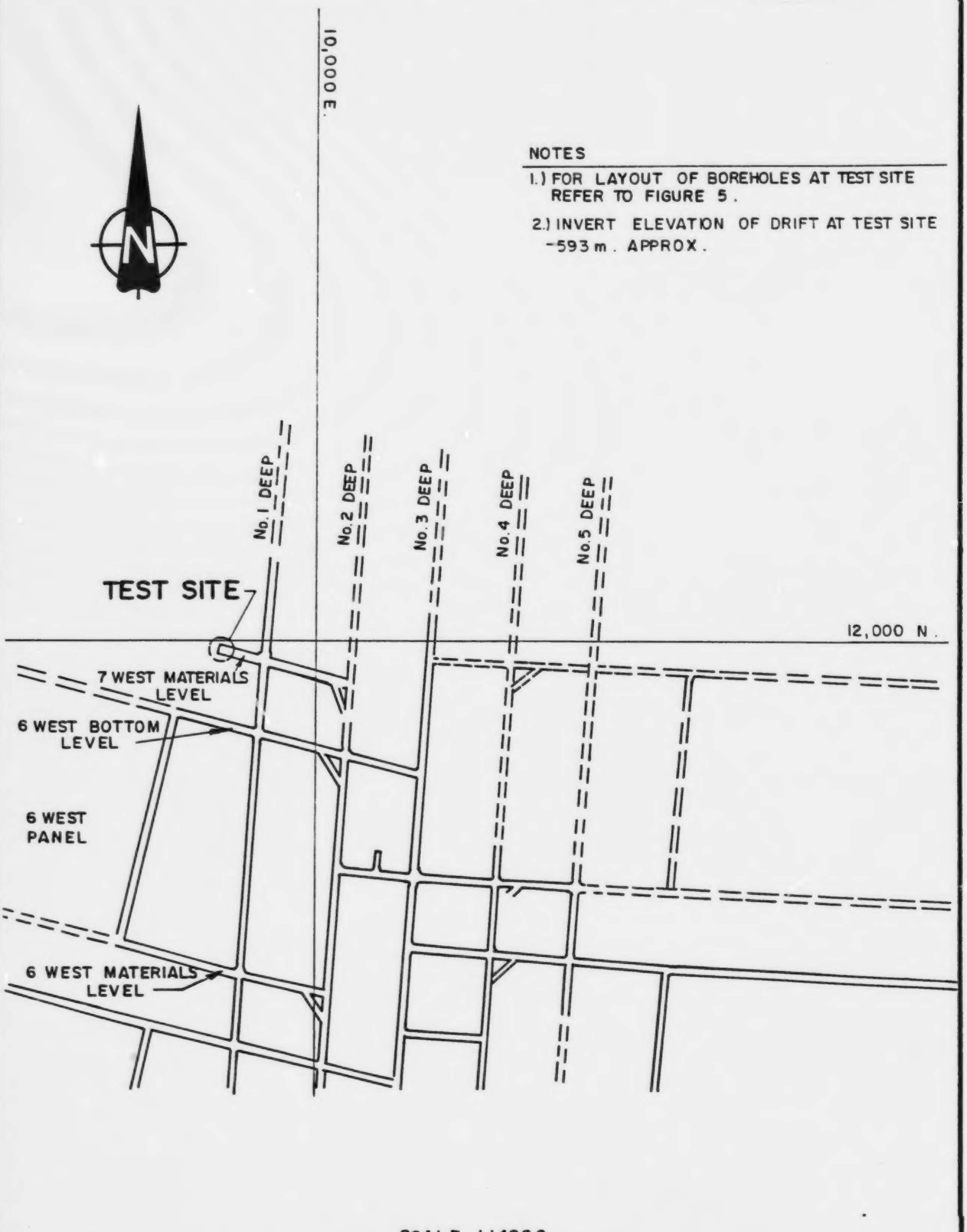
10,000 E.
N
No.1 DEEP
No.2 DEEP
No.3 DEEP
No.4 DEEP
No.5 DEEP
TEST SITE
12,000 N.
7 WEST MATERIALS LEVEL
6 WEST BOTTOM LEVEL
6 WEST PANEL
6 WEST MATERIALS LEVEL

NOTES

1.) FOR LAYOUT OF BOREHOLES AT TEST SITE REFER TO FIGURE 5.

2.) INVERT ELEVATION OF DRIFT AT TEST SITE -593 m. APPROX.

SCALE 1:4800

Date MAY 15, 1986

Project 851-6025

Golder Associates

Drawn D.M.

Chkd. J.G.

PLAN SHOWING LOCATIONS OF BOREHOLES FOR IN SITU STRESS MEASUREMENTS - PRINCE MINE

FIGURE 4

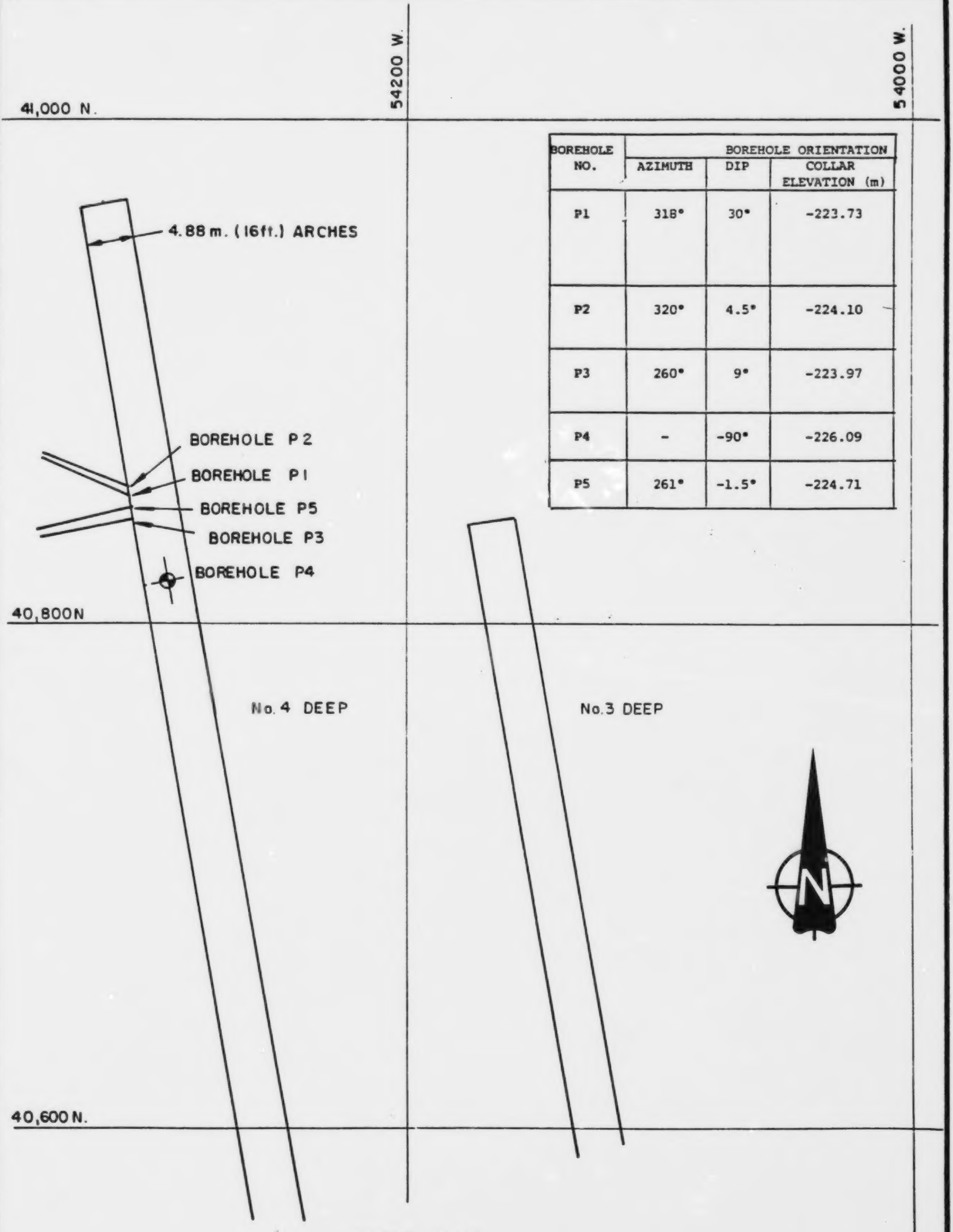
54200 W.
54000 W.
41,000 N.
4.88 m. (16ft.) ARCHES
BOREHOLE P2
BOREHOLE P1
BOREHOLE P5
BOREHOLE P3
BOREHOLE P4
40,800N
No. 4 DEEP
No. 3 DEEP
N
40,600 N.

BOREHOLE NO.	BOREHOLE ORIENTATION		
	AZIMUTH	DIP	COLLAR ELEVATION (m)
P1	318°	30°	-223.73
P2	320°	4.5°	-224.10
P3	260°	9°	-223.97
P4	-	-90°	-226.09
P5	261°	-1.5°	-224.71

SCALE 1:100

Date MAY 16, 1986
Project 851-6025

Golder Associates

Drawn D.M.
Chkd.

PLAN SHOWING LOCATIONS OF BOREHOLES FOR IN SITU STRESS MEASUREMENTS-LINGAN MINE

FIGURE 5

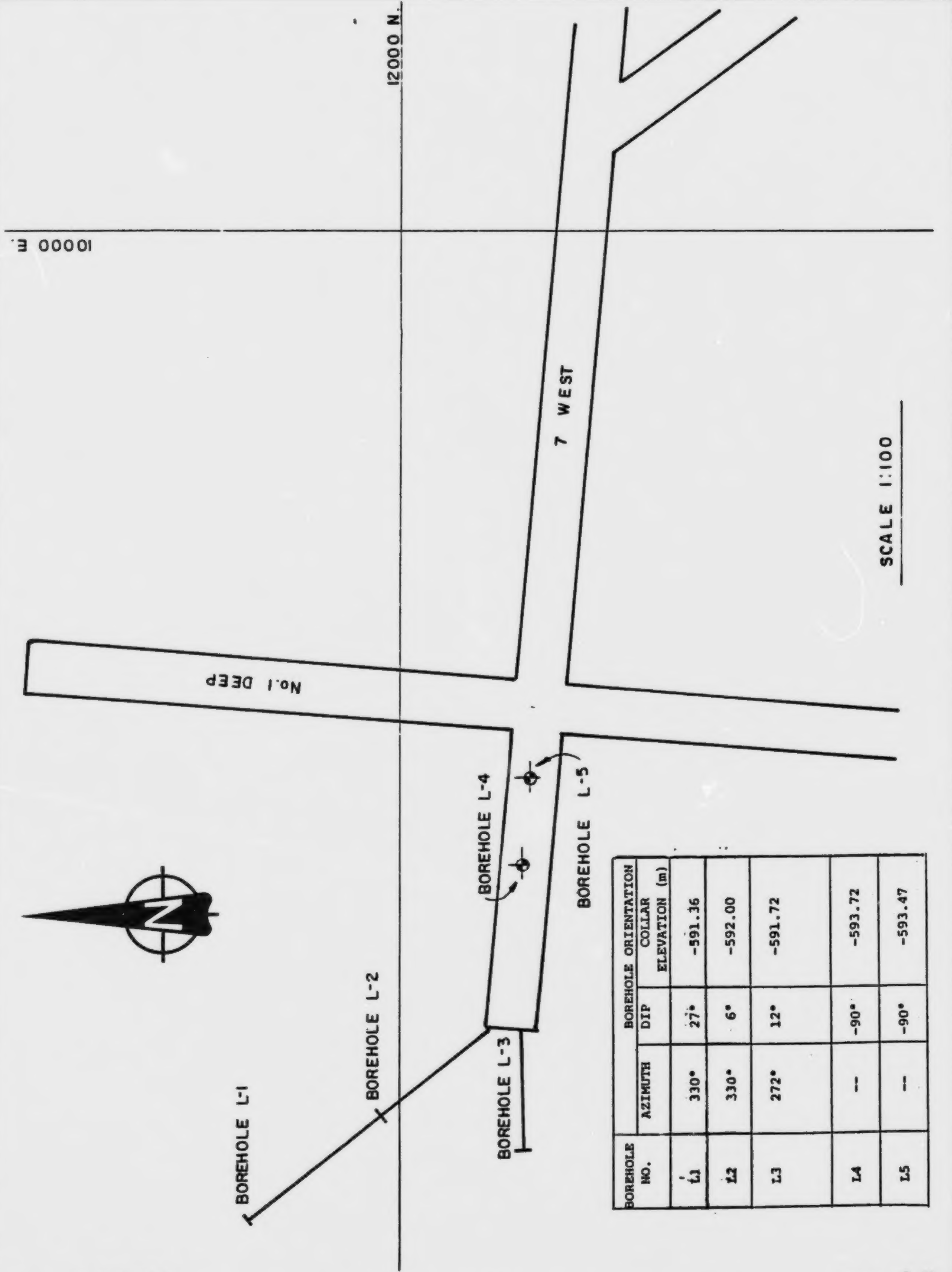
12000 N.
10000 E.
7 WEST
No.1 DEEP
BOREHOLE L-1
BOREHOLE L-2
BOREHOLE L-3
BOREHOLE L-4
BOREHOLE L-5
N
SCALE 1:100

BOREHOLE NO.	BOREHOLE ORIENTATION		
	AZIMUTH	DIP	COLLAR ELEVATION (m)
L1	330°	27°	-591.36
L2	330°	6°	-592.00
L3	272°	12°	-591.72
L4	—	-90°	-593.72
L5	—	-90°	-593.47

Date MAY 15,1986

Project 851-6025

Golder Associates

Drawn D. M.

Chkd.

STRESS MEASUREMENT BY OVERCORING METHOD

FIGURE 6

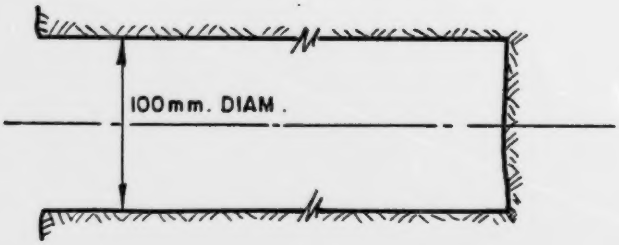

A) 100mm. DIAM. BOREHOLE DRILLED TO THE DEPTH AT WHICH THE STRESS IS TO BE DETERMINED

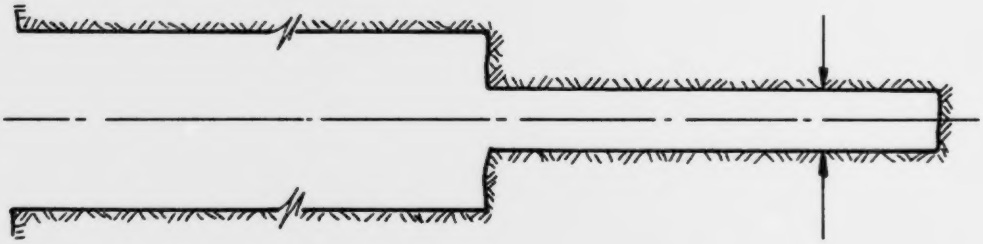

B) EXT BOREHOLE DRILLED FOR 500mm. TO 600mm. INTO THE END OF THE BOREHOLE

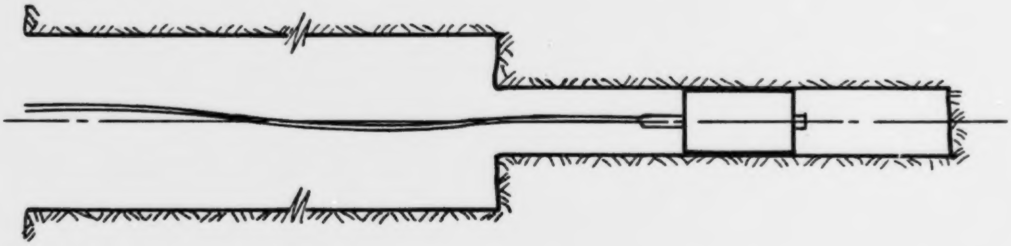

C) CSIRO OR USBM BOREHOLE GAUGE INSTALLED IN CENTRAL SECTION OF EXT BOREHOLE

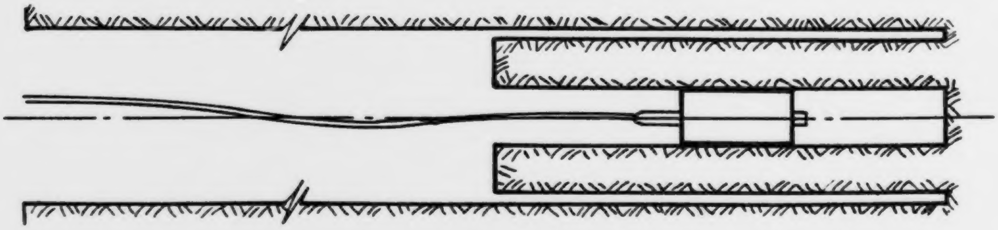

D) EXT BOREHOLE OVERCORED USING A 100mm. DIAM. THINWALL BIT

NOT DRAWN TO SCALE

Date MAY 15,1986
Project 851-6025

Golder Associates

Drawn D. M.
Chkd.

PRESSURE Vs. TIME
RECORD OF AN IDEALIZED HYDROFRACTURE TEST

FIGURE 7

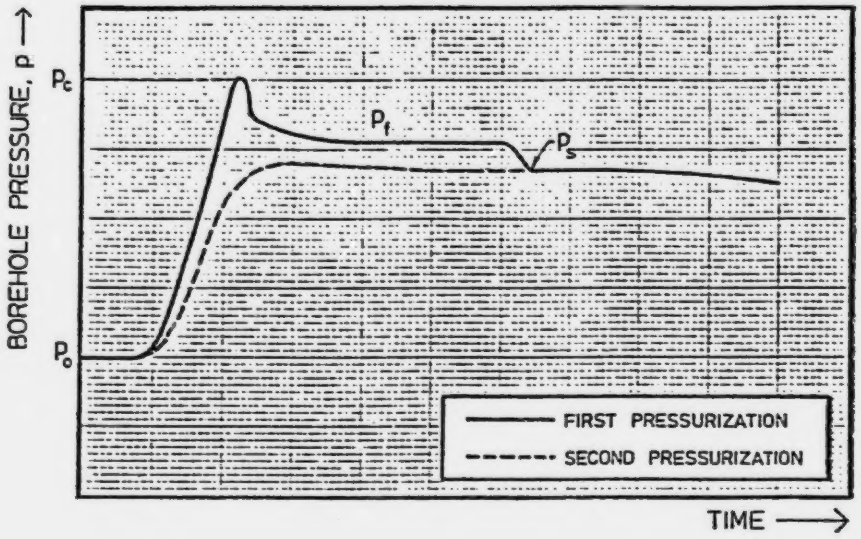

CASE (a): IDENTIFIABLE BREAKDOWN PRESSURE, P_c,

P_c - BREAKDOWN PRESSURE
P_f - FRACTURE PRESSURE
P_s - SHUT-IN PRESSURE
P_o - WELLBORE PRESSURE PRIOR TO TEST

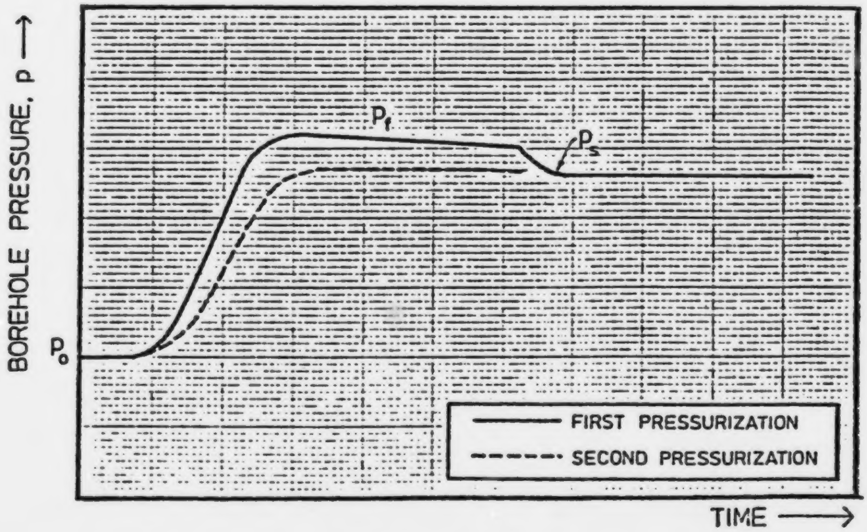

CASE (b): NON-IDENTIFIABLE BREAKDOWN PRESSURE, P_c,

Date MAY 21, 1986
Project 851-6025

Golder Associates

Drawn D.M.
Chkd.

SCHEMATIC LAYOUT OF HYDROFRACTURE TEST EQUIPMENT

FIGURE 8

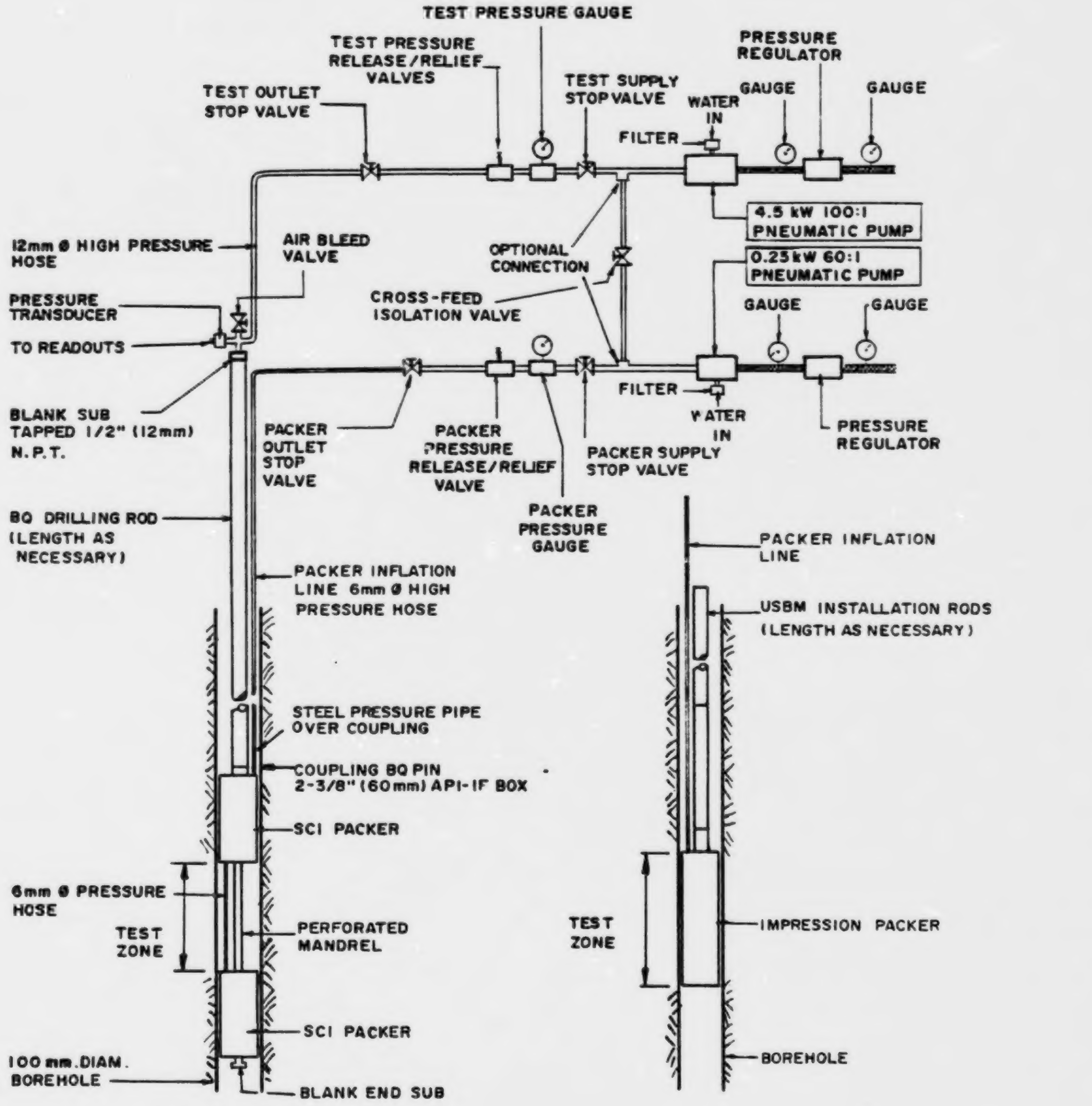
TEST PRESSURE GAUGE
TEST PRESSURE RELEASE/RELIEF VALVES
PRESSURE REGULATOR
TEST OUTLET STOP VALVE
TEST SUPPLY STOP VALVE
WATER IN
GAUGE
GAUGE
FILTER
4.5 kW 100:1 PNEUMATIC PUMP
12mm Ø HIGH PRESSURE HOSE
AIR BLEED VALVE
OPTIONAL CONNECTION
0.25 kW 60:1 PNEUMATIC PUMP
PRESSURE TRANSDUCER
CROSS-FEED ISOLATION VALVE
GAUGE
GAUGE
TO READOUTS
FILTER
WATER IN
BLANK SUB TAPPED 1/2" (12mm) N.P.T.
PACKER OUTLET STOP VALVE
PACKER PRESSURE RELEASE/RELIEF VALVE
PACKER SUPPLY STOP VALVE
PRESSURE REGULATOR
PACKER PRESSURE GAUGE
BQ DRILLING ROD (LENGTH AS NECESSARY)
PACKER INFLATION LINE 6mm Ø HIGH PRESSURE HOSE
PACKER INFLATION LINE
USBM INSTALLATION RODS (LENGTH AS NECESSARY)
STEEL PRESSURE PIPE OVER COUPLING
COUPLING BQ PIN 2-3/8" (60mm) API-IF BOX
SCI PACKER
6mm Ø PRESSURE HOSE
TEST ZONE
PERFORATED MANDREL
TEST ZONE
IMPRESSION PACKER
SCI PACKER
100 mm. DIAM. BOREHOLE
BOREHOLE
BLANK END SUB

A) PRESSURIZATION OF TEST ZONE

B) IMPRESSION PACKER TEST TO RECORD FRACTURE DETAILS IN TEST ZONE

NOT DRAWN TO SCALE

Date MAY 16, 1986
Project 851-6025

Golder Associates

Drawn RWR
Chkd.

STRADDLE PACKER ASSEMBLY FOR HYDROFRACTURE TESTS

FIGURE 9

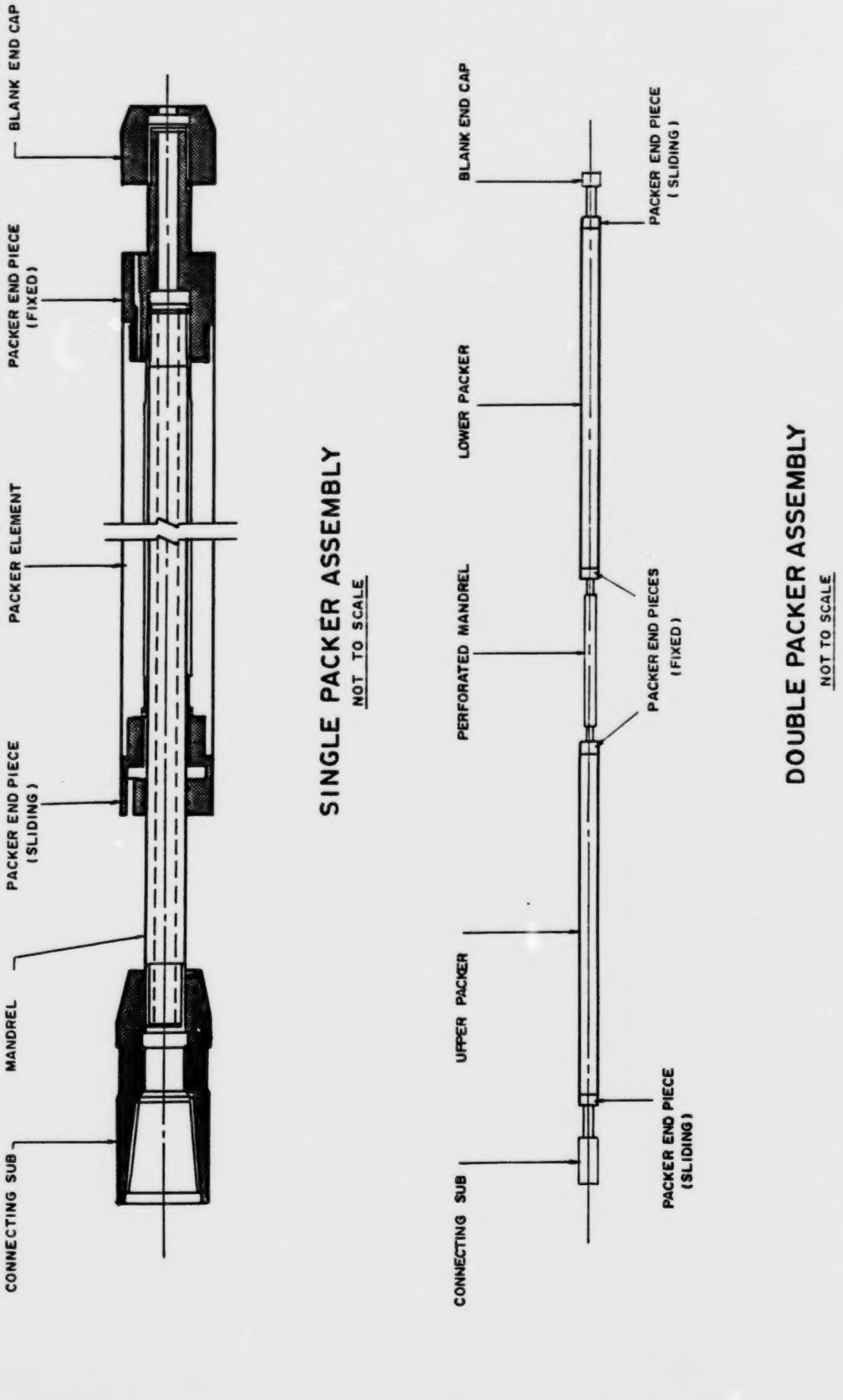
BLANK END CAP
PACKER END PIECE (FIXED)
PACKER ELEMENT
PACKER END PIECE (SLIDING)
MANDREL
CONNECTING SUB
BLANK END CAP
PACKER END PIECE (SLIDING)
LOWER PACKER
PACKER END PIECES (FIXED)
PERFORATED MANDREL
UPPER PACKER
PACKER END PIECE (SLIDING)
CONNECTING SUB

SINGLE PACKER ASSEMBLY
NOT TO SCALE

DOUBLE PACKER ASSEMBLY
NOT TO SCALE

Date MAY 16, 1986
Project 851-6025

Golder Associates

Drawn RWR
Chkd.

PRINCIPAL STRESS DIRECTIONS MEASURED IN SYDNEY COALFIELD

FIGURE 10

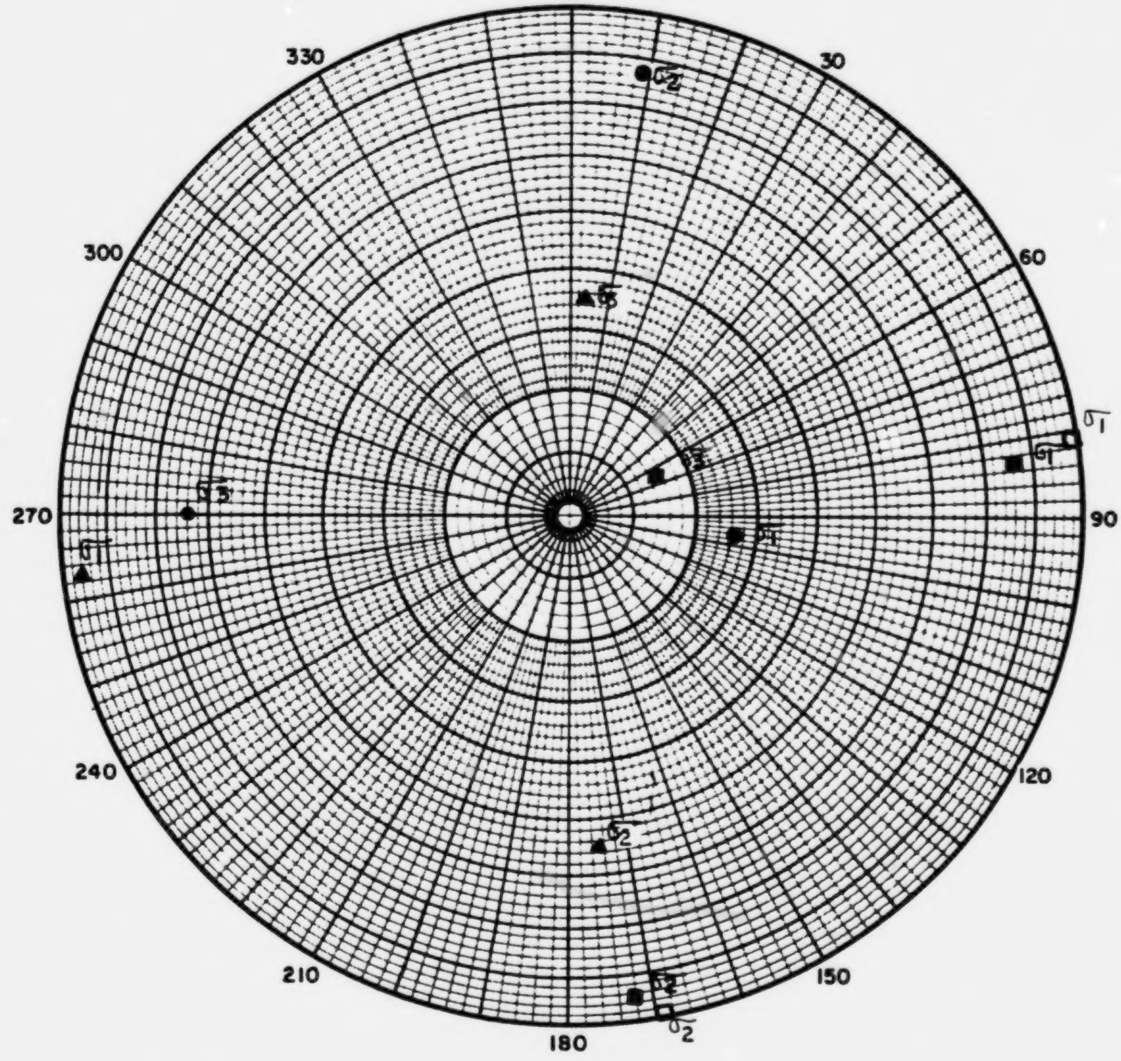

POLAR EQUAL AREA STEREONET
LOWER HEMISPHERE PROJECTION

NOTES

1) σ_1, σ_2, σ_3 = MAJOR, INTERMEDIATE AND MINOR PRINCIPAL STRESSES RESPECTIVELY

2) ● DATA FROM No. 26 COLLIERY
■ DATA FROM PRINCE MINE
▲ DATA FROM LINGAN MINE
} OBTAINED FROM OVERCORING TESTS USING USBM GAUGE.

□ DATA FROM PRINCE MINE - OBTAINED FROM HYDROFRACTURE TEST

Date MAY 21, 1986
Project No. 851-6025

Golder Associates

Drawn D.M.
Chkd.

STRESS COMPONENTS MEASURED AT DIFFERENT MINES IN THE SYDNEY COALFIELD

FIGURE 11

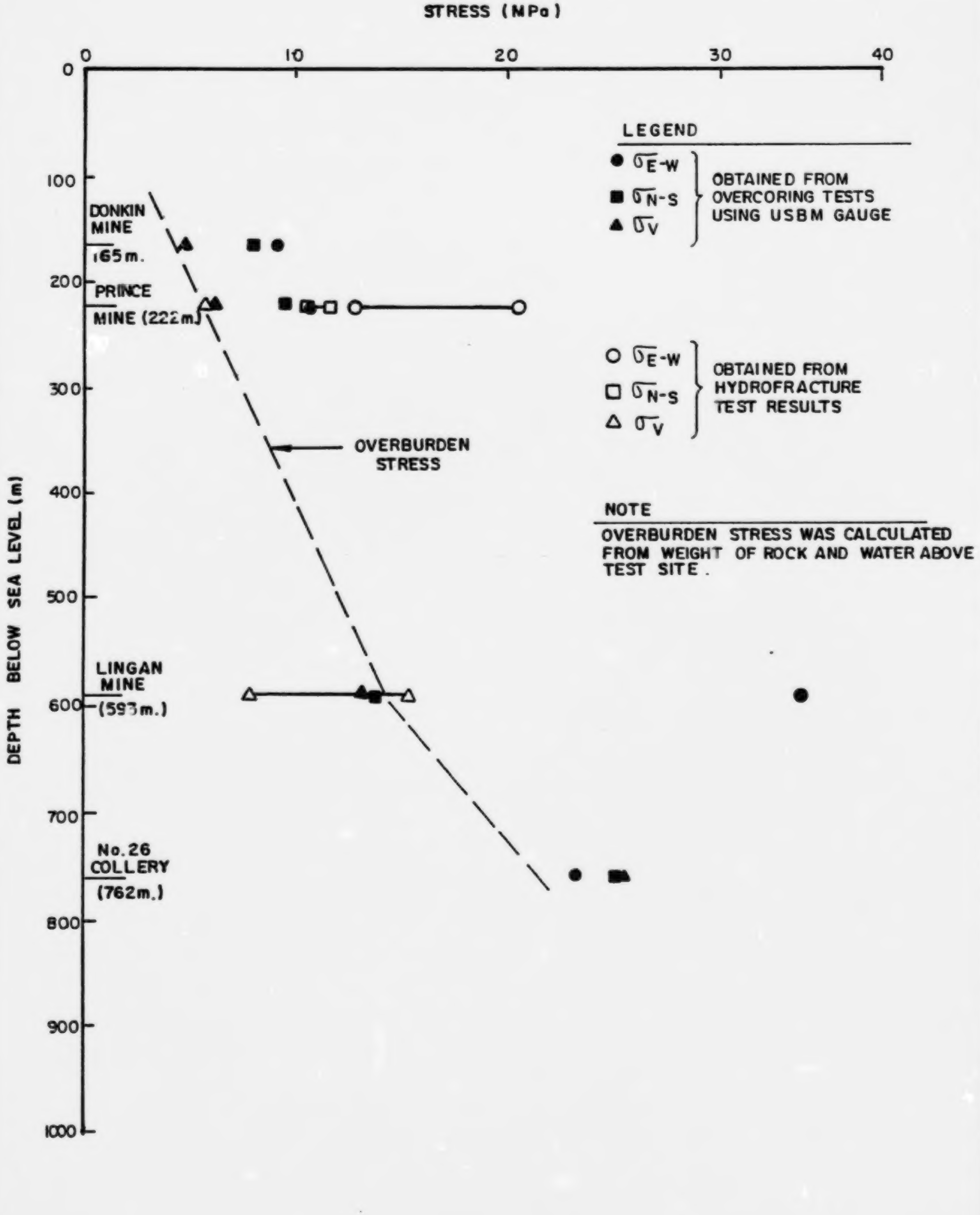

NOTE

OVERBURDEN STRESS WAS CALCULATED FROM WEIGHT OF ROCK AND WATER ABOVE TEST SITE.

Date MAY 21, 1986

Project 851-6025

Golder Associates

Drawn D. M.

Chkd.

PLATE 1. a) USBM DEFORMATION GAUGE

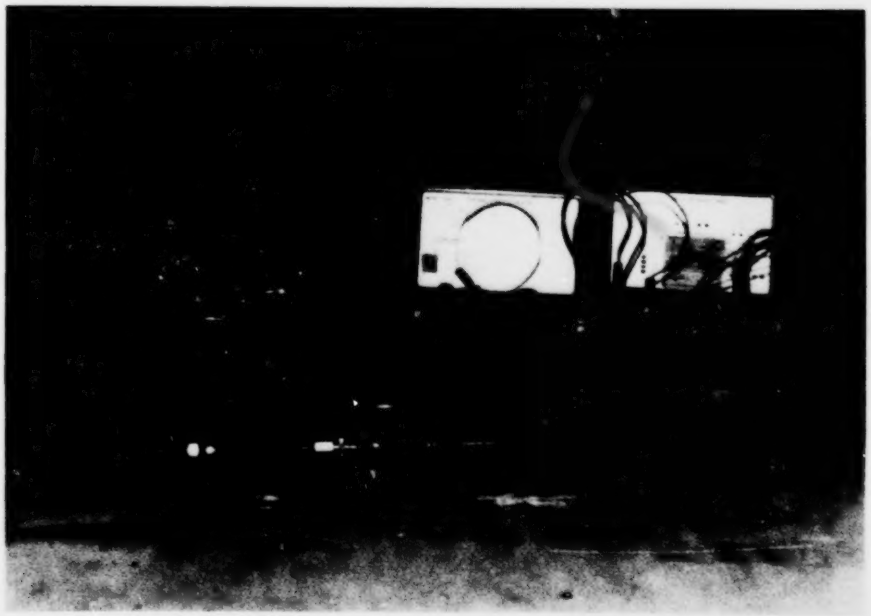

PLATE 1. b) SET-UP FOR BIAXIAL TEST

PLATE 2. a) GENERAL ARRANGEMENT OF DRILL RIG AT PRINCE MINE.

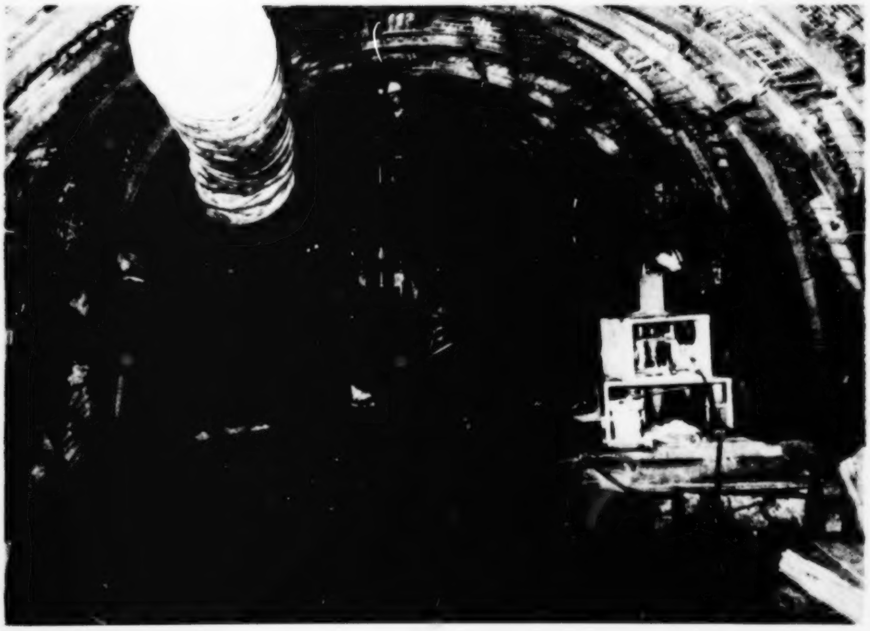

PLATE 2. b) GENERAL ARRANGEMENT OF DRILL RIG AT PRINCE MINE SHOWING HYDROFRACTURE EQUIPMENT,

PLATE 3. a) HYDROFRACTURE STRADDLE PACKER ASSEMBLY.

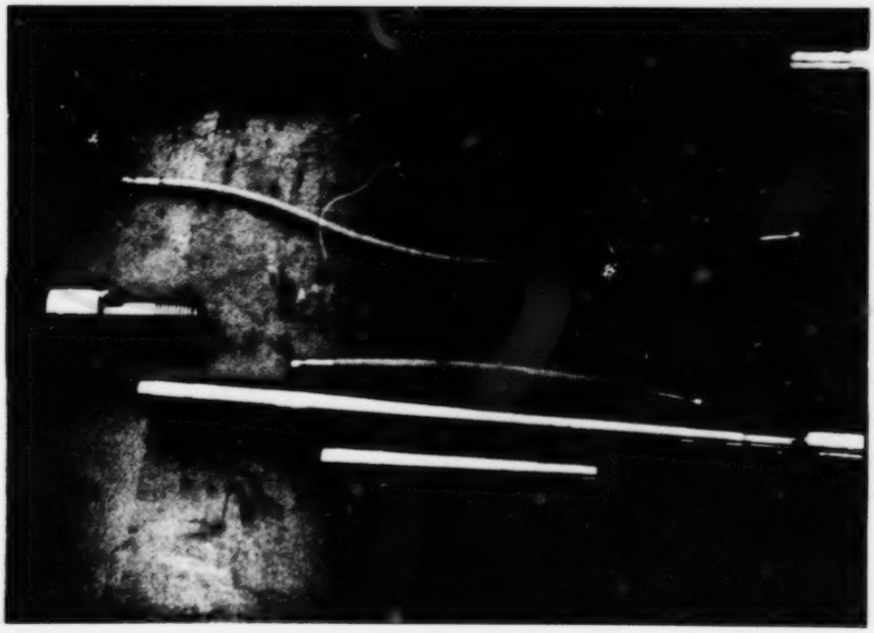

PLATE 3. b) HYDROFRACTURE PERFORATED MANDREL.

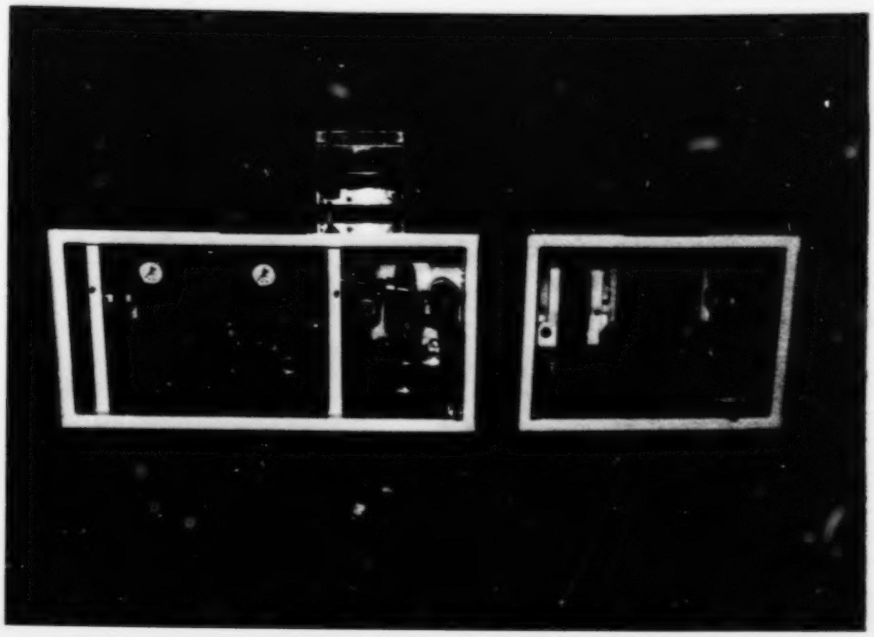

PLATE 4. a) HYDROFRACTURE TEST ZONE AND PACKER INFLATION PUMPS.

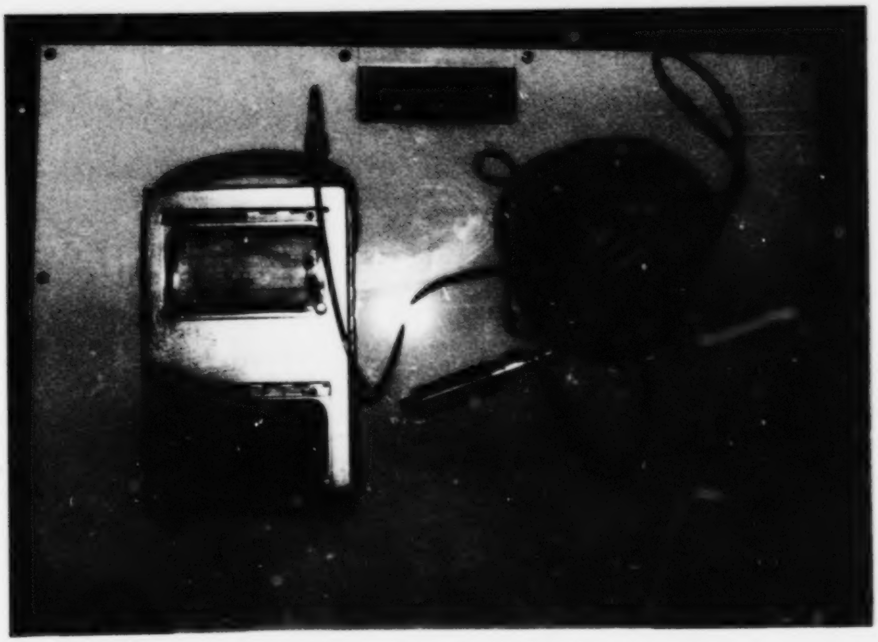

PLATE 4. b) HYDROFRACTURE CHARGE RECORDER AND PRESSURE TRANSDUCER.

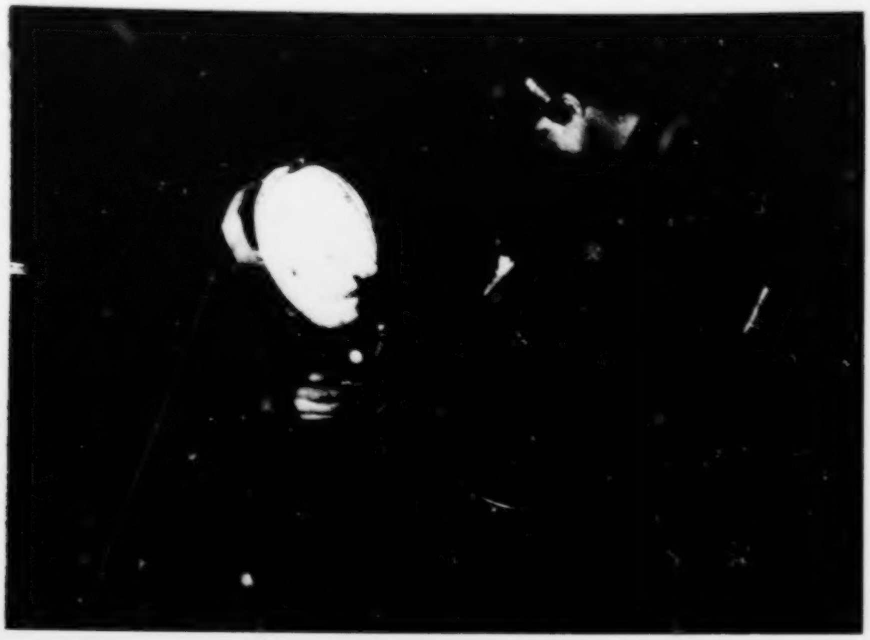

PLATE 5. HYDROFRACTURE IMPRESSION PACKER WITH TYPICAL FRACTURE TRACE SHOWN.

APPENDIX A

BOREHOLE RECORDS

ORM 1076

CAPE BRETON DEVELOPMENT CORPORATION

LOG SHEET

BOREHOLE NUMBER PM - 35 (P-1) LOCATION PRINCE MINE

COORDINATES N ~~S~~ 40,769 ELEVATION TOP OF CASING

~~E~~ W 54,245 TOP OF GROUND

TOTAL LENGTH 79'0"

DATE STARTED FINISHED

PURPOSE OF HOLE Determination of in situ stress by overcoring and minifracturing

SEAM OF INTEREST Hub

SEAM INTERSECTED None

CONTRACTOR Logan; Golder

DRILL PERSONNEL FOREMAN John Newsome

RUNNERS Bill Gillis

DRILLING METHOD Diamond

CORE SIZE HQ BEARING OF HOLE 323°

INCLINATION +28° OVERBURDEN DEPTH N.A.

CASING USED CEMENTED YES ☐ NO ☐

TESTS TAKEN IN HOLE

GEOPHYSICAL LOGGING None

REMARKS 1. Canmet program - Tim Aston

2. Hole drilled on 4 Deep

LOGGED BY Steve Forgeron

PM - 35

0 - 29'3"	SANDSTONE (29'3")	Light grey; minor siltstone, competent; entire sandstone section is noncalcareous and locally has high porosity (visual estimate 10-20%) : 0 - 26'1"; light grey; fine to medium grained (80% medium); locally coarse grained; core generally shows ghost cross bedding (3 inches to 3 feet apart); several well developed bedding planes marked with carbonaceous material. : 2'0"; bedding at 30° to long core axis. : 25'8" to 26'1"; sandstone fines upward : 26'1"; sandstone cut off by siltstone. : 26'1" - 26'5"; siltstone; dark grey; laminated; sharp contacts with overlying and underlying sandstone. : 26'5" - 27'9"; fine grained sandstone; light grey; contains rounded fragments and lenses of mudstone (up to 1") parallel to bedding. : 27'9" - 29'3"; medium grained; cross bedded. : abrupt contact at 29'3".
29'3" - 39'2"	LAMINITE (9'11")	Interbedded siltstone (dark grey) and sandstone (fine grained; light grey); unit is competent. : 29'3" - 29'6"; laminated siltstone; grades into laminite. : 29'6" - 33'0"; approximately 60% siltstone and 40% sandstone; laminations are mainly parallel but some are curved; beds are less than 1 cm thick. : 33'0" - 35'1"; approximately 80% sandstone and 20% siltstone; beds are generally thicker than below; mainly parallel bedding; cross bedding present. : 35'1" - 39'2"; approximately 80% siltstone and 20% sandstone; beds are generally less than 1 cm thick; bedding at 35° to long core axis.

39'2" - 66'8"	SANDSTONE (27'6")	Light grey; fine to medium grained (locally coarse); competent. : 39'2" - 39'5"; very coarse grained; quartz fragments up to 1 cm long; lithic fragments up to 2 cm long; fragments angular to sub-rounded. : 39'5" - 41'5"; generally massive; ghost bedding present. : 41'5" - 43'8"; some carbonaceous material parallel to bedding; several thin lenses (1-2 mm) of coarse grained sandstone; bedding at 45° to long core axis. : 43'8" - 45'5"; coarse grained; contains quartz grains up to 4 mm in size; contains a few mudstone fragments up to 1 cm in size; grains generally angular to sub-rounded; carbonaceous material and shards quite common; dickite common between grains; becomes fine to medium grained in top 3" of section. : 45'5" - 48'7"; generally massive; bedding becoming developed near top of section; bedding at 50° to C.A. : 48'7" - 49'7"; parallel bedding; some carbonaceous material along bedding. : 49'7" - 51'6"; fairly massive; ghost bedding. : 51'6" - 61'6"; bedding faintly developed; several coal shards present; minor amount of dickite. : 61'0"; bedding at 35° to long core axis. : 61'6" - 66'8"; bedding developed; carbonaceous material along bedding. : 63'6"; bedding at 40° to long core axis. : 66'8"; abrupt contact : entire sandstone unit is non calcareous locally quite porous
66'8" - 70'0"	MUDSTONE (3'4")	grey; unit consists of mudstone with approximately 25% sandstone as thin sandstone lenses. Slumping and discontinuous features main characteristic of section.

70'0" - 79'0"	MUDSTONE (9'0")	grey; little to no silt; rock unit is weak, incompetent. : 74'10" - 79'0"; core highly broken in core box; listric surfaces are common.
79'0"	END OF	HOLE

4 Slant Deep
PM - 35

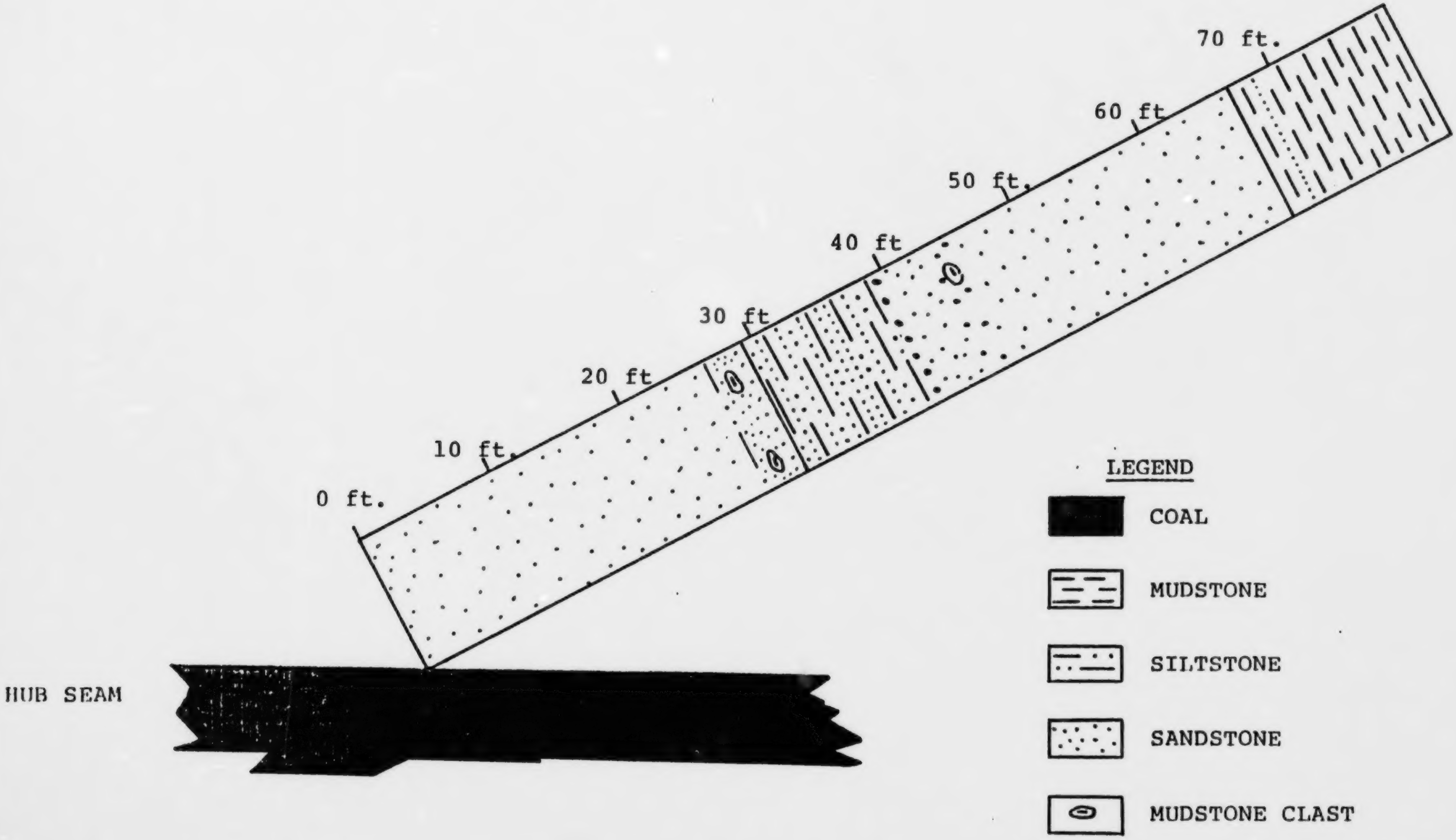
70 ft.
60 ft
50 ft.
40 ft
30 ft
20 ft
10 ft.
0 ft.
HUB SEAM
LEGEND
COAL
MUDSTONE
SILTSTONE
SANDSTONE
MUDSTONE CLAST

FORM 1076

CAPE BRETON DEVELOPMENT CORPORATION

LOG SHEET

BOREHOLE NUMBER PM-36 (P-2) LOCATION Prince Mine

COORDINATES N S ________ ELEVATION TOP OF CASING ________

E W ________ TOP OF GROUND ________

TOTAL LENGTH 43.7'

DATE STARTED ________ FINISHED ________

PURPOSE OF HOLE Determination of in situ stress by overcoring and minifracturing

SEAM OF INTEREST Hub

SEAM INTERSECTED None

CONTRACTOR Logan; Golder

DRILL PERSONNEL FOREMAN John Newsome

RUNNERS Bill Gillis

DRILLING METHOD Diamond

CORE SIZE ________ BEARING OF HOLE 323°

INCLINATION +6° OVERBURDEN DEPTH ________

CASING USED ________ CEMENTED YES ☐ NO ☐

TESTS TAKEN IN HOLE ________

GEOPHYSICAL LOGGING None

REMARKS 1. Canmet program - Tim Aston

2. Hole drilled on 4 Deep

LOGGED BY Steve Forgeron

PM - 36

0 - 2.5'	COAL (2.5')	
2.5' - 4.8'	COAL AND SANDSTONE - (2.3')	Top of seam and immediate roof
4.8' - 43.7'	SANDSTONE - (38.9')	Fine to medium grained; light grey; generally massive (minor ghost bedding and cross bedding marked with carbonaceous material). : 29.0' - 38.0'; several coarse grained lenses 5 mm to 2 cm thick. : 40.9' - 43.7'; approximately 30% coarse grained, entire section is noncalcareous and locally porous
43.7'	END OF HOLE	

PRINCE MINE
4 Slant Deep
PM - 36

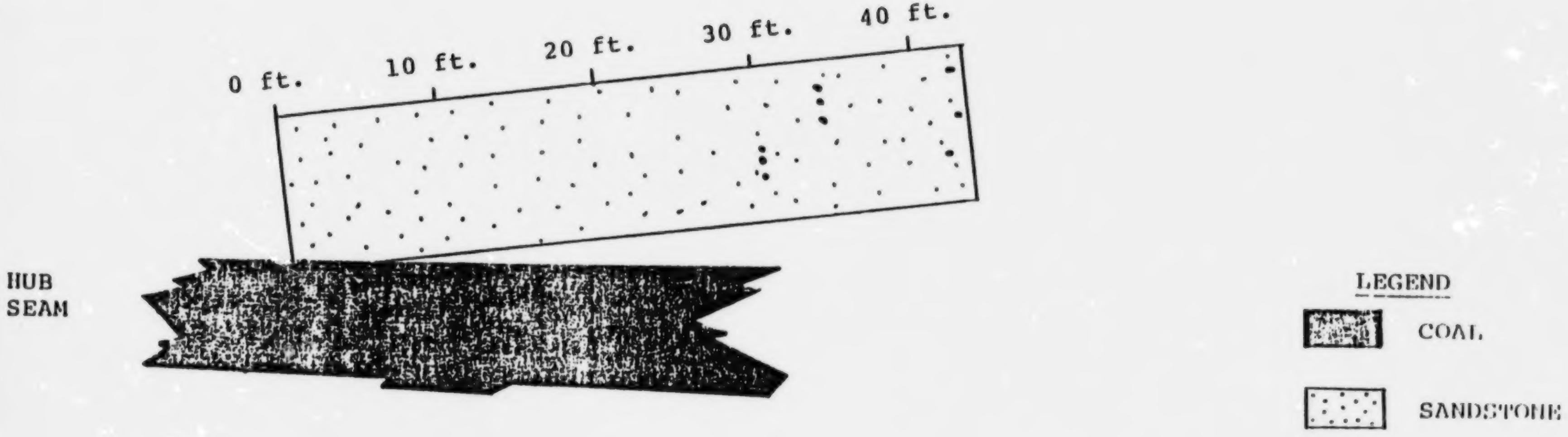
0 ft.
10 ft.
20 ft.
30 ft.
40 ft.
HUB
SEAM
LEGEND
COAL
SANDSTONE

FORM 1076

CAPE BRETON DEVELOPMENT CORPORATION

LOG SHEET

BOREHOLE NUMBER PM-37 (P-3) LOCATION Prince Mine

COORDINATES N S ____ ELEVATION TOP OF CASING ____

E W ____ TOP OF GROUND ____

TOTAL LENGTH 32' 0"

DATE STARTED ____ FINISHED ____

PURPOSE OF HOLE Determination of in situ stress by overcoring and minifracturing

SEAM OF INTEREST Hub

SEAM INTERSECTED None

CONTRACTOR Logan, Golder

DRILL PERSONNEL FOREMAN John Newsome

RUNNERS Bill Gillis

DRILLING METHOD Diamond

CORE SIZE ____ BEARING OF HOLE 261°

INCLINATION +6° OVERBURDEN DEPTH ____

CASING USED ____ CEMENTED YES ☐ NO ☐

TESTS TAKEN IN HOLE ____

GEOPHYSICAL LOGGING None

REMARKS 1. Canmet program - Tim Aston

2. Hole drilled on 4 Deep

LOGGED BY Steve Forgeron

PM - 37

0 - 3' 11"	COAL	
3' 11" - 5' 7"	COAL and SANDSTONE	- top of seam and immediate roof
5' 7" - 32' 0"	SANDSTONE	- Medium to coarse grained; light grey; carbonaceous bands common throughout section; competent.
32.0"	END OF HOLE	

PRINCE MINE
4 Slant Deep
PM - 37

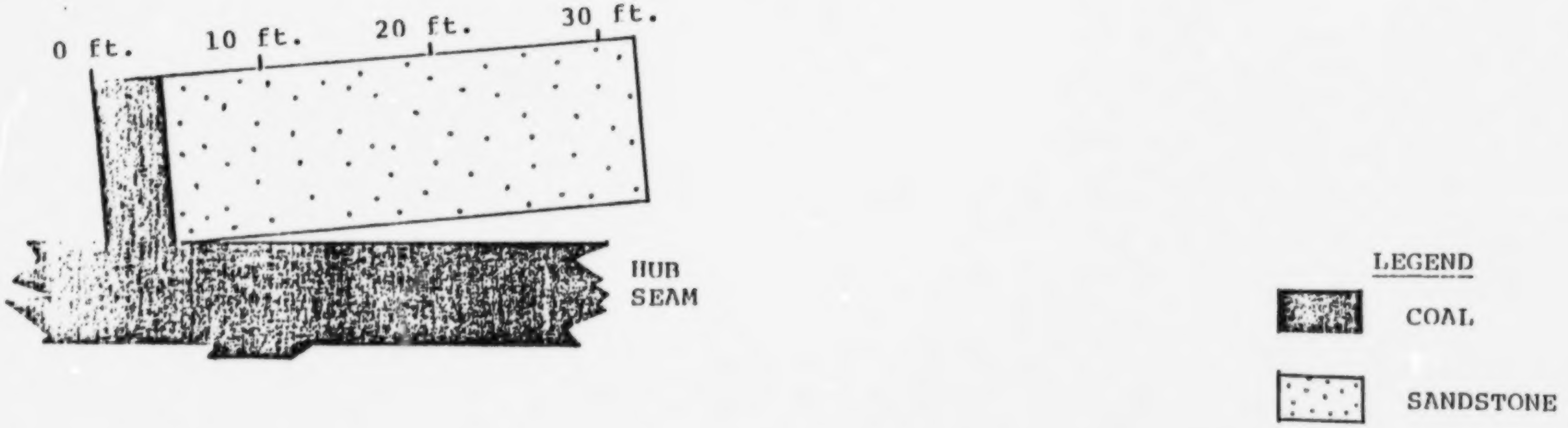
0 ft.
10 ft.
20 ft.
30 ft.
HUB
SEAM
LEGEND
COAL
SANDSTONE

M 1076

CAPE BRETON DEVELOPMENT CORPORATION

LOG SHEET

BOREHOLE NUMBER PM-38 (P-4) LOCATION Prince Mine

COORDINATES N ~~S~~ 40,760 ELEVATION TOP OF CASING

~~E~~ W 54,235 TOP OF GROUND

TOTAL LENGTH 98'0"

DATE STARTED FINISHED

PURPOSE OF HOLE Determination of in situ stress by overcoring and minifracturing

SEAM OF INTEREST Hub

SEAM INTERSECTED None

CONTRACTOR Logan; Golder

DRILL PERSONNEL FOREMAN John Newsome

RUNNERS Bill Gillis

DRILLING METHOD Diamond

CORE SIZE BEARING OF HOLE N.A.

INCLINATION -90° OVERBURDEN DEPTH N.A.

CASING USED CEMENTED YES ☐ NO ☐

TESTS TAKEN IN HOLE

GEOPHYSICAL LOGGING None

REMARKS 1) CANMET program - Tim Aston.

2) Hole drilled on 4 Deep.

LOGGED BY Steve Forgeron

PM - 38

0 - 3'5"	SILTSTONE (3'5")	- Medium grey; competent; stigmaria present; a few slickensided planes; sharp irregular lower contact.
3'5" - 32'7"	SANDSTONE (29'2")	- Fine to medium grained; light grey, noncalcareous, slightly porous. : 3'5" - 8'6"; well laminated; beds dip at 15° to long core axis; carbonaceous material and mica abundent along bedding planes; cross-bedded; becomes more massive near bottom of unit. : 8'6" - 32'7"; beds range from 60 cm to 1 mm thick; carbonaceous material and mica along bedding planes. : 19' - 21'; massive. : 25'7" - 27'8"; trace of bedding. : 22'; beds dip at 15° to long core axis. : 32'7"; sharp contact.
32'7" - 34'7"	SHALE (2'0")	- Medium to dark grey; soft; slickensided planes abundent; several clay zones 0.25" thick. : 32'7" - 33'1"; siderite nodules present. : 32'7" - 33'1"; black shale; fissile; abundent plant fossils; highly broken in core box.
34'7" - 36'3"	COAL (1'8")	- Rider seam; well developed cleat with pyrite and ankerite; core intact.
36'3" - 39'6"	MUDSTONE (3'3")	- Slightly silty; seatearth; ironstone nodules present; abundent stigmaria; gradational lower contact.
39'6" - 45'6"	SHALE (6'0")	- Medium grey; slity (30%); well laminated; thin (1 cm) grey siltstone beds throughout section; irregular nodules and bands of siderite throughout section; gradational lower contact.
45'6" - 48'6"	SANDSTONE (3'0")	- Fine grained; light grey; laminated; very hard; some carbonaceous material along bedding.

...../2

48'6" - 56'10"	MUDSTONE (8'4")	- Medium to dark grey; silty (30%); siltstone generally occurs as bed 3 to 5" thick; calcite nodules common. : 52'10" - 53'10"; dark grey. : 55'10" - 56'10"; dark grey. : 56'10"; sharp contact.
56'10" - 58'0"	SILTSTONE (1'2")	- Grey; massive; hard. : 58'0"; gradational contact.
58'0" - 61'1"	SANDSTONE (3'1")	- Light grey; massive; very hard. : 60'1" - 61'1"; minor irregular contorted bedding. : 61'1"; sharp erosional contact.
61'1" - 65'2"	INTERBEDDED SEQUENCE (4'1")	- 33% each of siltstone, fine grained sandstone and shale; laminated; beds 3 to 6" thick; competent.
65'2" - 68'9"	MUDSTONE (3'7")	- Dark grey. : 67'4" - 68'8"; red-brown; nodules and disseminated grains of calcite. : 68'9"; abrupt contact.
68'9" - 69'7"	SILTSTONE (0'10")	- Medium grey; massive. : 69'7"; grades quickly to dark grey mudstone.
69'7" - 72'4"	MUDSTONE (2'9")	- Medium to dark grey; highly slickensided; greasy; several red-brown bands (less than 1" thick); quite massive; irregular streaks and patches of carbonaceous material.
72'4" - 76'0"	SILTSTONE (3'8")	- Medium grey; very hard. : 76'0"; gradational contact.
76'0" - 83'0"	MUDSTONE (7'0")	- Silty (20 to 30%); bedding marked by siltstone beds up to 6" thick; several lenses and thin bands of ironstone. : 83'0"; gradatioral contact.

...../3

83'0" - 88'0"	MUDSTONE (5'0")	- Medium to dark grey; slightly fissile (almost a shale); competent; a few plant fossils parallel to bedding. : 88'0"; grades quickly to siltstone.
88'0" - 98'0"	SILTSTONE (10'0")	- Medium grey; coarse grained; very hard; several ironstone or calcareous nodules; generally massive (minor bedding); a few plant fossils.
98'0"	END OF HOLE	

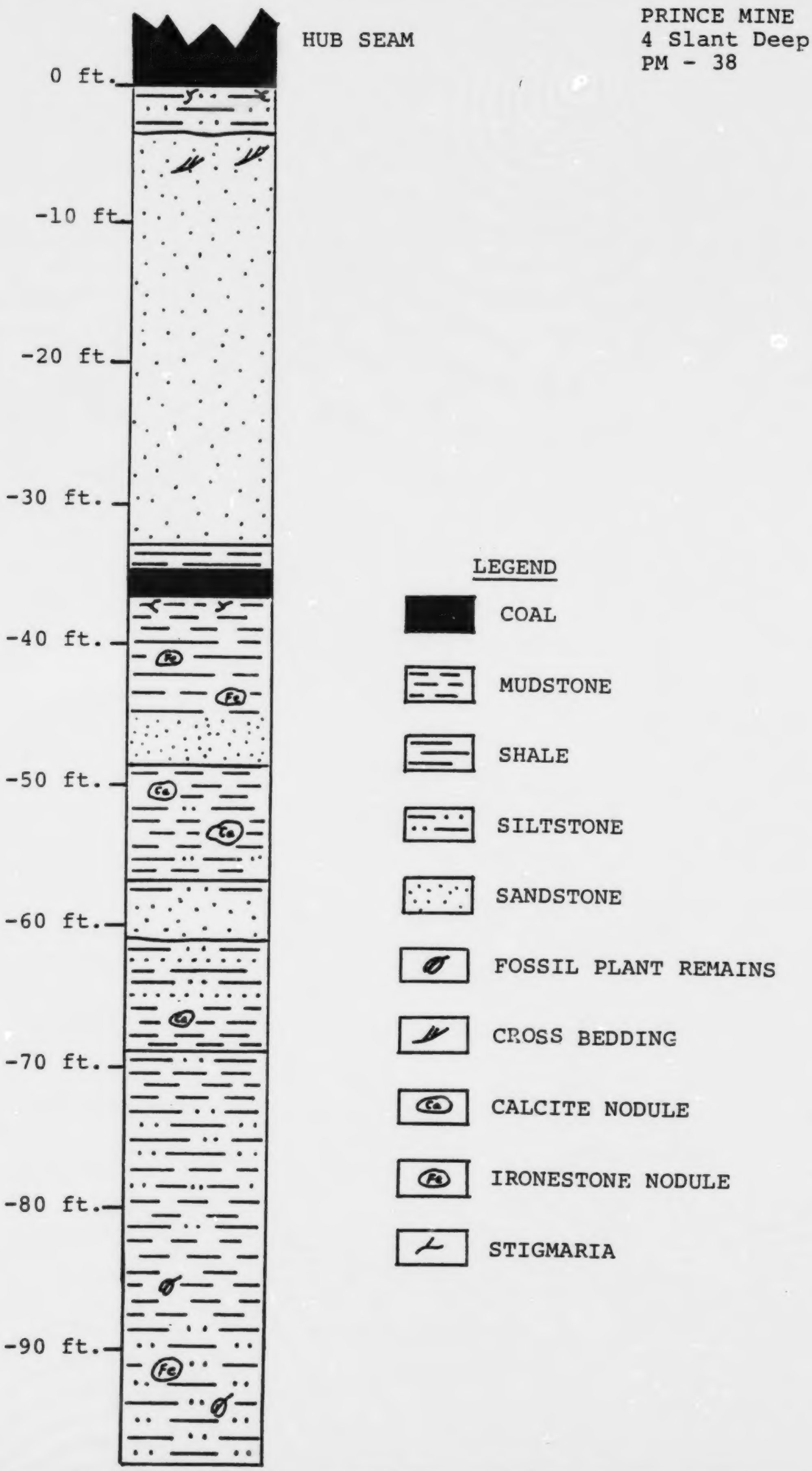

PRINCE MINE
4 Slant Deep
PM - 38

HUB SEAM
0 ft.
-10 ft.
-20 ft.
-30 ft.
-40 ft.
-50 ft.
-60 ft.
-70 ft.
-80 ft.
-90 ft.
LEGEND
COAL
MUDSTONE
SHALE
SILTSTONE
SANDSTONE
FOSSIL PLANT REMAINS
CROSS BEDDING
CALCITE NODULE
IRONESTONE NODULE
STIGMARIA
Fe
Ca

HOLE NO. L-1

DEPTH (m)	DESCRIPTION
0 - 7.44	SILTSTONE - medium grey; fine to medium grained; numerous fossiliferous pods; laminated wispy sandy sections throughout; crossbedded in places; micaceous; ironstone staining; carbonaceous partings; gradational contact; competent.
7.44 - 8.23	SANDSTONE - light to medium grey; fine grained; contains 30% laminated siltstone; entire unit is highly laminated; abundant carbonaceous material; gradational contact; competent.
8.23 - 13.41 (NOTE: 9.45 - 10.85 is missing)	SILTSTONE - medium grey; fine grained; micaceous; slightly fossiliferous; slightly cross bedded; a few small (wispy) beds of sandstone noted; gradational contact.
13.41 - 15.01	MUDSTONE - medium to dark grey; very silty; fossiliferous; slightly banded; erosive contact.
15.01 - 15.69	SANDSTONE - light to medium grey; fine grained; highly laminated; grades to a siltstone at base; slightly crossbedded; ironstone staining; gradational contact.
15.69 - 20.88	MUDSTONE - medium to dark grey; very silty in sections (≃25%); highly broken 18.11 - 18.28; siltstone from 19.81 to 20.24; gradational contact.
20.88 - 23.87	SANDSTONE - light to medium grey; highly laminated; micaceous; gradational contact; competent.
23.87 - 26.51	LIMESTONE - brownish grey; sugary texture; massive; sharp contact; competent.
26.51 - 30.40	SHALE/MUDSTONE - medium to dary grey; very little silt; bedded; slightly fossiliferous.

END OF HOLE

HOLE NO. L-2

DEPTH (m)	DESCRIPTION
0 - 0.33	MUDSTONE - dark grey; very silty fossiliferous; gradational contact.
0.33 - 7.82	SILTSTONE - medium grey; fine to medium grained; numerous wispy sandstone bands; slightly fossiliferous; coal shards; micaceous; gradational contact; competent.
7.82 - 12.32	SANDSTONE - light to medium grey; fine grained; highly laminated (contains ≈ 30% siltstone); siltstone beds up to 15 cm thick throughout; micaceous carbonaceous; last 25 cm of unit is bordering on a coarse siltstone; competent.

END OF HOLE

HOLE NO. L-3

DEPTH (m)	DESCRIPTION
0 - 0.91	MUDSTONE - medium grey; very silty; no plant fossils noted; noncalcareous; non micaceous; slickensided surfaces noted; gradational contact.
0.91 - 4.04	SILTSTONE - medium grey; fine grained; massive; calcareous; fossiliferous; competent.
4.04 - 4.29	SANDSTONE - light to medium grey; fine grained; crossbedded; slightly carbonaceous; contact (see Diagram); competent. 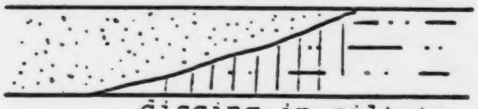 discing in siltstone
4.29 - 10.99	SILTSTONE - medium grey; medium grained; numerous wispy sandstone bands throughout (last 30 cm is quite sandy); only a few plant fossils noted; micaceous; competent.

END OF HOLE

HOLE NO. L-4

DEPTH (m)	DESCRIPTION
0 - 4.27	MUDSTONE - medium to dary grey; first 15 cm is quite silty; highly fossiliferous; first 3 m is highly broken up along bedding; gradational contact.
4.27 - 4.37	SILTSTONE - medium grey; laminated; slightly crossbedded; micaceous; fossiliferous; gradational contact; competent.
4.37 - 5.76	SANDSTONE - light grey; fine to medium grained; micaceous; slightly crossbedded; carbonaceous beds; erossive contact; competent.
5.76 - 6.75	MUDSTONE - medium to dark grey; highly fossiliferous; slickensided surfaces throughout; weak.
6.75 - 6.96	COAL
6.96 - 7.59	MUDSTONE - medium grey; seatearth; silty; gradational contact; weak.
7.59 - 8.17	SILTSTONE - medium grey; slightly laminated; sandy sections; micaceous; erosive contact; competent.
8.17 - 8.92	MUDSTONE - medium to dark grey; silty; fossiliferous; erosive contact.
8.92 - 10.67	SANDSTONE - light grey; fine to medium grained; massive; micaceous; silty sections; discing noted; gradational contact; competent.
10.67 - 12.62	SILTSTONE - medium to dark grey; fossiliferous; micaceous; laminated; competent.
12.62 - 12.80	COAL
12.80 - 13.16	MUDSTONE - dark grey; seatearth; fossiliferous; weak.
13.16 - 13.99	SILTSTONE - medium grey; medium grained; micaceous; carbonaceous; sandy sections; gradational contact; competent.
13.99 - 20.55	MUDSTONE - medium to dark grey; quite silty; sandstone clasts; slightly laminated; micaceous where silty; erosive contact; competent.
20.55 - 20.93	LAMINITE (70% Siltstone/30% Sandstone) - light to medium grey; fine grained; micaceous; carbonaceous; erosive contact; competent.

HOLE NO. L-4 (cont)

DEPTH (m)	DESCRIPTION
20.93 - 24.08	MUDSTONE - medium to dark grey; somewhat silty; fossiliferous; gradational contact.
24.08 - 26.31	SILTSTONE - medium grey; fine grained; mudstone sections; fossiliferous; micaceous; erosive contact; competent.
26.31 - 26.77	SANDSTONE - medium grey; medium grained; highly calcareous; carbonaceous flecks; sharp contact; competent.
26.77 - 26.97	MUDSTONE - medium to dark grey; non fossiliferous; no noticeable grain; nonmicaceous; massive; sharp contact.
26.97 - 28.45	SANDSTONE - light grey; medium to coarse grained; calcareous; large flakes of mica and carbonaceous material along bedding; crossbedded; gradational contact; competent.
28.45 - 28.83	SANDSTONE - medium to dark grey; fine grained; micaceous; slightly laminated; noncalcareous; gradational contact; competent.
28.83 - 31.29	SANDSTONE - light grey; fine to medium grained; carbonaceous flecks; massive; competent.

END OF HOLE

HOLE NO. 1-5

DEPTH (m)	DESCRIPTION
0 - 0.63	Not cored
0.63 - 1.11	MUDSTONE - medium grey; quite silty fossiliferous; sharp lower contact.
1.11 - 1.45	SANDSTONE - light to medium grey; fine to medium; first 12 cm is massive; remaining section is laminated (65% sandstone/35% siltstone); erosive lower contact; competent.
1.45 - 3.05	MUDSTONE - dark grey; slightly laminated; silty; fossiliferous; siltstone (1.49 - 1.70); calcareous shale section (2.20 - 2.44).
3.05 - 3.73	SANDSTONE - light to medium grey; first 10 cm is massive (fine to medium grained); remaining section contains interbeds of siltstone; micaceous; gradational lower contact; competent.
3.73 - 4.01	MUDSTONE - medium to dark grey; silty; fossiliferous; ironstone staining; slightly laminated; gradational contact.
4.01 - 4.21	SILTSTONE - medium grey; fine grained; micaceous; gradational contact; competent.
4.21 - 5.05	SANDSTONE - light to medium grey; medium grained; carbonaceous; large mica flakes; crossbedded; silty bands; gradational contact; competent.
5.05 - 5.49	SILTSTONE - medium grey; fine grained; micaceous; noncalcareous; gradational contact; competent.
5.49 - 6.63	MUDSTONE - medium to dark grey; laminated sections; highly fossiliferous.
6.63 - 6.93	COAL (6.40 - 7.01 m is spread over 0.91 m in the coal box, ∴. Rider Seam thickness is an estimate.
6.93 - 7.39	MUDSTONE - seatearth; medium to dary grey; highly fossiliferous; very weak.
7.39 - 8.23	SILTSTONE - medium grey; fossiliferous; medium grained; micaceous; small sandy beds noted; gradational lower contact; competent.
8.23 - 9.04	MUDSTONE - dark grey; shaley; slightly laminated; numerous slickensided surfaces; erosive lower contact;

HOLE NO. L-3 (cont)

DEPTH (m)	DESCRIPTION
9.04 - 10.08	SANDSTONE - light grey; medium grained; carbonaceous; streaks; micaceous; silty toward base; gradational lower contact; slight core discing noted at 9.78 m (9.09 - 9.78 - missing core).
10.08 - 12.70	LAMINITE (80% mudstone/15% siltstone/5% sandstone) light to dark grey; wispy sandy beds throughout; fossiliferous; micaceous; sharp lower contact.
12.70 - 13.23	COAL (17.7 cms in core box)
13.23 - 13.59	MUDSTONE - seatearth; dark grey; slightly silty; gradational contact.
13.59 - 14.12	SILTSTONE - medium grey; very coarse grained; ironstone staining; micaceous; gradational lower contact; competent.
14.12 - 19.45	MUDSTONE - dark grey to black; numerous silty beds throughout; slightly micaceous where silty; noncalcareous; laminated appearance; fossiliferous; 5 cm sandstone bed at 19.15; gradational contact; competent.
19.45 - 19.78	SILTSTONE - medium grey; sandy sections; micaceous; noncalcareous; gradational contact; competent.
19.78 - 20.98	MUDSTONE - medium to dark grey; silty; non-fossiliferous; gradational lower contact; competent.
20.98 - 21.16	SANDSTONE - light grey; fine to medium grained; highly calcareous; micaceous; carbonaceous; erosive lower contact.
21.16 - 24.58	MUDSTONE - medium grey to black; very shaley in sections; fossiliferous; laminated appearance; calcareous shale at 24.56; sharp lower contact.
24.58 - 25.30	LIMESTONE - brownish grey; sugary texture; very impure.

END OF HOLE

APPENDIX B

OVERCORING TEST RESULTS

INSITU STRESS MEASUREMENT - PRINCE MINE USBM TEST No. P101

FIGURE B1-1

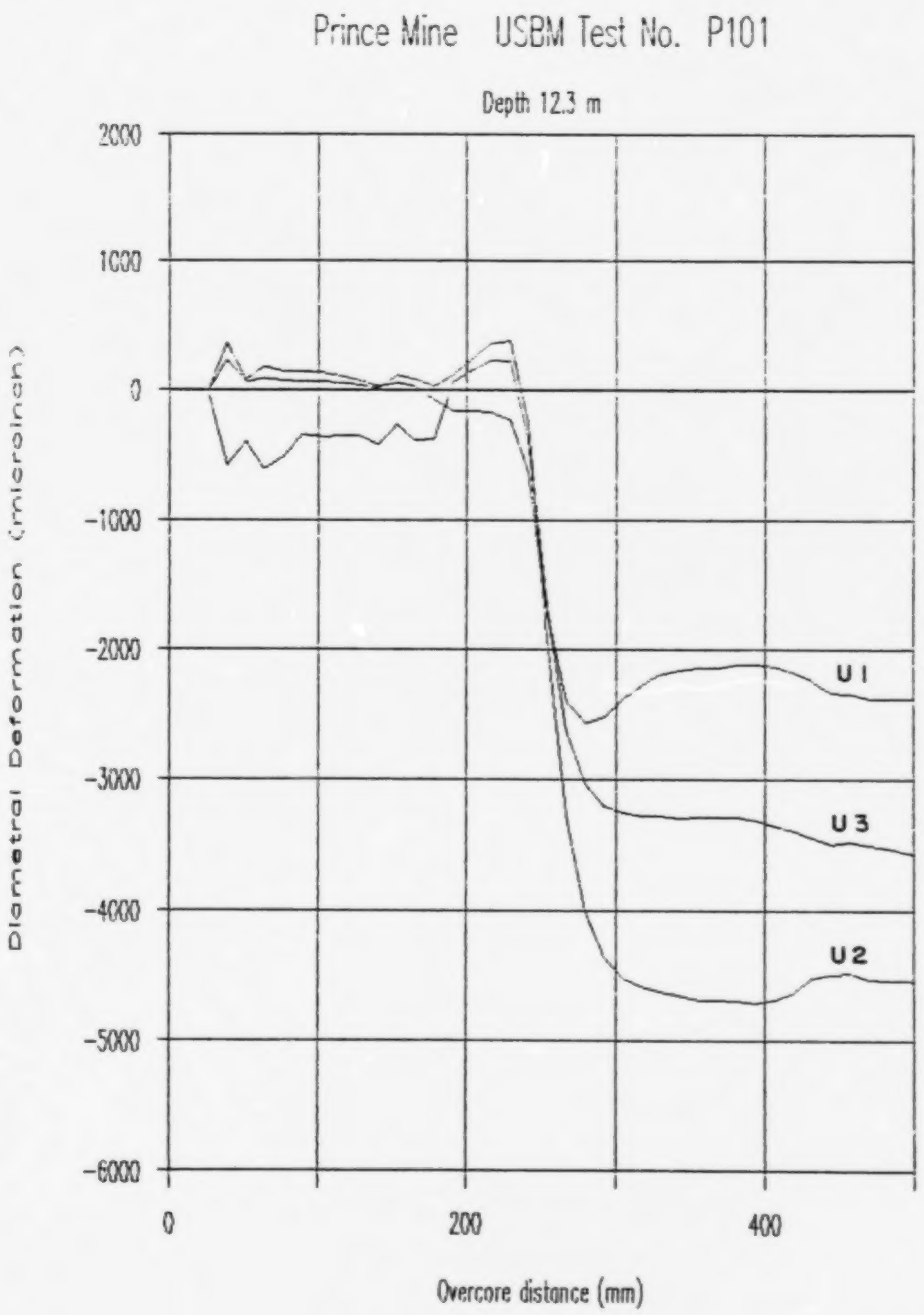

Date MAY 14, 1986

Project 851-6025

Golder Associates

Drawn D.M.

Chkd.

INSITU STRESS MEASUREMENT - PRINCE MINE
USBM TEST No. P104

FIGURE BI-2

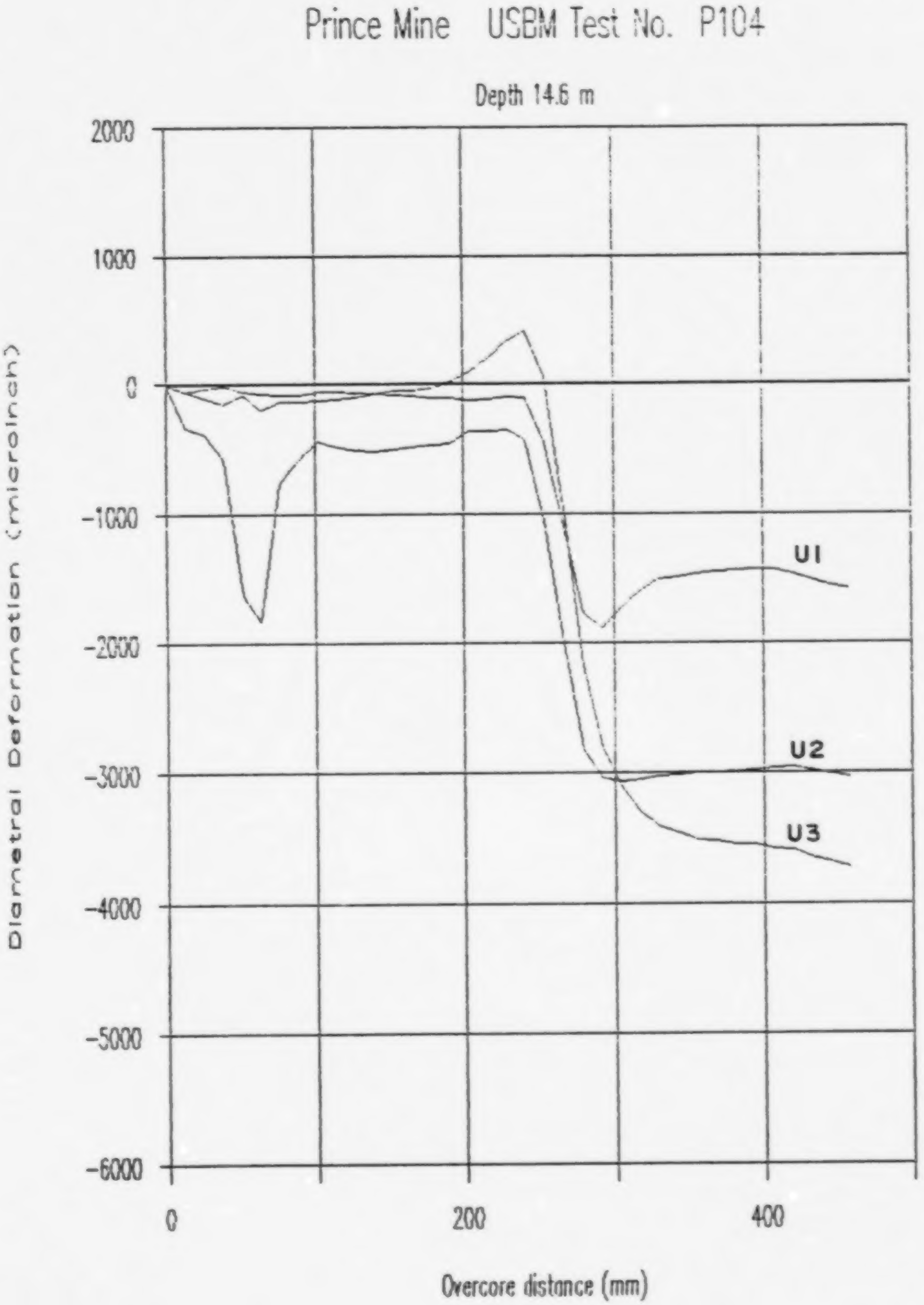

Date MAY 14,1986
Project 851-6025

Golder Associates

Drawn D. M.
Chkd.

INSITU STRESS MEASUREMENT - PRINCE MINE
USBM TEST No. P201

FIGURE BI-3

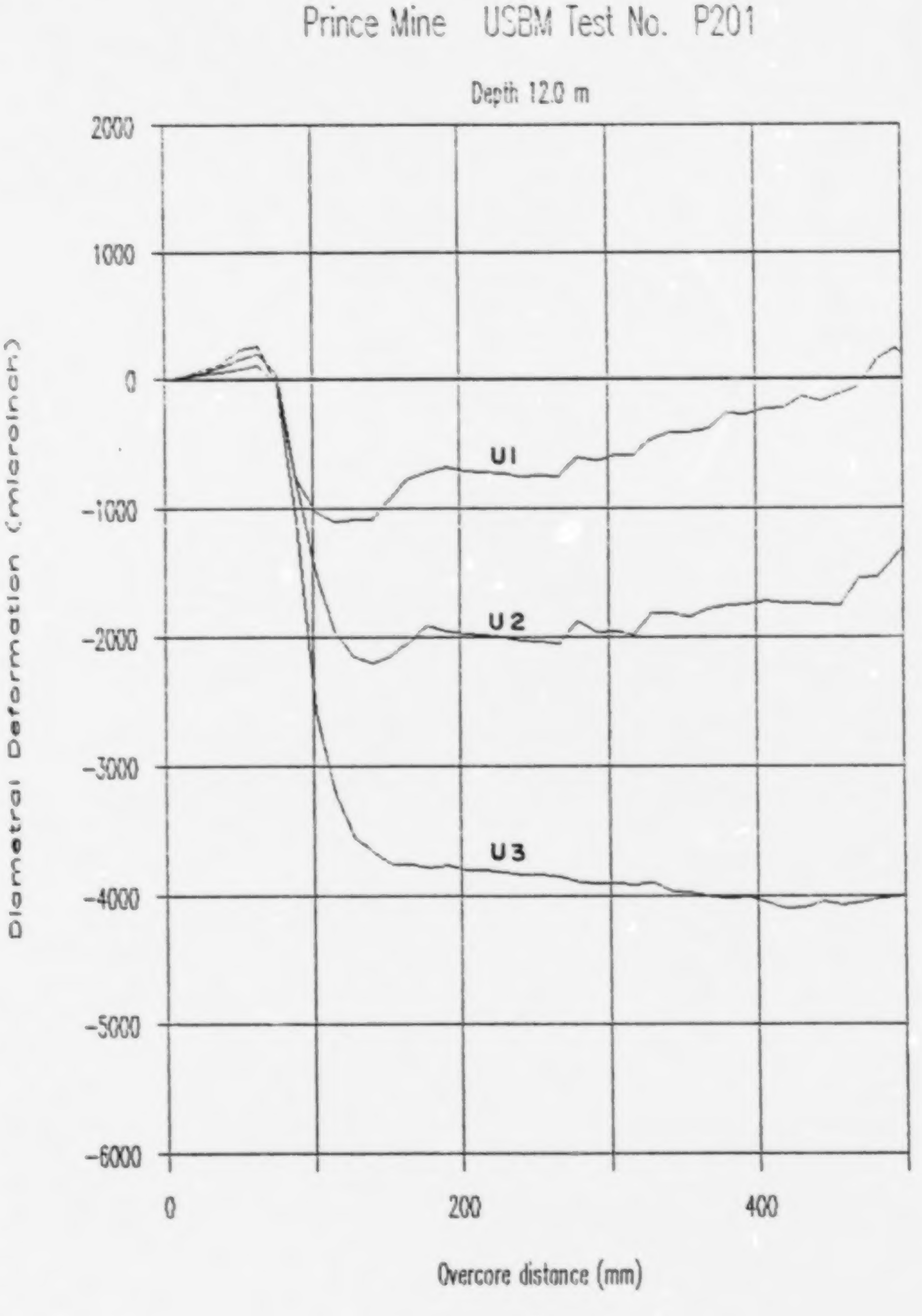

Date MAY 14, 1986
Project 851-6025

Golder Associates

Drawn D.M.
Chkd. JG

IN SITU STRESS MEASUREMENT - PRINCE MINE
USBM TEST No. P202

FIGURE BI-4

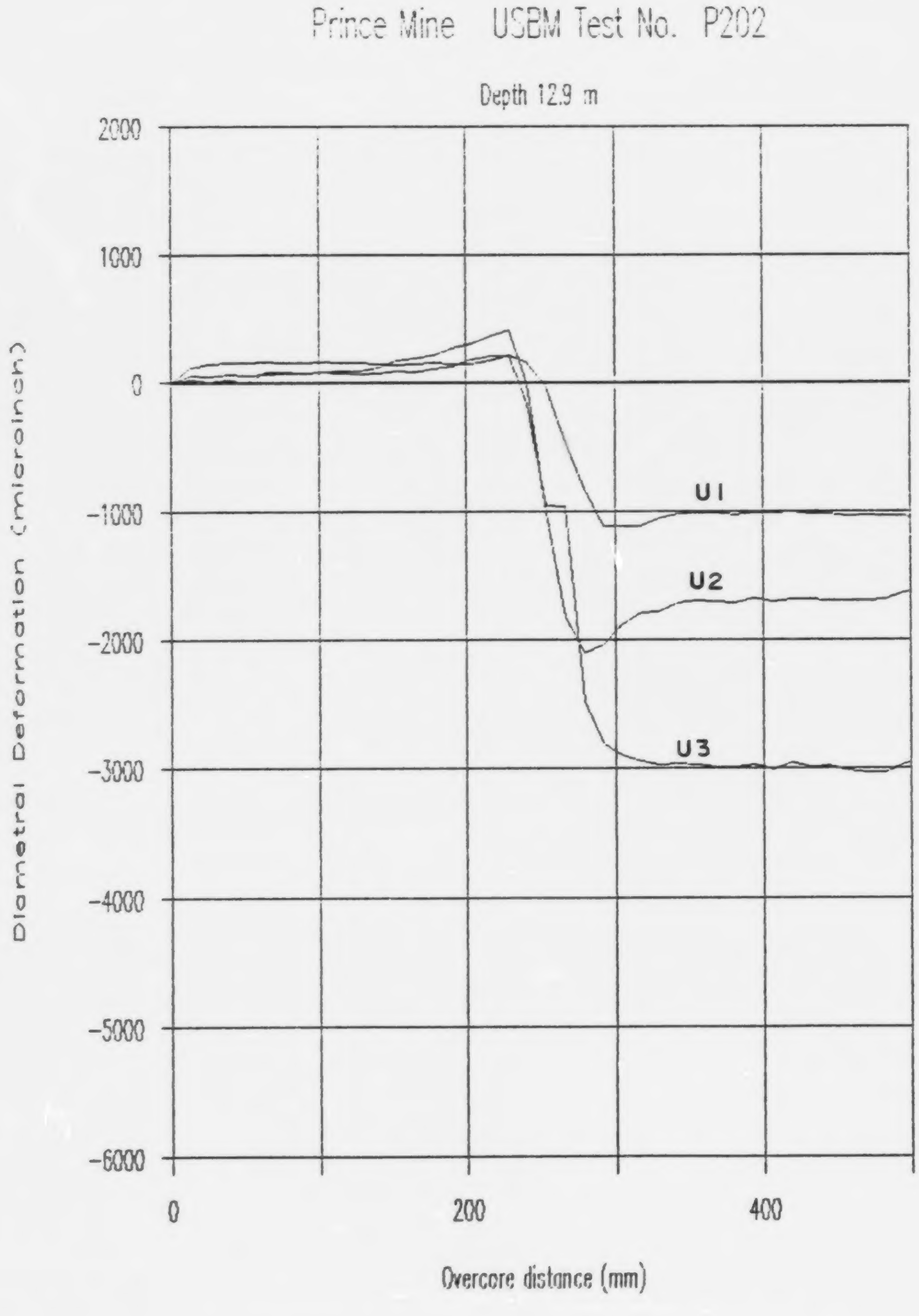

Date MAY 14, 1986
Project 851-6025

Golder Associates

Drawn D. M.
Chkd. JKG

INSITU STRESS MEASUREMENT- PRINCE MINE
USBM TEST No. P301

FIGURE BI-5

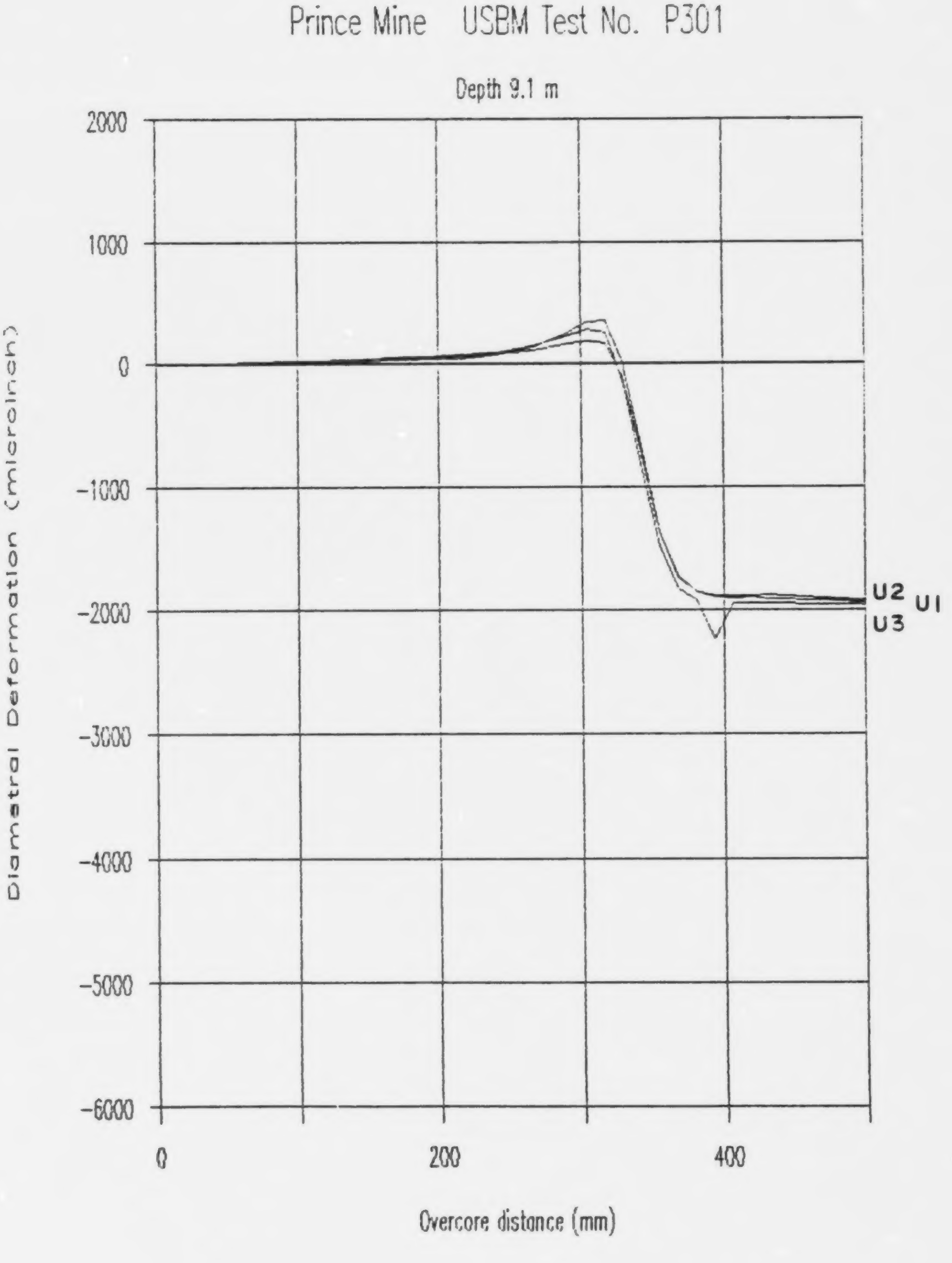

Date MAY 14, 1986
Project 851-6025

Golder Associates

Drawn D.M.
Chkd.

INSITU STRESS MEASUREMENT - PRINCE MINE
USBM TEST No. P302

FIGURE BI-6

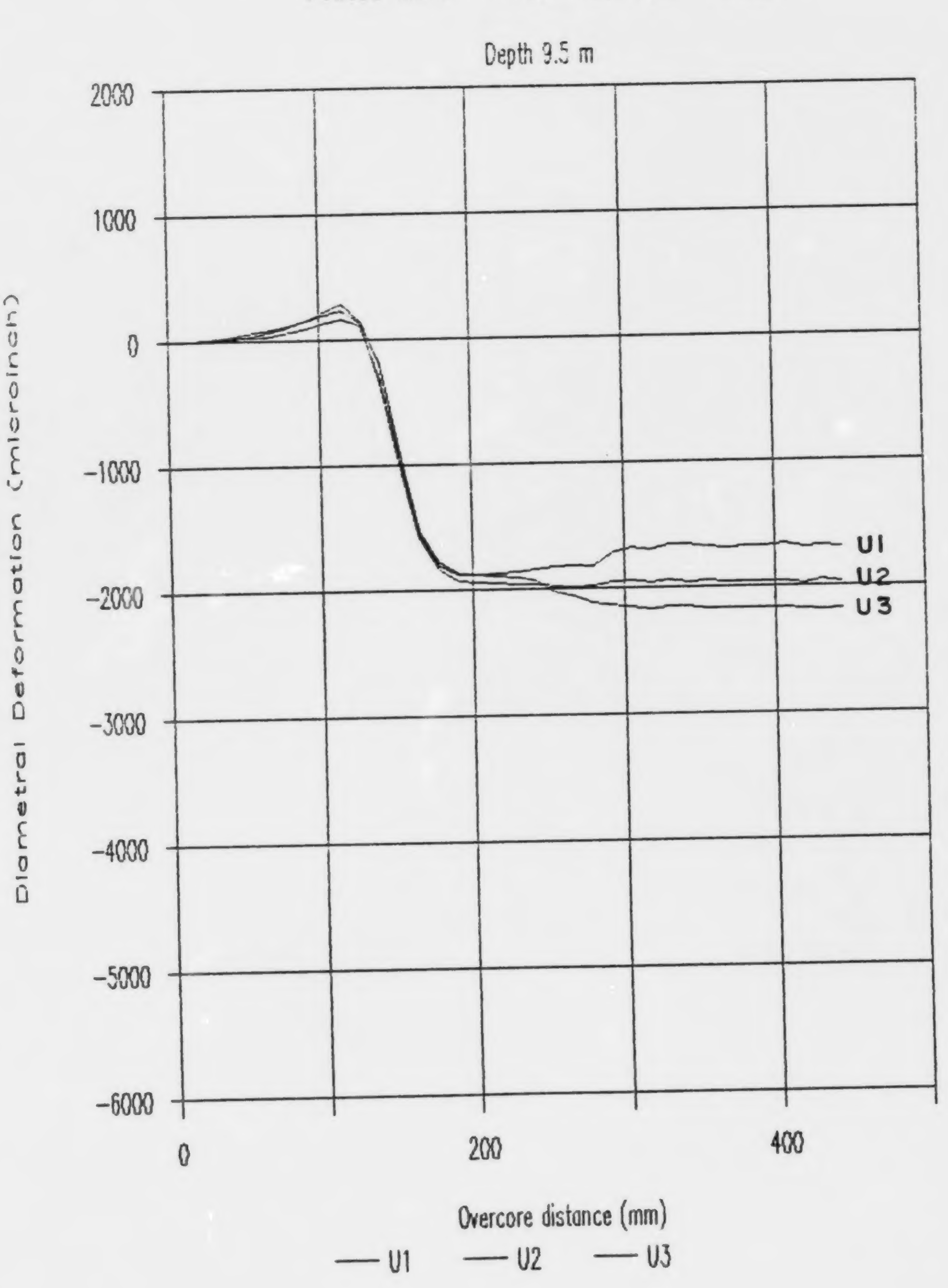

Date MAY 14,1986
Project 851-6025

Golder Associates

Drawn D.M.
Chkd.

INSITU STRESS MEASURENT- PRINCE MINE
USBM TEST No. P401

FIGURE BI-7

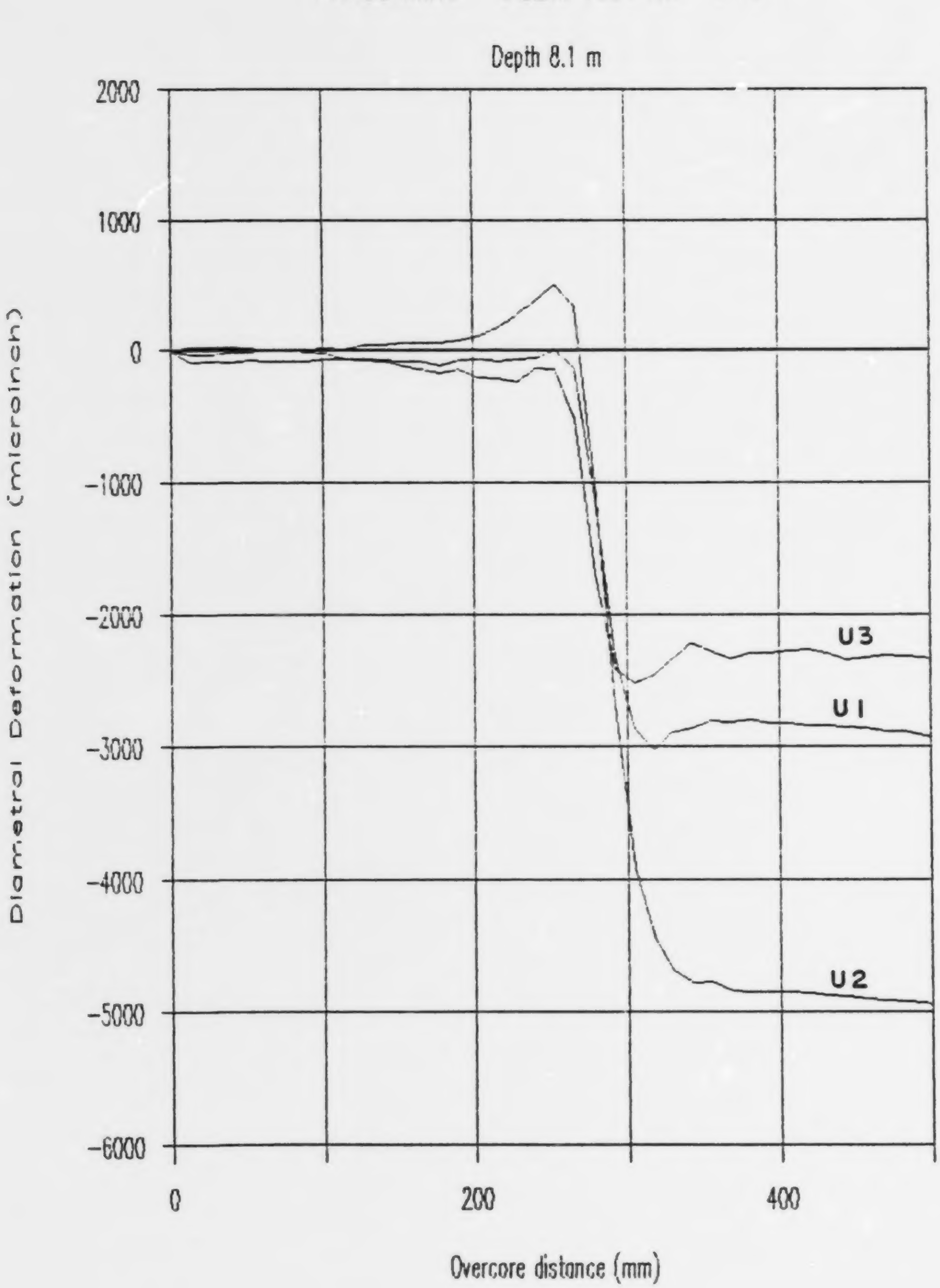

Date MAY 14, 1986
Project 851-6025

Golder Associates

Drawn D.M.
Chkd. JG

IN SITU STRESS MEASUREMENT-PRINCE MINE
BIAXIAL TEST No. P103B1

FIGURE B1-8

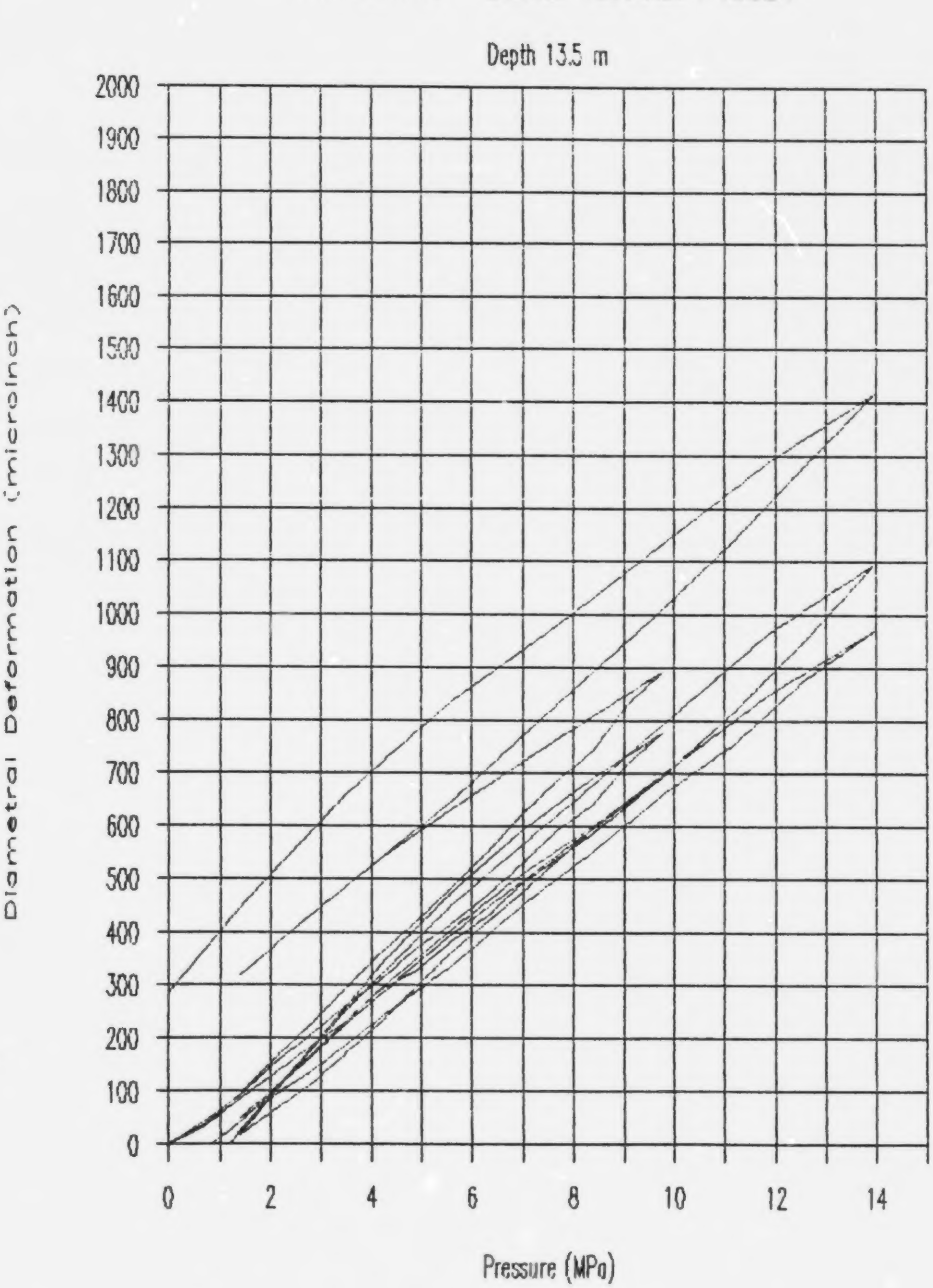

Date MAY 21, 1986
Project 851-6025

Golder Associates

Drawn D.M.
Chkd. JG

INSITU STRESS MEASUREMENT - LINGAN MINE
USBM TEST No. L102

FIGURE B2-1

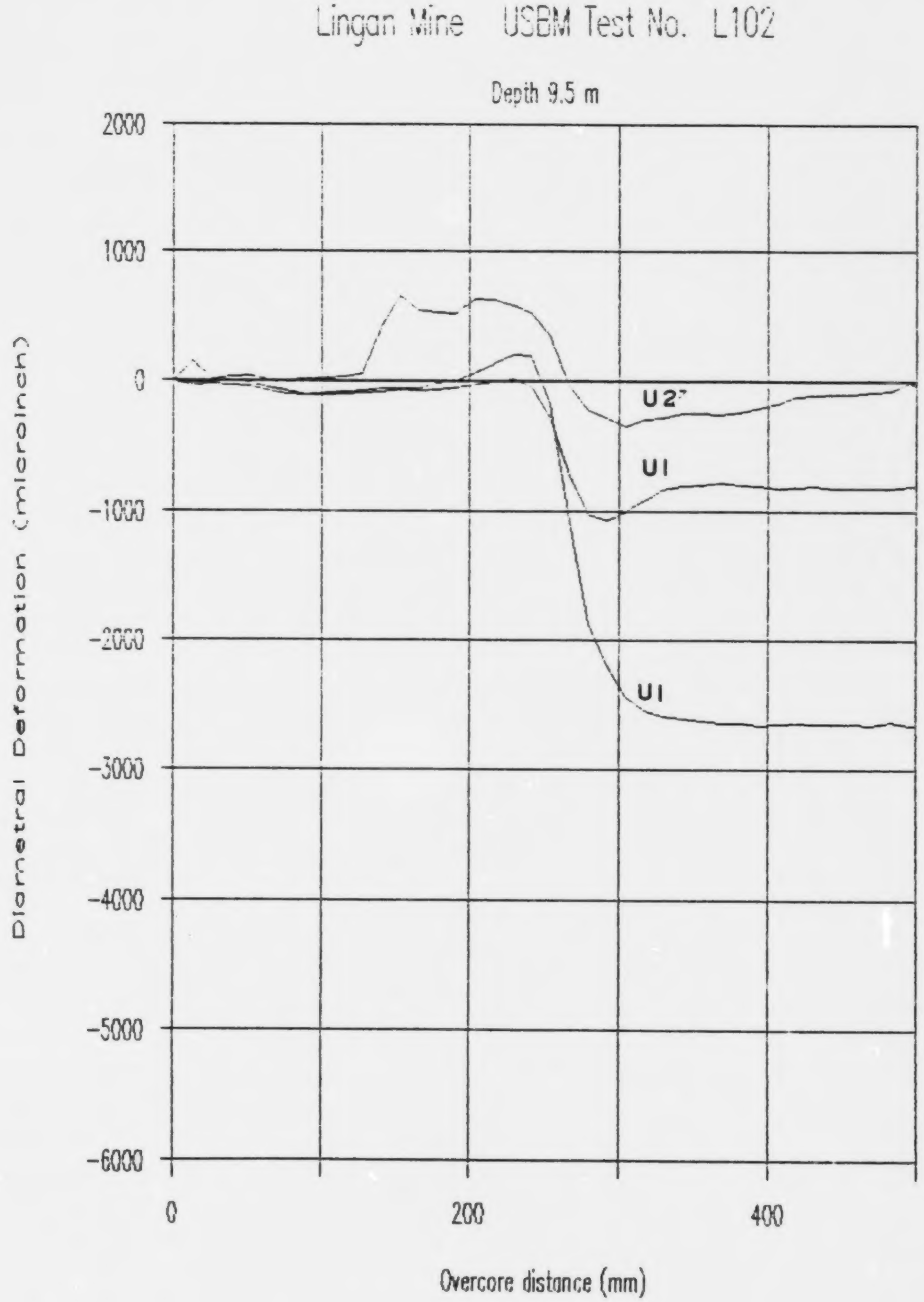

Date MAY 14,1986

Project 851-6025

Golder Associates

Drawn D.M.

Chkd. [illegible]

INSITU STRESS MEASUREMENT - LINGAN MINE
USBM TEST No. L103

FIGURE B2-2

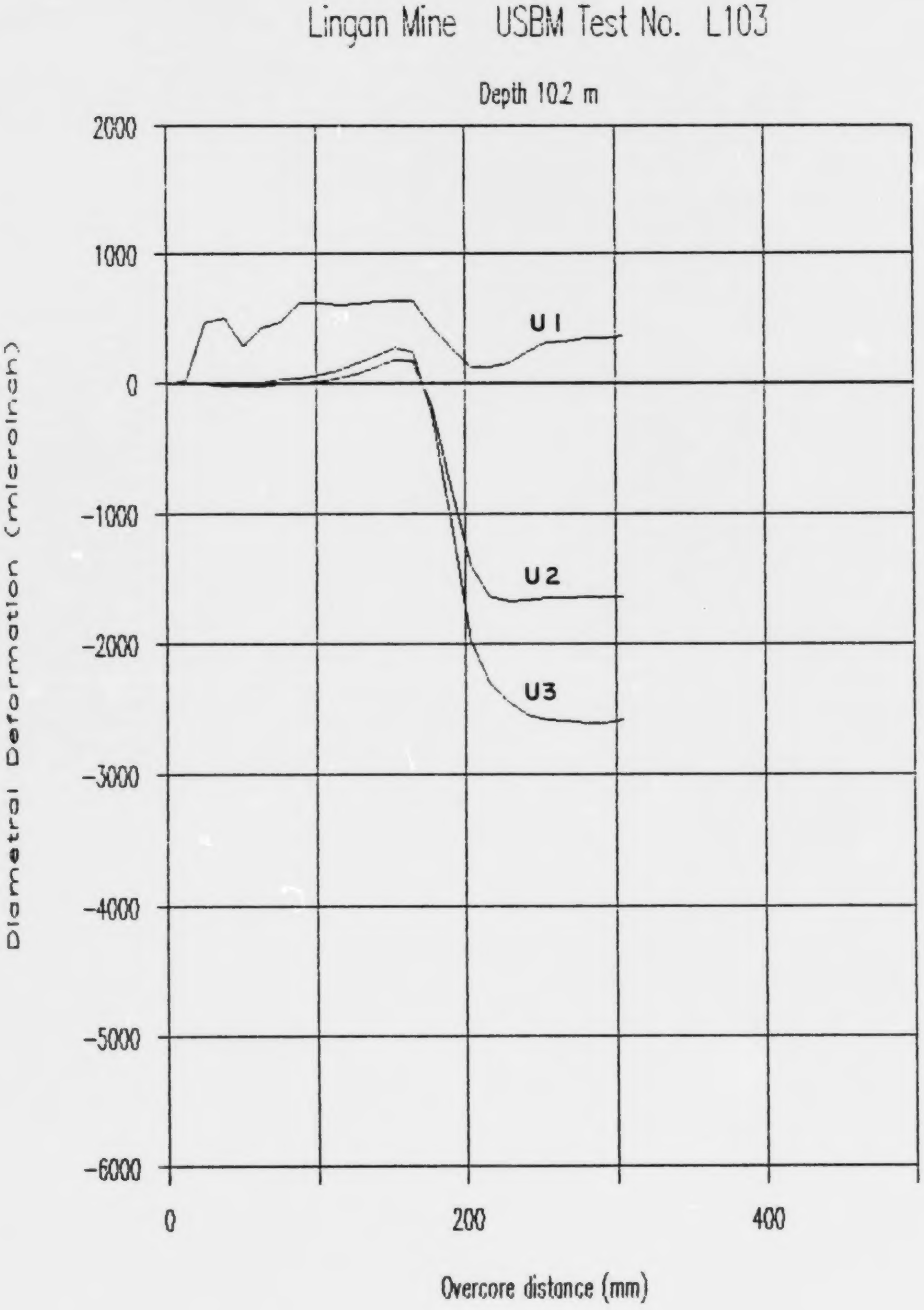

Date MAY 14, 1986
Project 851-6025

Golder Associates

Drawn D.M.
Chkd. JG

Form G.A.-D.-4 (M)

INSITU STRESS MEASUREMENT-LINGAN MINE
USBM TEST No. L203

FIGURE B2-3

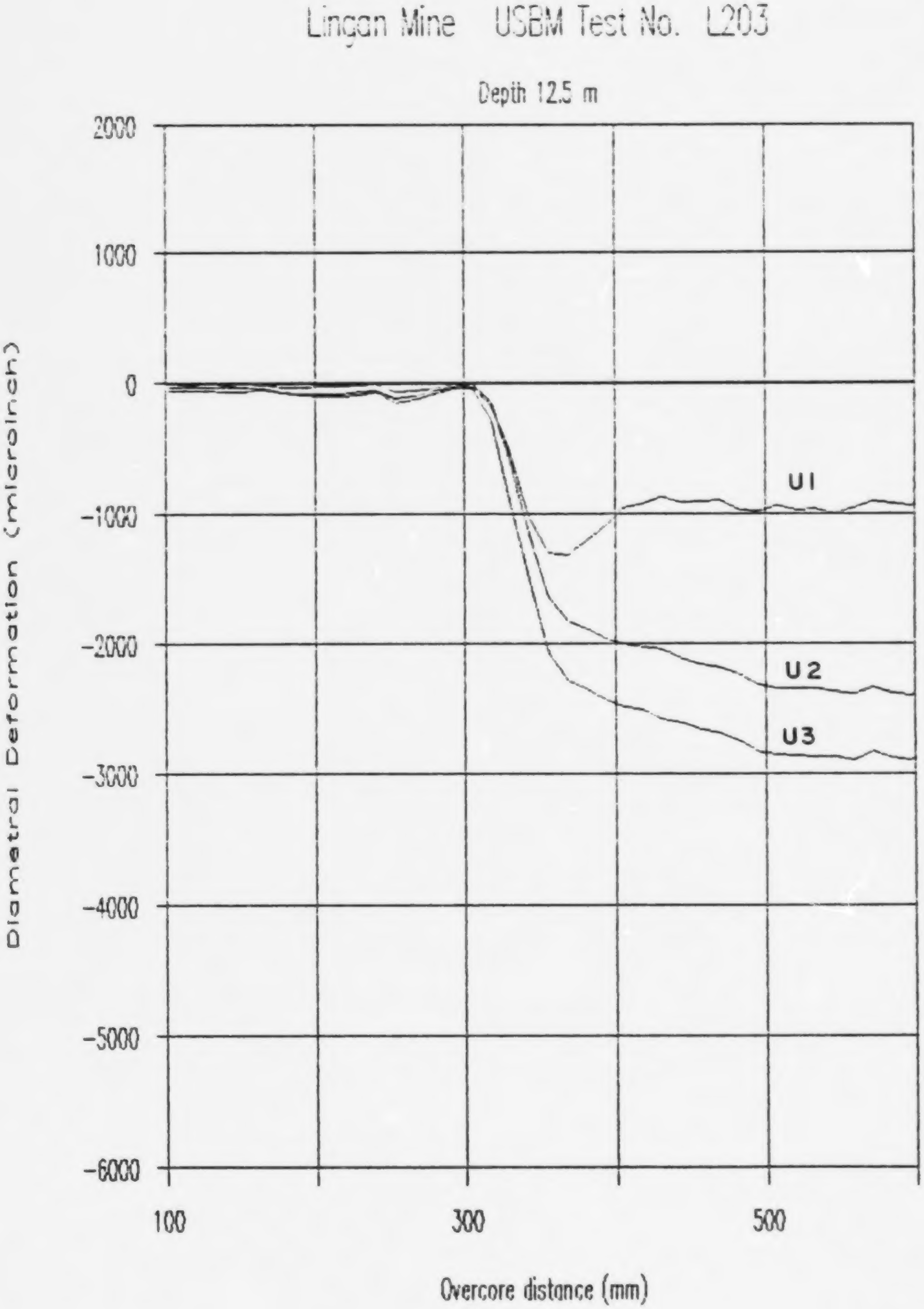

Date MAY 14, 1986
Project 851-6025

Golder Associates

Drawn D.M.
Chkd. J.C.

INSITU STRESS MEASUREMENT-LINGAN MINE
USBM TEST No. L 204

FIGURE B2-4

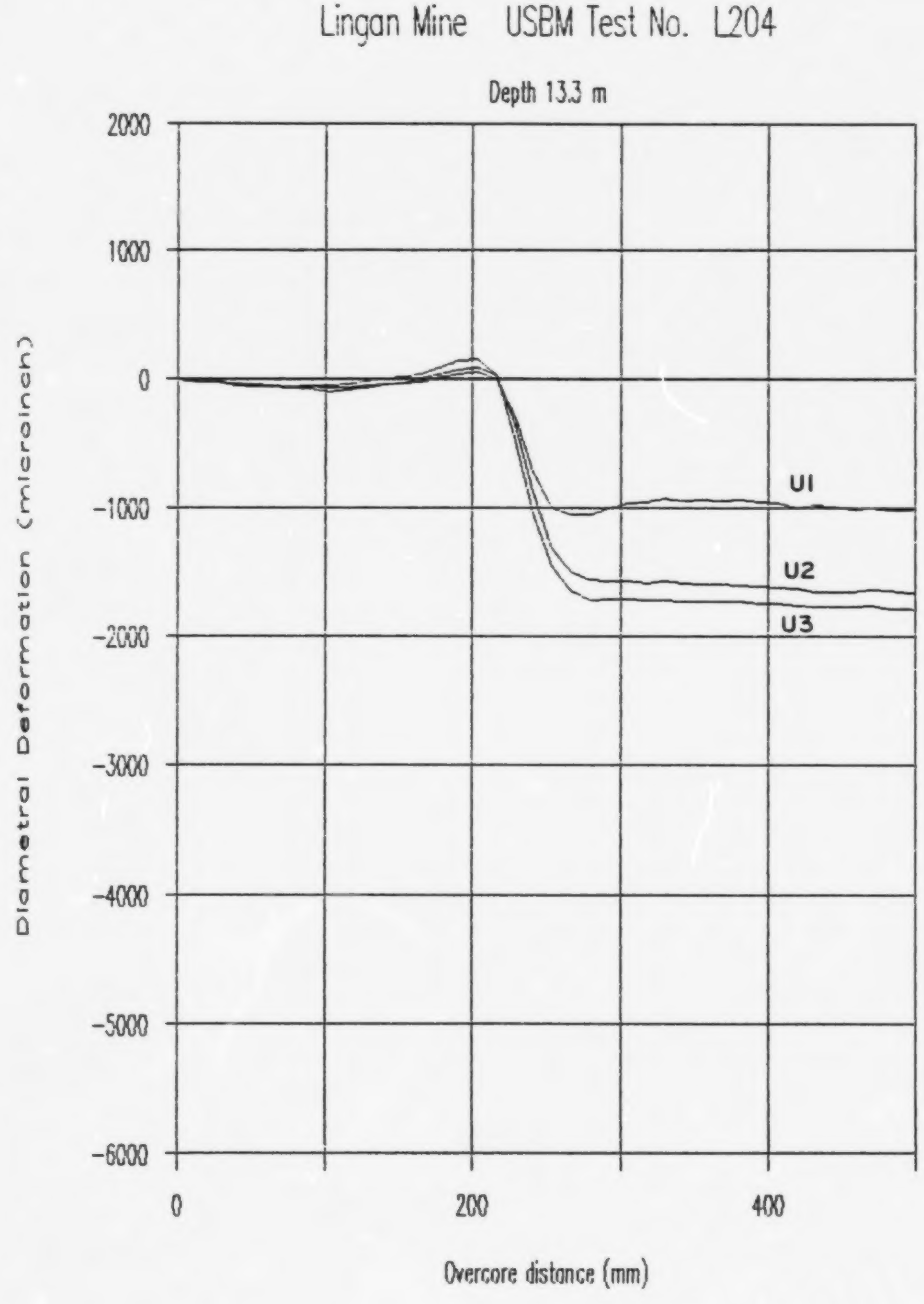

Date MAY 14, 1986
Project 851-6025

Golder Associates

Drawn D.M.
Chkd. JHC

INSITU STRESS MEASUREMENT - LINGAN MINE USBM TEST No. L301	FIGURE B2-5

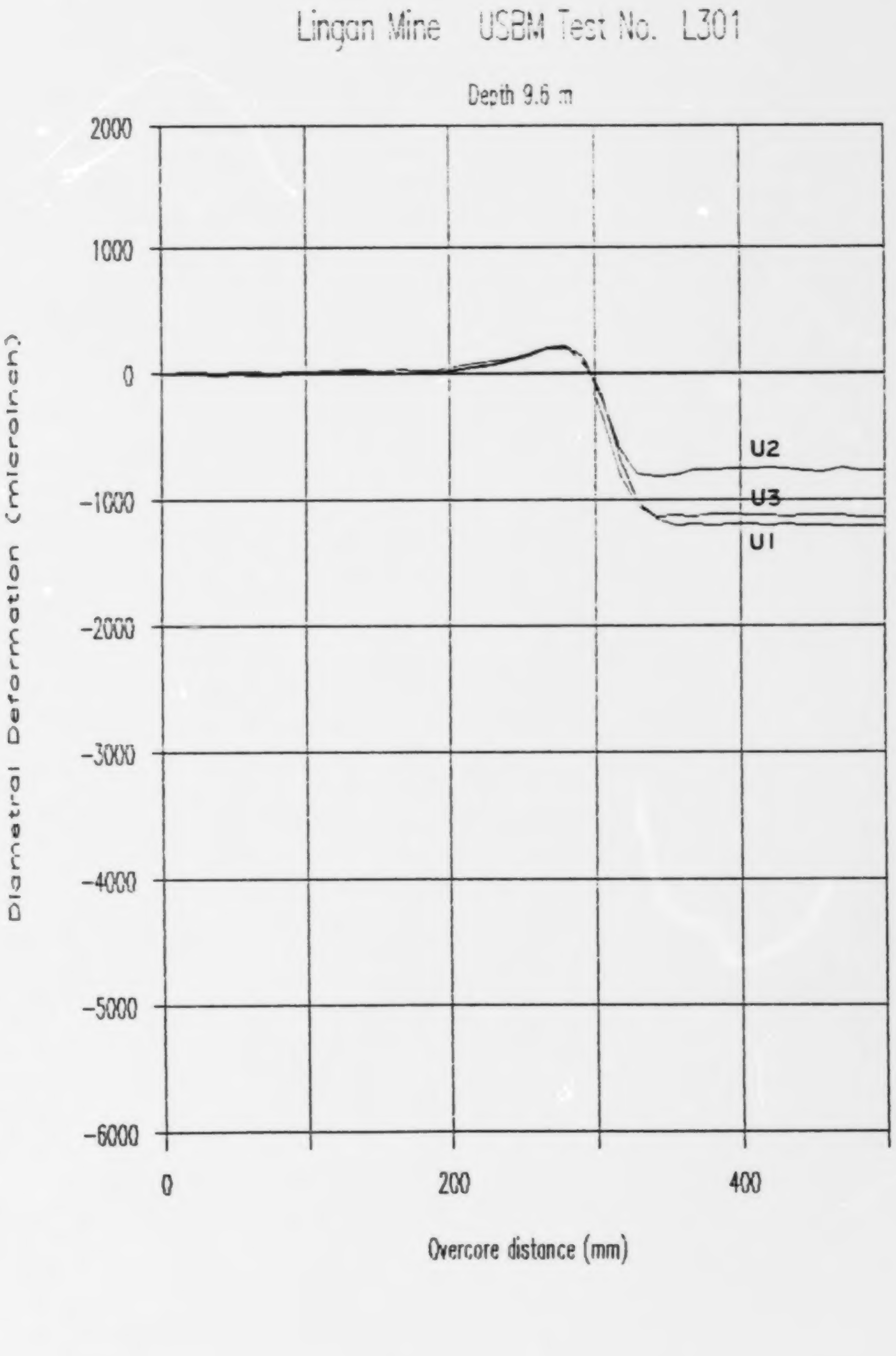

Date MAY 14, 1986
Project 851-6025

Golder Associates

Drawn D.M.
Chkd. J.G.

INSITU STRESS MEASUREMENT - LINGAN MINE
US B M TEST No. L303

FIGURE B2-6

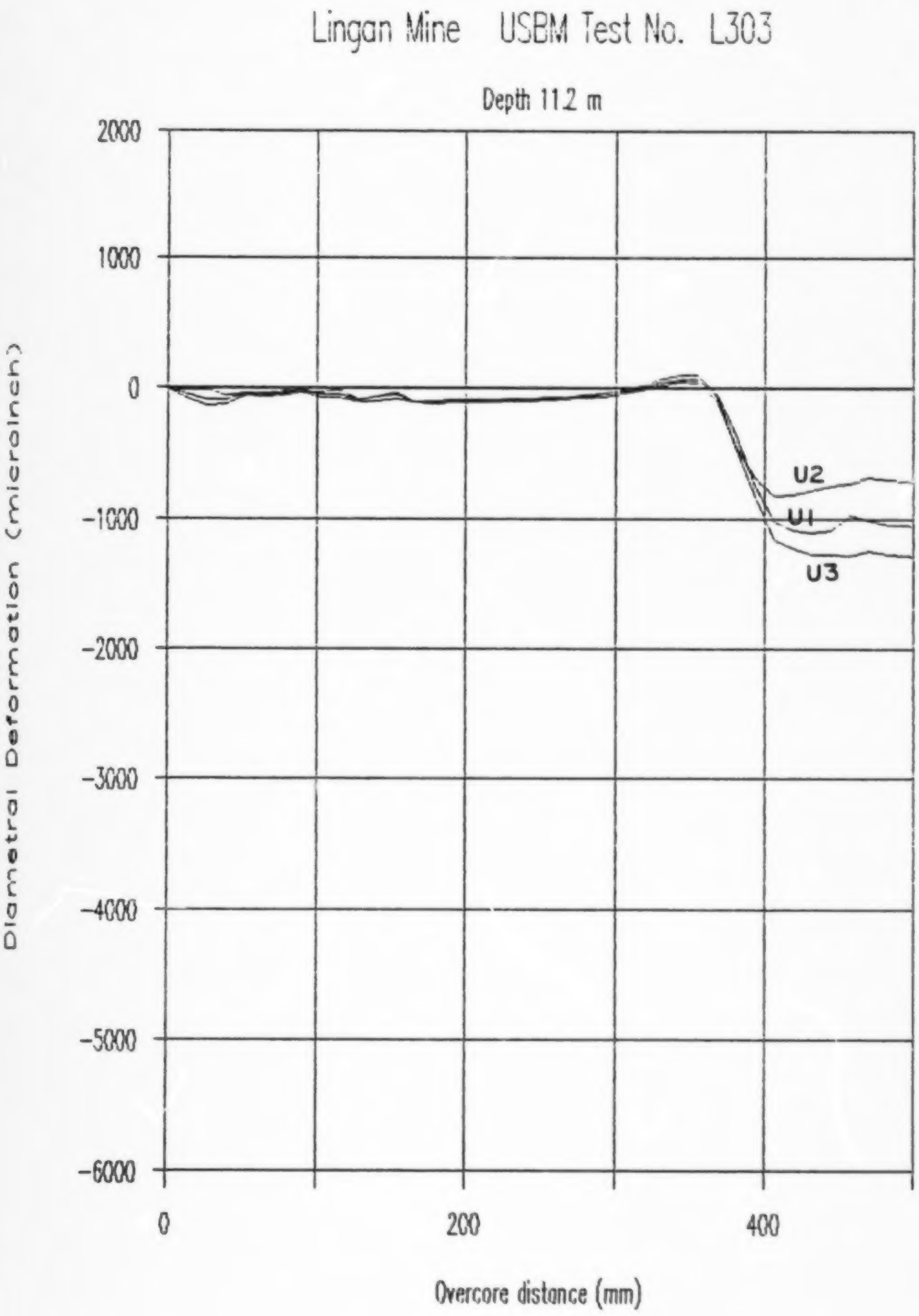

Date MAY 14, 1986
Project 851-6025

Golder Associates

Drawn D.M.
Chkd.

INSITU STRESS MEASUREMENT - LINGAN MINE USBM TEST No. L501

FIGURE B2-7

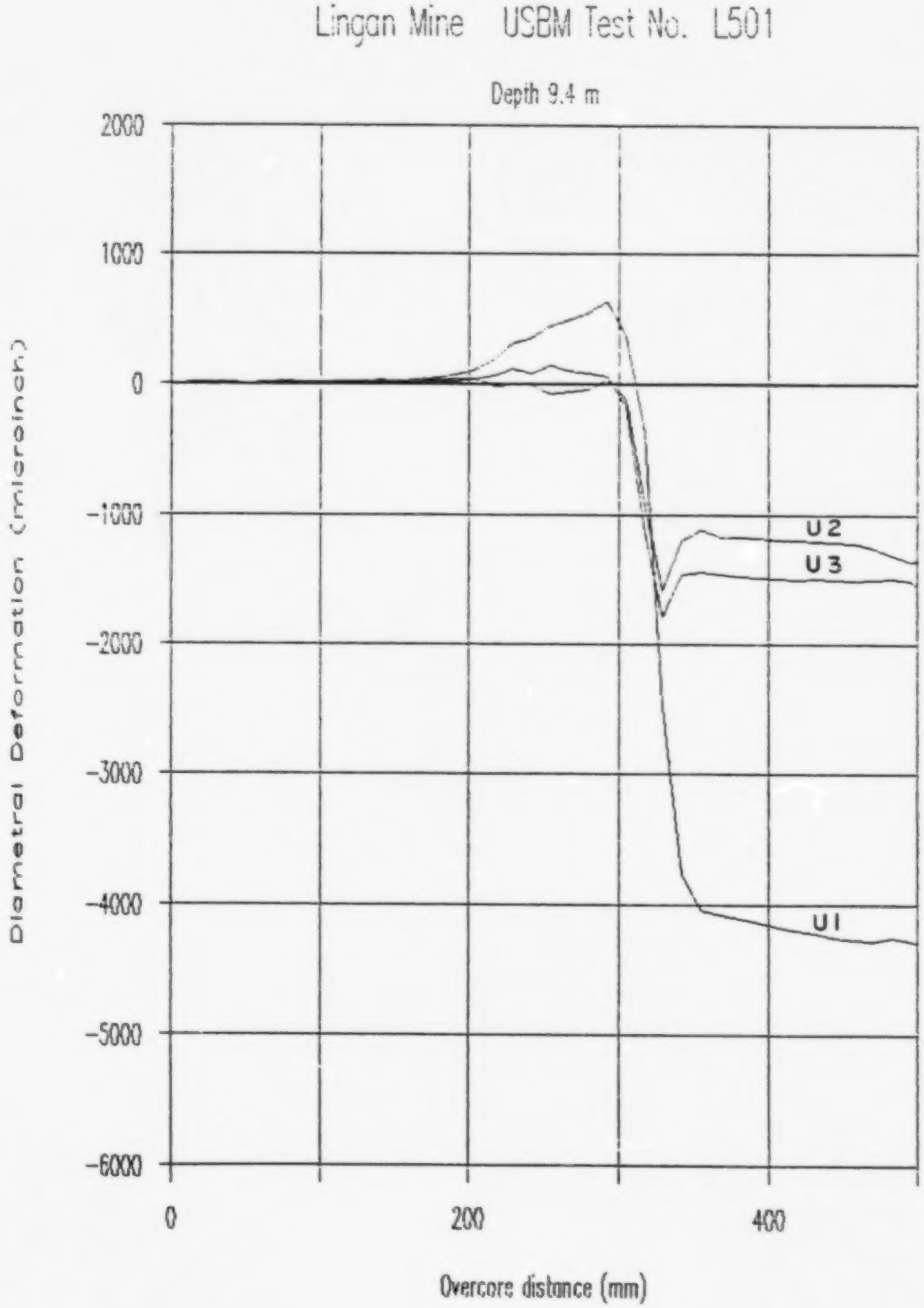

Date MAY 14, 1986

Project 851-6025

Golder Associates

Drawn D.M.

Chkd.

INSITU STRESS MEASUREMENT - LINGAN MINE BIAXIAL TEST No. L102B1	FIGURE B2-8

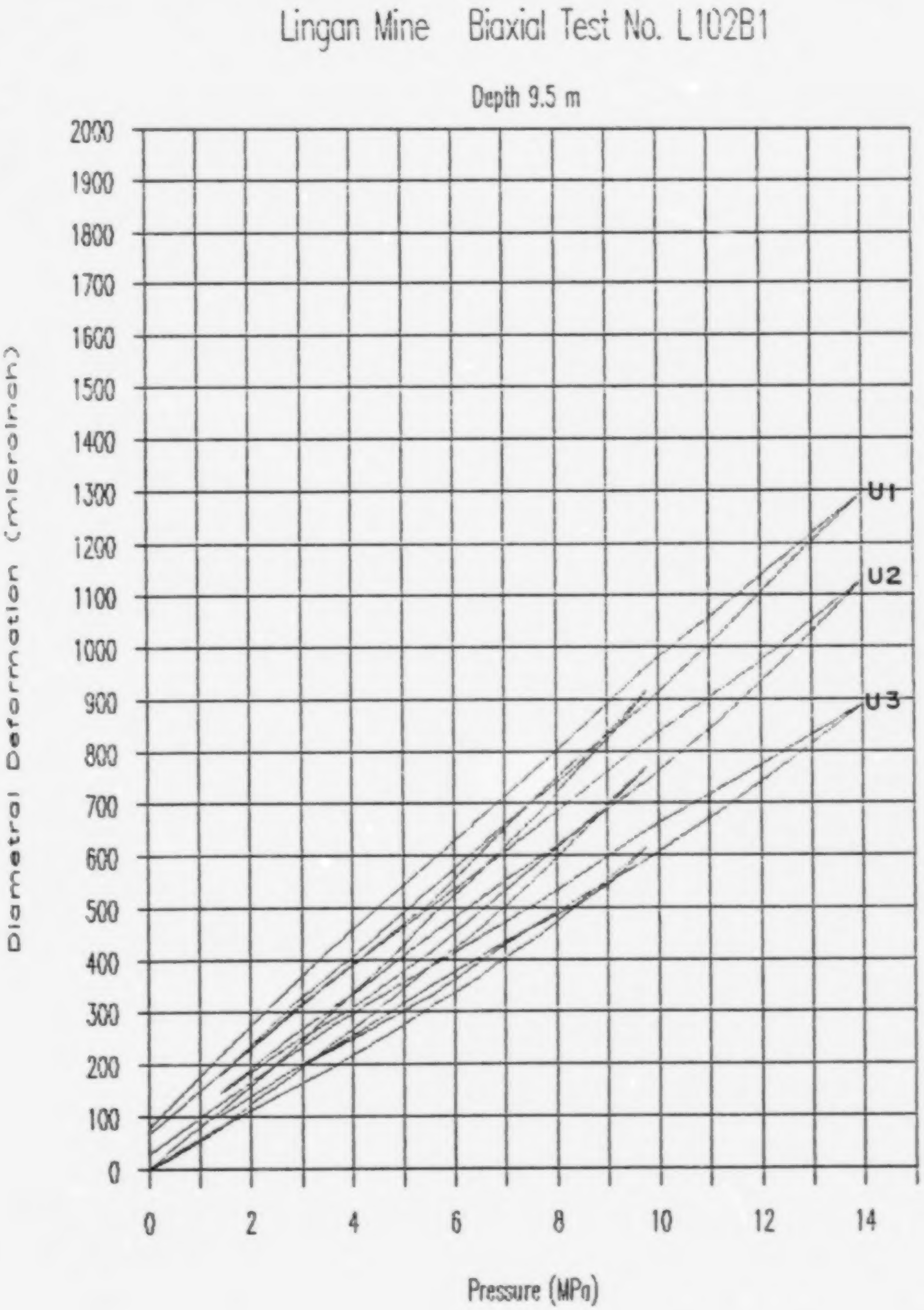

Date MAY 14, 1986
Project 851-6025

Golder Associates

Drawn D.M.
Chkd. JHC

APPENDIX C

HYDROFRACTURE RESULTS

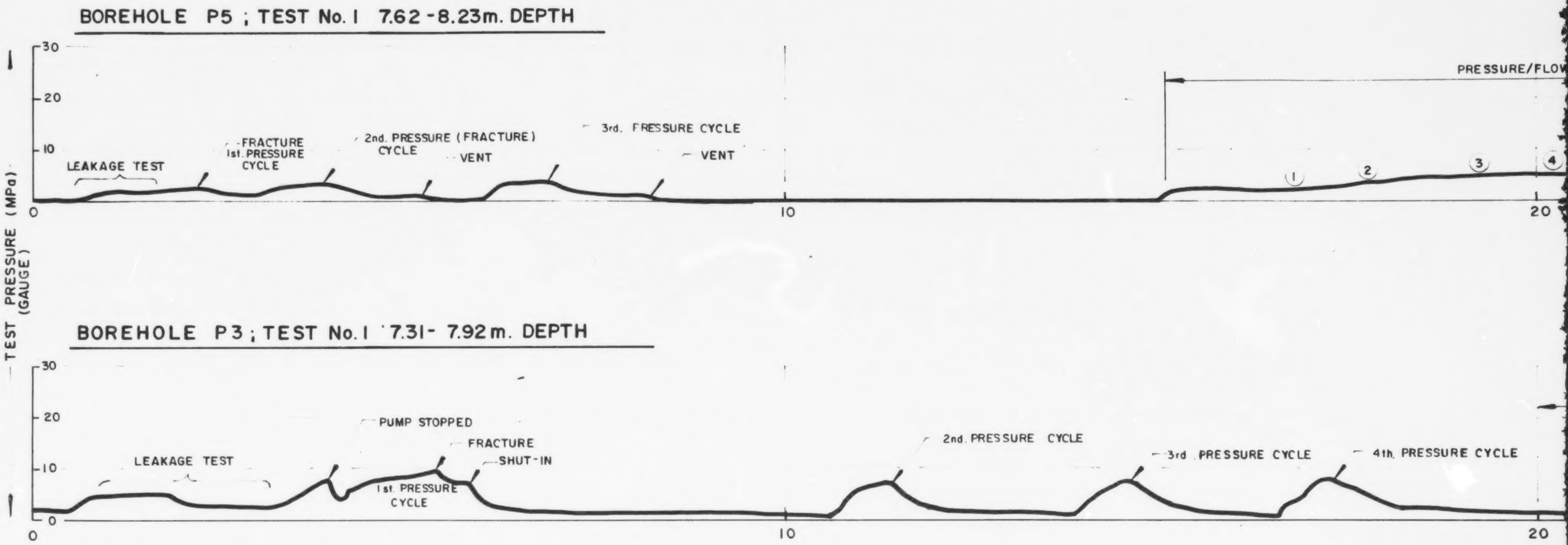

BOREHOLE P5 ; TEST No. 1 7.62 - 8.23m. DEPTH

BOREHOLE P3 ; TEST No. 1 7.31 - 7.92m. DEPTH

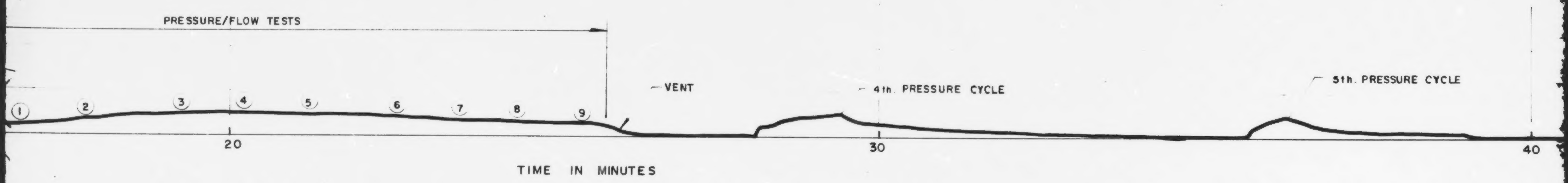
PRESSURE/FLOW TESTS
1
2
3
4
5
6
7
8
9
VENT
4th. PRESSURE CYCLE
5th. PRESSURE CYCLE
20
30
40
TIME IN MINUTES

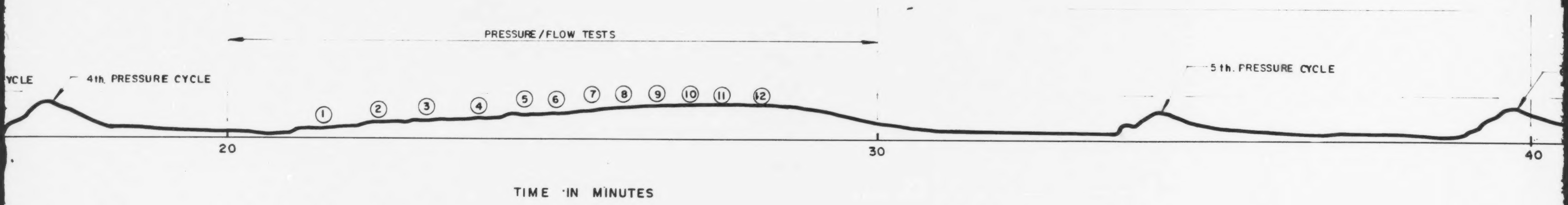
PRESSURE/FLOW TESTS
YCLE
4th. PRESSURE CYCLE
①
②
③
④
⑤
⑥
⑦
⑧
⑨
⑩
⑪
⑫
5th. PRESSURE CYCLE
20
30
40
TIME IN MINUTES

HYDROFRACTURE TEST
PRINCE MINE
BOREHOLE P-3,TES
BOREHOLE P-5,TES

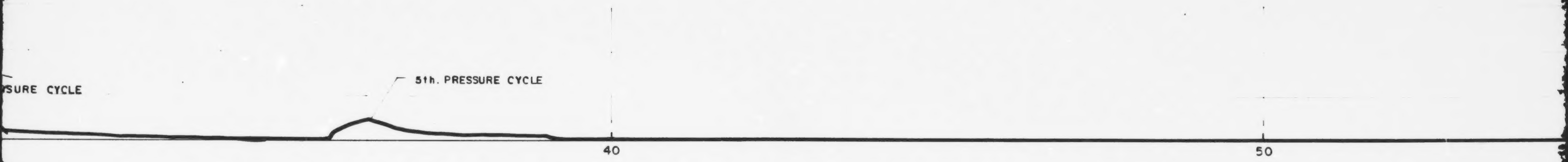

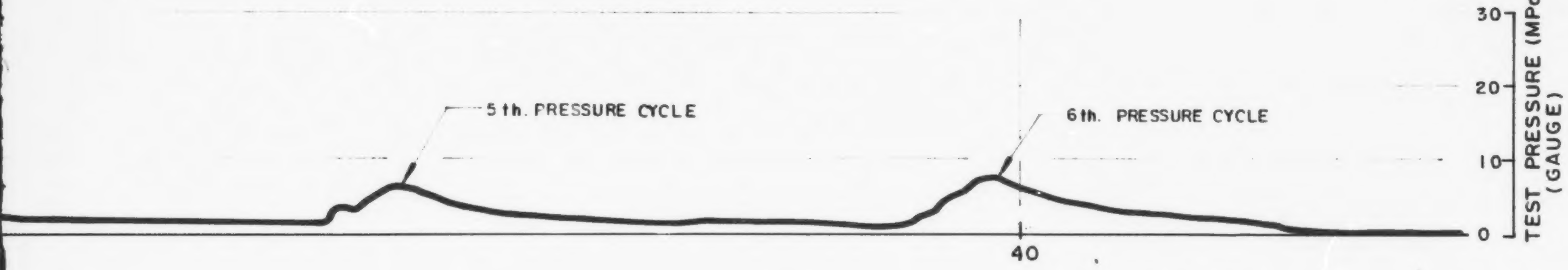

NOTES

1.) RESULTS SHOWN WERE TR

2.) ① - STAGE 1 PRE

Date MAY 12, 1986
Project 851-6025

Golder

HYDROFRACTURE TEST RESULTS
PRINCE MINE
BOREHOLE P-3, TEST No. 1
BOREHOLE P-5, TEST No. 1

FIGURE CI-1

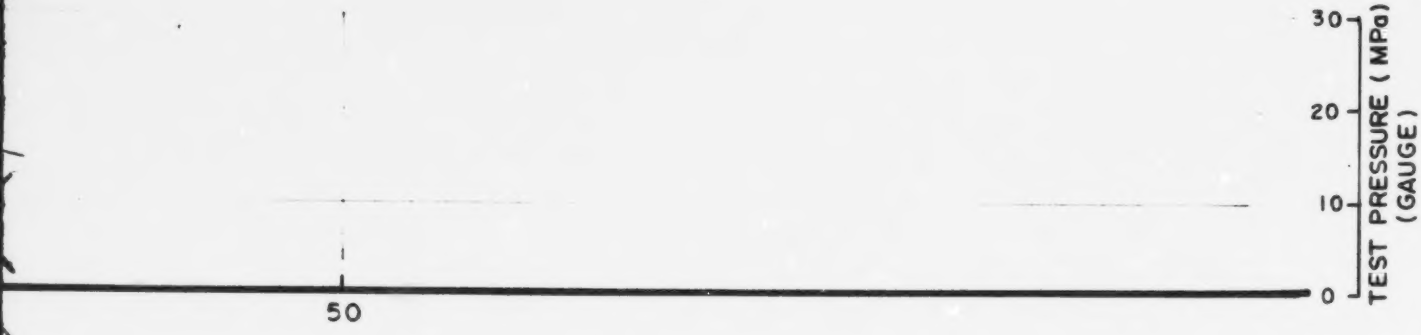

NOTES

1.) RESULTS SHOWN WERE TRACED DIRECTLY FROM CHART RECORDS
2.) ① - STAGE 1 PRESSURE FLOW TESTS

Date MAY 12, 1986
Project 851-6025

Golder Associates

Drawn D.M.
Chkd

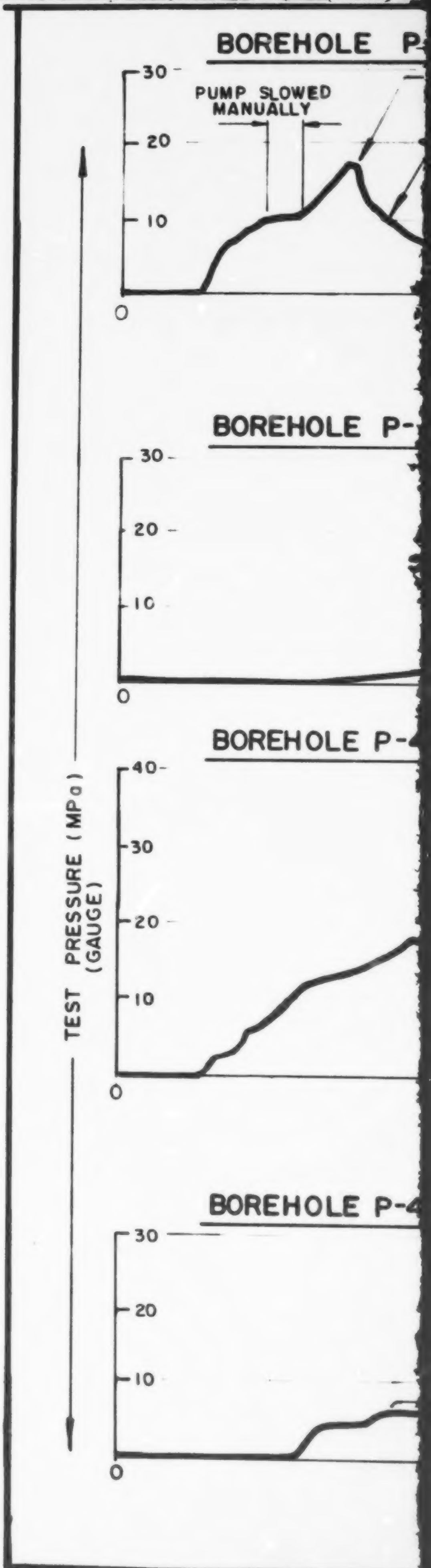
BOREHOLE P-
PUMP SLOWED MANUALLY
30
20
10
0
BOREHOLE P-
30
20
10
0
BOREHOLE P-
40
30
20
10
0
TEST PRESSURE (MPa) (GAUGE)
BOREHOLE P-
30
20
10
0

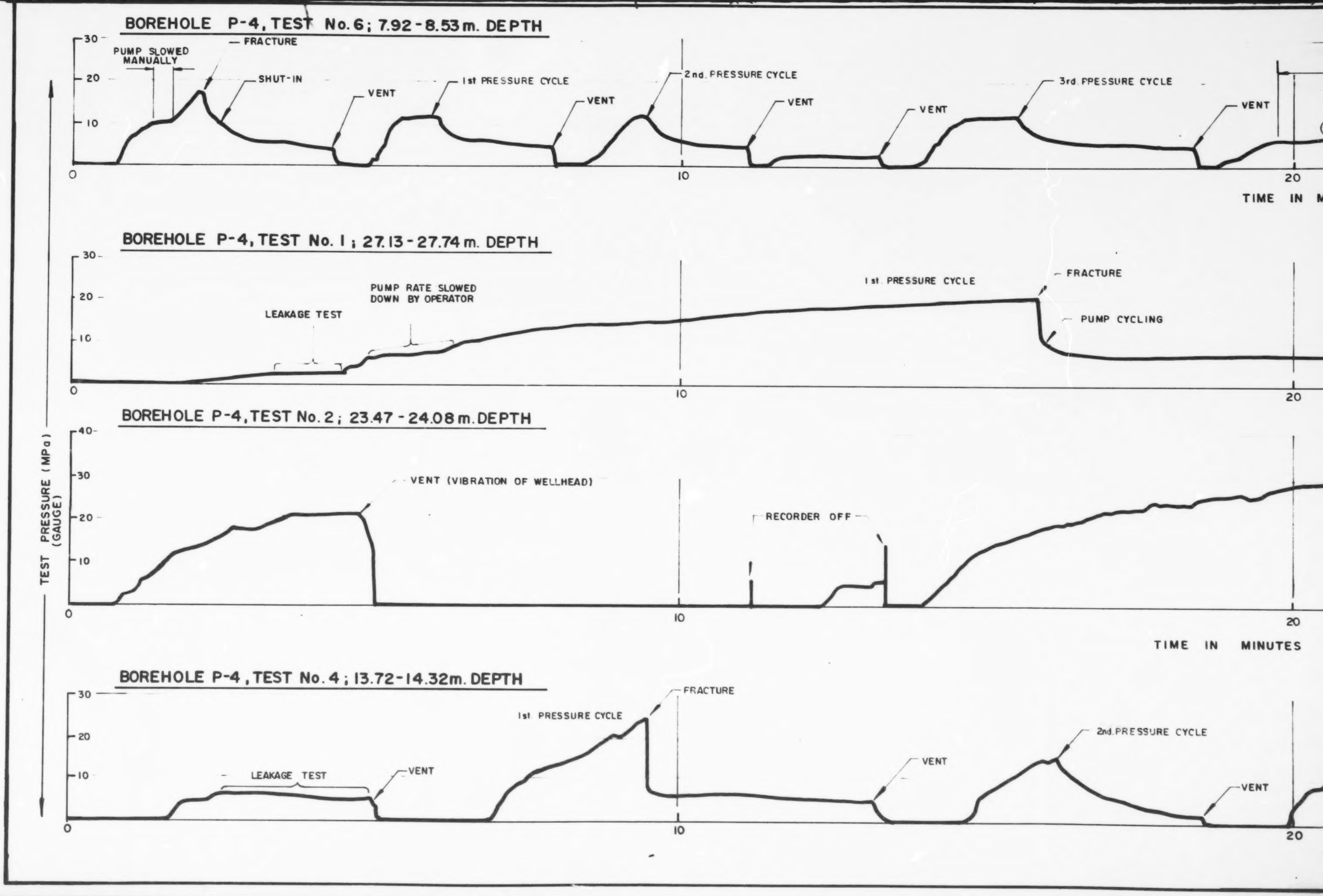

BOREHOLE P-4, TEST No. 6; 7.92-8.53 m. DEPTH

BOREHOLE P-4, TEST No. 1; 27.13-27.74 m. DEPTH

BOREHOLE P-4, TEST No. 2; 23.47-24.08 m. DEPTH

BOREHOLE P-4, TEST No. 4; 13.72-14.32 m. DEPTH

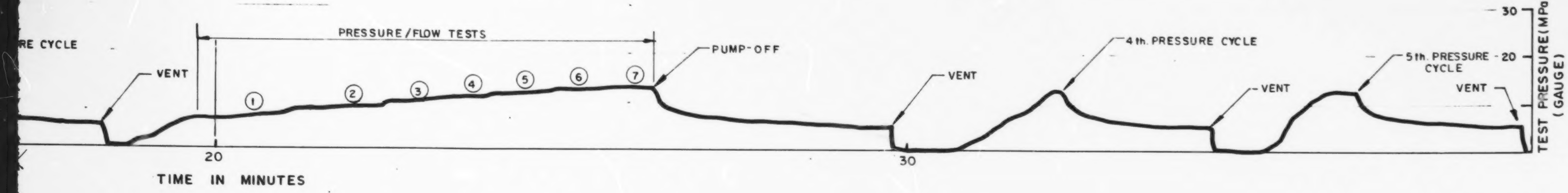

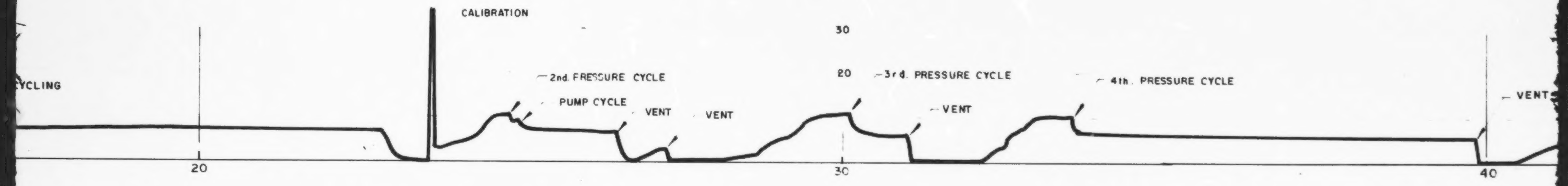

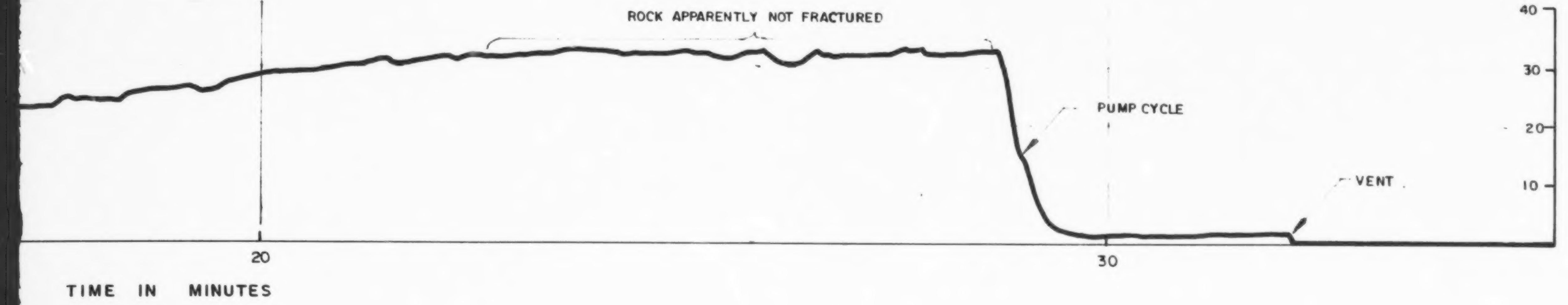

BOREHOLE P-4, TEST No. 3 ;

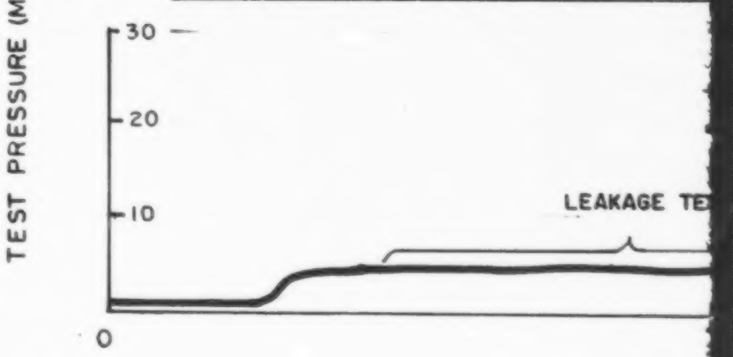

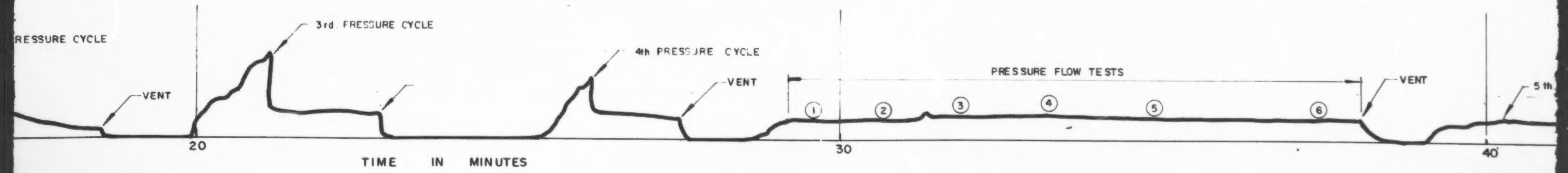

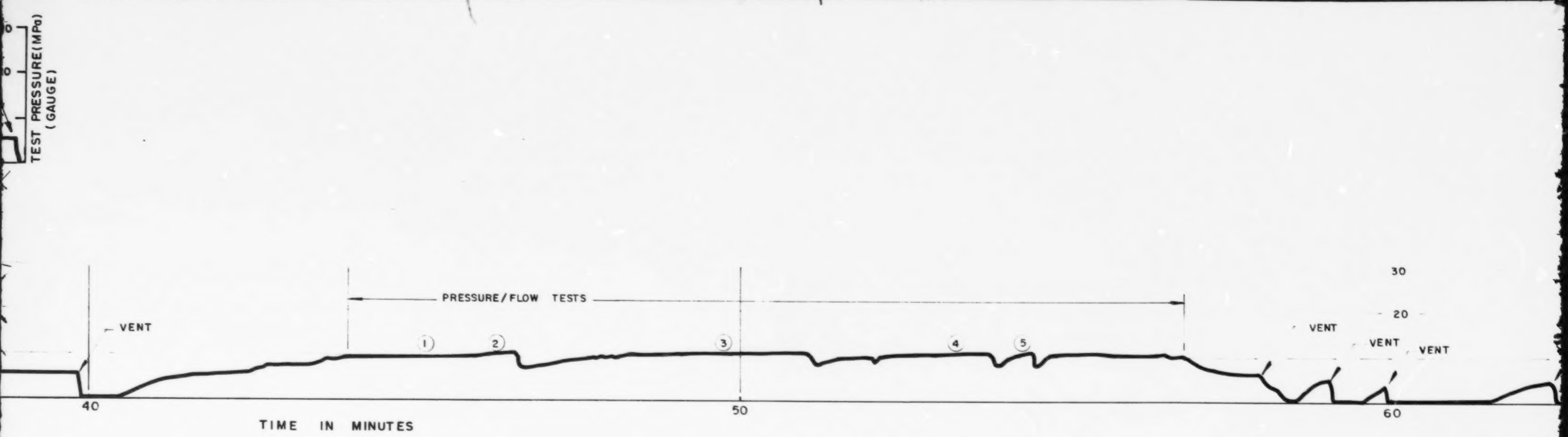

P-4, TEST No. 3 ; 17.98 - 18.59m. DEPTH

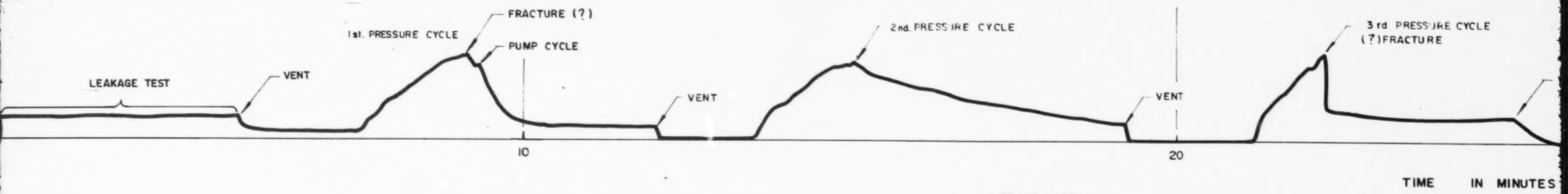

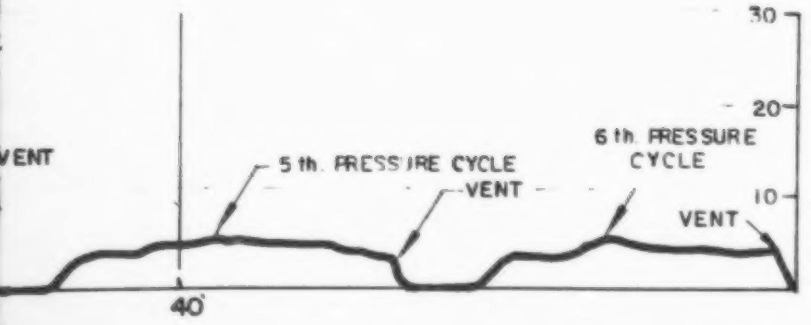

BOREHOLE P-4, TEST No. 5; 11.88 - 12.50m. DEPTH

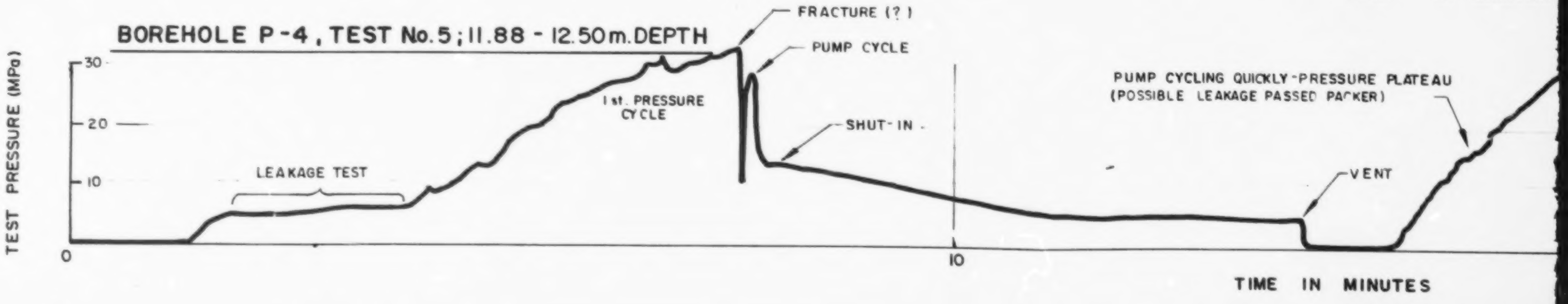

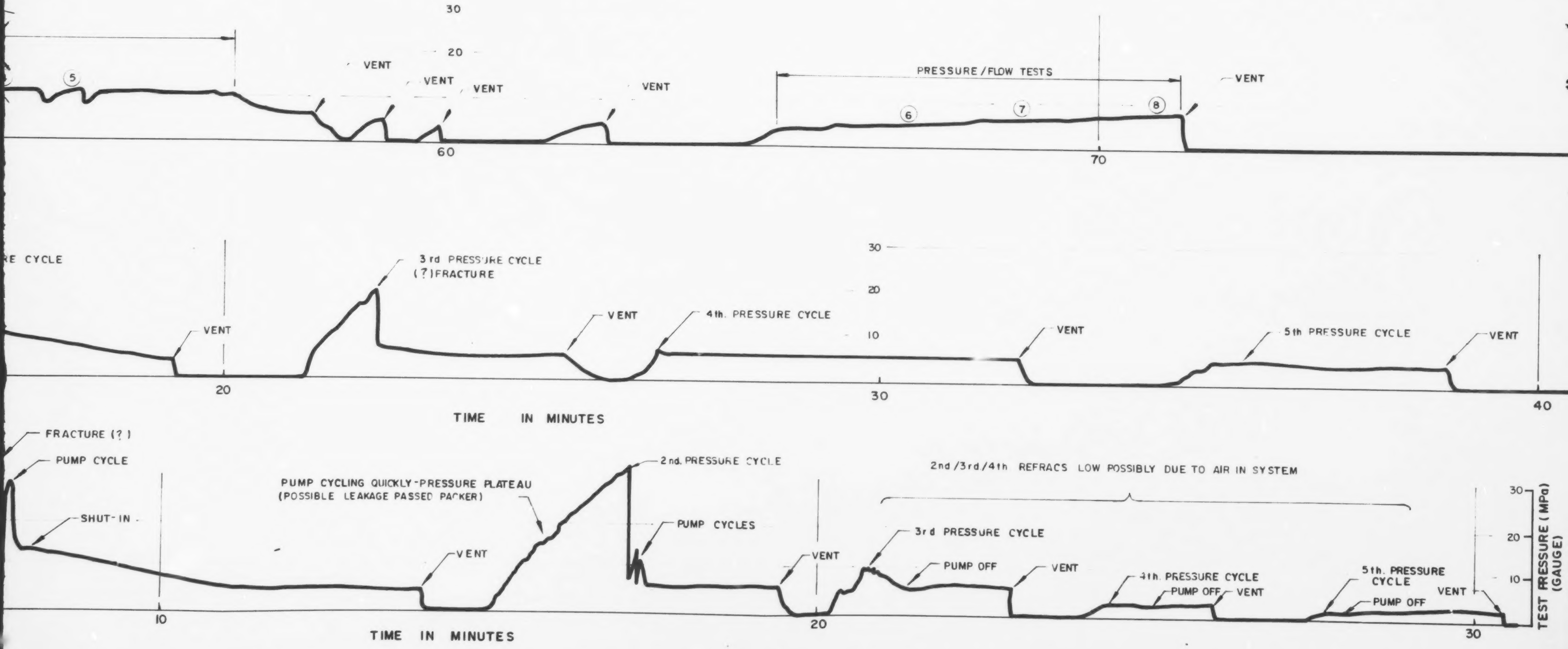
30
20
VENT
VENT
VENT
VENT
5
PRESSURE / FLOW TESTS
6
7
8
VENT
60
70
RE CYCLE
3rd PRESSURE CYCLE
(?) FRACTURE
VENT
VENT
4th. PRESSURE CYCLE
30
20
10
VENT
5th PRESSURE CYCLE
VENT
20
30
40
TIME IN MINUTES
FRACTURE (?)
PUMP CYCLE
SHUT-IN
PUMP CYCLING QUICKLY-PRESSURE PLATEAU
(POSSIBLE LEAKAGE PASSED PACKER)
VENT
2nd. PRESSURE CYCLE
PUMP CYCLES
2nd/3rd/4th REFRACS LOW POSSIBLY DUE TO AIR IN SYSTEM
3rd PRESSURE CYCLE
VENT
PUMP OFF
VENT
4th. PRESSURE CYCLE
PUMP OFF
VENT
5th. PRESSURE CYCLE
PUMP OFF
VENT
30
20
10
TEST PRESSURE (MPa) (GAUGE)
10
20
30
TIME IN MINUTES

HYDROFRACTURE TEST RESULTS PRINCE MINE
BOREHOLE P-4 TEST Nos. 1 - 6 incl.

FIGURE CI-2

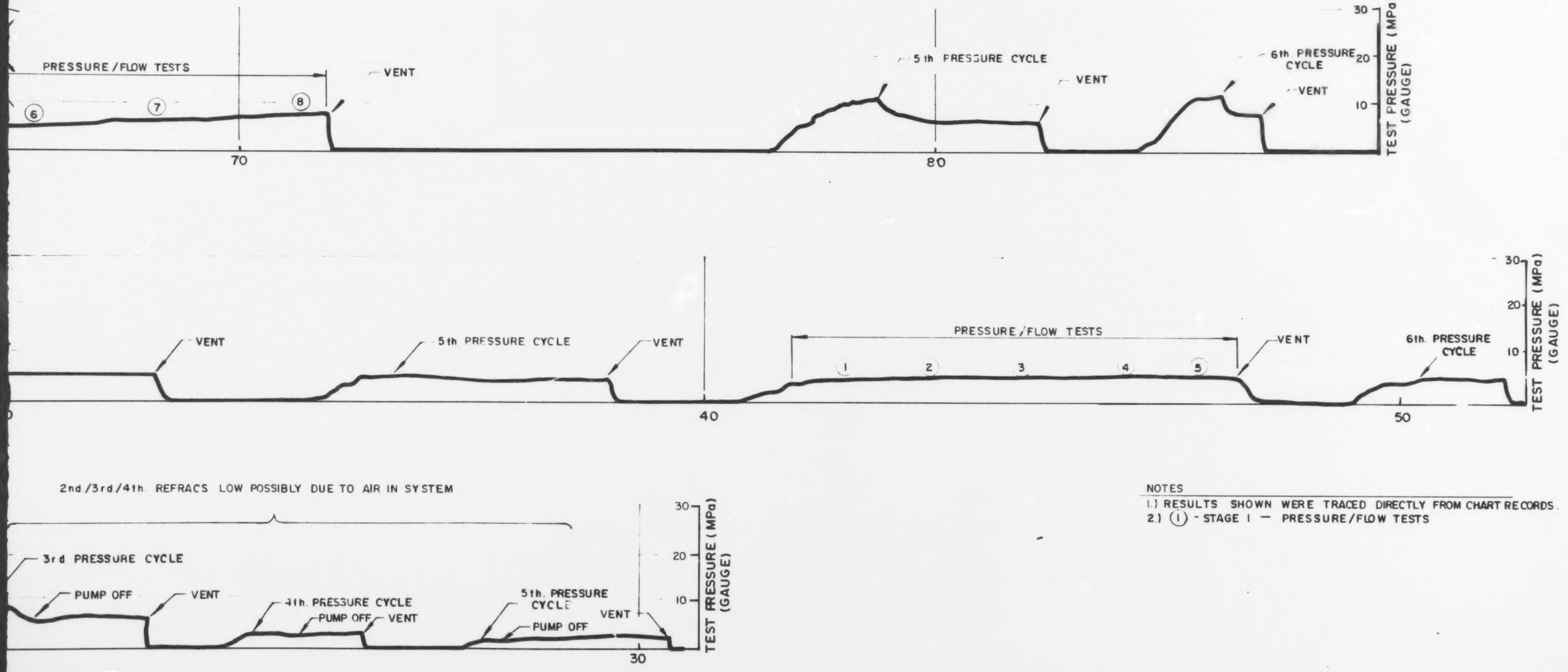

NOTES
1.) RESULTS SHOWN WERE TRACED DIRECTLY FROM CHART RECORDS.
2.) ① - STAGE 1 — PRESSURE/FLOW TESTS

Date MAY 20, 1986
Project 851-6025

Golder Associates

Drawn D. M.
Chkd JG

HYDROFRACTURE PRESSURE / FLOW TEST
PRINCE MINE
BOREHOLE P4 TEST No. 1

FIGURE C1-3

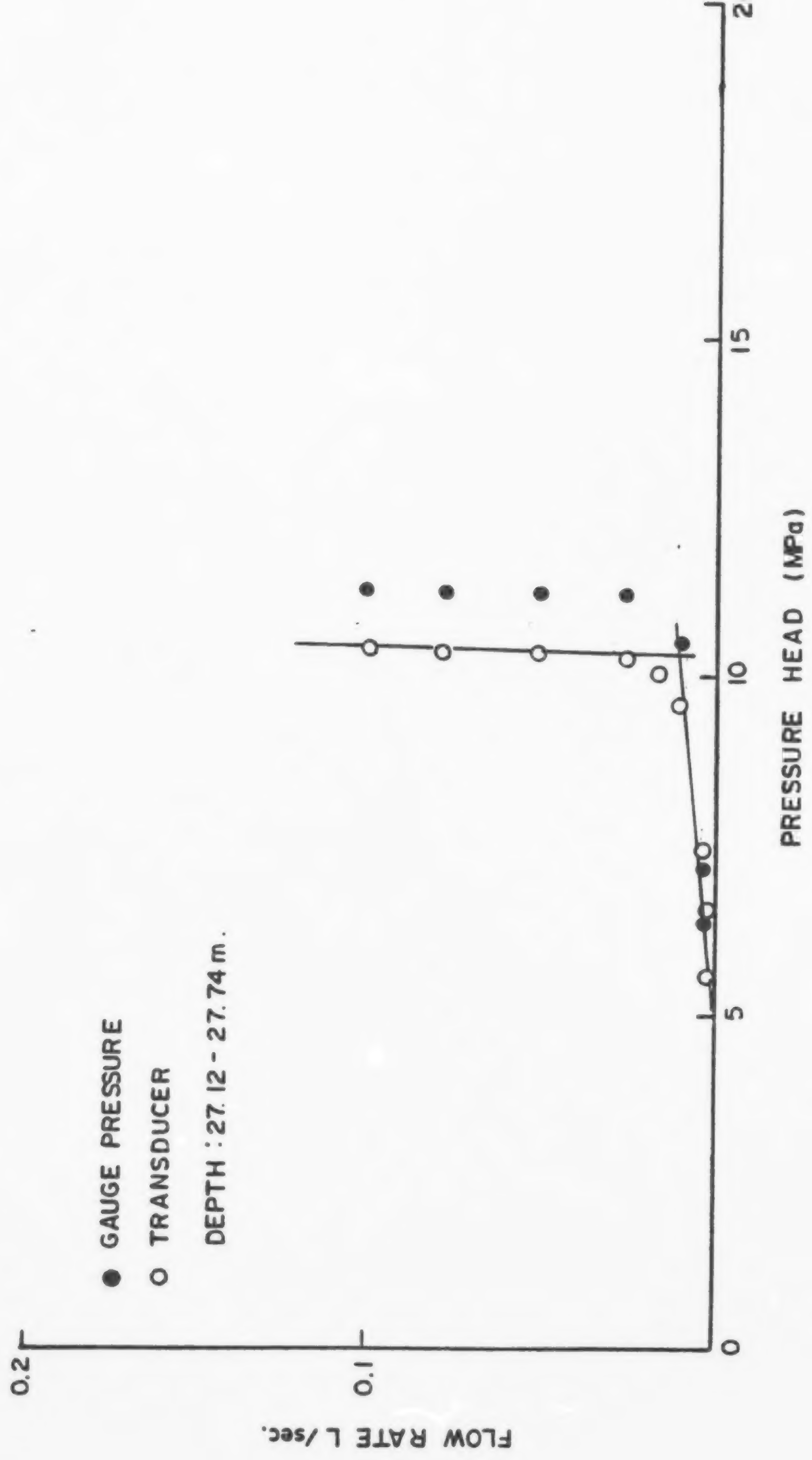

Date MAY 14, 1986

Project 851-6025

Golder Associates

Drawn D.M.

Chkd.

HYDROFRACTURE PRESSURE / FLOW TEST
PRINCE MINE
BOREHOLE P4 TEST No. 3

FIGURE CI-4

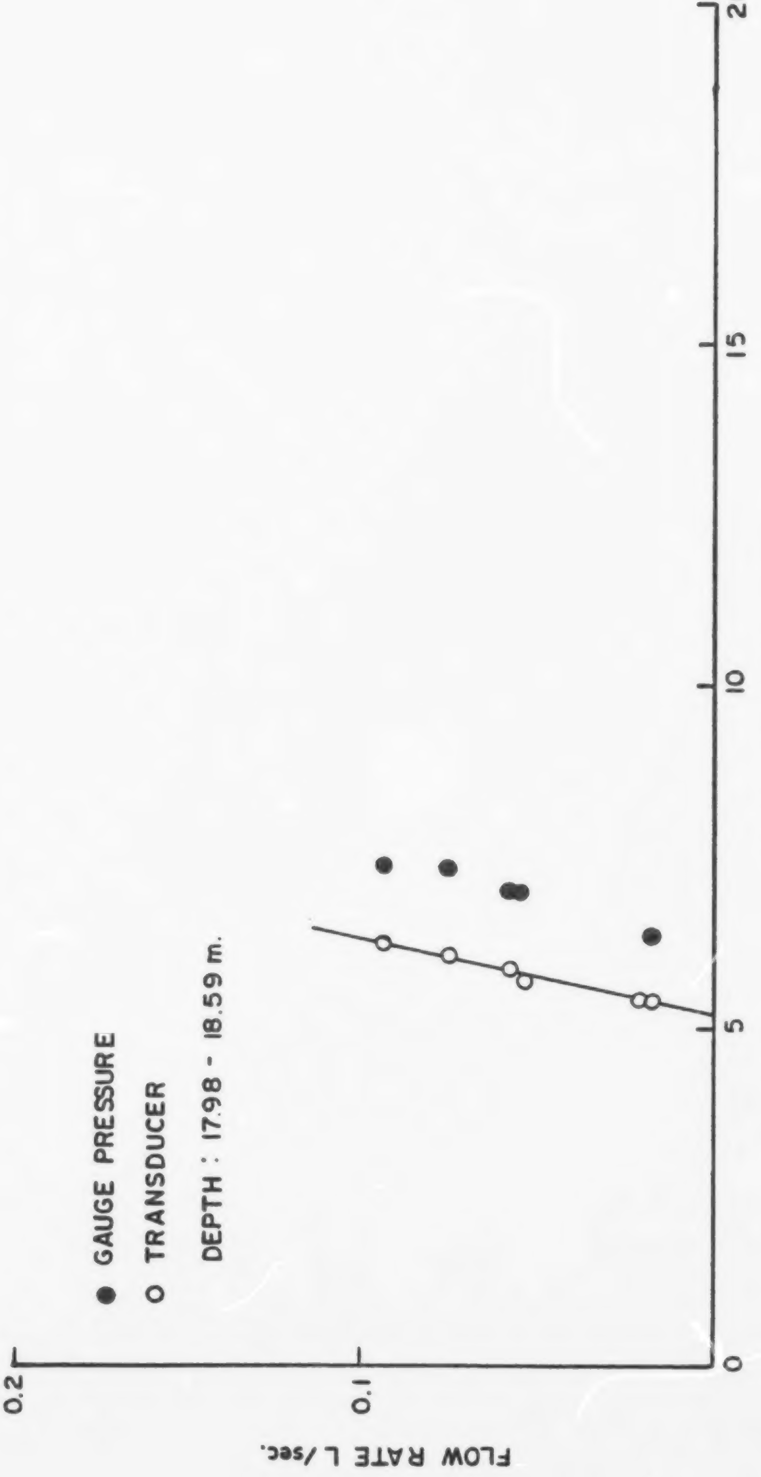

Date MAY 14, 1986
Project 851-6025

Golder Associates

Drawn D.M.
Chkd.

HYDROFRACTURE PRESSURE / FLOW TEST
PRINCE MINE
BOREHOLE P4 TEST No. 4

FIGURE CI - 5

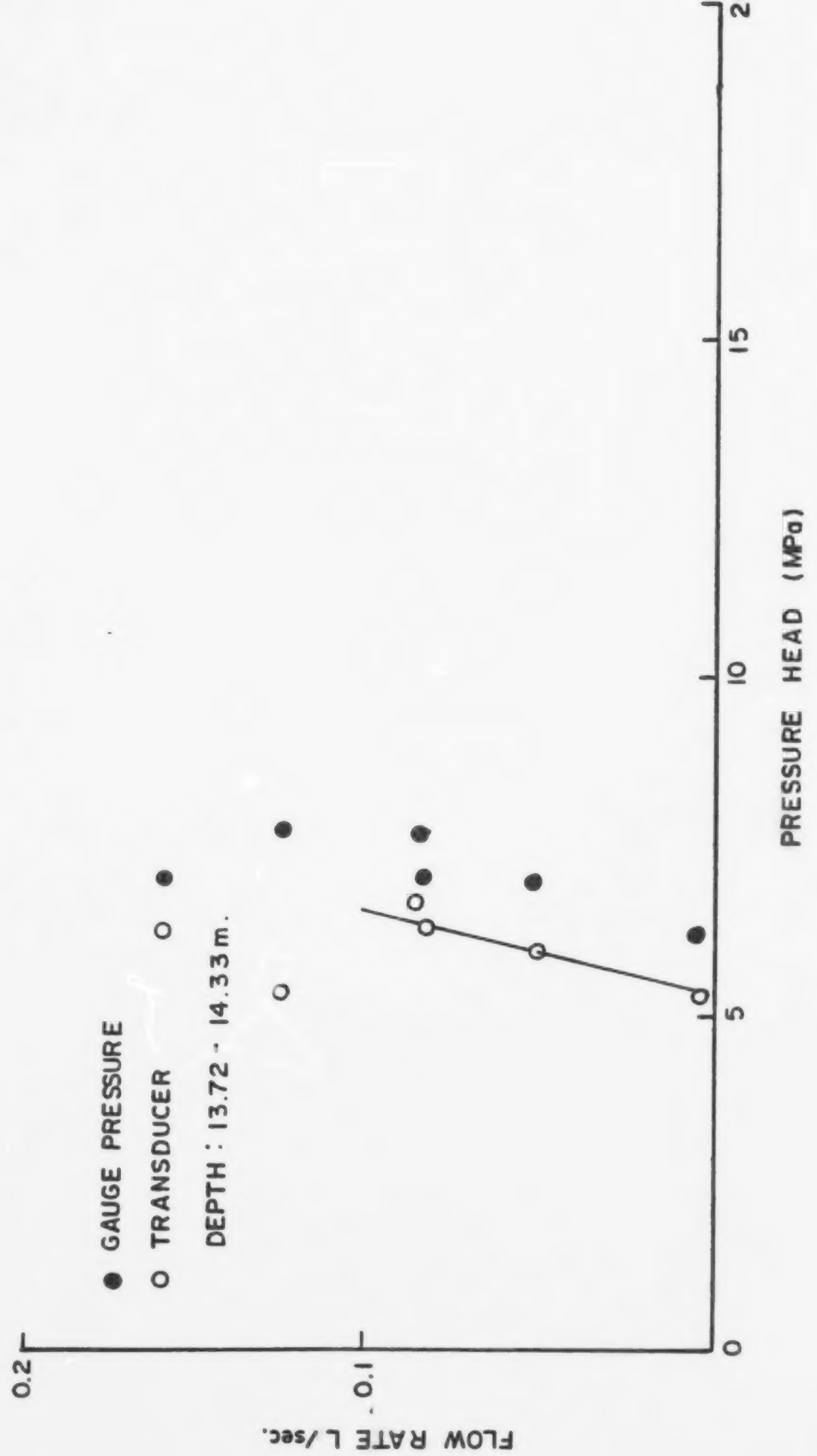

Date MAY 14, 1986
Project 851-6025

Golder Associates

Drawn D.M.
Chkd.

HYDROFRACTURE PRESSURE / FLOW TEST
PRINCE MINE
BOREHOLE P4 TEST No. 6

FIGURE CI - 6

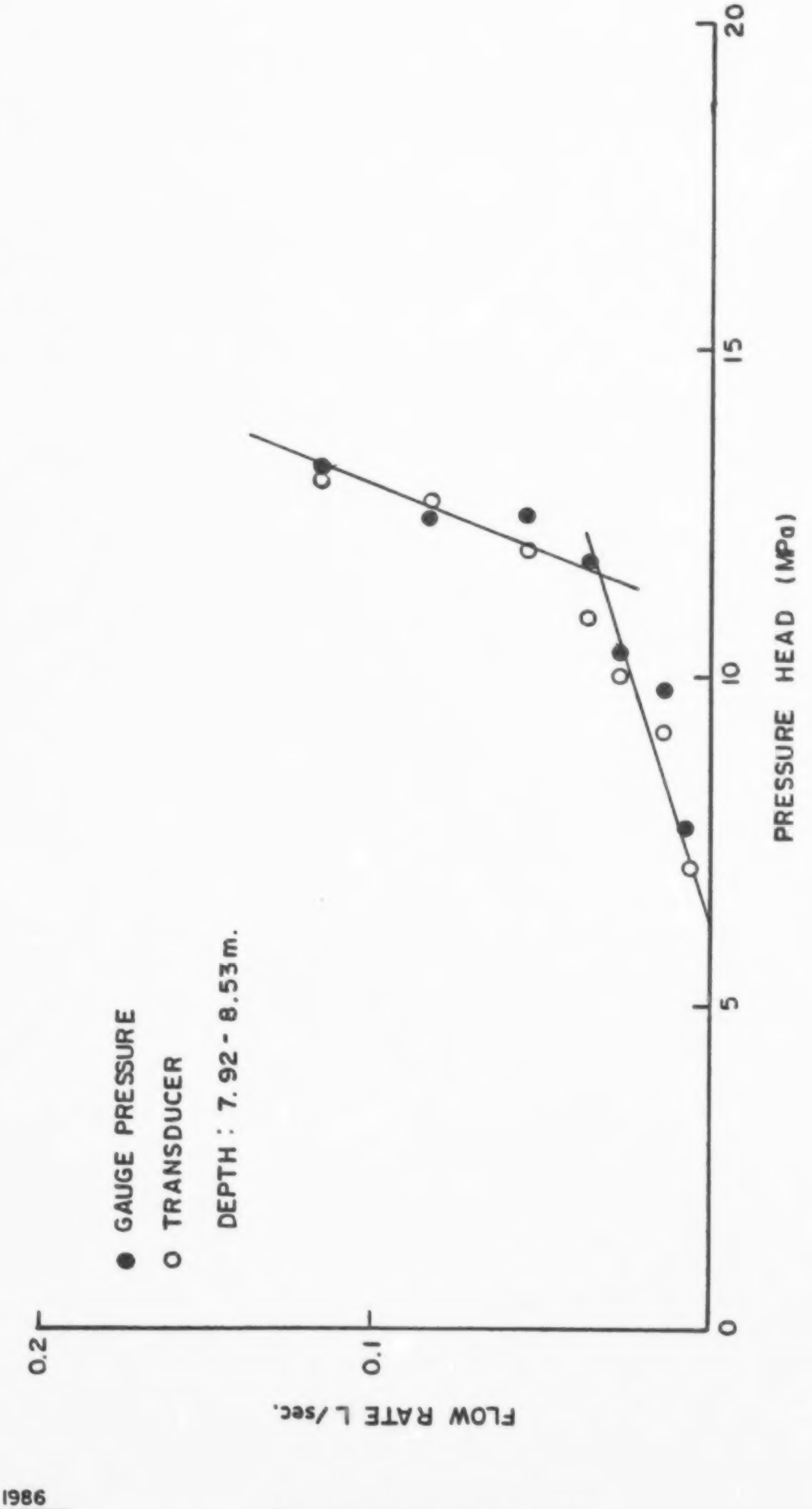

Date MAY 14, 1986
Project 851-6025

Golder Associates

Drawn D.M.
Chkd.

HYDROFRACTURE PRESSURE / FLOW TEST
PRINCE MINE
BOREHOLE P3 TEST No. 1

FIGURE C1-7

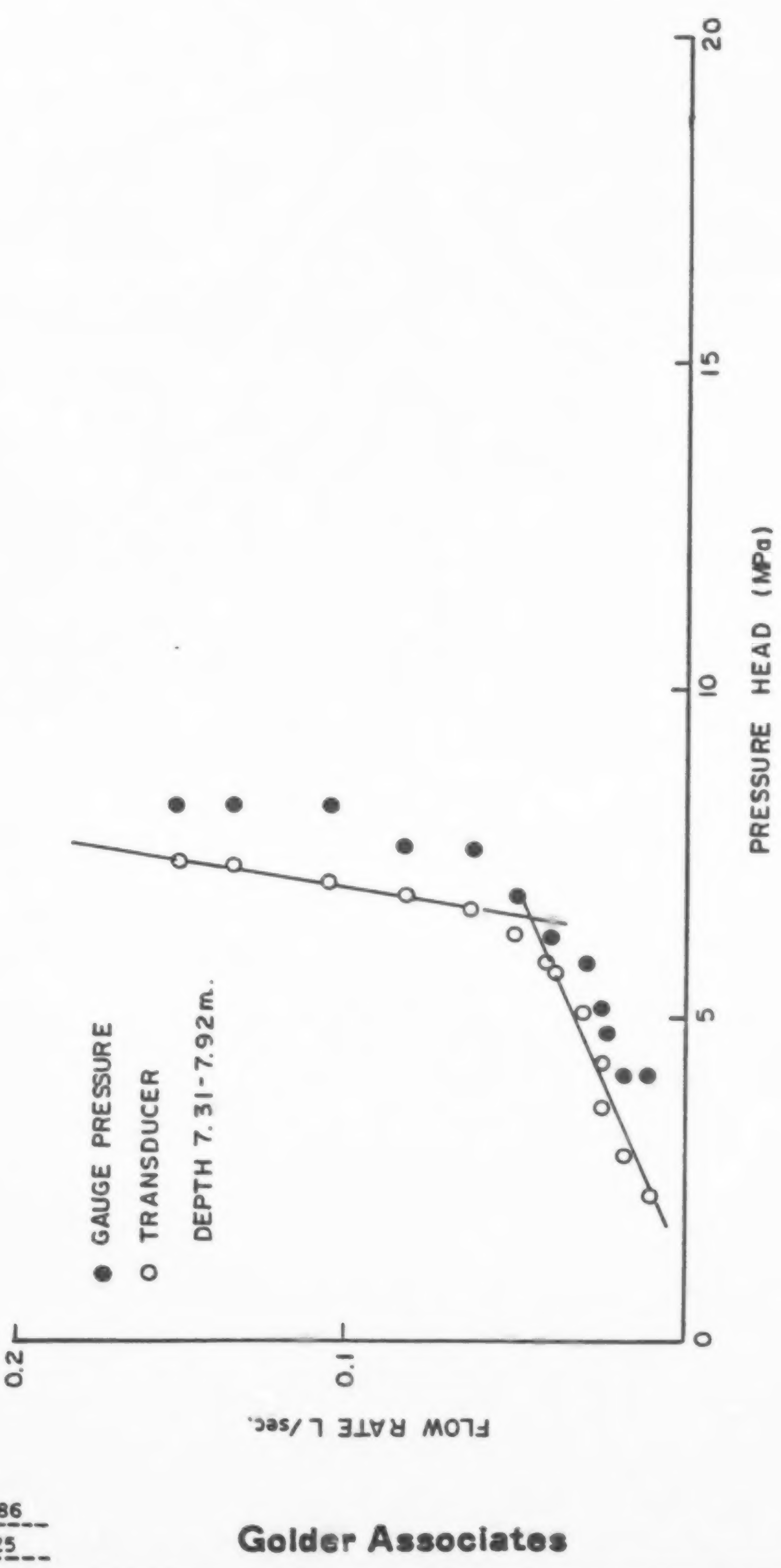

Date MAY 14, 1986
Project 851-6025

Golder Associates

Drawn D.M.
Chkd.

HYDROFRACTURE PRESSURE / FLOW TEST
PRINCE MINE
BOREHOLE P5 TEST No. 1

FIGURE C1-8

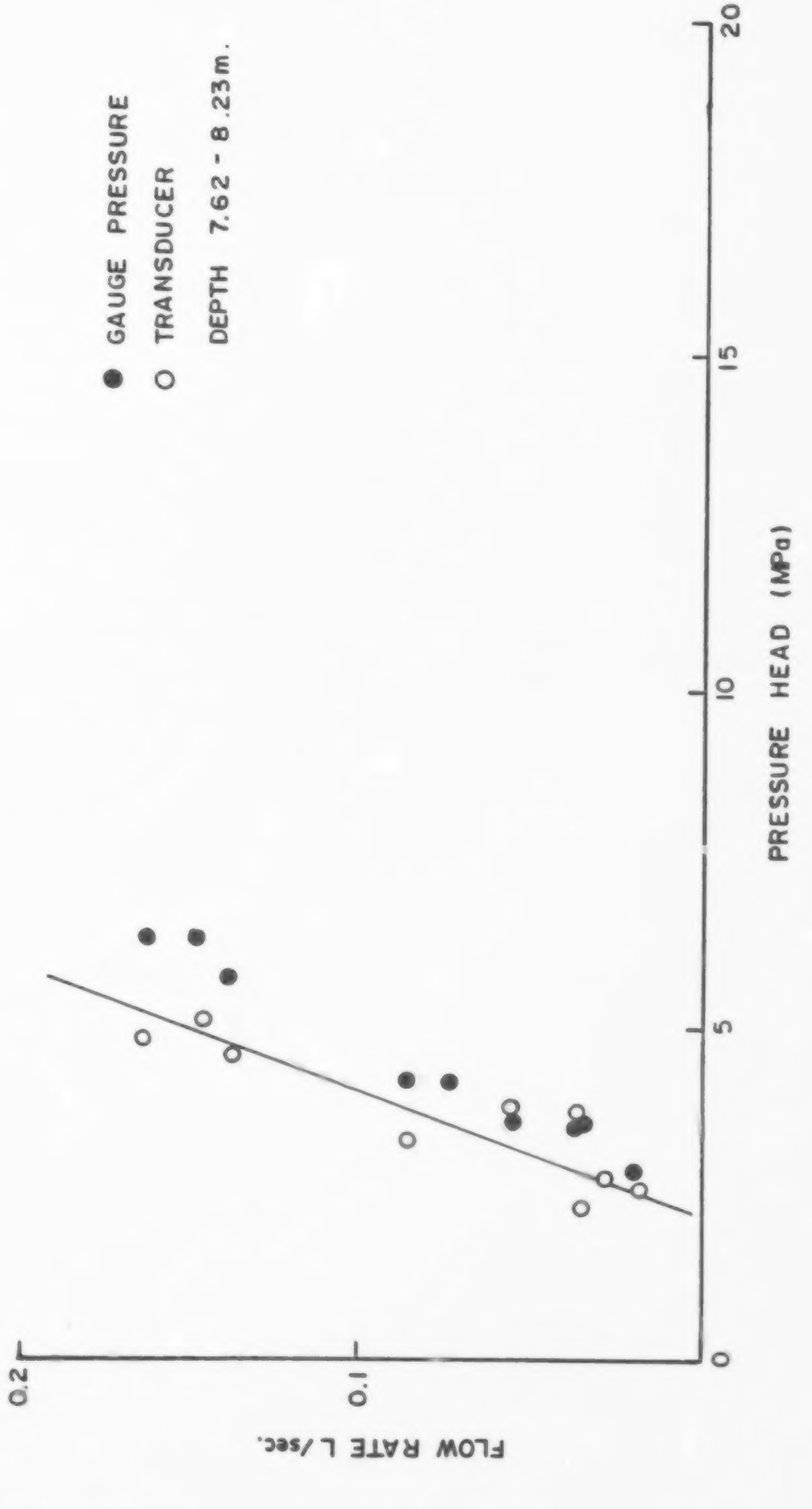

Date MAY 14, 1986
Project 851-6025

Golder Associates

Drawn D.M.
Chkd.

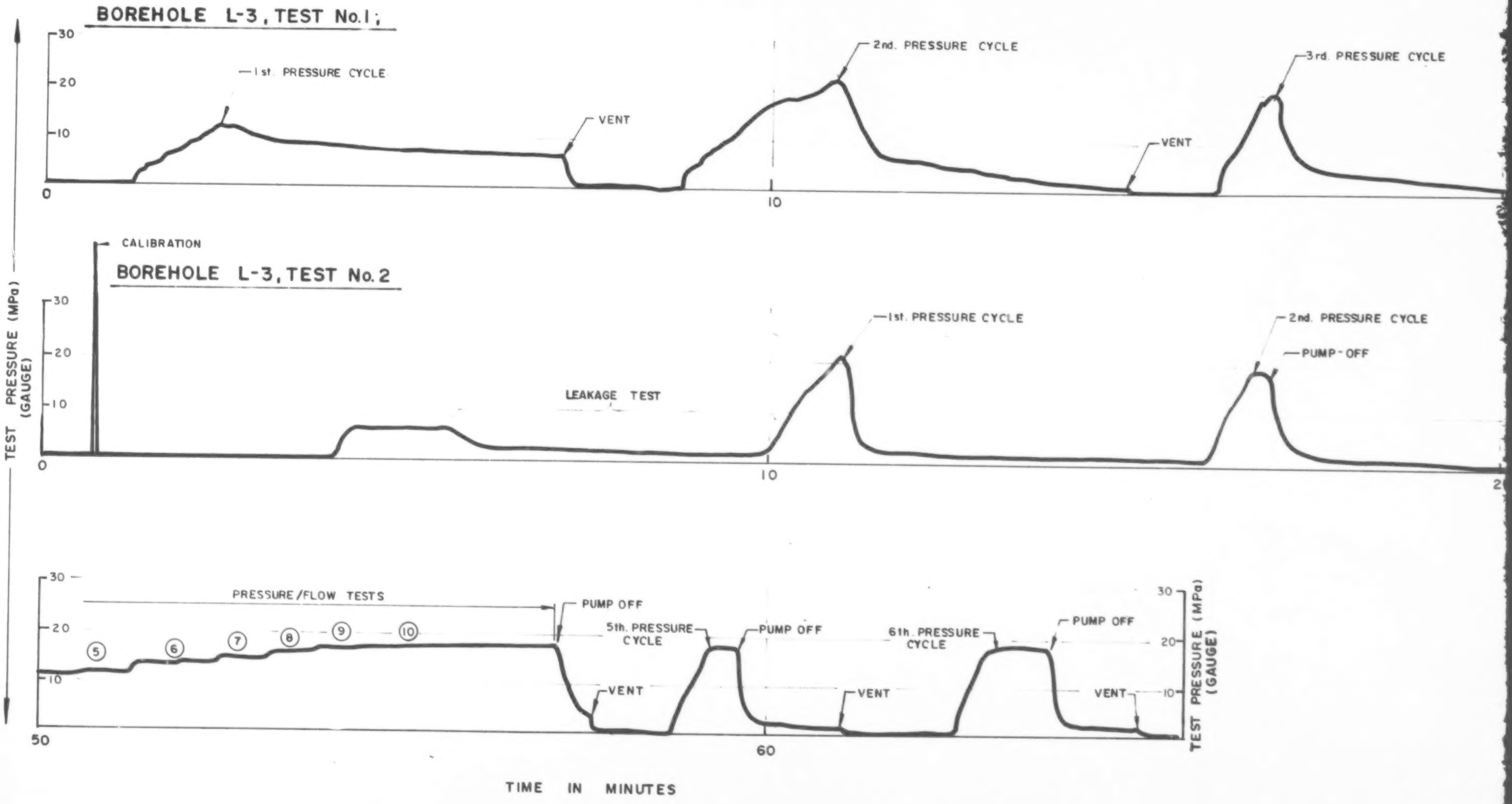
BOREHOLE L-3, TEST No.1;
30
20
10
0
1st. PRESSURE CYCLE
VENT
2nd. PRESSURE CYCLE
VENT
3rd. PRESSURE CYCLE
10
CALIBRATION
BOREHOLE L-3, TEST No. 2
30
20
10
0
LEAKAGE TEST
1st. PRESSURE CYCLE
2nd. PRESSURE CYCLE
PUMP-OFF
10
TEST PRESSURE (MPa) (GAUGE)
30
20
10
PRESSURE/FLOW TESTS
⑤
⑥
⑦
⑧
⑨
⑩
PUMP OFF
5th. PRESSURE CYCLE
PUMP OFF
VENT
6th. PRESSURE CYCLE
PUMP OFF
VENT
VENT
50
60
30
20
10
TEST PRESSURE (MPa) (GAUGE)
TIME IN MINUTES

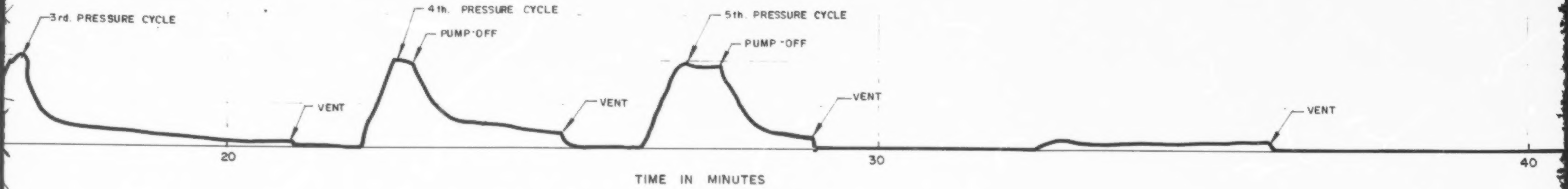
3rd. PRESSURE CYCLE
4th. PRESSURE CYCLE
PUMP-OFF
5th. PRESSURE CYCLE
PUMP-OFF
VENT
VENT
VENT
VENT
20
30
40
TIME IN MINUTES

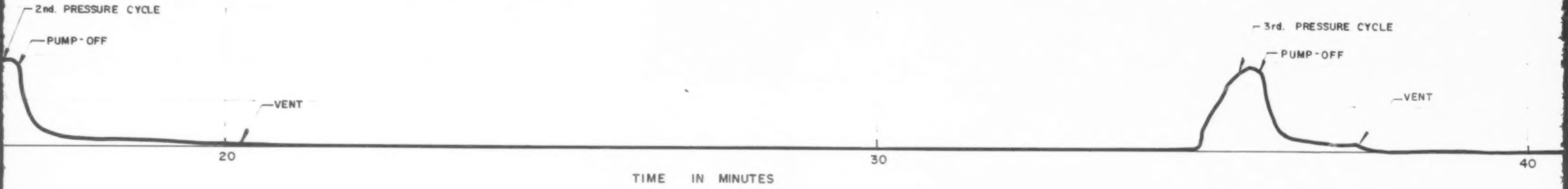
2nd. PRESSURE CYCLE
PUMP-OFF
VENT
3rd. PRESSURE CYCLE
PUMP-OFF
VENT
20
30
40
TIME IN MINUTES

HYDROFRAC
LIN
BOREHOLE

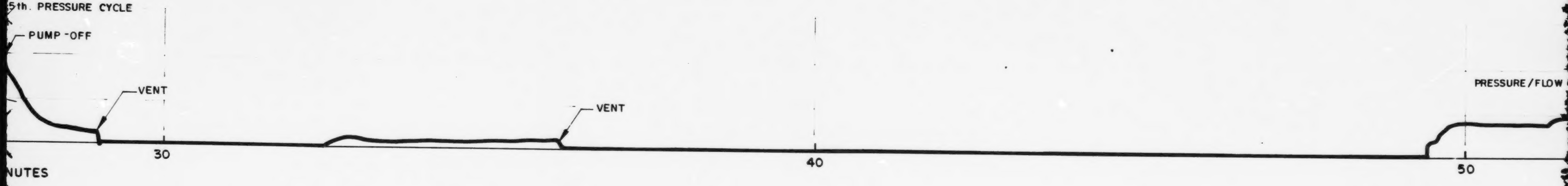

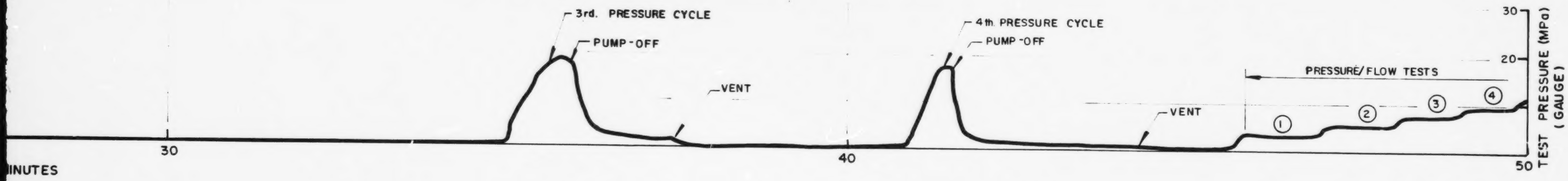

Date MAY 12,1986
Project 851-6025

HYDROFRACTURE TEST RESULTS
LINGAN MINE
BOREHOLE L-3, TEST Nos. 1 and 2

FIGURE C2-1

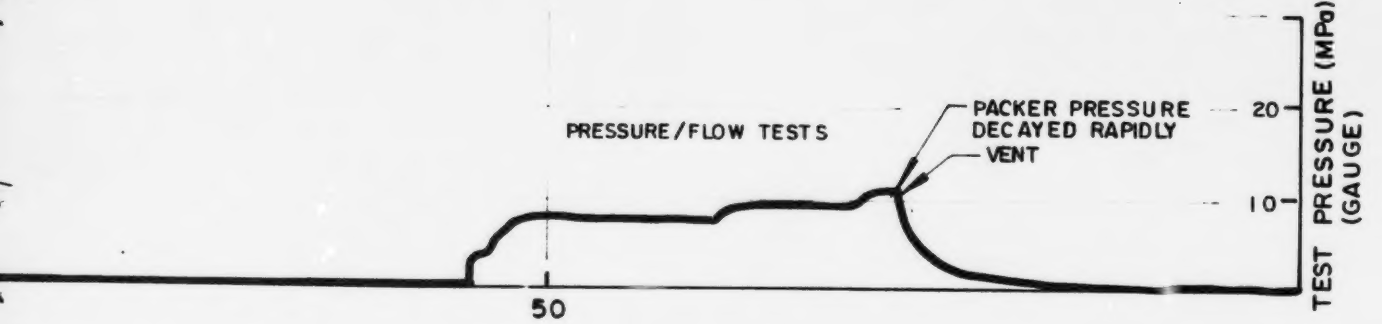

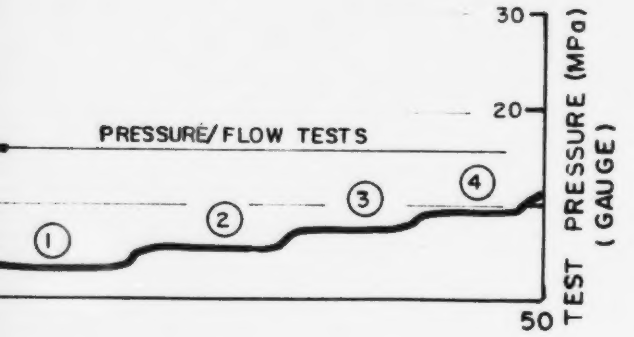

NOTES

1.) RESULTS SHOWN WERE TRACED DIRECTLY FROM CHART RECORDS

2) ① STAGE 1 ≃ PRESSURE/FLOW TESTS.

Date MAY 12, 1986
Project 851-6025

Golder Associates

Drawn D.M.
Chkd

BOREHOLE L-4, TEST No. 1; 28.96 - 29.56 m. DEPTH

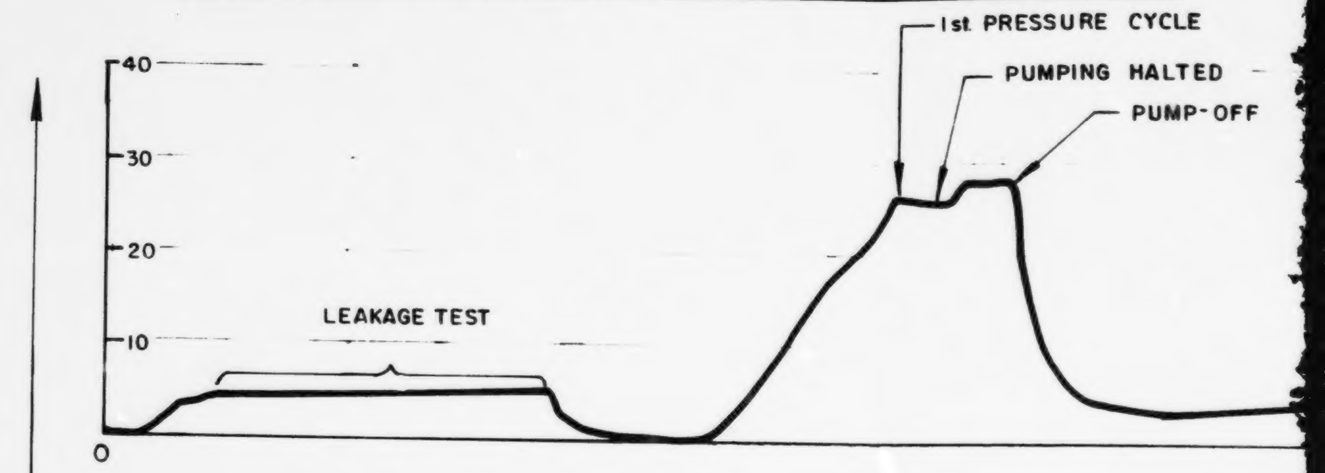

BOREHOLE L-4, TEST No. 2; 27.43 - 28.04 m. DEPTH

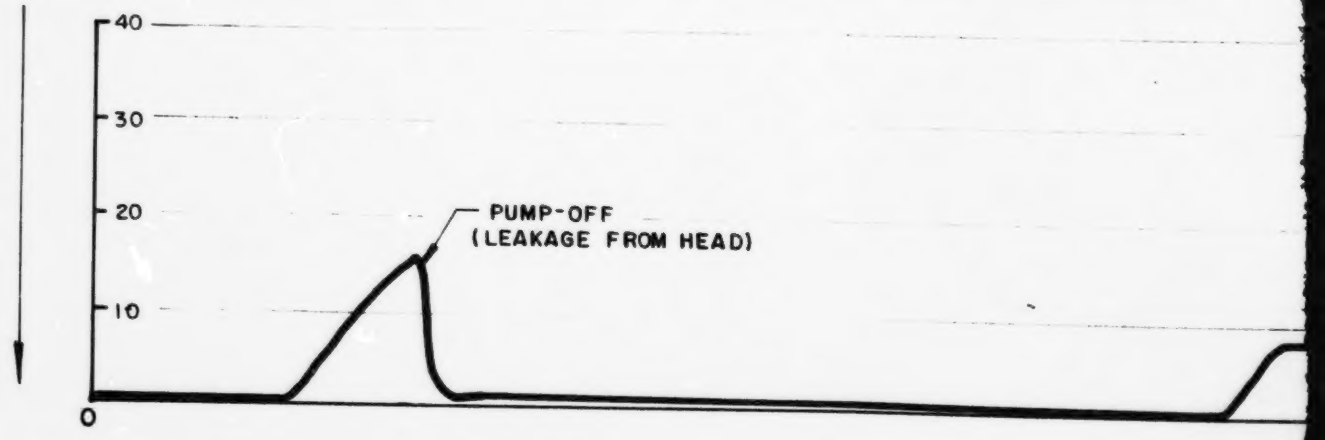

28.96 - 29.56 m. DEPTH

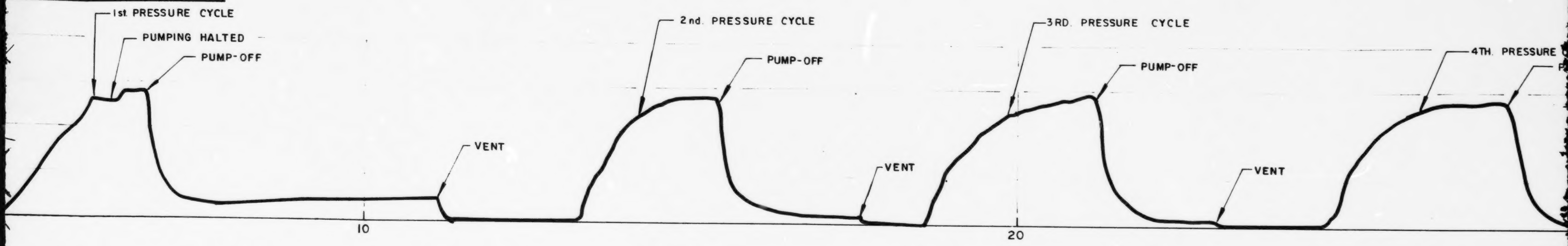

27.43 - 28.04 m. DEPTH

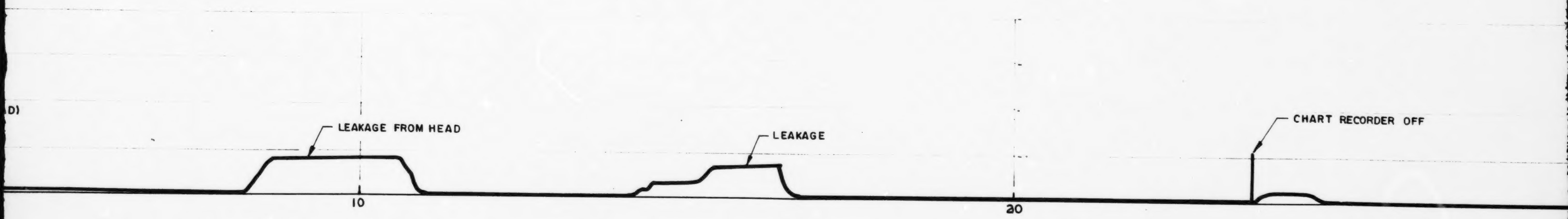

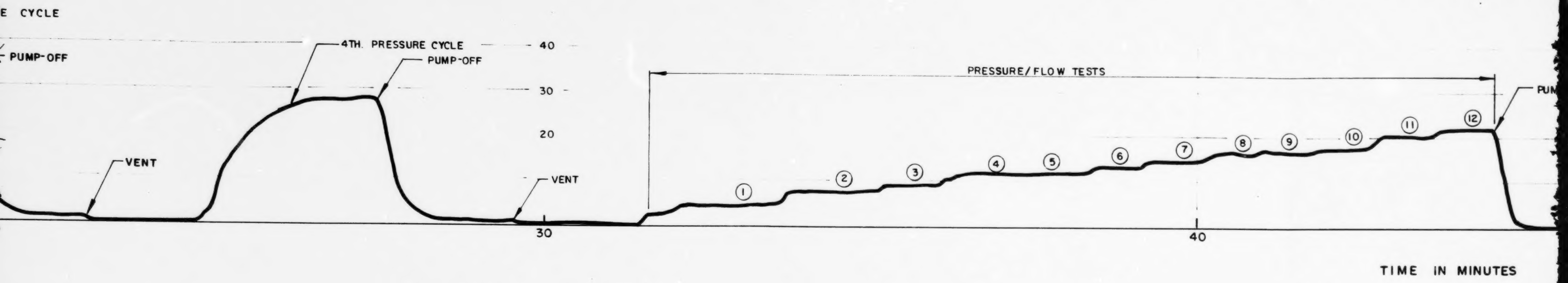
E CYCLE
PUMP-OFF
4TH. PRESSURE CYCLE
PUMP-OFF
VENT
VENT
40
30
20
PRESSURE/FLOW TESTS
PUM
①
②
③
④
⑤
⑥
⑦
⑧
⑨
⑩
⑪
⑫
30
40
TIME IN MINUTES

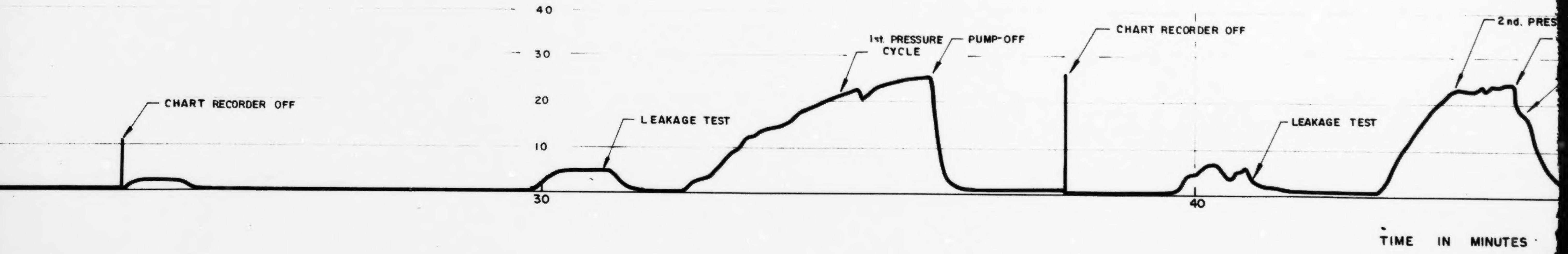
40
30
20
10
CHART RECORDER OFF
LEAKAGE TEST
1st. PRESSURE CYCLE
PUMP-OFF
CHART RECORDER OFF
LEAKAGE TEST
2nd. PRES
30
40
TIME IN MINUTES

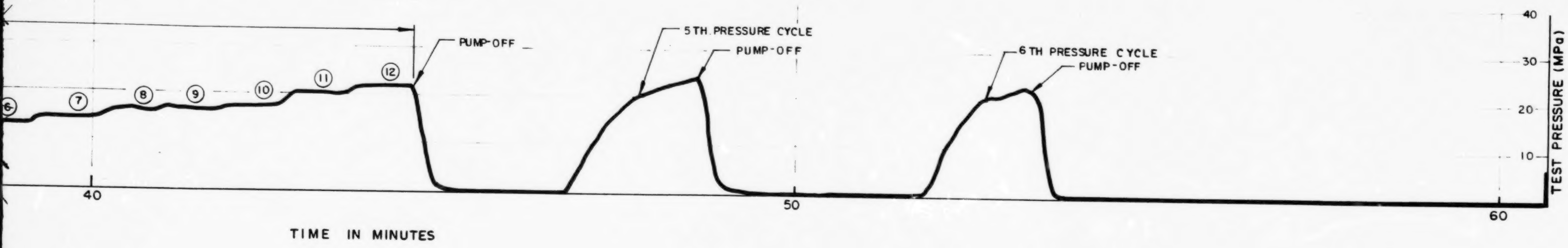

PUMP-OFF
5 TH. PRESSURE CYCLE
PUMP-OFF
6 TH PRESSURE CYCLE
PUMP-OFF
⑦
⑧
⑨
⑩
⑪
⑫
40
50
60
TIME IN MINUTES
40
30
20
10
TEST PRESSURE (MPa)

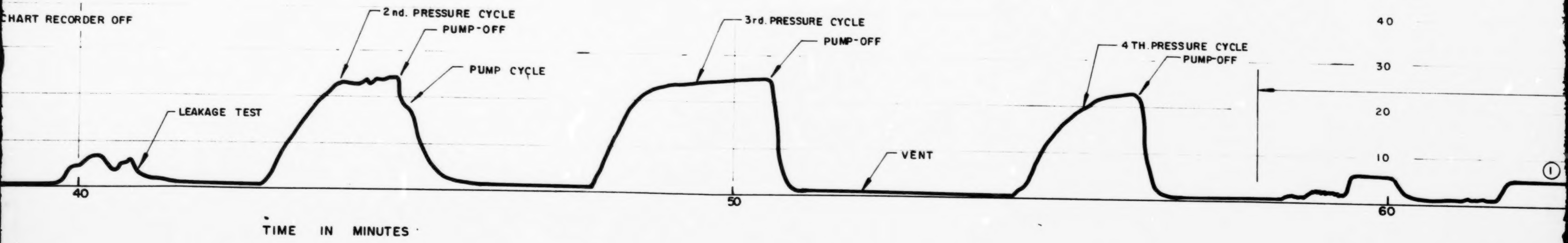

CHART RECORDER OFF
2nd. PRESSURE CYCLE
PUMP-OFF
PUMP CYCLE
LEAKAGE TEST
3rd. PRESSURE CYCLE
PUMP-OFF
VENT
4 TH. PRESSURE CYCLE
PUMP-OFF
①
40
30
20
10
40
50
60
TIME IN MINUTES

HYDROFRACTUR
LINGAN
BOREHOLE

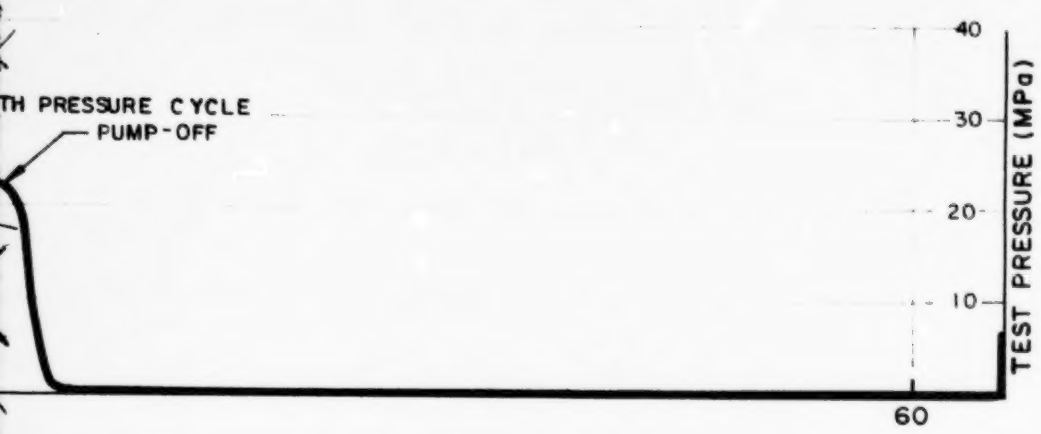

NOTES
1.) RESULT
2.) ①

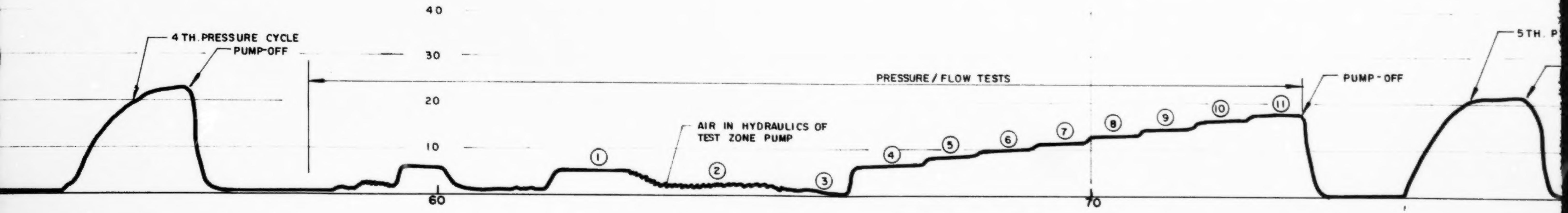

Date MAY 12, 1986
Project 851-6025

HYDROFRACTURE TEST RESULTS
LINGAN MINE
BOREHOLE L-4 TEST Nos.1 and 2

FIGURE C2-2

NOTES

1.) RESULTS SHOWN WERE TRACED DIRECTLY FROM CHART RECORDS.

2.) ① STAGE 1 ≃ PRESSURE FLOW TESTS

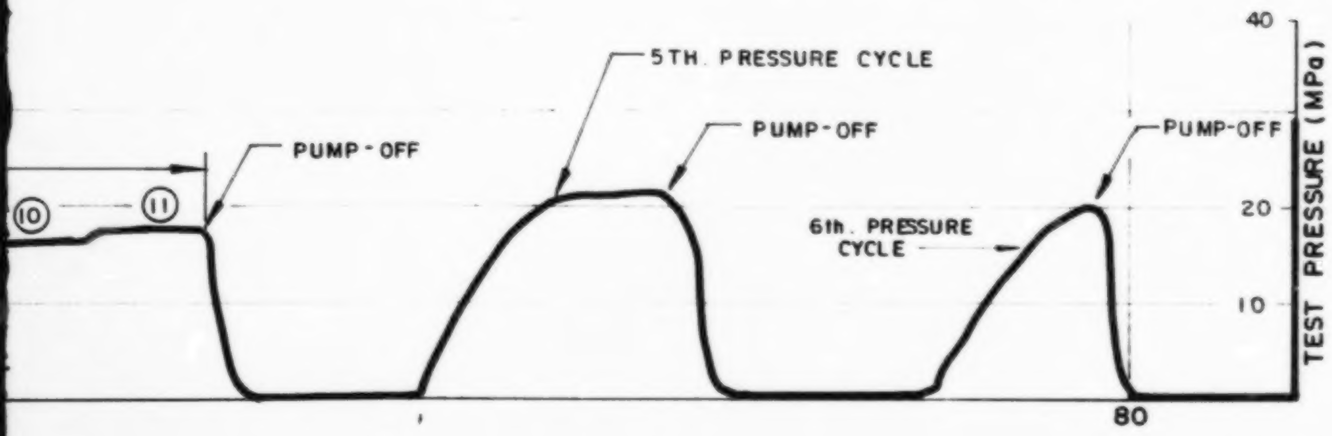

Date MAY 12, 1986
Project 851-6025

Golder Associates

Drawn D.M.
Chkd JcG

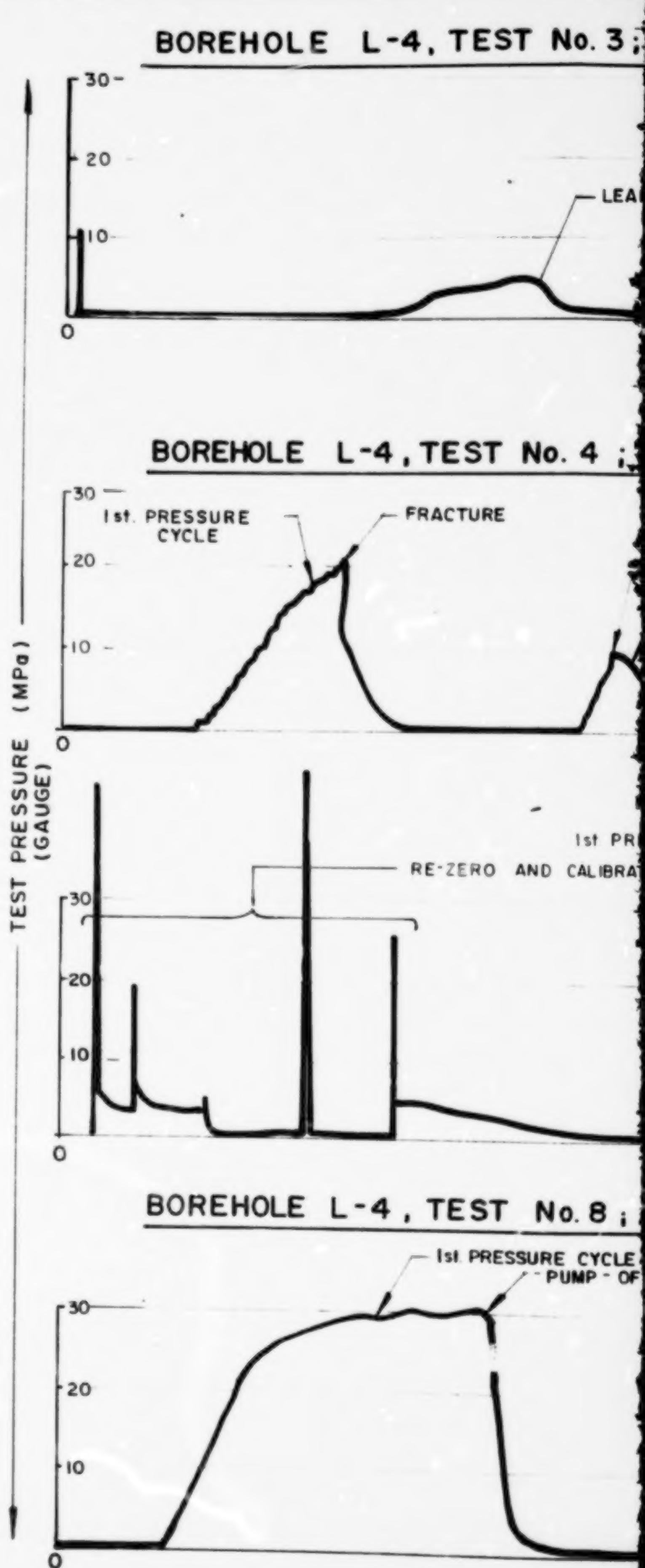
BOREHOLE L-4, TEST No. 3;

BOREHOLE L-4, TEST No. 4 ;

BOREHOLE L-4, TEST No. 8 ;

HOLE L-4, TEST No. 3 ; 24.38-24.99 m. DEPTH

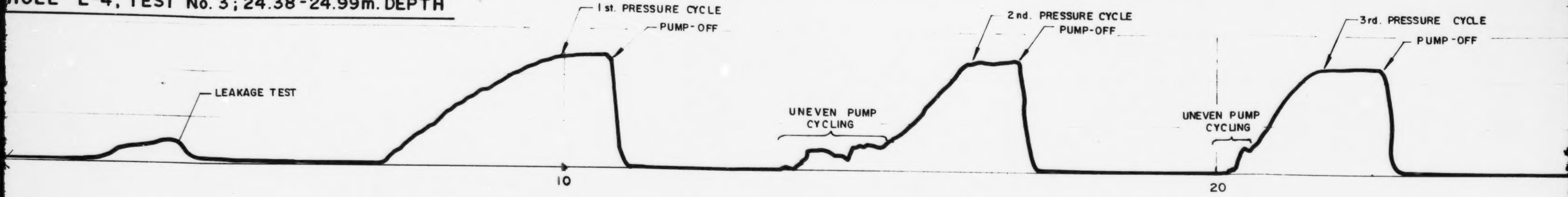

HOLE L-4, TEST No. 4 ; 9.14-9.75 m. DEPTH

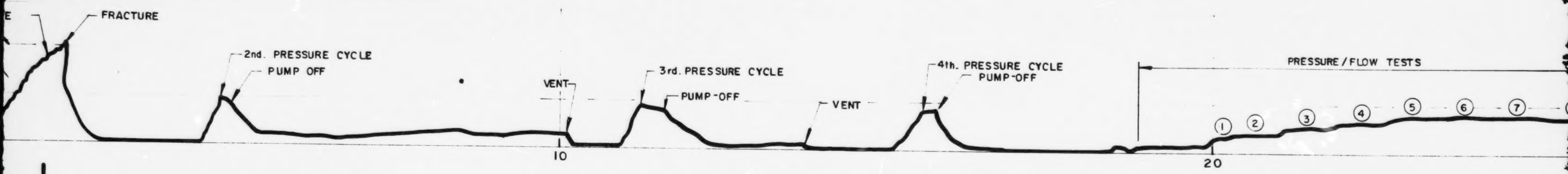

BOREHOLE L-4, TEST No. 6 ; 13.11-13.72 m. DEPTH

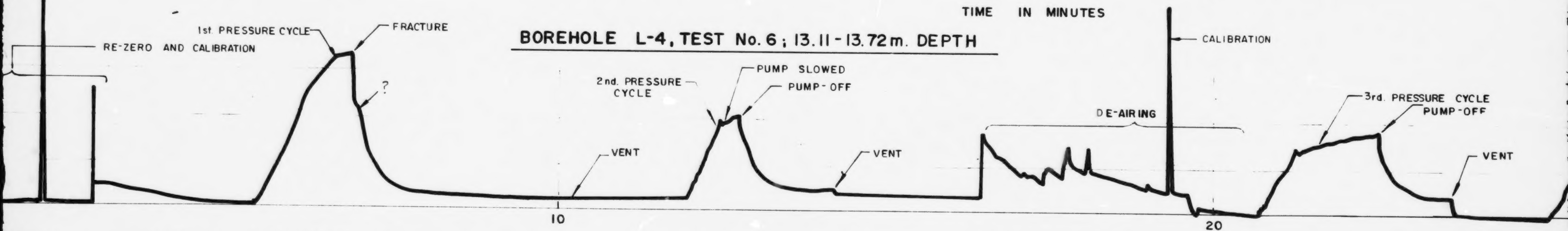

HOLE L-4, TEST No. 8 ; 24.38-24.99 m. DEPTH

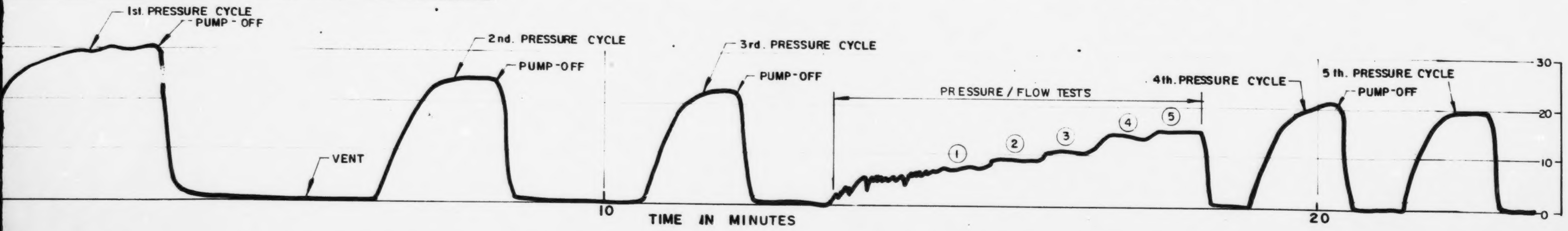

BOREHOLE

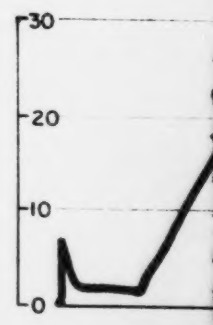

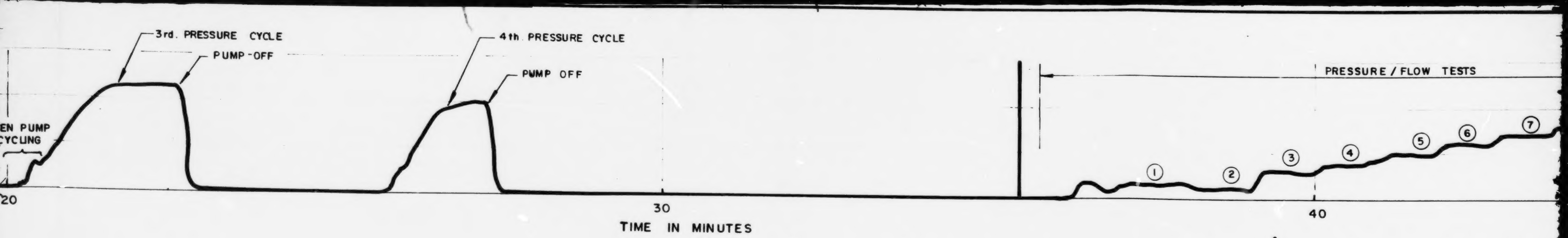

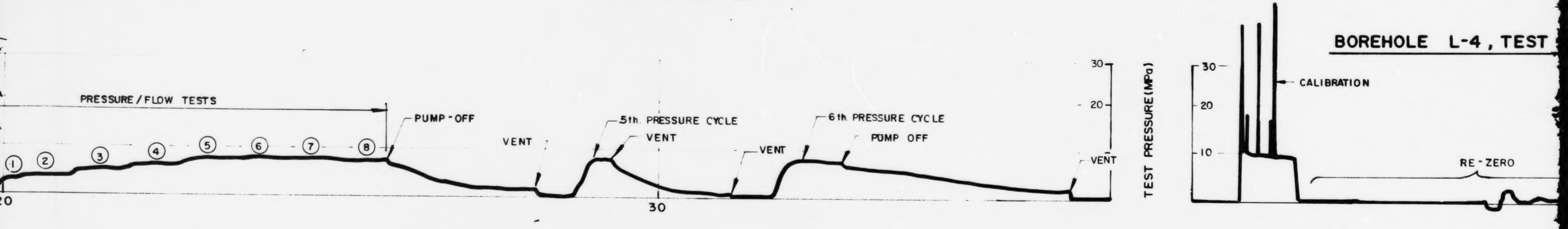

BOREHOLE L-4, TEST

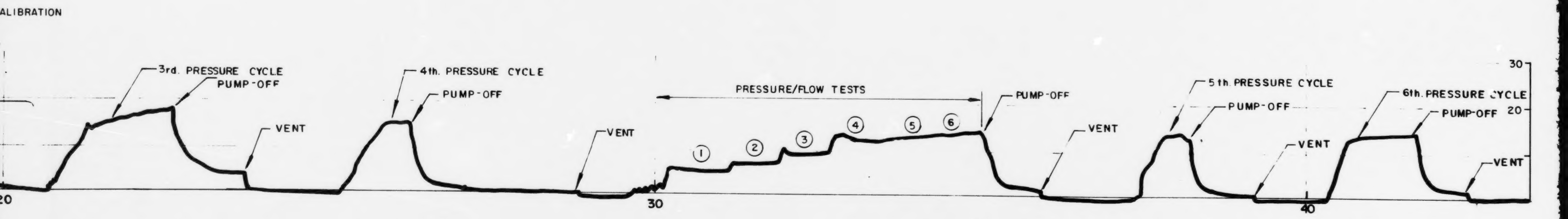

BOREHOLE L-4, TEST No.9 ; 28.19 - 28.80 m. DEPTH

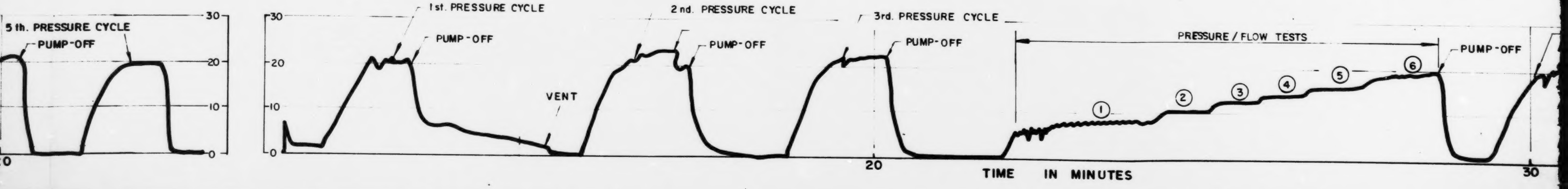

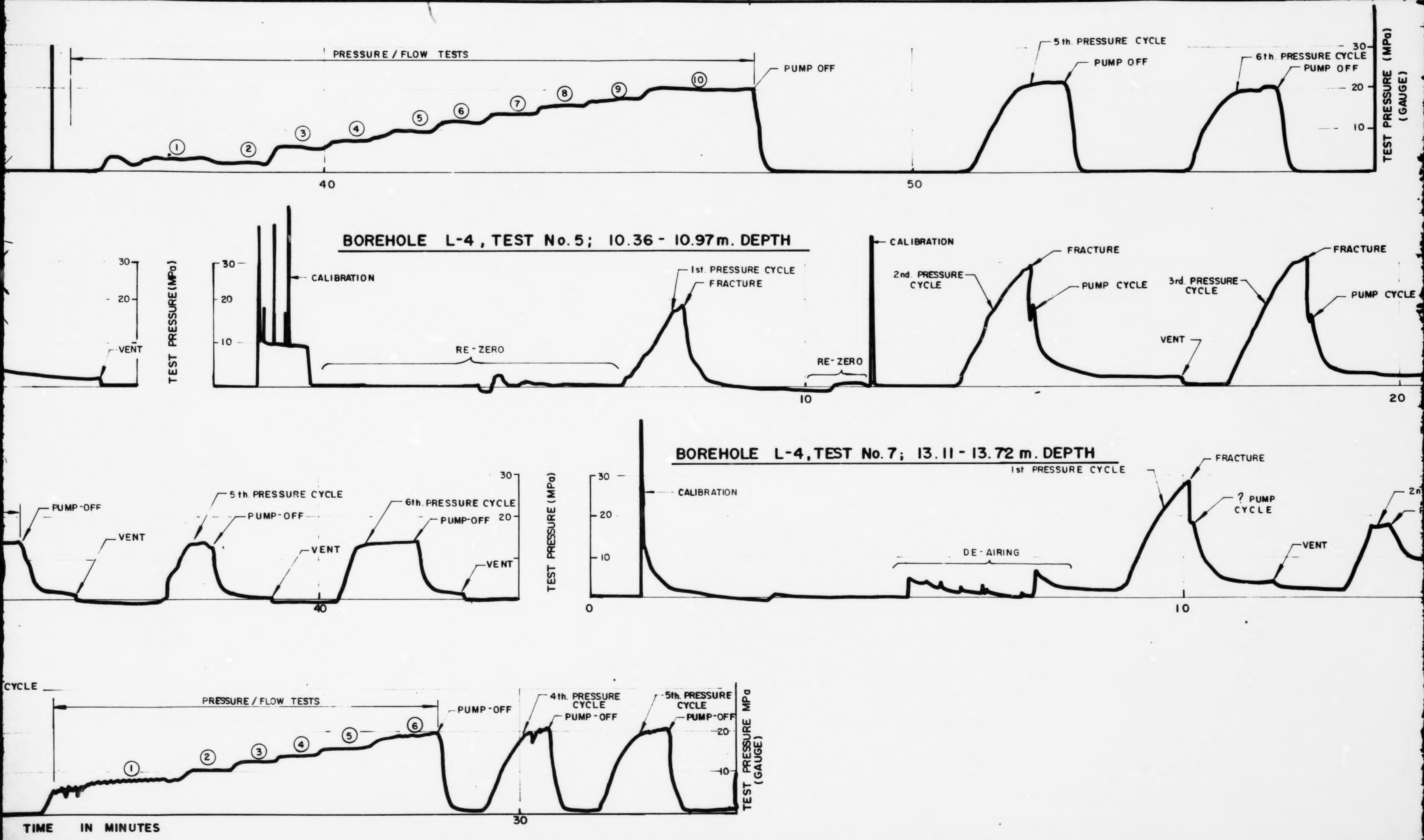

BOREHOLE L-4, TEST No. 5; 10.36 - 10.97 m. DEPTH

BOREHOLE L-4, TEST No. 7; 13.11 - 13.72 m. DEPTH

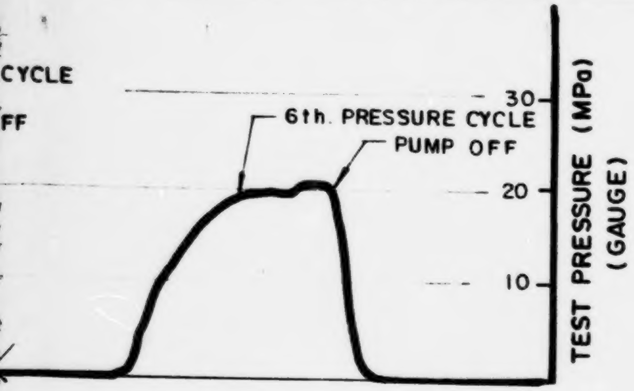
CYCLE
FF
6th. PRESSURE CYCLE
PUMP OFF
30
20
10
TEST PRESSURE (MPa) (GAUGE)

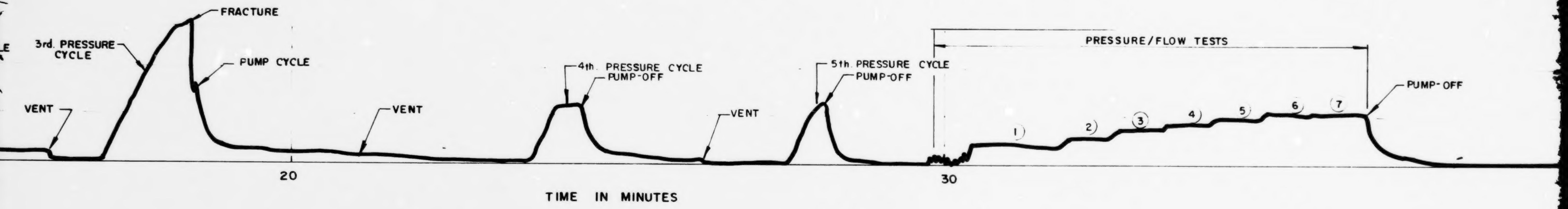
LE
FRACTURE
3rd. PRESSURE CYCLE
PUMP CYCLE
VENT
VENT
4th. PRESSURE CYCLE
PUMP-OFF
VENT
5th. PRESSURE CYCLE
PUMP-OFF
PRESSURE/FLOW TESTS
PUMP-OFF
1
2
3
4
5
6
7
20
30
TIME IN MINUTES

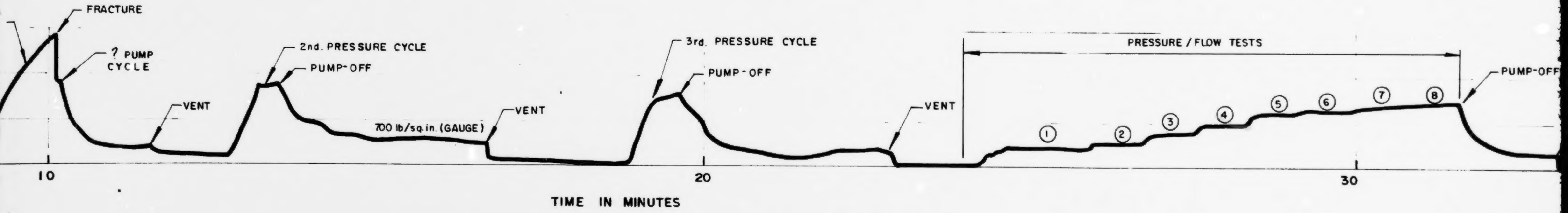
FRACTURE
? PUMP CYCLE
2nd. PRESSURE CYCLE
PUMP-OFF
VENT
700 lb/sq.in. (GAUGE)
VENT
3rd. PRESSURE CYCLE
PUMP-OFF
VENT
PRESSURE / FLOW TESTS
PUMP-OFF
①
②
③
④
⑤
⑥
⑦
⑧
10
20
30
TIME IN MINUTES

HYDROFRACTURE TEST RESULTS
LINGAN MINE
BOREHOLE L-4 TEST Nos. 3,4,5,6,7,8 and 9

FIGURE C2-3

NOTES

1) RESULTS SHOWN WERE TRACED DIRECTLY FROM CHART RECORDS

2) ① - STAGE I — PRESSURE/FLOW TESTS.

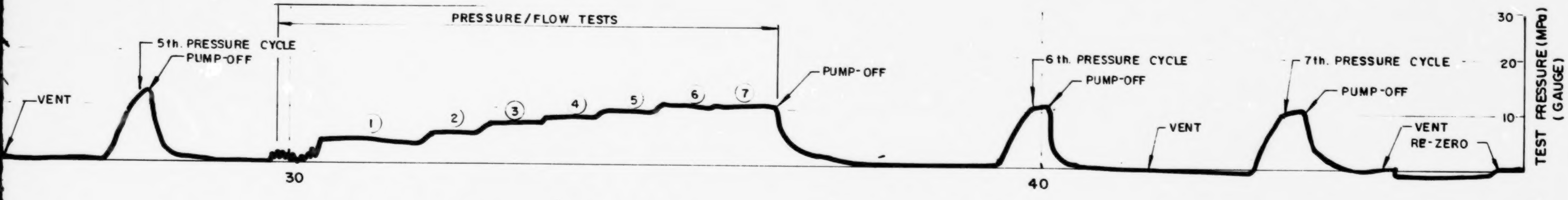

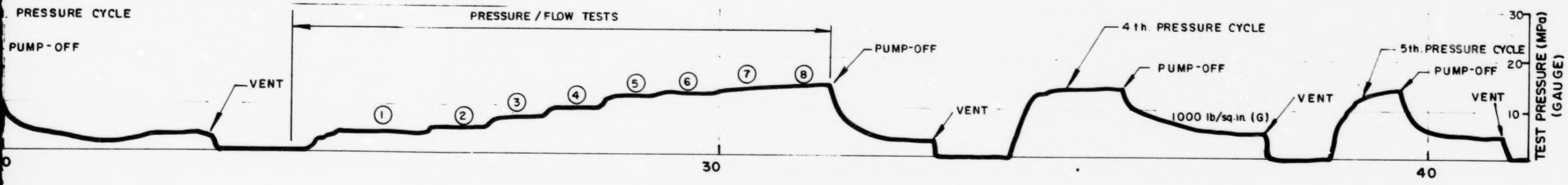

Date MAY 9, 1986
Project 851-6025

Golder Associates

Drawn D.M.
Chkd

BOREHOLE L-5, TEST No. 1; 11.6-12.2 m. DEPTH

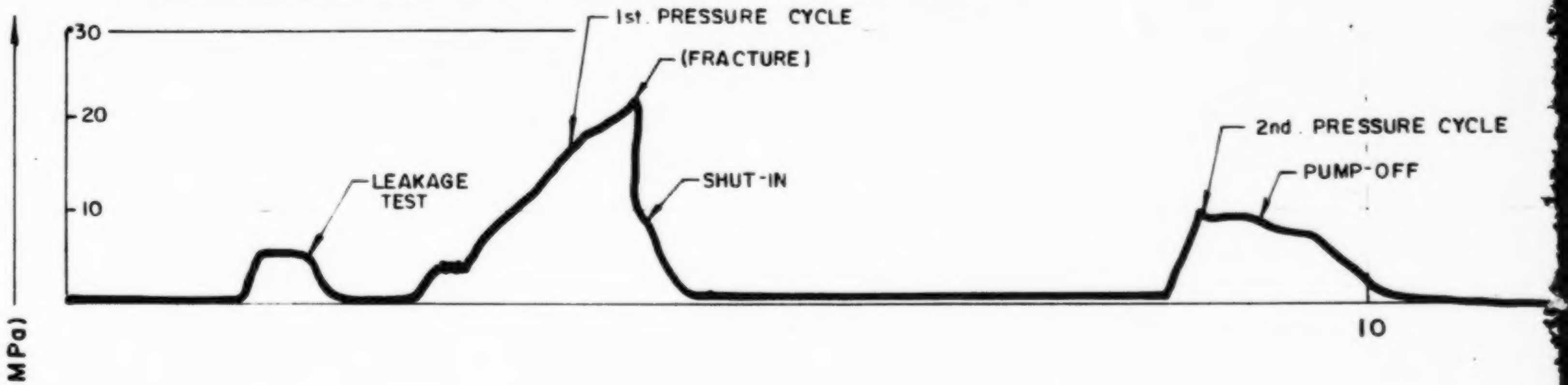

BOREHOLE L-5, TEST No. 2; 13.72 -14.32 m. DEPTH

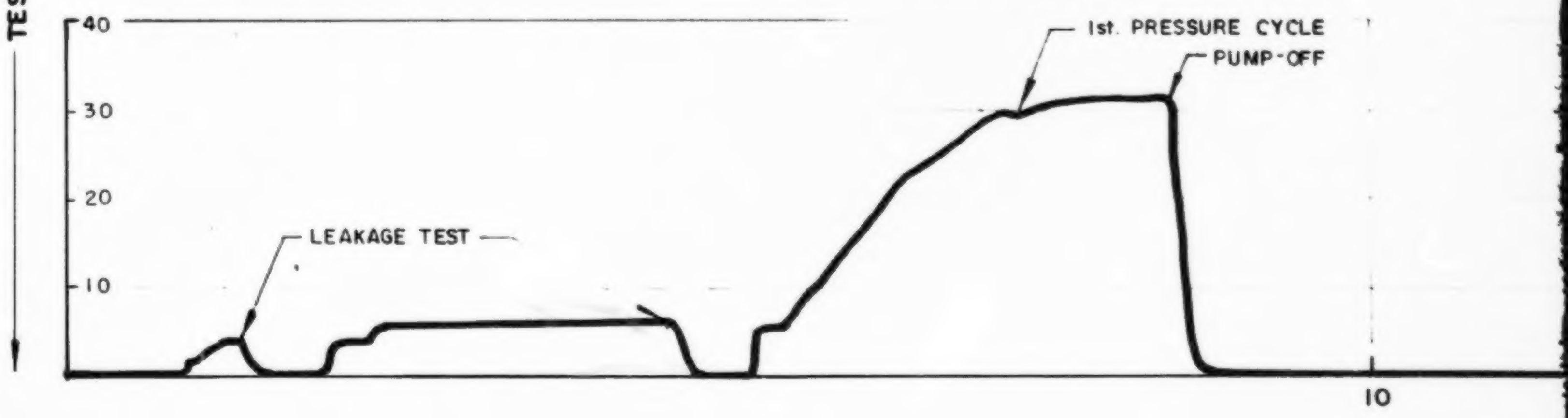

. DEPTH

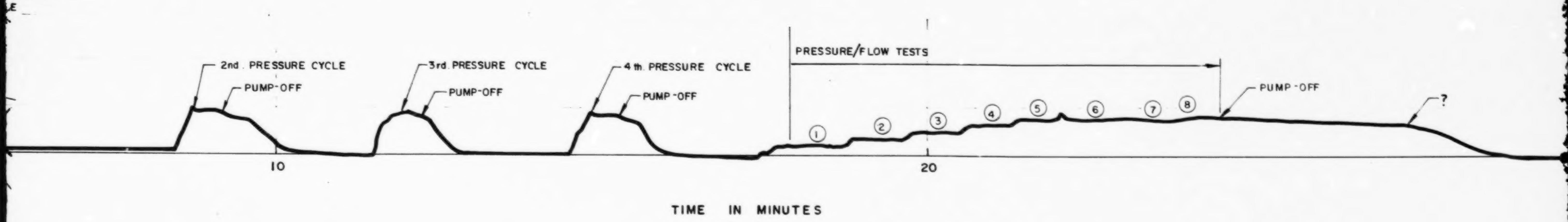

2 m. DEPTH

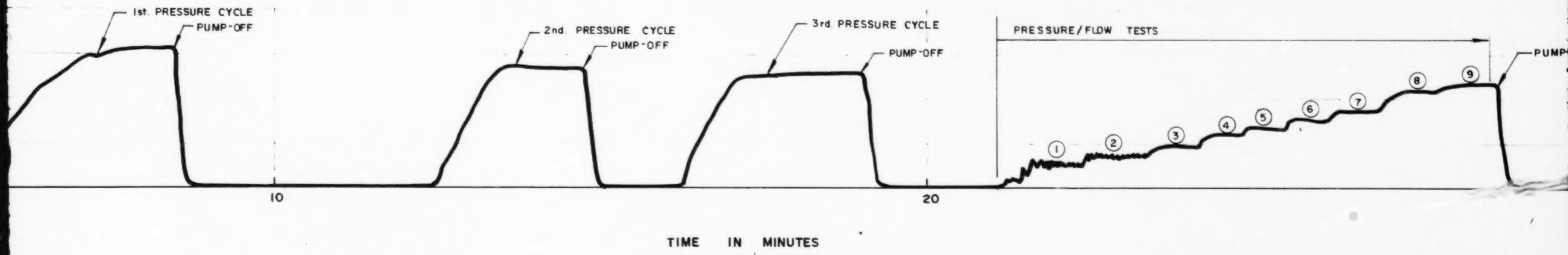

HYDROFRACTURE TEST RESULTS
LINGAN MINE
BOREHOLE L-5 TEST Nos. 1 and 2

FIGURE C2-4

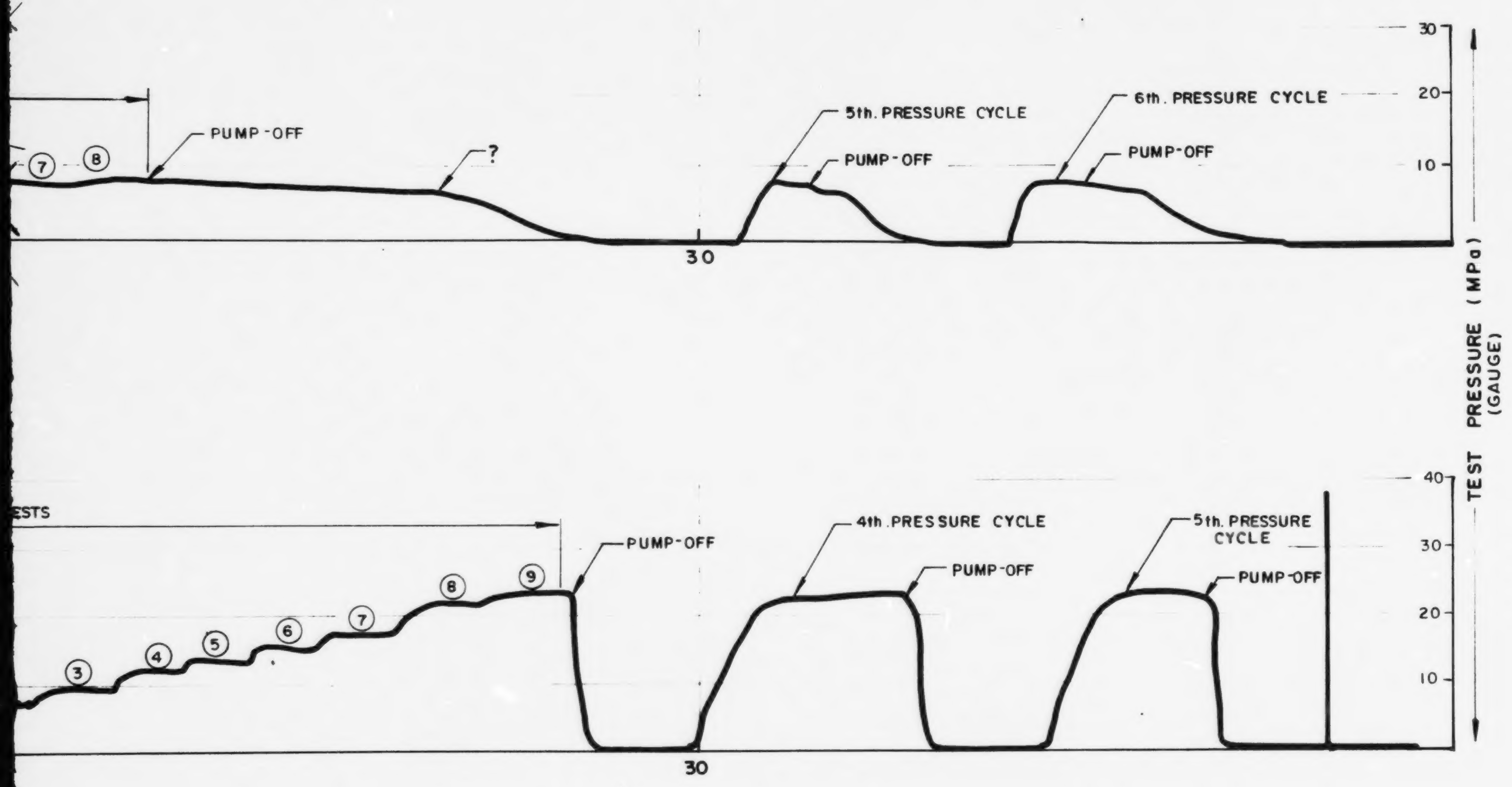

NOTES

1.) RESULTS SHOWN WERE TRACED DIRECTLY FROM CHART RECORDS

2.) ① - STAGE 1 ≈ PRESSURE / FLOW TESTS

Date MAY 9, 1986
Project 851-6025

Golder Associates

Drawn D. M.
Chkd JLC

HYDROFRACTURE PRESSURE / FLOW TEST
LINGAN MINE
BOREHOLE L3 TEST No. 1

FIGURE C2-5

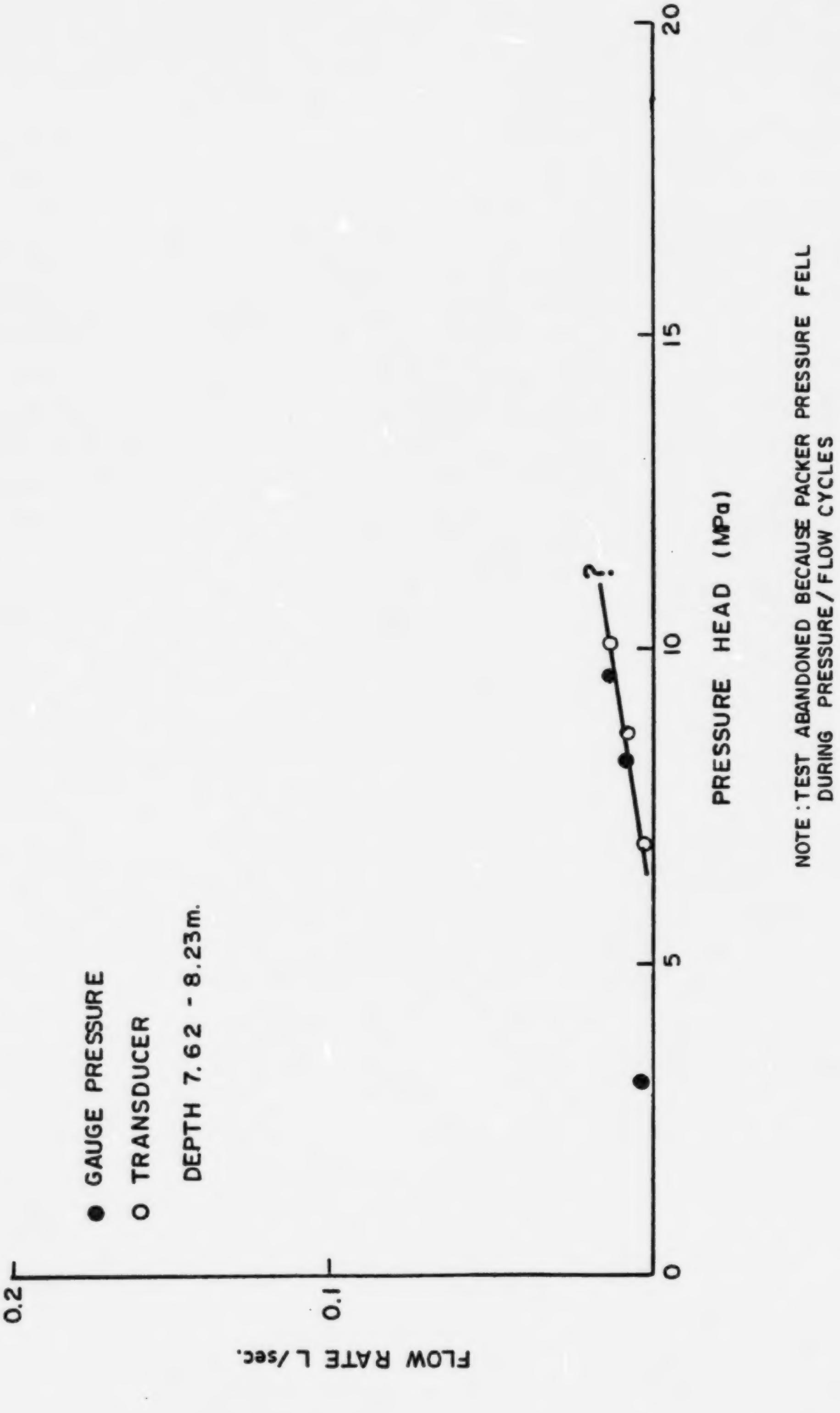

NOTE: TEST ABANDONED BECAUSE PACKER PRESSURE FELL DURING PRESSURE / FLOW CYCLES

Date MAY 14, 1986
Project 851-6025

Golder Associates

Drawn D.M.
Chkd. sh

HYDROFRACTURE PRESSURE / FLOW TEST
LINGAN MINE
BOREHOLE L3 TEST No. 2

FIGURE C2-6

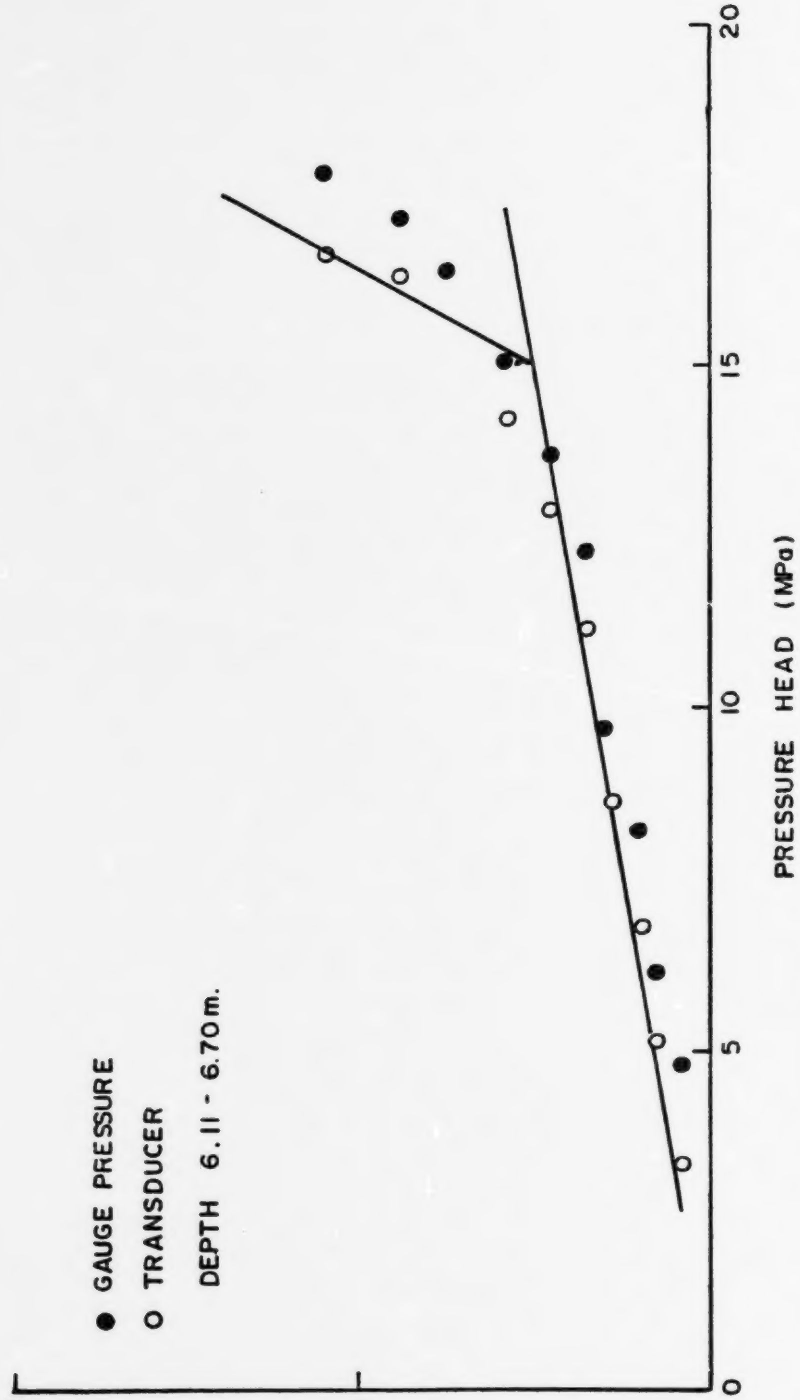

Date MAY 14, 1986
Project 851-6025

Golder Associates

Drawn D.M.
Chkd.

HYDROFRACTURE PRESSURE / FLOW TEST
LINGAN MINE
BOREHOLE L4 TEST No. 1

FIGURE C2-7

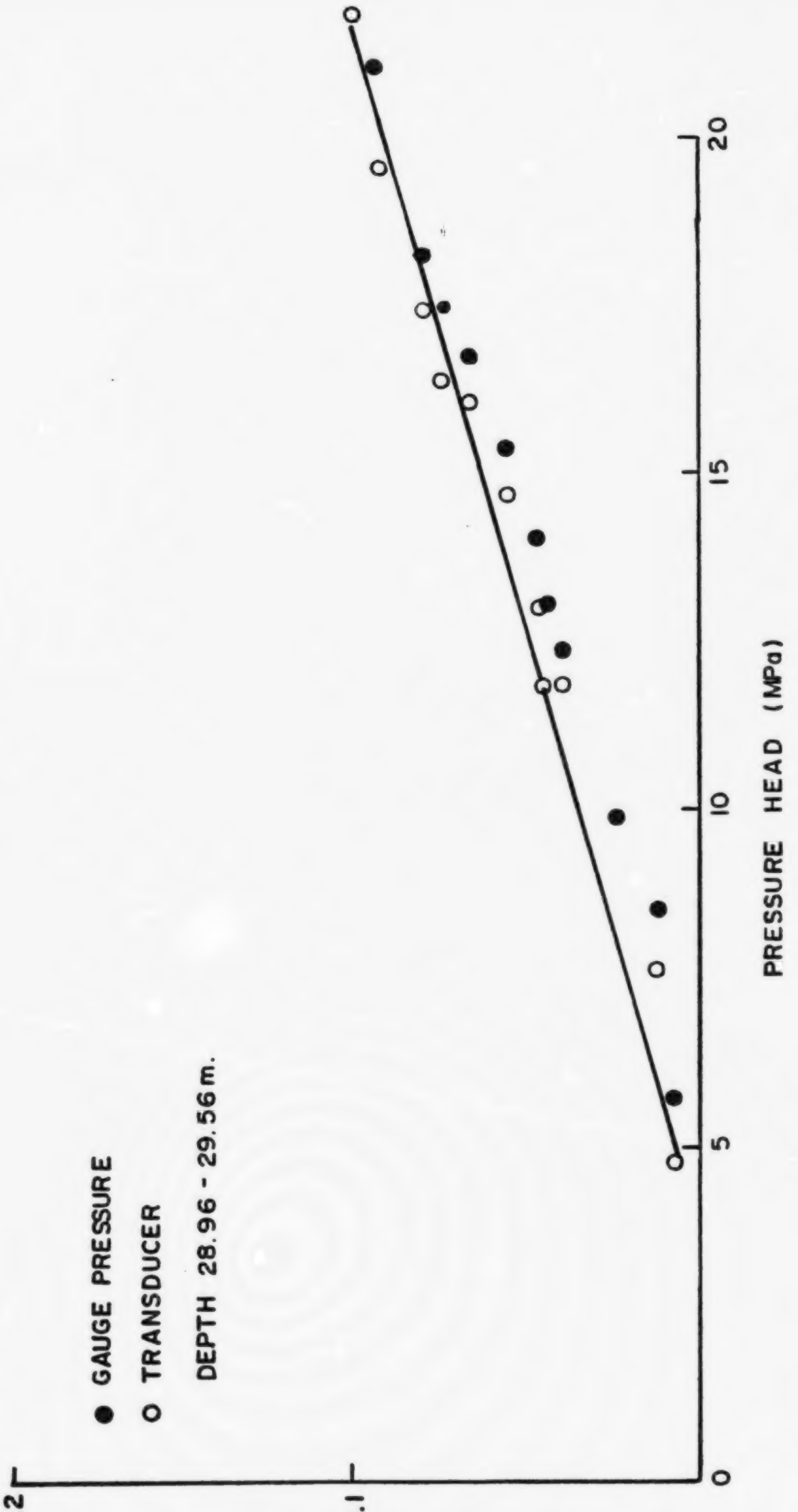

Date MAY 14, 1986
Project 851-6025

Golder Associates

Drawn D.M.
Chkd. JLC

HYDROFRACTURE PRESSURE / FLOW TEST
LINGAN MINE
BOREHOLE L4 TEST No. 2

FIGURE C2-8

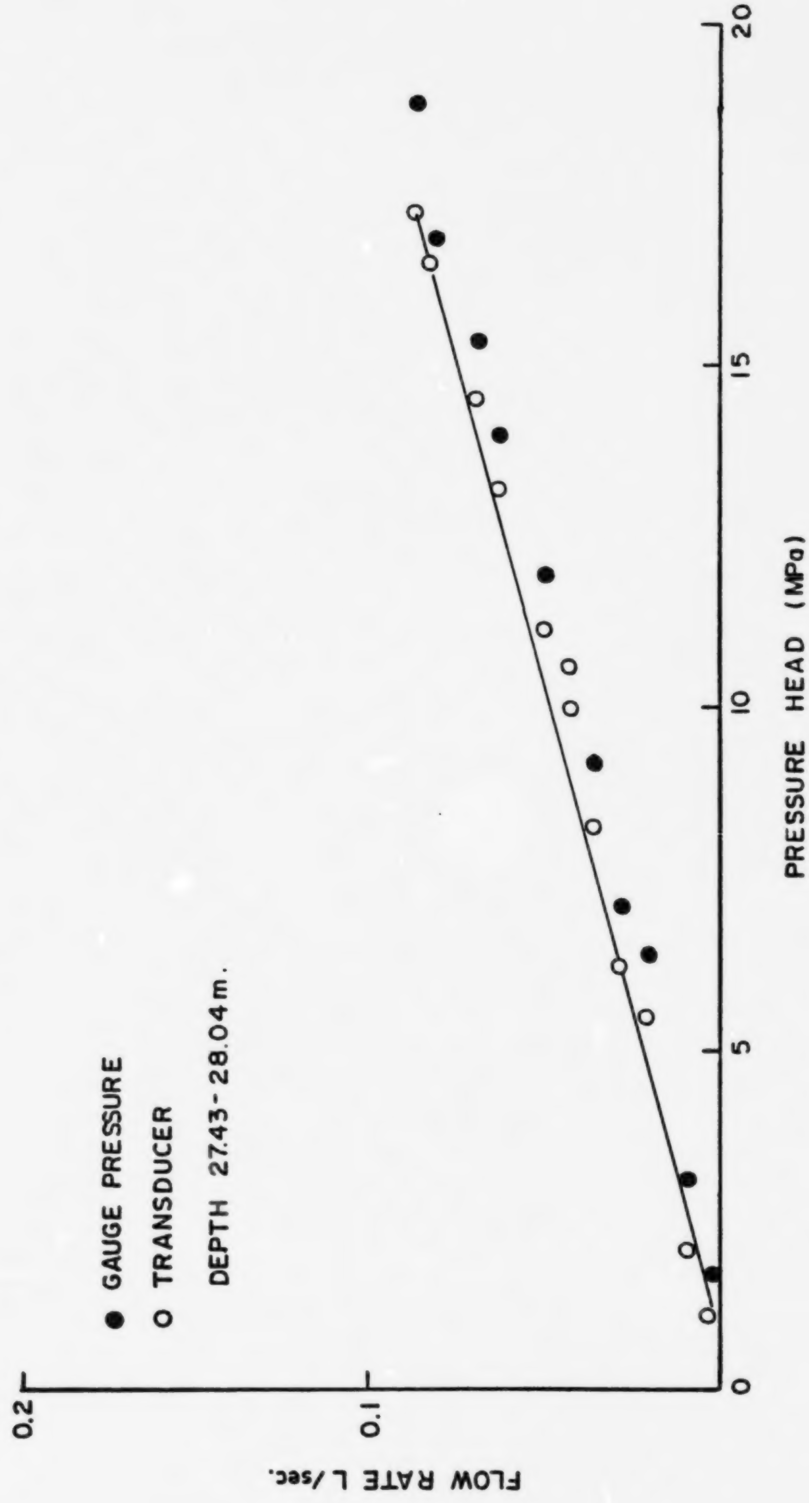

Date MAY 14, 1986
Project 851-6025

Golder Associates

Drawn D.M.
Chkd.

HYDROFRACTURE PRESSURE / FLOW TEST
LINGAN MINE
BOREHOLE L4 TEST No. 3

FIGURE C2-9

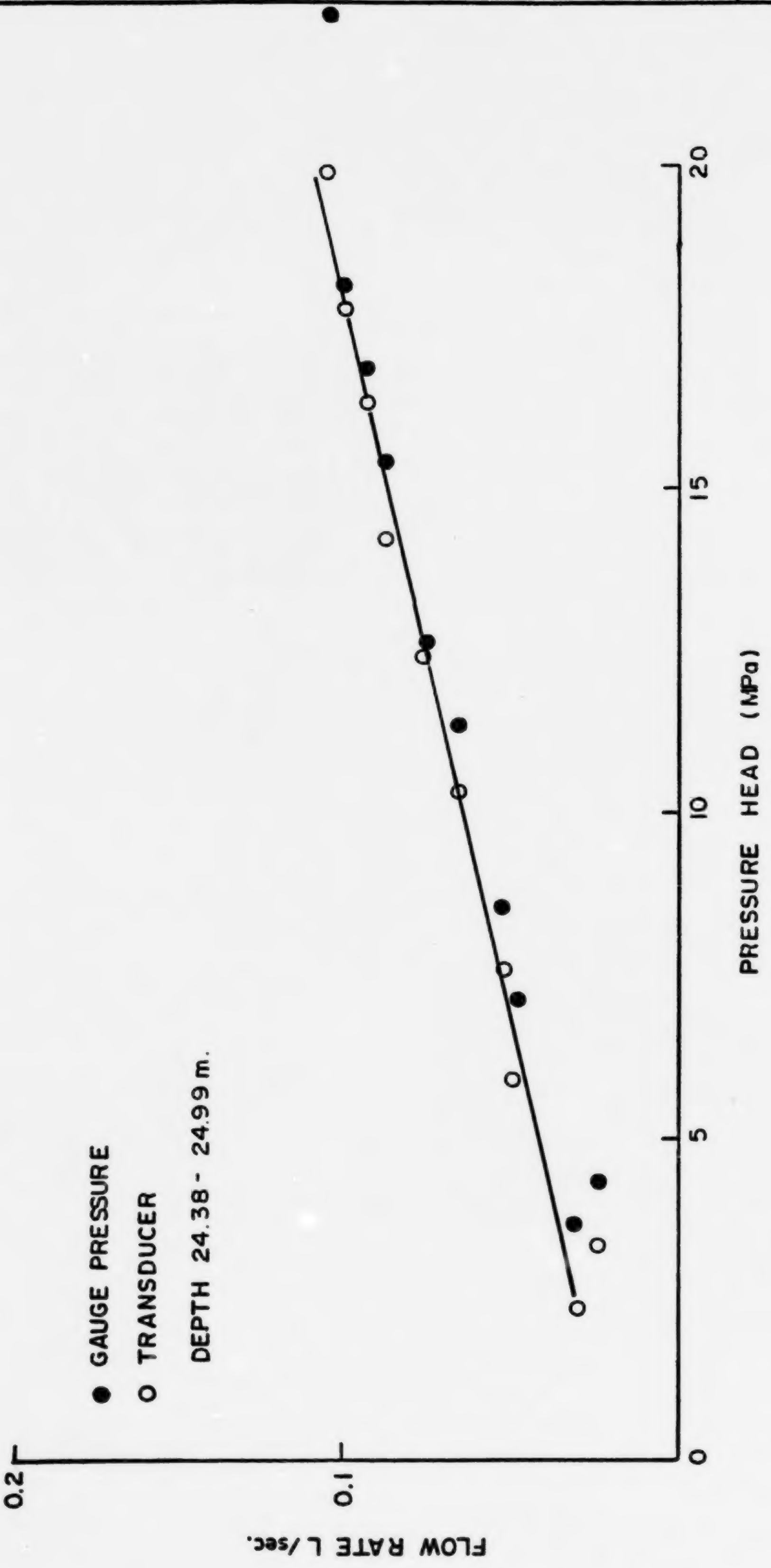

Date MAY 14, 1986

Project 851-6025

Golder Associates

Drawn D.M.

Chkd.

HYDROFRACTURE PRESSURE / FLOW TEST
LINGAN MINE
BOREHOLE L4 TEST No. 4

FIGURE C2-10

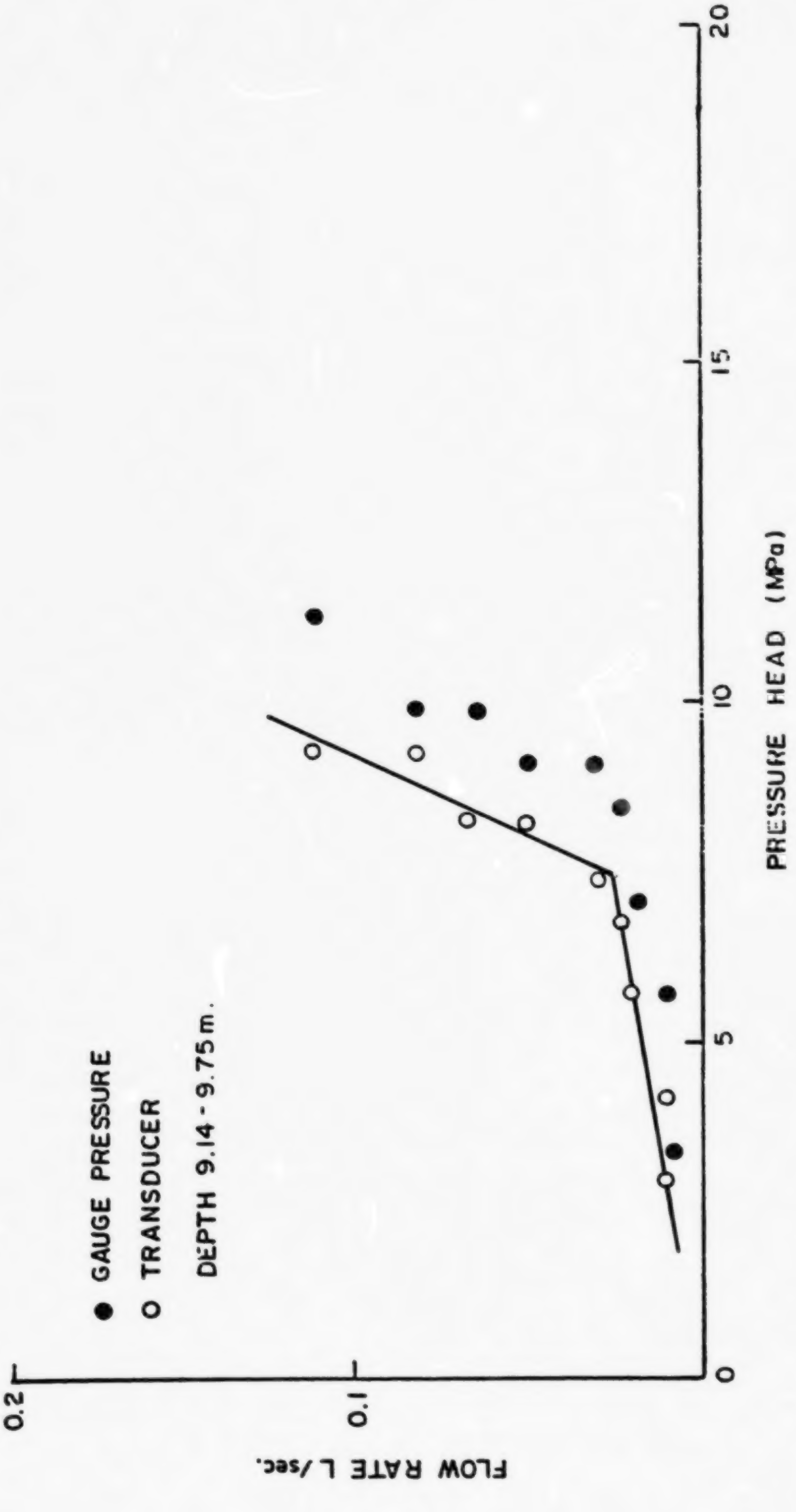

Date MAY 14, 1986
Project 851-6025

Golder Associates

Drawn D.M.
Chkd. JLC

HYDROFRACTURE PRESSURE / FLOW TEST
LINGAN MINE
BOREHOLE L4 TEST No. 5

FIGURE C2-11

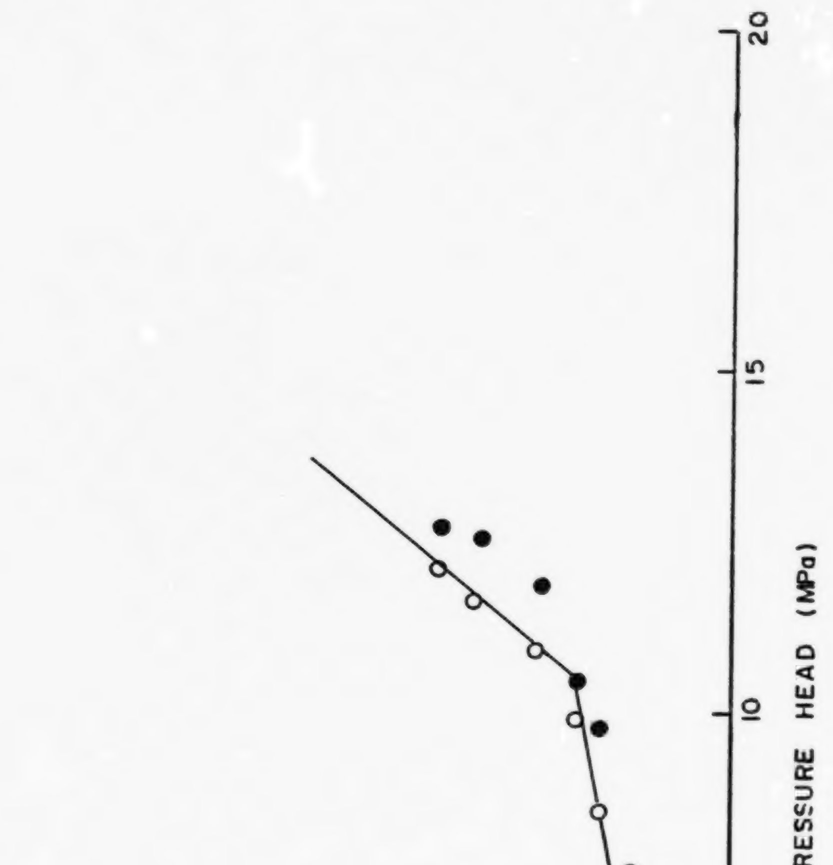

Date MAY 14, 1986
Project 851-6025

Golder Associates

Drawn D.M.
Chkd.

HYDROFRACTURE PRESSURE / FLOW TEST
LINGAN MINE
BOREHOLE L4 TEST No. 6

FIGURE C2-12

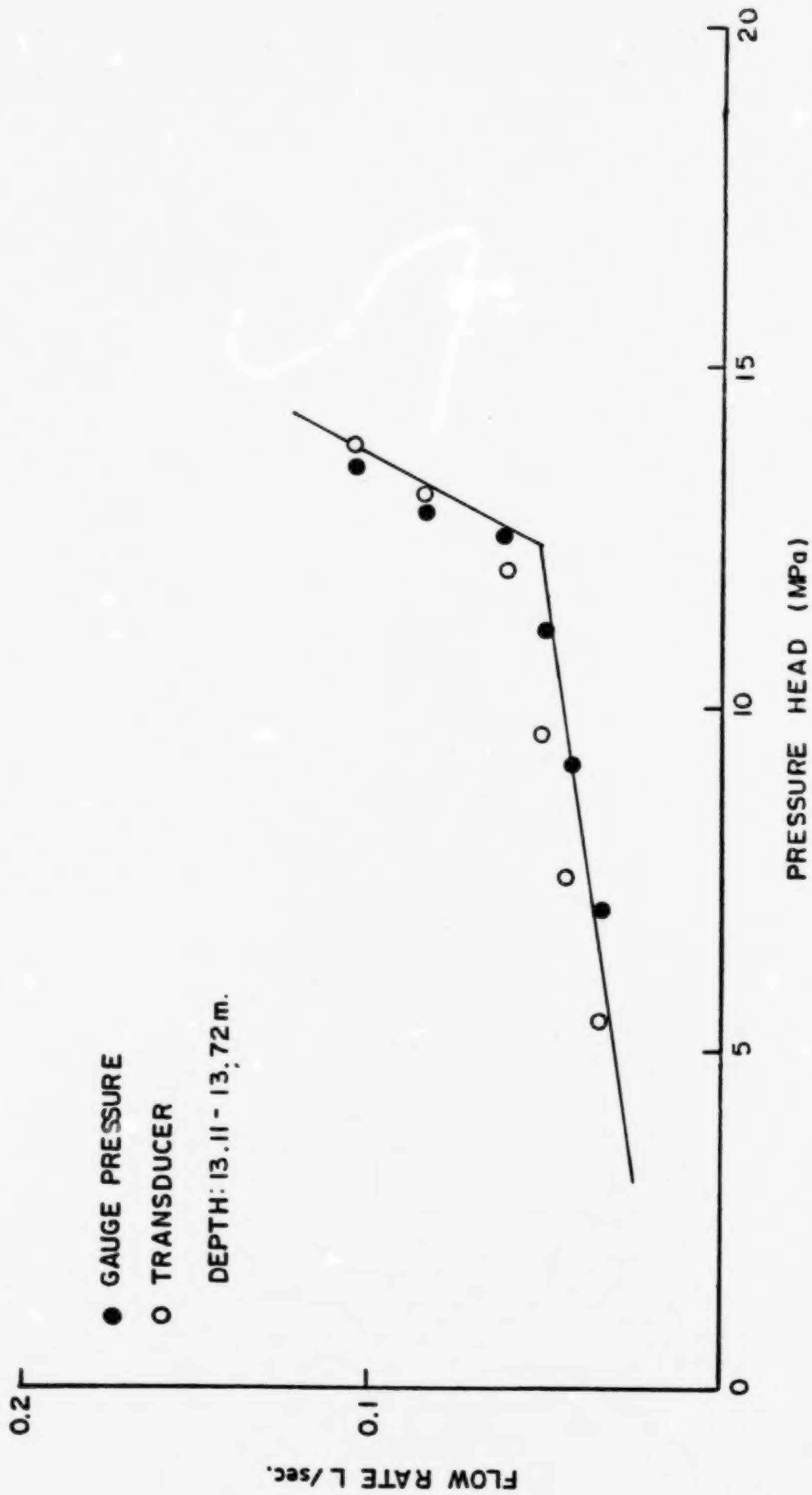

Date MAY 14, 1986
Project 851-6025

Golder Associates

Drawn D.M.
Chkd.

HYDROFRACTURE PRESSURE / FLOW TEST
LINGAN MINE
BOREHOLE L4 TEST No. 7

FIGURE C2-13

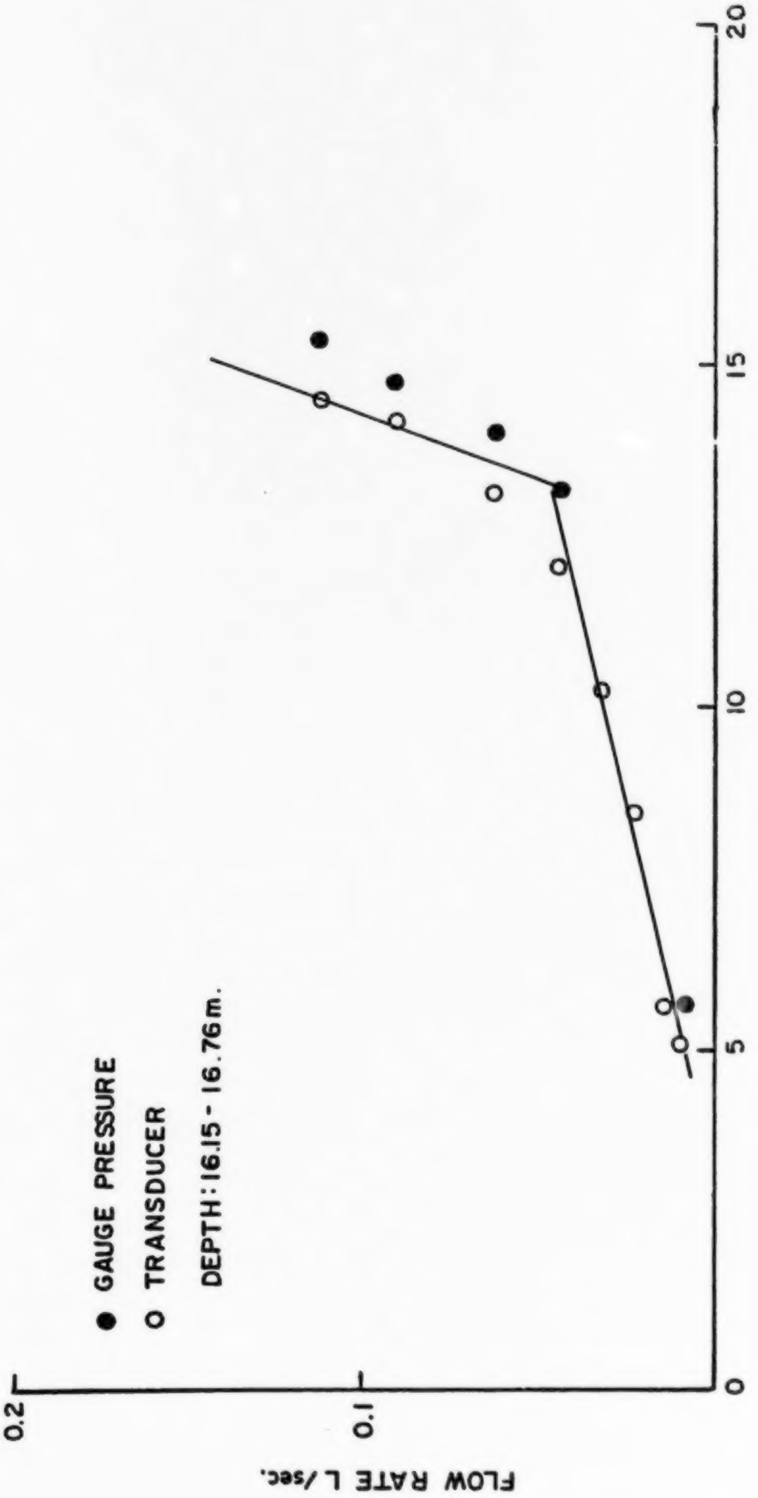

Date MAY 14, 1986
Project 851-6025

Golder Associates

Drawn D.M.
Chkd. SHG

HYDROFRACTURE PRESSURE / FLOW TEST
LINGAN MINE
BOREHOLE L4 TEST No. 8

FIGURE C2-14

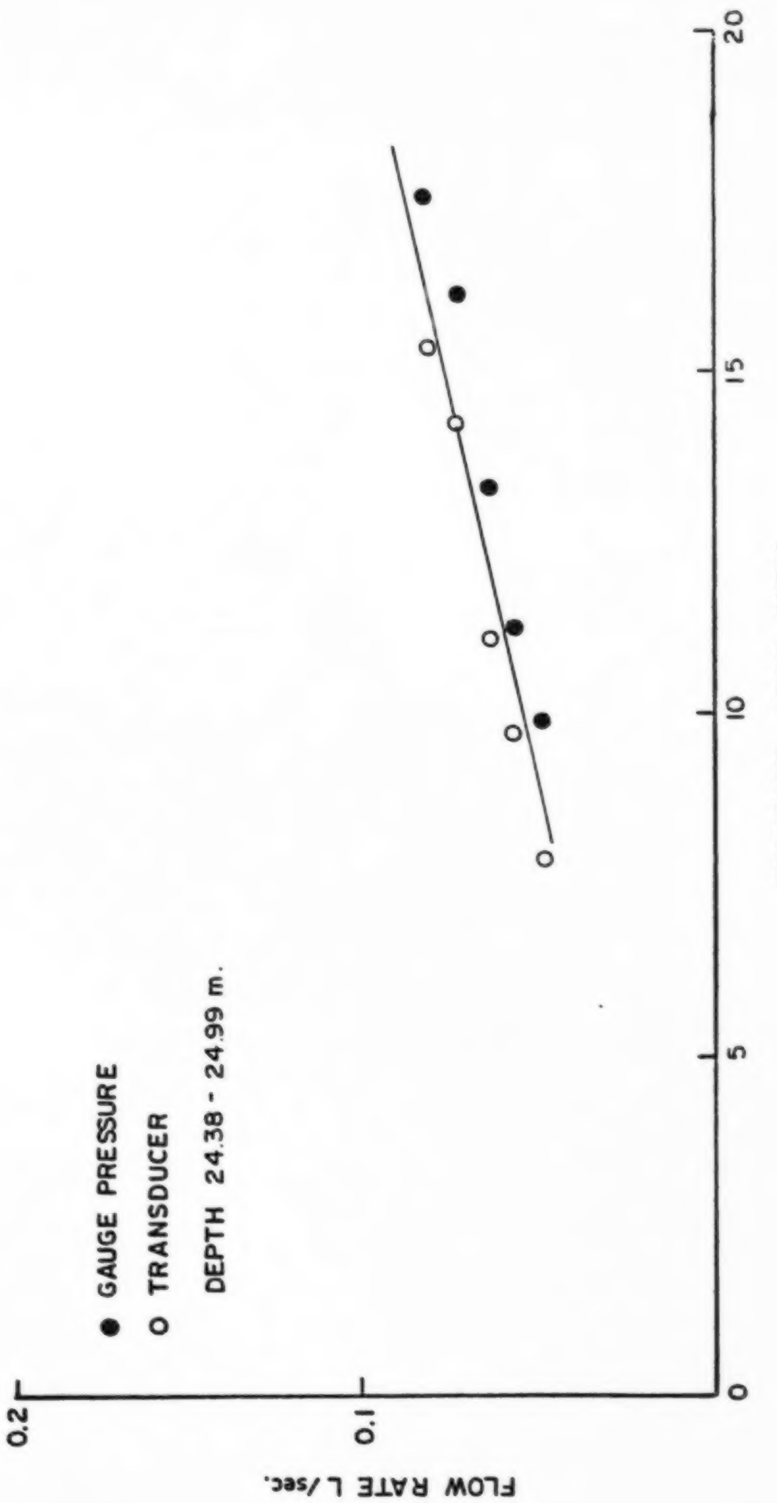

Date MAY 14, 1986
Project 851-6025

Golder Associates

Drawn D.M.
Chkd.

HYDROFRACTURE PRESSURE / FLOW TEST
LINGAN MINE
BOREHOLE L4 TEST No. 9

FIGURE C2-15

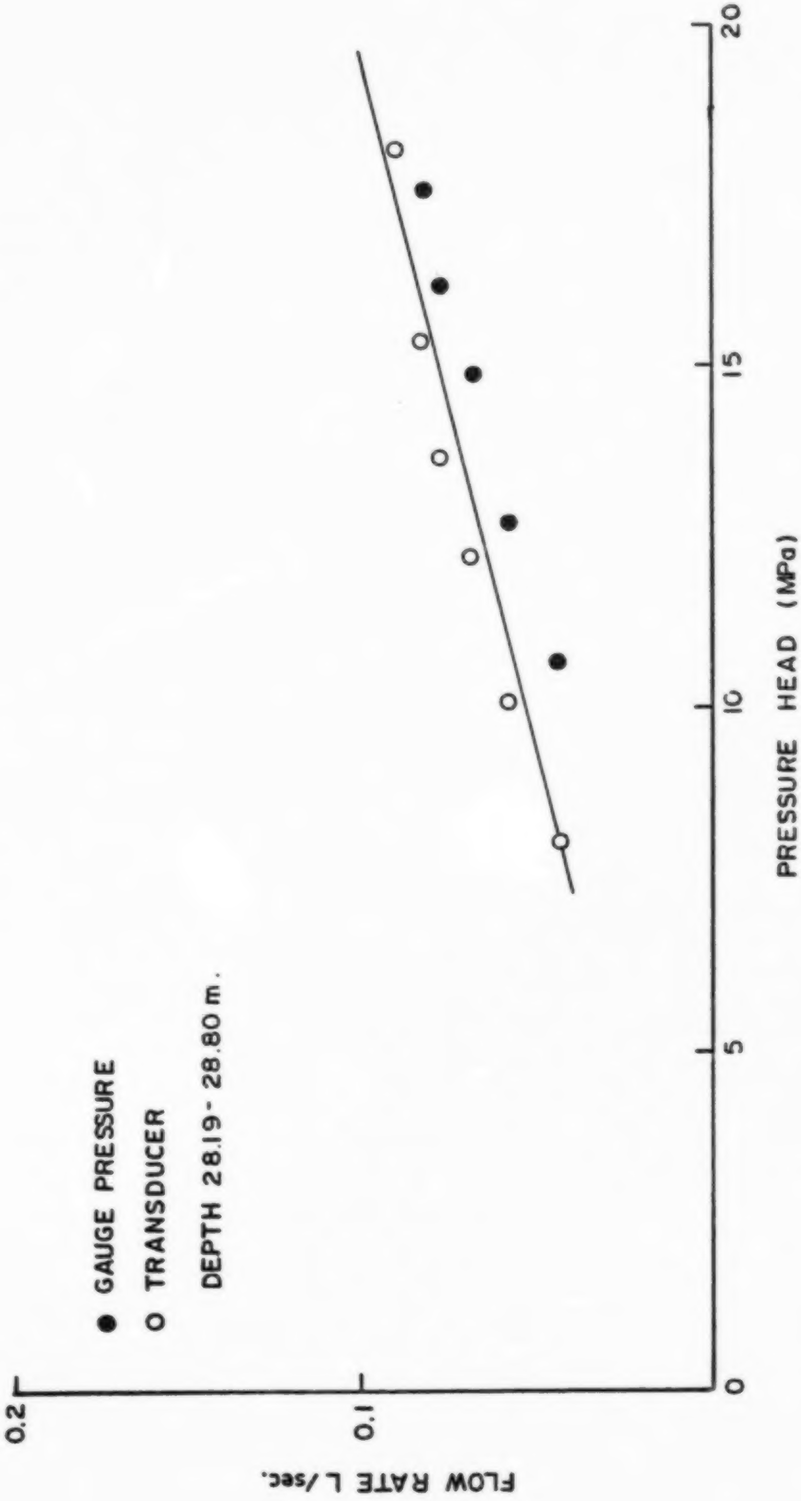

Date MAY 14, 1986
Project 851-6025

Golder Associates

Drawn D.M.
Chkd.

HYDROFRACTURE PRESSURE / FLOW TEST
LINGAN MINE
BOREHOLE L5 TEST No. 1

FIGURE C2-16

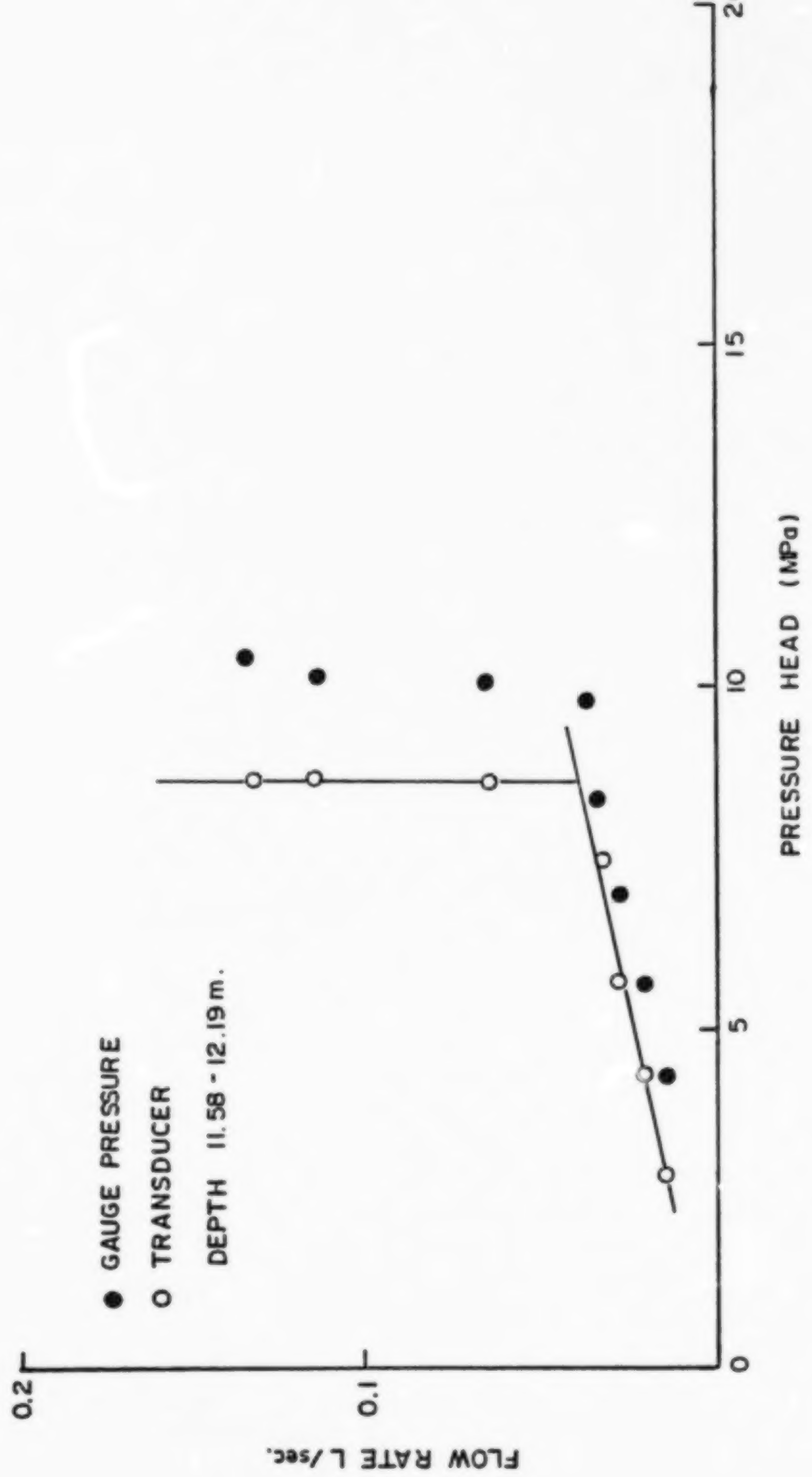

Date MAY 14, 1986
Project 851-6025

Golder Associates

Drawn D.M.
Chkd. JG

HYDROFRACTURE PRESSURE / FLOW TEST
LINGAN MINE
BOREHOLE L5 TEST No. 2

FIGURE C2-17

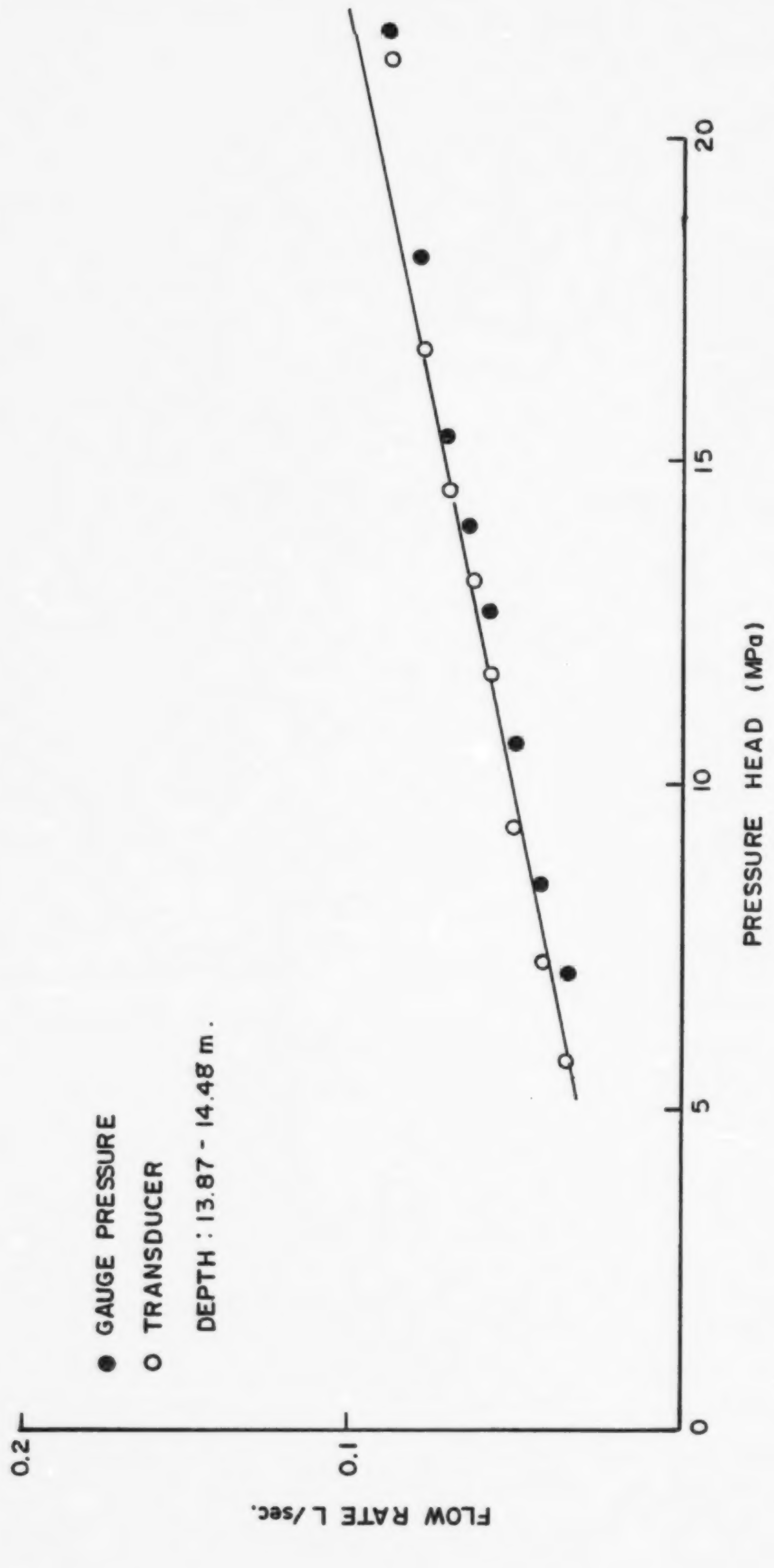

Date MAY 14, 1986
Project 851-6025

Golder Associates

Drawn D.M.
Chkd. dJC

APPENDIX D

PROCEDURES FOR EVALUATION OF INSITU STRESSES FROM OVERCORING TEST DATA

D.1 EVALUATION OF SECONDARY PRINCIPAL STRESSES FROM OVERCORING TEST DATA

Based on the deformations measured across the three diameters, the secondary principal stresses on the plane perpendicular to the axis of the drillhole are given by the following expressions(Obert and Duvall, 1967).

$$P = \frac{E}{6d(1-\nu^2)} \left(U_1+U_2+U_3 + \frac{1}{\sqrt{2}} [(U_1-U_2)^2 + (U_2-U_3)^2 + (U_3-U_1)^2]^{\frac{1}{2}}\right)$$

$$Q = \frac{E}{6d(1-\nu^2)} \left(U_1+U_2+U_3 - \frac{1}{\sqrt{2}} [(U_1-U_2)^2 + (U_2-U_3)^2 + (U_3-U_1)^2]^{\frac{1}{2}}\right)$$

where E is the average deformation modulus.

ν is the Poisson's ratio.

d is the diameter of the pilot hole

and U_1, U_2, U_3 are the measured changes in borehole diameter across three diameters at 60° rotation.

U is positive for an increasing diameter.

P is the maximum secondary principal stress.

Q is the minimum secondary principal stress.

The direction of P is given by:

$$\theta = \frac{1}{2} \tan^{-1} \left[\frac{\sqrt{3}\,(U_2 - U_3)}{2U_1-U_2-U_3}\right]$$

where θ is the angle to P measured counterclockwise from the direction of the U_1 diameter.

The quadrant of θ may be determined as follows,

if $U_2 > U_3$ and $U_2+U_3 < 2U_1$ then θ is between 0° and 45°

$U2 > U_3$ and $U_2+U_3 > 2U_1$ then θ is between 45° and 90°

$U_2 < U_3$ and $U_2+U_3 > 2U_1$ then θ is between 90° and 135°

$U_2 < U_3$ and $U_2+U_3 < 2U_1$ then θ is between 135° and 180°

The above equations are derived for plane strain condition with zero axial strain ($\varepsilon_2=o$) along the drillhole. If the effect of axial strain is taken into account, an estimate of the axial stress along the borehole is required. Based on the results obtained from the complete solution of the stress tensor, it was noted that the secondary principal stresses based on non-zero axial strain is only about 7 percent higher than those based on zero axial strain.

The deformation modulus of the rock was evaluated based on the results of the biaxial tests using the following expression and assuming isotropic elasticity.

$$E = \frac{4ab^2P_o}{(b^2-a^2)U}$$

where E = Deformation modulus
a = the inner radius of the overcore
b = the outer radius of the overcore
P_o = pressure on the outer surface of the overcore
and U = Diametral deformation of pilot hole in the overcore

D.2 EVALUATION OF THE STRESS TENSORS USING LEAST SQUARES SOLUTION

The procedure for using the least squares solution for the stress tensor is described in detail by Panek (1966). The following is an outline of the proposed method.

D.2.1 Formulation of the General Equation for Diametral Deformation

In this formulation, the drillhole is assigned a right hand rectangular co-ordinate system with axis h_1, h_2 and h_3, as shown on Figure D.1. Axis h_2 is parallel to the borehole axis and axis h_3 is vertical if h_2 is horizontal. The three-dimensional stress system with respect to this co-ordinate system is completely defined by the six stress components σ_1, σ_2, σ_3, τ_{12} ,τ_{23} and τ_{31}.

Of these six stress components, it may be assumed that the stresses τ_{12} and τ_{23} (or τ_{32}) which act parallel to the axis of the drillhole, have negligible influence on the diametral deformation of the drillhole when the stress system is relieved around the drillhole. Consequently, the diametral change of the drillhole is a function only of the following stress components:

σ_1, σ_3 and τ_{13} acting normal to the drillhole axis,
and σ_2 acting parallel to the drillhole axis

The effect of σ_2 is through the Poissons's effect of the strain ε_2 in the direction of axis h_2.

The contributions to the diametral deformation of the drillholes from σ_1, σ_3, τ_{13} and ε_2 are:

$$U_{(\sigma_1)} = \sigma_1\ d\ (1+ 2 \cos 2\theta)(1-\nu^2)/E \qquad \text{(D1)}$$

$$U_{(\sigma_3)} = \sigma_3\ d\ (1+ 2 \cos 2\theta)(1-\nu^2)/E \qquad \text{(D2)}$$

$$U_{(\tau_{13})} = \tau_{13}\ d\ (4 \sin 2\theta)(1-\nu^2)/E \qquad \text{(D3)}$$

$$U_{(\varepsilon_2)} = (\sigma_1 d\nu^2 - \sigma_2 d\nu + \sigma_3 d\nu^2)/E \qquad \text{(D4)}$$

where U is the deformation across the diameter oriented at the angle θ with respect to the h_1 axis

E is the modulus of deformation

ν is the Poisson's ratio

d is the diameter of the drillhole

θ is the angle with respect to h_1 axis measured in the h_1-h_3 plane

Equations D1 to D4 can be combined to give the total diametral deformation:

$$U = \sigma_1 f_1 + \sigma_2 f_2 + \sigma_3 f_3 + \tau_{13} f_4 \qquad \text{(D5)}$$

where

$$\begin{aligned} f_1 &= [d(1+ 2 \cos 2\theta)(1-\nu^2) + d\nu^2]/E \\ f_2 &= -d\nu/E \\ f_3 &= [d(1-2 \cos 2\theta)(1-\nu^2) + d\nu^2]/E \\ f_4 &= d(4 \sin 2\theta)(1-\nu^2)/E \end{aligned} \qquad \text{(D6)}$$

D.2.2 Diametral Deformation in a Common Co-ordinate System

When the drillhole deformations are determined from tests in more than one drillhole as in the present case, it becomes necessary to relate all the measurements to a common co-ordinate system. Hence, in addition to the co-ordinate system (h_1, h_2

and h_3) for each drillhole, a set of common co-ordinate system x, y and z should be assigned to the medium. For convenience, x is chosen to be parallel to the EW (East being positive) and y parallel to the NS (North being positive) direction. z is chosen to be the vertical direction (Figure D.1). The six independent stress components of the stress tensor with respect to the x, y, z co-ordinate systems are σ_x, σ_y, σ_z, τ_{xy}, τ_{yz} and τ_{zx}.

The formulae for transformation of stresses in three dimensions may be written as:

$$\begin{bmatrix} \sigma_1 \\ \sigma_2 \\ \sigma_3 \\ \tau_{12} \\ \tau_{23} \\ \tau_{31} \end{bmatrix} = \begin{bmatrix} \ell_1^2 & m_1^2 & n_1^2 & 2\ell_1 m_1 & 2m_1 n_1 & 2n_1 \ell_1 \\ \ell_2^2 & m_2^2 & n_2^2 & 2\ell_2 m_2 & 2m_2 n_2 & 2n_2 \ell_2 \\ \ell_3^2 & m_3^2 & n_3^2 & 2\ell_3 m_3 & 2m_3 n_3 & 2n_3 \ell_3 \\ \ell_1 \ell_2 & m_1 m_2 & n_1 n_2 & (\ell_1 m_2 + \ell_2 m_1) & (m_1 n_2 + m_2 n_1) & (n_1 \ell_2 + n_2 \ell_1) \\ \ell_2 \ell_3 & m_2 m_3 & n_2 n_3 & (\ell_2 m_3 + \ell_3 m_2) & (m_2 n_3 + m_3 n_2) & (n_2 \ell_3 + n_3 \ell_2) \\ \ell_1 \ell_3 & m_1 m_3 & n_1 n_3 & (\ell_1 m_3 + \ell_3 m_1) & (m_1 n_3 + m_3 n_1) & (n_1 \ell_3 + n_3 \ell_1) \end{bmatrix} \times \begin{bmatrix} \sigma_x \\ \sigma_y \\ \sigma_z \\ \tau_{xy} \\ \tau_{yz} \\ \tau_{zx} \end{bmatrix} \qquad \text{(D7)}$$

ℓ_1, m_1, n_1 are the direction cosines for the positive h_1 axis with the positive x, y, z axis. For a given azimuth of drillhole orientation, α, and dip of drillhole (uphole), Ψ, the direction cosines are given by the following relationships:

$$\begin{vmatrix} \ell_1 & \ell_2 & \ell_3 \\ m_1 & m_2 & m_3 \\ n_1 & n_2 & n_3 \end{vmatrix} = \begin{vmatrix} \cos\alpha & \sin\alpha \cos\Psi & -\sin\alpha \sin\Psi \\ -\sin\alpha & \cos\alpha \cos\Psi & -\cos\alpha \sin\Psi \\ 0 & \sin\Psi & \cos\Psi \end{vmatrix} \qquad \text{(D7A)}$$

Substituting the relevant equations from (D7) into equation D5 and collecting terms.

$$U = b_1 J_1 + b_2 J_2 + b_3 J_3 + b_4 J_4 + b_5 J_5 + b_6 J_6 \qquad \text{(D8)}$$

where U = total diametral deformation

$$b_1 = \sigma_x, \quad b_4 = \tau_{xy},$$
$$b_2 = \sigma_y, \quad b_5 = \tau_{yz}, \qquad (D9)$$
$$b_3 = \sigma_z, \quad b_6 = \tau_{zx},$$

$$J_1 = f_1 \ell_1{}^2 + f_2 \ell_2{}^2 + f_3 \ell_3{}^2 + f_4 \ell_1 \ell_3$$

$$J_2 = f_1 m_1{}^2 + f_2 m_2{}^2 + f_3 m_3{}^2 + f_4 m_1 m_3$$

$$J_3 = f_1 n_1{}^2 + f_2 n_2{}^2 + f_3 n_3{}^2 + f_4 n_1 n_3$$

$$J_4 = 2f_1 \ell_1 m_1 + 2f_2 \ell_2 m_2 + 2f_3 \ell_3 m_3 + f_4 (\ell_1 m_3 + \ell_3 m_1)$$
$$J_5 = 2f_1 m_1 n_1 + 2f_2 m_2 n_2 + 2f_3 m_3 n_3 + f_4 (m_1 n_3 + m_3 n_1)$$
$$J_6 = 2f_1 n_1 \ell_1 + 2f_2 n_2 \ell_2 + 2f_3 n_3 \ell_3 + f_4 (n_1 \ell_3 + n_3 \ell_1)$$

Equation D8 expresses the diametral deformation (U) of a drillhole as a linear function of bi. It may be noted that J is a function of the drillhole diameter and orientation (defined by the direction cosines), the orientation of the measured diametral deformation (θ) and the elastic constants (E and ν). Hence J is a known coefficient provided that the orientation of measurement and the elastic constants are specified. By determining U for six independent conditions and substituting the six sets of values in equation D8, six independent simultaneous equations are obtained. The six independent components of the stress tensor (b_i) can then be solved.

D.2.3 Least Squares Solution for the Stress Tensor

Although six independent determinations of U provide the minimum data required to calculate the six stress components, each measurement is subject to random effects as in all other types of field measurements. It is therefore desirable to make a number of sample measurements of U and to calculate from the collected data, an average value for each of the six stress components and an assessment of their accuracy.

The method of calculation is to apply the multilinear regression analysis to equation D5. The errors of b_i are minimized if the following conditions are satisfied.

$$\begin{aligned}
&b_1\Sigma J_1{}^2 + b_2\Sigma J_1J_2 + b_3\Sigma J_1J_3 + \ldots\ b_6J_1J_6 = \Sigma UJ_1 \\
&b_1\Sigma J_2J_1 + b_2\Sigma J_2{}^2 + b_3\Sigma J_2J_3 + \ldots\ b_6J_2J_6 = \Sigma UJ_2 \qquad \text{(D10)} \\
&\ldots\ldots\ldots\ldots\ldots\ldots\ldots\ldots\ldots\ldots\ldots\ldots \\
&b_1\Sigma J_6J_1 + b_2\Sigma J_6J_2 + b_3\Sigma J_6J_3 + \quad b_6\Sigma J_6{}^2 = \Sigma UJ_6
\end{aligned}$$

If we define

$a_{ij} = \Sigma J_iJ_j$ and $g_j = \Sigma UJ_j$

$(i,j = 1, 2, 3 \ldots\ldots 6)$

Equation D10 can be written as

$$\begin{aligned}
&b_1\ a_{11} + b_2\ a_{12} + b_3\ a_{13} \ldots + b_6\ a_{16} = g_1 \\
&b_1\ a_{21} + b_2\ a_{22} + b_3\ a_{23} \ldots + b_6\ a_{26} = g_2 \qquad \text{(D11)} \\
&\ldots\ldots\ldots\ldots\ldots\ldots\ldots\ldots\ldots\ldots \\
&b_1\ a_{61} + b_2\ a_{62} + b_3\ a_{63} \ldots + b_6\ a_{66} = g_6
\end{aligned}$$

where $a_{21} = a_{12}$, $a_{31} = a_{13}$ etc.

The mathematical operation is to find a set of coefficients C_{ij} such that:

$$\begin{aligned}
b_1 &= C_{11}g_1 + C_{12}g_2 + C_{13}g_3 + \ldots\ldots C_{16}g_6 \\
b_2 &= C_{21}g_1 + C_{22}g_2 + C_{23}g_3 + \ldots\ldots C_{26}g_6 \\
&\cdots\cdots\cdots\cdots\cdots\cdots\cdots\cdots\cdots\cdots \\
b_6 &= C_{61}g_1 + C_{62}g_2 + C_{63}g_3 + \ldots\ldots C_{66}g_6
\end{aligned} \qquad \text{(D12)}$$

where $C_{12} = C_{21}$, $C_{13} = C_{31}$, etc.

Expressing equations D11 and D12 in matrix form and defining the following matrices:

$$A = \begin{bmatrix} a_{11} & a_{12} & a_{13} & \cdots & a_{16} \\ a_{21} & a_{22} & a_{23} & \ldots & a_{26} \\ - & - & - & - & - \\ a_{61} & a_{62} & a_{63} & \ldots & a_{66} \end{bmatrix} \qquad b = \begin{bmatrix} b_1 \\ b_2 \\ b_3 \\ b_4 \\ b_5 \\ b_6 \end{bmatrix}$$

$$C = \begin{bmatrix} C_{11} & C_{12} & C_{13} & \cdots & C_{16} \\ C_{21} & C_{22} & C_{23} & \ldots & C_{26} \\ - & - & - & - & - \\ C_{61} & C_{62} & C_{63} & \ldots & C_{66} \end{bmatrix} \qquad g = \begin{bmatrix} g_1 \\ g_2 \\ g_3 \\ g_4 \\ g_5 \\ g_6 \end{bmatrix}$$

Then equation D11 can be represented by

$$[A] * [b] = [g] \qquad \text{(D13)}$$

then

$$[b] = [A]^{-1} * [g] \qquad \text{(D14)}$$

$[A]^{-1}$ is the inverse of $[A]$ and defining

$[C] = [\ A\ ]^{-1}$ thus

$[b] = [C] x [g]$, a matrix form of equation D12 (D15)

D.2.4 Statistical Interpretation of the Least Squares Solution

The parameters which are significant in the statistical interpretation of the least squares solution for the stress tensor are:

(a) The error sum of squares

$$\Sigma e^2 = \Sigma U^2 - \Sigma b_i g_i \quad (i = 1, 2....6) \tag{D16}$$

(b) The multiple correlation coefficient R, where

$$R^2 = 1 - \frac{\Sigma e^2}{\Sigma U^2} \tag{D17}$$

(c) The standard deviation, S, about the fitted regression line, equation D8

$$S = \left(\frac{\Sigma e^2}{(n-p)}\right)^{\frac{1}{2}} \tag{D18}$$

where n is the total number of U measurements
p is the number of b_i calculated from the data (the degree of freedom)

(d) The standard deviations of the stress components, b_i, are given by

$$\begin{aligned} S_{b_1} &= S\,(C_{11})^{\frac{1}{2}} \\ S_{b_2} &= S\,(C_{22})^{\frac{1}{2}} \\ &- - - - - - - - \\ S_{b_6} &= S\,(C_{66})^{\frac{1}{2}} \end{aligned} \tag{D19}$$

where S is given by equation D18 and the coefficients C_{11}, C_{22} etc. are coefficients of [C] from equation D15.

D.2.5 Evaluation of Principal Stresses

With the six independent components of the stress tensor determined with respect to the x, y, z, co-ordinate system, it is possible to calculate the stress components with respect to any other cartesian co-ordinates. One transformation which will be of interest is the evaluation of the principal stresses and their directions from the six stress components.

If S_1, S_2 and S_3 are defined as the three principal stress components, there is a set of co-ordinate axes, 1, 2 and 3 such that the shear stresses $S_{12} = S_{23} = S_{31} = 0$. These axes are then the principal stress axes, the formulae for determining the principal stresses and their directions are given below.

The principal stresses are the three roots of the following cubic equation.

$$S^3 + 3BS^2 + 3CS + D = 0 \tag{D20}$$

where

$$\begin{aligned} B &= -(\sigma_x^{*} + \sigma_y + \sigma_z)/3, \\ C &= (\sigma_x\sigma_y + \sigma_y\sigma_z + \sigma_z\sigma_x - \tau_{xy}^{2} - \tau_{yz}^{2} - \tau_{zx}^{2})/3, \\ \text{and} \quad D &= -\sigma_x\sigma_y\sigma_z - 2\tau_{xy}\tau_{yz}\tau_{zx} + \sigma_x\tau_{yz}^{2} + \sigma_y\tau_{zx}^{2} + \sigma_z\tau_{xy}^{2} \end{aligned} \tag{D21}$$

The three roots S_1, S_2, S_3 of equations D20 are found by calculating:

$$\begin{aligned} E &= (B^2 - C)^{\frac{1}{2}}, \\ F &= -B^3 + (3BC - D)/2, \\ \cos 3A &= \pm F/E^3, \\ S_1 &= -B \pm 2E \cos A, \\ S_2 &= -B \pm 2E \cos (A + 120^{\circ}), \\ S_3 &= -B \pm 2E \cos (A + 240^{\circ}), \end{aligned} \tag{D22}$$

(where ± appears, use + if F is positive, use - if F is negative)

---

* compressive stresses are taken as -ve in this formulation

The direction cosines for principal direction 1 with respect to x, y, z are found from the following equations:

$$\begin{aligned}(S_1 - \sigma_x)\, l_1' - \tau_{xy} m_1' - \tau_{zx} n_1' &= 0,\\ -\tau_{xy} l_1' + (S_1 - \sigma_y) m_1' - \tau_{yz} n_1' &= 0,\\ -\tau_{zx} l_1' - \tau_{yz} m_1' + (S_1 - \sigma_z) n_1' &= 0,\\ (l_1')^2 + (m_1')^2 + (n_1')^2 &= 1\end{aligned} \qquad \text{(D23)}$$

The direction cosines for principal direction 2 are found from the same equations, except that each subscript 1 is replaced by a 2, and similarly for principal direction 3.

The bearing and inclination of any principal stress can be found as follows. It is easily shown that, for direction 1,

$$[\cos\ (\text{angle of inclination of } S_1)] \times [\cos\ (\text{bearing of } S_1)] = m_1', \qquad \text{(D24)}$$

$$[\cos\ (\text{angle of inclination of } S_1)] \times [\sin\ (\text{bearing of } S_1)] = l_1', \qquad \text{(D25)}$$

from which

$$\tan\ (\text{bearing of } S_1) = l_1'/m_1'. \qquad \text{(D26)}$$

Given the bearing angle, the inclination can be found from equation D24 or D25.

In the case where the magnitudes of the principal stresses are close (ie. the stress system is fairly isotropic) the accuracy of the orientation calculation would reduce due to the small difference between the principal stresses.

CO-ORDINATE SYSTEMS FOR EVALUATION OF INSITU STRESSES

FIGURE D-1

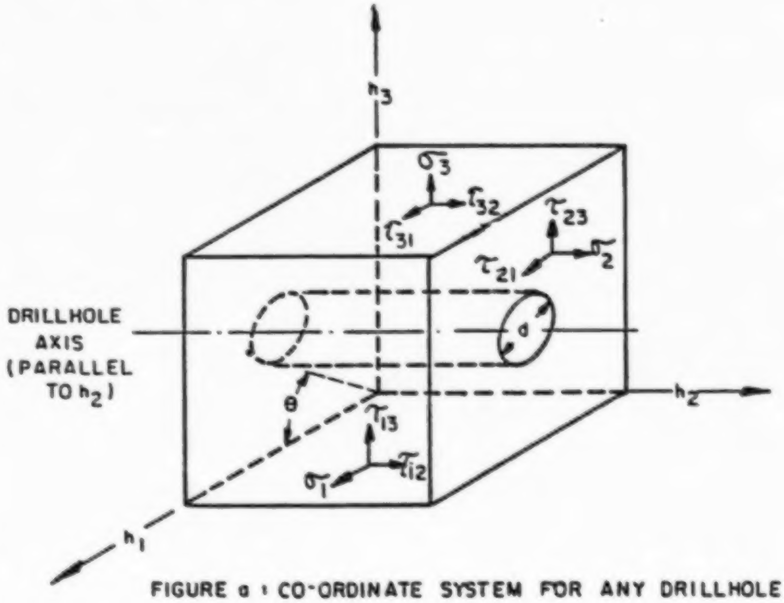
h_3
σ_3
τ_{32}
τ_{31}
τ_{23}
τ_{21}
σ_2
DRILLHOLE AXIS (PARALLEL TO h_2)
d
h_2
θ
τ_{13}
σ_1
τ_{12}
h_1

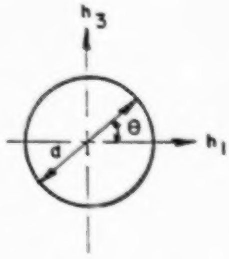

θ = ORIENTATION OF DIAMETRAL DEFORMATION (MEASURED FROM h_1 AXIS)

FIGURE a : CO-ORDINATE SYSTEM FOR ANY DRILLHOLE

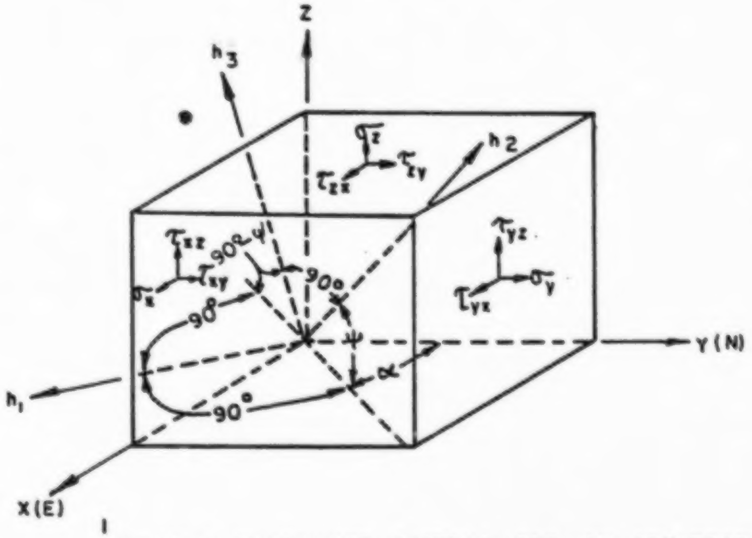
Z
h_3
σ_z
τ_{zx}
τ_{zy}
h_2
τ_{xz}
σ_x
τ_{xy}
90°-ψ
90°
90°
ψ
α
90°
τ_{yz}
τ_{yx}
σ_y
Y (N)
h_1
X (E)

NOTES

ALL CO-ORDINATE AXES ARE SHOWN IN THEIR POSITIVE DIRECTIONS.

FIGURE b : CO-ORDINATE SYSTEMS FOR AN ARBITRARILY ORIENTED DRILL HOLE IN AN x, y, z CO-ORDINATE SYSTEM (x - EAST ; y - NORTH ; AND z - VERTICAL)

α - AZIMUTH OF DRILL HOLE

ψ - INCLINATION OF DRILL HOLE

Date MAY 15, 1986
Project 851-6025

Golder Associates

Drawn D.M.
Chkd. [illegible]

APPENDIX E

LABORATORY TEST RESULTS

TABLE E1-1

UNIAXIAL COMPRESSIVE STRENGTH TESTS

PRINCE MINE

Drill Hole	Depth Interval (m)	Rock Type	Q_u MPA	E (GPa)	ν
P1	4.75	Medium grained sandstone	41.11	12.86	0.21
P1	5.27		41.45	14.51	0.17
P1	5.48		41.85	14.57	0.20
P1	19.50		68.63	17.05	0.24
P1	19.70		67.78	16.00	0.26
P2	10.29		38.70	13.79	0.28
P2	10.85		46.72	16.85	0.20
P2	11.06		50.69	17.18	0.24
P3	7.09		56.18	16.11	0.23
P3	7.29		52.32	14.92	0.22
P3	7.40		53.66	14.38	0.20
P4	7.95		71.65	19.15	0.16
P4	8.34		74.49	17.84	0.17
P4	8.54		82.32	20.98	0.17
		mean	56.25	16.16	0.21
		standard deviation	±14.26	± 2.22	±0.04
P4	17.38	Fine grained sandstone	142.87	38.75	0.17
P4	27.85	Siltstone	82.08	15.82	0.16
P4	13.26	Mudstone	89.30	20.36	0.12

TABLE E1-2

MULTIPLE TRIAXIAL TEST RESULTS

PRINCE MINE

Bore-hole	Depth (m)	Rock Type	σ_3 = 0.34 (MPa)	σ_3 = 3.45 (MPa)	σ_3 = 6.89 (MPa)	σ_3 = 13.79 (MPa)	σ_3 = 20.68 (MPa)	Modulus	Poissons Ratio
			σ_1 (MPa)	σ_1 (MPa)	σ_1 (MPa)	σ_1 (MPa)	σ_1 (MPa)	E (GPa)	ν
P1	4.65	Medium grained sandstone	49.77	70.58	92.68	117.43	149.18	17.75	0.18
	4.85		52.42	69.70	92.46	120.29	148.39	19.15	0.14
	4.96		51.68	73.50	92.40	120.27	152.66	16.93	0.15
	5.17		52.61	70.89	90.14	118.52	151.19	17.45	0.20
	5.37		44.51					15.32	0.21
	18.89		54.30	79.40	95.12	122.56	149.71	14.62	0.16
	18.99		47.69	56.01	91.56	122.50	163.48	11.74	0.15
	19.09		48.06	67.85	95.41	122.43	169.49	11.24	0.25
P2	2.55		38.14	53.93	79.28	106.20	145.91	12.20	0.12
	10.39		37.51	55.79	66.26	99.72	136.27	12.76	0.12
	10.49		36.35	59.11	84.09	103.93	139.88	14.25	0.14
	10.60		38.30	52.00	71.70	92.13	141.74	15.29	0.24
	10.75		41.30	57.83	74.33	103.41	138.00	14.88	
	10.95		45.56	64.29	74.08	100.80	141.74	13.52	0.17
P3	5.41		39.51	53.24	80.27	100.39	137.97	12.27	
	7.19		51.73	64.51	80.24	108.20	150.19	12.91	0.24
	7.58		40.65	60.56	77.58	103.76	147.22	14.52	
	7.68		39.71	62.49	83.31	108.59	146.93	13.21	0.13
	7.78		38.06	60.97	77.94	104.57	141.26	12.64	0.20
	7.89		41.90	60.74	78.60	109.68	141.61	12.96	0.16
P4	7.85		45.56	71.62	88.10	103.48	150.40	16.20	0.20
	8.05		53.46	82.56	86.10	121.51	152.77	16.20	0.12
	8.16		54.68	85.71	98.72	120.03	152.58	18.52	0.11
	8.44		71.17	92.56	117.10	144.96	179.10	22.74	0.12
		mean	46.44	66.34	85.54	111.97	149.03	14.97	0.17
		standard deviation	±8.08	±10.91	±11.00	±11.65	±10.25	±2.76	±0.04
P4	13.81	Fine grained sandstone	95.68	112.38	133.64	139.34	174.41	20.73	
	17.93		170.83	196.34	203.71	249.63	279.50	55.39	0.18
	18.04		199.21	218.81	224.46	250.46	309.49	53.88	0.20
	18.14		146.48	147.36	148.68	185.70	235.35	40.21	0.15
		mean	153.05	168.72	177.62	206.28	249.69	42.55	0.18
		standard deviation	±43.90	±47.97	±43.38	±53.96	±58.70	±16.07	±0.03
P1	9.53	Siltsone	60.03	66.73				16.64	
P4	23.38		31.31					5.31	
	27.54		71.14	92.34	105.37	118.84	162.11	16.38	0.16
	27.64		75.86	78.52	96.72	141.05	161.36	16.13	0.19
	27.74		65.98	83.44	106.24	127.83	157.85	14.99	0.21
	27.95		76.56	94.09	95.88	126.03	157.18	13.85	0.12
		mean	63.48	83.02	101.05	128.44	159.63	13.88	0.17
		standard deviation	±16.95	±11.13	±5.51	±9.26	±2.47	±4.33	±0.04
P4	13.16	Mudstone	51.67	56.16	87.45	114.82	140.67	13.98	0.23
	13.36		82.25	87.63	115.61	142.19	174.04	17.85	
		mean	66.96	71.90	101.53	128.51	157.36	15.92	
		standard deviation	±21.62	±22.25	±19.91	±19.35	±23.60	±2.74	

TABLE E1-3

LABORATORY TENSILE STRENGTH TESTS

PRINCE MINE

Drill Hole	Depth Interval (m)	Rock Type	Tensile Strength σ_t (MPa)
P1	5.01	Medium grained sandstone	-2.99
P1	19.60		-5.44
P1	19.61		-4.71
P1	19.62		-5.62
P1	19.80		-5.07
P2	2.60		-4.22
P2	11.16		-3.88
P2	11.17		-3.66
P3	5.37		-1.98
P3	7.45		-3.28
P4	8.26		-4.81
P4	8.27		-6.53
		mean standard deviation	-4.35 ±1.27
P4	13.71	Fine grained sandstone	-7.30
P4	13.72		-9.46
P4	13.91		-10.70
P4	17.73		-8.63
P4	17.74		-12.11
P4	17.75		-11.59
		mean standard deviation	-9.97 ± 1.84
P1	9.22	Siltstone	-5.92
P1	9.32		-6.74
P1	9.42		-6.72
P1	9.63		-5.35
P1	9.64		-4.90
P4	23.28		-2.15
P4	23.29		-4.14
P4	23.30		-5.13
P4	23.92		-6.54
P4	24.08		-4.06
P4	24.09		-4.65
P4	24.10		-4.21
P4	28.05		-7.41
P4	28.15		-6.27
P4	28.16		-9.60
		mean standard deviation	-5.59 ±1.76
P4	13.46	Mudstone	-7.96

TABLE E2-1

UNIAXIAL COMPRESSIVE STRENGTH TESTS

LINGAN MINE

Drill Hole	Depth Interval (m)	Rock Type	Q_u (MPa)	E (GPa)	ν
L1	11.03	Siltstone	47.27	39.79	0.20
L1	11.16		32.42	37.18	0.17
L1	11.26		34.02	-	-
L5	13.83		80.84	32.78	0.25
		mean	48.64	36.58	0.21
		standard deviation	±22.48	±3.54	±0.04
L1	23.10	Sandstone	88.91	31.60	0.22
L1	23.42		96.60	26.26	0.16
L1	23.73		54.56	33.26	0.15
		mean	80.02	30.37	0.18
		standard deviation	±22.38	±3.66	±0.04
L5	17.70	Mudstone	59.40	15.49	0.11

TABLE E2-2

MULTI-STAGE TRIAXIAL TEST RESULTS

LINGAN MINE

			σ_3 = 3.45 MPa	σ_3 = 6.89 MPa	σ_3 = 13.79 MPa	σ_3 = 20.68 MPa
Drill Hole	Depth (m)	Rock Type	σ_1 (MPa)	σ_1 (MPa)	σ_1 (MPa)	σ_1 (MPa)
L1	12.08	Siltstone	24.15	36.22	58.32	80.68
L5	7.65		50.50	65.45	97.16	129.54
L5	14.13		48.31	61.35	80.28	95.11
L5	14.23		38.00	46.78	64.09	93.32
		mean	40.24	52.45	74.96	99.66
		standard deviation	±12.03	±13.46	±17.48	±20.93
L1	23.20	Sandstone	100.74	119.67	164.54	193.37
L1	23.32		83.57	-	-	-
		mean	92.16	-	-	-
		standard deviation	±12.14	-	-	-
L5	16.18	Mudstone	41.58	50.10	69.98	102.63

TABLE E2-3

LABORATORY TENSILE STRENGTH TESTS

LINGAN MINE

Drill Hole	Depth Interval (m)	Rock Type	Tensile Strength σt (MPa)
L1	11.99	Siltstone	-8.00
L1	12.02		-6.15
L5	7.71		-6.04
L5	7.74		-7.99
L5	13.74		-4.66
L5	13.77		-6.83
L5	14.07		-9.09
		mean	-6.97
		standard deviation	±1.50
L1	23.26	Sandstone	-9.28
L1	23.80		-5.29
L1	23.83		-6.05
		mean	-6.87
		standard deviation	±2.12
L5	16.25	Mudstone	-10.60
L5	16.28		-6.96
		mean	-8.78
		standard deviation	±2.57

APPENDIX F

SPECIALIZED DRILLING EQUIPMENT FOR OVERCORING

APPENDIX F - SPECIALIZED DRILLING EQUIPMENT FOR OVERCORING

The equipment described in this Appendix pertains to overcoring using a 100 mm diameter hole and a 38 mm diameter pilot hole. The overcoring equipment was designed to adapt to the commercially available HQ wireline drilling equipment and can be used either in horizontal or vertical down holes. The components of the drilling equipment are as follows:

a) Underground drillrig capable of driving HQ equipment such as the Longyear 38 or equivalent.

b) Water pump complete with pressure gauge readable to 1 psi.

c) Special water swivel and water pressure regulator (to limit pressure to 40 psi).

d) Standard HQ wireline drilling equipment with HQ driving rods.

e) Modified inner tube assembly for the HQ system which carries the starter barrel for the E hole and the 1 m longer double tube E core barrel. This modified assembly latches in place of the conventional HQ inner tube assembly and is rotated and/or fed with the HQ rods are rotated and/or fed. As the modified inner tube assembly was machined to set concentrically with the HQ outer tube, the E hole drill with this assembly would be concentric with the H hole.

   This system of drilling is especially advantageous when carrying out deep measurements in vertical downholes because the wireline system allows substantial saving in the time for breaking up and assembling drill rod for drilling the holes. This system has been used successfully in stress measurements in Nova Scotia and Ontario.

f) 100 mm diameter thin-walled overcoring bit adaptable to and driven by HQ rods acting as a continuous string of stabilizers along the drillhole. This eliminates the use of individual stabilizers and hence improves the efficiency.

The above equipment performed satisfactorily during the tests.

APPENDIX G

NOMENCLATURE

APPENDIX G - NOMENCLATURE

		First Reference Page
P	Maximum secondary principal stress	5
Q	Minimum secondary principal stress	5
σ_x	Stress component (east-west)	12
σ_y	Stress component (north-south)	12
σ_z	Stress component (vertical)	12
τ_{xy}	Shear stresses	12
τ_{yz}		12
τ_{zx}		12
σ_H	Maximum horizontal principal stress	13
σ_h	Minimum horizontal principal stress	13
σ_r	Radial stress	13
σ_θ	Tangential stress	13
T	Tensile strength	14
P_c	Critical fluid pressure for rupture	15
P_p	Pore water pressure	15
α	$1 - Cv/Cb$	16
Cv	Coefficient of rock matrix compressibility	16
Cb	Coefficient of rock bulk compressibility	16
K	Rock permeability	16
ν	Poissons ratio	16
σ_v	Vertical stress	48
σ_1	Major Principal Stress	49
σ_2	Intermediate Principal Stress	49
σ_3	Minor Principal Stress	49